THE UNIVERSITY OF HULL

Investigation of monolithic materials for protein sample preparation

being a thesis submitted for the Degree of Doctor of Philosophy
in the University of Hull

by

Eman Saad Alzahrani

MSc (University of Hull)

December 2012

Contents

Abstract

Proteomics plays an important role in the recognition of diseases and the understanding of biological processes. Sample preparation is a bottleneck in systems for chemical analysis and it is a required step in proteomics in order to remove interferences and preconcentrate the proteins. In addition, protein reduction and alkylation before digestion is a required step in proteomics to facilitate protein unfolding and increase the efficiency of enzymes in digesting proteins. The purpose of this study was to develop new techniques to address some of the shortcomings of current sample preparation methods, and provide short sample preparation time. Much research in recent years has focused on porous monolithic materials since they are highly permeable to liquid flow and show high mass transfer compared with common packed beds. This study has focused on the use of organic polymer- and inorganic silica-based monolithic materials for protein sample preparation.

The organic polymer monolith used in this study was a butyl methacrylate-*co*-ethylene dimethacrylate (BuMA-*co*-EDMA) monolith that was fabricated inside the borosilicate tube using photoinitiated polymerisation. The porous properties of the fabricated monolith were controlled by adjusting the composition of the porogenic solvent in the polymerisation mixture. The results indicated that using MeOH/1-propanol as a porogenic solvent produced a polymer-based monolith with high surface area (56.89 m^2 g^{-1}); however, it lacked the desired permeability and porosity when fabricated inside a glass microchip. Evaluation of its performance was carried out by extraction of four standard proteins that were insulin, cytochrome C, myoglobin, and hemoglobin and the extraction recovery was in the range (79.1-98.4 %).

A monolithic silica rod was fabricated without cracks inside a heat shrinkable tube and then compared with the same material whose surface has been modified with octadecyl groups in order to use them for preconcentration/extraction of proteins. Their performance was evaluated using eight standard proteins, namely insulin, cytochrome C, lysozyme, myoglobin, β-lactoglobulin, ovalbumin, hemoglobin, and bovine serum albumin. The results show that recovery of the proteins was achieved by both columns with variable yields; however, the octadecylated silica monolith gave higher recoveries (92.7 - 109.7%) than the non-modified silica monolith (25.5 - 97.9%). This was followed by a new process for the fabrication of a silica-based

monolith inside a glass microchip, which was successfully developed for use in microchip-based solid phase extraction of proteins. This was achieved by placement of the monolithic silica disk inside the extraction chamber in the base plate of the microchip, followed by thermal bonding of the two plates of the glass microchip at 575 °C for 3 hours. By doing this, the problem of shrinkage in the silica skeleton during preparation was avoided completely. The monolithic silica disk inside the glass microchip was subsequently modified with octadecyl groups for increased protein binding capacity. The performance of the microchip was evaluated using the extraction of standard proteins mixed with a high concentration of the detergent 3-[(3-cholamidopropyl)dimethylammonio]-1-propanesulfonate (CHAPS). The results show that the octadecylated silica monolith was permeable, has the ability to remove impurities, and achieved a high extraction recovery of the proteins (94.8-99.7%) compared with conventional octadecylated silica particles (48.3-91.3%). The intra-batch and inter-batch RSDs were in the range of 2.0-4.5% and 2.9-6.4%, respectively. Comparison between the fabricated device and a commercial cartridge for the preconcentration of proteins in skimmed cows milk and hen egg white showed the ability of the device to successfully enrich protein mixtures from more realistic samples. This new microfluidic device for protein extraction may find an application in the area of proteomic research.

A novel approach for immobilisation of the reducing reagent on the surface of the silica-based monolith in order to use it for protein reduction and alkylation was successfully developed. This was carried out by silanisation of the surface of the silica-based monolith with (3-aminopropyl)triethoxysilane (APTES), followed by immobilisation of the reducing reagent, tris (2-carboxyethyl) phosphine hydrochloride (TCEP) on the surface of the amino-bonded silica monolith. The fabricated monolith was characterised using IR spectroscopy, EDX analysis, BET model, and measuring the contact angle of deionised water. The fabricated monolith was evaluated for its use in protein reduction and alkylation in one single step at 60 °C by injection of a mixture consisting of 40 μL denatured protein and 60 μL iodoacetamide solution into the fabricated microchip, followed by using MALDI-TOF-MS instrument for qualitative confirmation. The results show that the fabricated microchip-based silica monolith has the ability to reduce and alkylate insulin in 30 min, and lysozyme in 45 min. Although this method was shown to require sample desalting to remove denaturant (urea) and

the performance of the fabricated monolith had low intra-chip reproducibility, the method was simple, reduced the risk of contamination, decreased the number of processing steps, and results in lower amounts of the sample and reagents compared with the conventional techniques for proteomics sample preparation. More work is required to fully optimise this approach to protein sample preparation.

Acknowledgements

First of all, I would like to express unlimited thanks to my first supervisor Dr. Kevin Welham for his continuous encouragement, given time to guiding, and patience throughout this work. I would like to express my appreciation to my second supervisor Dr. Tom McCreedy.

I would also like to thank all members of the Analytical Research Group at Hull University and all the people in lab C222. A special mention must go to Dr. Alberto Diego-Taboada for technical assistance. I would like to acknowledge Dr. Steve Clark for microfluidic device manufacture and Mr. Tony Sinclair for production of the monolith SEM images.

I offer my profound thanks to the Saudi Arabian Culture Bureau generally, and to Taif University specifically for their spiritual and financial support.

I would like to give my deep thanks to my husband Mohammed and my kids Rahaf, Sultan, and Amir for their endless support, love, and care. In addition, I would like to thank my parents, and my sisters and brothers for their continual motivation and support.

Finally, I wish to thank those who have positively affected my life with their support, wisdom, love, and care.

Abbreviations

4HCCA	α-cyano-4-hydroxycinnamic acid
γ-MAPS	3-(trimethoxysilyl) propyl methacrylate
μTAS	micro total analysis systems
ACN	acetonitrile
AFM	atomic force microscopy
AIBN	2,2′-azobis(2-methylpropionitrile)
APTES	(3-aminopropyl)triethoxysilane
BET	Brunauer-Emmett-Teller
BJH	Barrett-Joyner-Halenda
BME	2-mercaptoethanol
BPO	dibenzoyl peroxide
BSA	bovine serum albumin
BuMA	butyl methacrylate
CCD	charge-coupled device
CDMOS	chlorodimethyl octadecyl silane
CE	capillary electrophoresis
CEC	capillary electrochromatography
CHAPS	3-[(3-cholamidopropyl)dimethylammonio]-1-propanesulfonate
CNC	computer numerical control
CZE	capillary zone electrophoresis
DCC	N,N'-dicyclohexylcarbodiimide
DCU	dicyclohexyl urea
DHB	2,5-dihydroxybenzoic acid
DMPA	2,2-dimethoxy-2-phenyl acetophenone
DNA	deoxyribonucleic acid
DTT	dithiothreitol
DVB	divinylbenzene
EDC	N-(3-dimethylaminopropyl)-N′-ethylcarbodiimide hydrochloride

EDMA	ethylene dimethacrylate
EDX	energy dispersive X-ray analysis
EOF	electro-osmotic flow
ER	extraction recovery
ESI	electrospray ionisation
ETFE	ethylenetetrafluoroethylene
EtOH	ethanol
FITC	fluorescein isothiocyanate
FT-IR	Fourier transform infrared
GC	gas chromatography
GFP	green fluorescent protein
GMA	glycidyl methacrylate
HCl	hydrochloric acid
HEMA	2-hydroxyethyl methacrylate
HF	hydrogen fluoride
HMDS	hexamethyldisilazane
HPLC	high performance liquid chromatography
HSA	human serum albumin
IA	iodoacetic acid
IAA	iodoacetamide
ICP	inductively coupled plasma
i.d.	internal diameter
IE	ion-exchange
IgG	immunoglobulin G
ISEC	inverse size exclusion chromatography
ITO	indium tin oxide
KOH	potassium hydroxide
LC	liquid chromatography
LLE	liquid-liquid extraction

LPO	lauroyl peroxide
MALDI	matrix-assisted laser desorption/ionisation
MCC	monolithic capillary column
MeOH	methanol
MES	4-morpholineethanesulfonic acid
META	[2-(methacryloyloxy)ethyl]trimethylammonium chloride
MIP	mercury intrusion porosimetry
MPTS	3-mercaptopropyltrimethoxysilane
MS	mass spectrometry
MTMS	methyltrimethoxysilane
MTS	(3-methacryloyloxypropyl) trimethoxysilane
MudPit	multidimensional protein identification technology
MW	molecular weight
m/z	mass to charge ratio
NaCl	sodium chloride
NaOH	sodium hydroxide
NEM	N-ethylmaleimide
NP	normal-phase
o.d.	outer diameter
ODS	octadecyl-bonded silica
PAGE	polyacrylamide gel electrophoresis
PBS	phosphate-buffered saline
PC	packed column
PDF	pressure-driven flow
PDMS	polydimethylsiloxane
PE	polyethylene
PEEK	polyetheretherketone
PEO	polyethylene oxide
pI	isoelectric point

PMMA	polymethylmethacrylate
PP	polypropylene
PPM	porous polymer monolith
PS	polystyrene
PTFE	polytetrafluoroethylene
PTM	post-translational modification
RBITC	rhodamine B isothiocyanate
RNA	ribonucleic acid
RP	reversed-phase
RSD	relative standard deviation
SA	sinapinic acid
SCX	strong cation exchange
SDS	sodium dodecyl sulphate
SEM	scanning electron microscopy
SPE	solid phase extraction
Sulfo-NHS	N-hydroxysulfosuccinimide sodium salt
TCEP	tris (2-carboxyethyl) phosphine hydrochloride
TEM	transmission electron microscopy
TEOS	tetraethyl orthosilicate
TFA	trifluoroacetic acid
TMCS	trimethylchlorosilane
TMOS	tetramethyl orthosilicate
TOF	time of flight
TRIM	trimethylolpropane trimethacrylate
UV	ultraviolet light
VP	vinylpyridine

1.0 Introduction

The work performed throughout the PhD will be divided into different sections in this thesis. Chapter one provides a brief introduction, and presents a literature review of key concepts, which are related to this thesis. Then, chemicals, materials, instruments, the experimental setup, and procedures utilised for the work in this thesis will be detailed in the experimental chapter. The results and discussion section will be broken into two main sections. The first section is about evaluation of fabrication of monolithic materials and characterisation of the fabricated materials using different techniques (chapter 3). The second section evaluates the use of fabricated polymer- and silica-based monoliths in protein extraction, and an investigation of the performance of the TCEP-immobilised silica monolith in reduction and alkylation of proteins (chapter 4). A conclusions chapter will summarise the work performed and present recommendations for the future of the work, followed by a list of references. Finally, Publications related to the work described here will be mentioned.

1.1 Proteomics

Study of proteins is very important because they are related to cellular structure and function. Proteomics deals with the large-scale determination of gene and cellular function directly at the protein level. It is increasingly important in the development of new medicines and as a tool for identifying proteins implicated in disease pathways. As the search for novel molecules to tackle diseases increases, the need to identify proteins as biological targets increases. In addition, proteome analysis can identify the presence of post-translational modifications (PTMs).[1, 2]

The name “protein”, derived from the Greek term ‘proteios’ that means “the first rank”, was firstly utilised by Berzelius in 1838 to emphasise the importance of proteins.[3] They consist of long chains of amino acids linked together by peptide bonds. There are twenty common amino acids and they contain amine and carboxyl functional groups. The order of these amino acids, which is called the amino acid sequence, can differ from protein to protein, and real samples tend to be very complex mixtures of proteins.[1] The term “proteome” (PROTEins expressed by a genOME) was coined by Wilkins *et al.*[4] in 1996. The proteome can be defined as the entire complement of proteins expressed by a genome and which are present in a cell, a body

fluid, a tissue, or an organism under different conditions. Proteomics plays an important role in the study of proteins and protein identification.[2]

Analysis of proteins is more difficult than that of deoxyribonucleic acid (DNA) or ribonucleic acid (RNA) because the genome is stable while the proteome is dynamic and changes depending on the type and the functional state of a cell.[3] Another reason is the complexity of proteins since they contain heterogeneous groups.[5] Moreover, the structure of proteins can be modified by adding chemical groups to chemical functionalities in the amino acid sequence and this can cause changes in the properties of the proteins. In addition, the life of proteins can be very short, sometimes minutes or hours. Another challenge is the vast dynamic range of proteins present in a cell, ranging from tens to millions, and this poses a challenge for analysis that no one analytical technique can overcome.[6, 7] In addition, dealing with proteins is difficult because they stick to many different surfaces such as metals, plastic, and glass.[8] This is because of the electrostatic interaction between the charged functional groups in proteins with a negatively charged surface.[9] For these reasons, study of an entire complex mixture of proteins is still a great challenge for analytical chemistry.

1.2 Analysis techniques in proteomics

The main steps in proteomics are sample preparation, extraction, digestion, separation, and detection. In order to analyse proteins, the protein samples should be isolated from the matrix. The biological sample should be pulverised and disrupted to make a soup, which contains a mixture of cells and biological components. This is followed by protein extraction, which needs to be carried prior to the following analysis.[10]

The most traditional method to detect and identify proteins from a biological sample is the "top-down" approach. It depends on studying the intact proteins using the characteristics of a protein; for example, molecular weight, isoelectric point, and hydrophobicity to isolate the intact protein.[11] The top-down approach consists of intact protein separation using one- or two-dimensional polyacrylamide gel electrophoresis (1D- or 2D-PAGE), followed by off-line static infusion of sample into the mass spectrometer for intact protein mass measurement and intact protein fragmentation. The advantage of this approach is the ability for direct detection of the native

molecular mass of proteins.[12] Moreover, it is used to find any post-translational modification (PTM) occurring in a protein.[13] Other advantages of this approach are simplified sample preparation and elimination of the time consuming protein digestion required for bottom-up approach. However, the problem with this technique is that using 2D-PAGE tends to exclude low abundance proteins, highly hydrophobic membrane proteins, and highly basic or acidic proteins.[7]

The other method is known as the "bottom-up" approach. This approach, referred to as "shotgun proteomics", has gained popularity in the proteomics field.[12] It refers to the direct study of complex protein mixture to obtain a global profile of the proteins in the mixture. This approach is based on proteolytic digestion of the intact proteins into peptides, followed by separation of the peptides using the MudPit method (multidimensional protein identification technology), which incorporates multidimensional high-pressure liquid chromatography (LC/LC), tandem mass spectrometry (MS/MS) and database-searching algorithms.[14] The main advantages of the bottom-up approach are automation and the ability to obtain high resolution separation.[11] However, it can cause an increase in the complexity of the mixture; for example, 5-15 peptides per protein. Additionally, it is difficult to screen for biomarkers for smaller proteins and peptides that have fewer proteolytic coverage sites. In addition, the sequence coverage of a protein is rarely 100 %; therefore, there will be a chance of missing modifications.[13]

1.3 Protein sample preparation

Proteomic samples are commonly complex because proteins differ in their physical properties such as solubility, hydrophilicity/hydrophobicity (some proteins are soluble in water, others only in very hydrophobic organic solvents), and isoelectric points (from 2 to 14), and the proteins of most interest could be in low abundance. Proteins also have a broad range of molecular weights (can be < 10000 Da to > 500000 Da).[15] In addition, they contain contaminants such as salts, buffers, nucleic acids, polysaccharides, lipids, and detergents that can interfere with the protein separation step, inhibit protein digestion, affect MS analysis, or make the statistical analysis difficult.[16] These challenges make efficient extraction of proteins the most critical step

in proteomics, and require the extraction technique to be of the highest efficiency and broadest range of applicability.[15]

Most instruments cannot handle such sample matrices directly, or the target analytes could be masked by the interfering compounds during the analysis. The benefit of the sample preparation method is to remove interfering materials, and preconcentrate the proteins. As a result, the signal intensities of the target analytes will be improved, and the quantities of the target analytes can be easily measured.[17]

The selection of an appropriate sample preparation procedure is therefore a key factor in the success of analysis, and the whole analytical process can be wasted if an unsuitable sample preparation is used.[18, 19] Commonly, the process of extraction and preconcentration of the biological samples is complicated, labour-intensive, and time consuming.[20] Therefore, an ideal sample preparation procedure should be as simple as possible, fast, and the procedure should be reproducible with high extraction recovery of the target analytes. In addition, it should require a minimum number of processing steps, minimise solvent consumption, be environmentally friendly, improve detection limits, and have potential for use in on-line method arrangement.[21, 22] Generally, sample preparation can be typically performed by liquid-liquid extraction (LLE), or solid phase extraction (SPE).[23]

1.3.1 Liquid-liquid extraction

The extraction of the sample can be performed by liquid-liquid extraction (LLE), which is also known as “solvent extraction” or “partitioning”. It is the oldest and most widely used sample preparation technique. It is based on using a separatory funnel for separating liquid phases from each other, and an immiscible organic solvent is mixed with an aqueous solvent, which could be plasma or urine, followed by evaporation of the organic solvent to dryness and reconstitution prior to analysis.[22]

In general, advantages of the LLE technique include large sample capacity, and good extraction recovery for a wide range of analytes. In addition, the broad polarity range of solvents makes this technique popular.[19] However, it is labour-intensive including multiple stages, non-selective, susceptible to errors, time consuming, needs a large volume of high-purity solvents with expensive disposal requirements for

environmental pollutants that adding extra cost to the analytical procedure, creates health hazards to the laboratory personnel, and is difficult to automate and connect with analytical instruments.[18, 22, 23] In addition, LLE can lead to loss of the analyte due to incomplete extraction, and commonly it has practical problems such as emulsion formation.[24, 25]

1.3.2 Solid phase extraction

Another extraction method that can be used to extract the target analyte from a solution is liquid solid extraction, which is often called solid phase extraction (SPE). It has become a popular pretreatment procedure in many areas such as clinical, environmental, pharmaceutical, food, and industrial applications.[25, 26] It was invented in the mid 1970s in order to avoid the labour-intensive liquid-liquid extraction, and the first paper describing the SPE approach was published in 1998.[27]

Solid phase extraction has been identified as "a method of sample preparation that concentrates and purifies analytes from solution by sorption onto a disposable solid-phase cartridge, followed by elution of the analyte with solvent appropriate for instrumental analysis".[28] The benefit of using SPE is not only to extract and concentrate the analytes of interest in a single step, but also to remove the interfering compounds of complex matrices to get a cleaner extract containing the target analytes.[29]

There are many advantages of SPE compared with LLE; for example, it is relatively fast, obtains relatively high recoveries, is more reproducible, has good accuracy and precision, entails low solvent consumption, involves minimal waste, no emulsions are formed, and a smaller volume of the sample is required.[30] Moreover, the eluent of the SPE can be injected directly into high performance liquid chromatography (HPLC) or gas chromatography (GC) while the extracted analytes using LLE need to be dried and the residue prepared in a suitable solvent before analysis.[31]

Nevertheless, there are some disadvantages to SPE; for example, SPE cartridges or columns can be relatively expensive and are manufactured for single use only.[32] In addition, if the sample solution contains any solid particles, they can block the

cartridge/columns.[33] Another problem with SPE is the reproducibility of fabrication of the sorbent. In addition, SPE has a higher level of contamination by manufacturing and packaging materials than is the case for LLE. Another problem in SPE is related to the limited sorption capacity of the sorbents, which can lead to sample overload, compared with LLE.[25] In some cases, solvent evaporation is needed, which is more time consuming than in LLE because protic solvents are mainly utilised such as methanol, which has lower vapour pressure than the apolar solvents utilised for LLE.[18, 34] Although conventional SPE cartridges are easy to handle using a vacuum, it is not easy to control the flow rate and additional care should be taken in order to avoid drying the cartridges. However, these shortcomings do not prevent SPE being the most widely utilised sample preparation technique.[22]

The SPE technique can be carried out on-line by direct connection between the sorbent and the chromatographic analysis, or off-line, which means the sample preparation is separated from the subsequent chromatographic system. The advantages of the on-line technique are that it is fast, the extracted analytes do not need further handling between the extraction and separation steps, the risk of sample contamination is decreased, and the loss of the sample by evaporation and transfer is minimised. SPE can be coupled with HPLC or GC, followed by a detection system. Integration of SPE with GC is more delicate because of incompatibility between the aqueous part of the SPE step and the dry part of the GC instrument, while HPLC is more compatible with SPE since both techniques are based on using the aqueous mobile phase.[35, 36] Although off-line sample preparation by SPE is time consuming, it is the most common approach since the extraction and separation efficiency can be optimised independently.[37]

1.3.2.1 Solid phase extraction procedure

A typical solid phase extraction technique involves five steps; firstly the sorbent is activated using an appropriate solvent, followed by equilibration of the sorbent bed in order to remove impurities, and to remove the air present in the cartridge. It is important to make sure that the sorbent is not dry between the conditioning and applying the sample solution; otherwise, the target analytes will not be efficiently retained and low extraction recovery will be obtained.[38] The sample solution is then

applied through the solid sorbent and the analytes of interest are adsorbed on the sorbent and retained with appropriate chemistry while the unwanted components are not bound to the sorbent. The concentration of the target analyte at the surface of the sorbent increases until the sorbent is saturated and breaks through into the next segment of the SPE adsorption bed. The sample solution could be applied to the sorbent by gravity, pumping, or by an automated system. The flow rate of the sample solution through the sorbent should be low in order to enable efficient retention of the analyte.[38] The final arrangement of adsorbed analyte in the sorbent bed depends on the nature of the target analyte and type of sorbent. After loading the aqueous sample, the sorbent is washed in order to remove interfering materials, while the target analytes retain on a solid phase sorbent. Finally, the target analytes are desorbed by eluting the target analytes from the sorbent.[39] The flow rate needs to be adjusted to ensure efficient elution of the target analytes.[31] Figure 1.1 shows a schematic view of the main steps of solid phase extraction.

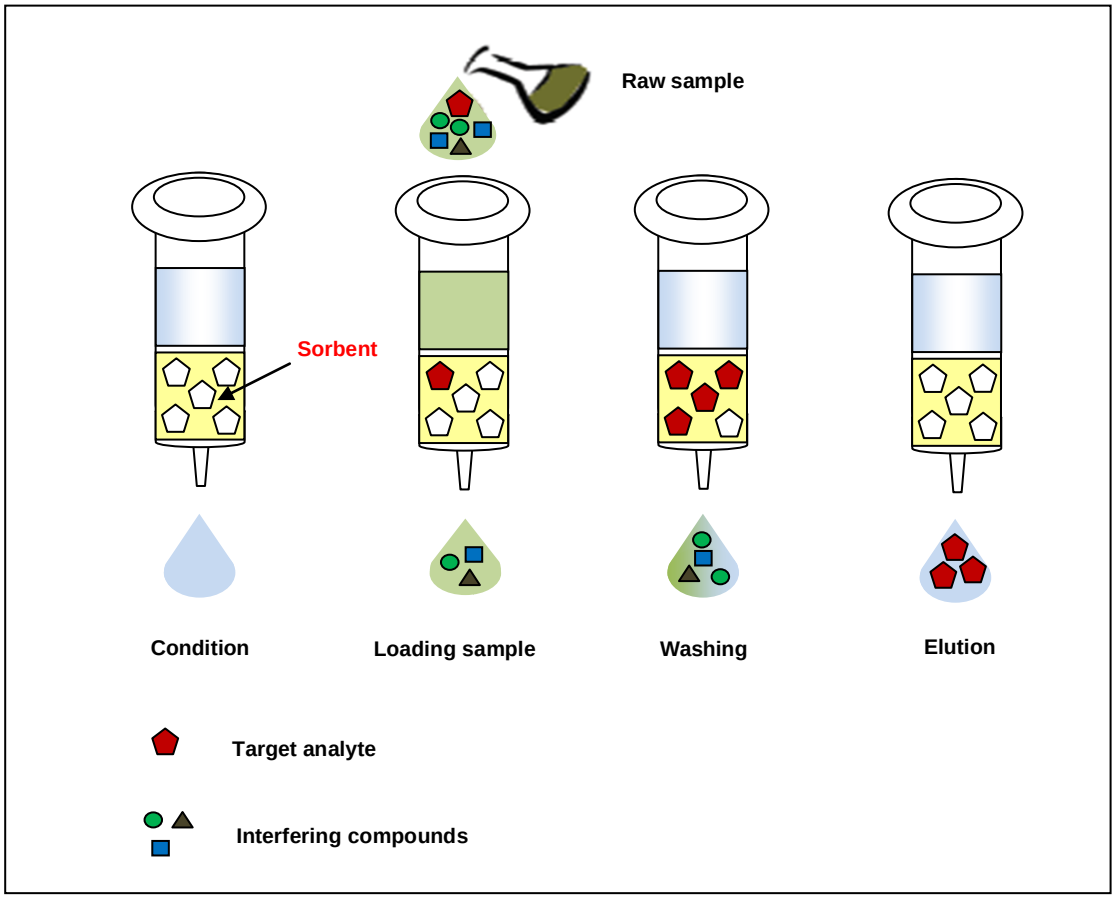

Figure 1.1 The main steps of solid phase extraction (SPE).

Solvents play an important role in SPE. Solvents used in each step of SPE must not react with analytes or the sorbent. Furthermore, they should have weak toxicity, not interfere with the target analytes, and be compatible with the chromatographic system used (HPLC or GC).[40] Commonly, organic solvents such as acetonitrile (ACN) could be added to the sample solution in order to precipitate salts and biopolymers such as proteins, polysaccharides, and DNA. In the conditioning step, commonly an organic solvent is used to clean up the sorbent and remove impurities from the sorbent. In addition, it is used to wet and solvate hydrophobic groups. In the washing step, the washing solution plays an important role in removal of unwanted materials without affecting the adsorbed target analytes. The type of eluting solvent depends on the mechanism of retention in SPE and the volume of the eluting solvent should be enough to elute all the components of the target analyte from the surface of the sorbent. Commonly, eluting solvent such as ACN containing 0.1% trifluoroacetic acid (TFA) or 5% triethylamine in methanol is suitable for direct injection onto HPLC.[31]

1.3.2.2 Retention mechanisms applied in solid phase extraction

Conventionally, solid phase extraction can be divided into three categories: reversed-phase (RP), normal-phase (NP) and ion-exchange (IE).[41] Reversed-phase (RP) involves a polar or moderately polar sample matrix and a non-polar stationary phase, which can be octadecyl, octyl, cyclohexyl, or butyl. The attractive forces of this type are non-polar interactions, commonly called van der Waals forces or dispersion forces. The normal-phase (NP) involves a non-polar matrix (such as acetone, chlorinated solvents, and hexane) and a polar stationary phase such as bare silica, alumina, or silica chemically modified with polar groups such as amino, cyano or diol groups. The retention mechanism of this type is based on interaction between polar functional groups of the target analyte and the polar groups on the surface of the sorbent.[35] The ion-exchange (IE) method involves extraction of compounds in solution: anionic (negatively charged) compounds can be extracted using an aliphatic quaternary amine group that is bonded to the silica surface while cationic (positively charged) compounds can be extracted using aliphatic sulfonic acid or carboxyl groups that are bonded to the silica surface. The mechanism of reaction is based on the electrostatic attraction between the charged functional groups in the target analyte and the charged functional groups that are bonded on the surface of the silica.[29]

1.4 Materials used on SPE sorbent

The availability of different materials of SPE sorbents is the major advantage over the LLE technique. The selection of sorbent is the key factor in SPE, which depends on the properties of the target analyte, the kind of sample matrix, and the interfering materials that should be removed.[22, 40]

The ideal sorbent material to be used for SPE should not be degraded by micro-organisms when using a biological sample, and it should not be affected by high temperature or storage. The SPE sorbent should be chemically stable and not react with the cleaning, conditioning, washing, or eluting solvents. In addition, one of the most important properties of a suitable sorbent for SPE is a high surface area that is proportional to the capacity of the sorbent in order to increase its loadability. Another important property of the sorbent utilised is the permeability of the SPE sorbent in order to decrease the processing time by increasing the flow rate and decreasing the backpressure. In addition, a suitable sorbent for SPE should be able to separate desired from undesired components, and give batch-to-batch reproducibility.[31] The common materials that have been used as SPE sorbents are particles and monoliths, which will be discussed in the following sections.

1.4.1 Particles

The most common materials used as sorbents for solid phase extraction are silica-based particles. The fabrication of packed columns (PCs) is based on two steps; fabrication of frits inside the capillary or microchip and then filling the capillary or microchip with small diameter particles in the range of 50-60 µm between the porous frits.[42]

The advantages of packed particles are the high surface area to volume ratio, they are widely available, well characterised, and easily functionalised.[43] However, the main problem with particles is their inability to fill completely the available space or possibility of being mislocalised, which means particle preparation requires special instruments and skilled technicians since the efficiency of extraction depends on the quality of packing. Furthermore, this type of stationary phase requires frits to keep the particles in place. The frits should be highly porous and rigid, which is commonly difficult to achieve. In addition, using frits can cause air bubbles to be formed that can

cause an unstable baseline, interrupt the electric current, and decrease the electroosmotic flow. Moreover, proteins can be adsorbed into the frits and remain trapped inside the capillary or microchip.[44-47] Extraction efficiency can be increased by increasing the surface area, which can be performed by reduction of the particle size; however, decreasing the particle diameter can cause an increase in the backpressure, which is inversely proportional to the square of particle size.[46, 47] In order to solve this problem, the bed length needs to be decreased to decrease the backpressure; on the other hand, this can decrease the number of interaction sites on the surface of the sorbent, resulting in decreasing the capacity of the sorbent. Moreover, the movement of the particles from their position by either pressure or a high electric field leads to formation of channels after a few usages, resulting in rapid movement of the analytes through these channels before they interact with the sorbent. As a result, the extraction efficiency of the analytes will be reduced.[48, 49]

1.4.2 Monolithic materials

Monolithic materials were introduced by Hjerten *et al*.[50] when compressed soft gels, called "continuous beds" were developed in 1989 and utilised in chromatographic separation. A further innovation by Svec and Frechet in the early 1990s was fabrication of rigid macroporous polymer monoliths, which were fabricated by a very simple "moulding" process and used as high performance liquid chromatography separation media.[51] Due to their unique properties, these organic monolithic materials have been used in a variety of applications.[52] Later, inorganic silica-based monolith was fabricated by several groups starting in 1996.[53, 54]

The word "monoliths" is from the Greek, "mono", which means 'one', and "lithos", which means 'stone'. It defines a geological or technological feature such as a mountain or boulder, consisting of a single massive rock; for example, a rock, which was collected by a famous Chinese Empress and used to decorate the access to one of her palaces,[55] as shown in figure 1.2.

Figure 1.2 Photograph of the porous monolith erected at the entrance of the Summer Palace Park, Beijing, China.[55]

The monolithic column can be defined as a single piece of a continuous rigid porous polymer that possess an interconnected skeletal structure and contains pores. Based on the size of the pores, they can be divided into three types; micropores (< 2 nm), mesopores (2-50 nm), and macropores or through-pores (> 50 nm). Each of these pores has a special benefit; micropores are the most important pores in terms of separation. However, in some cases, the molecules are too big to diffuse through these micropores; therefore, they will interact with mesopores. The main benefit of the macropores is to control the column permeability resulting in reducing the backpressure of the column.[56] For extraction, besides the macropores, the mesopores are the important pores since they can increase the surface area of the monolith, resulting in increased loadability of the monolith.[57]

Figure 1.3 shows the structural differences between a conventional chromatographic column, tightly packed with particles, figure 1.3 (A), and a monolithic column

fabricated of a single piece of a porous solid with relatively large channels for convective flow, figure 1.3 (B). The comparison between the scanning electron micrographs of the packed and monolithic chromatographic beds illustrates that the monolithic bed contains a much greater number of channels penetrating the chromatographic bed compared with the column packed with particles.

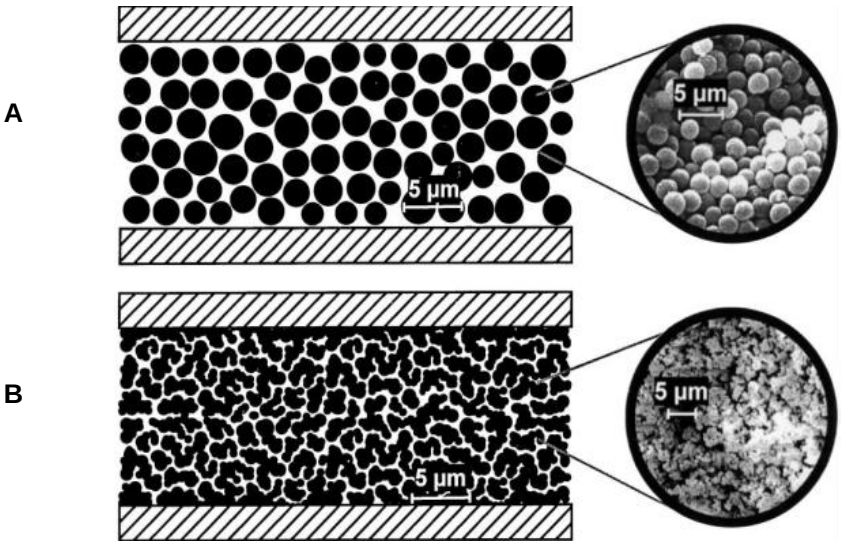

Figure 1.3 Structural characteristics of (A) packed, and (B) monolithic chromatographic beds.[58]

Monolithic materials have been shown to possess many advantages compared with packed particles. For example, they are easy to prepare, they have high surface area and high stability, and they are highly permeable to liquid flow compared with the packed bed since porous monoliths contain interconnected macro- and mesopores. This can increase the efficiency of extraction or separation and decrease the backpressure.[59, 60] Furthermore, the monolithic stationary phase does not need frits in comparison with the packed particles, which have mechanical problems related to the fragility of the columns and clogging of the column during use.[61, 62]

Several methods are commonly used for physical characterisation and measuring the porous properties of monolithic materials. For surface characterisation methods, they can be studied using optical methods such as scanning electron microscopy (SEM),

atomic force microscopy (AFM), and transmission electron microscopy (TEM).[60] These can give information about the morphology of the monolithic materials, which is closely related to their porous properties. Moreover, they are used to estimate the size of the pores, which will in turn determine the hydrodynamic properties and mechanical strength of the column.[62] The physical properties of monolithic materials, such as the porosity and pore size distribution, are studied using mercury intrusion porosimetry (MIP), which has the ability to measure large pores ranging from 10 nm to 150 µm. For measuring small pores (less than 50 nm), inverse size exclusion chromatography (ISEC) is commonly used. Moreover, the specific surface area and the pore size distribution can be studied using the Brunauer-Emmett-Teller (BET) method, which involves measuring the volume of N_2 adsorbed on the surface of the monolithic materials and the surface area can then be calculated from the adsorbed volume of an N_2 molecule.[52, 62]

Due to the unique properties of monolithic materials, they are finding their place in a variety of fields. For example, they have been used in various types of chromatography, such as gas chromatography (GC), high performance liquid chromatography (HPLC), and capillary electrochromatography (CEC). These applications have been described in many reviews.[52] However, less common applications of monoliths are as carriers for immobilisation of enzymes, static mixers, thermally responsive gates and valves, as well as a solid phase support for extraction and preconcentration.[63] According to their components, monolithic materials can be divided into organic polymer-based monoliths and inorganic silica-based monoliths, both of which will be described in the following sections.

1.4.2.1 Organic polymer-based monoliths

An organic monolith is a single block of highly porous material that consists of polymer globules separated by numerous interconnected cavities (pores), and held together through extensive crosslinking.[64] The preparation of a polymer-based monolith is produced by a "moulding" process, which is relatively simple and straightforward compared with silica-based monoliths.[60] Before fabrication of the polymer-based monolith inside a capillary or a microchip, its inner walls are silanised in order to prevent the movement of the monolith during the procedure. Commonly,

the capillary column or the microchip is rinsed with a strong basic solution in order to hydrolyse the siloxane groups at the inner surface resulting in increased density of the silanol groups. The silanisation of the inner walls is carried out using a bifunctional reagent solution, typically 3-(trimethoxysilyl) propyl methacrylate (γ-MAPS), which is allowed to react for a period of time. As a result, trimethoxysilane functional groups of the silanising agent will be anchored to the silanol groups while the methacrylate groups of the silanising agent will participate in the polymerisation reaction, causing the monolith to be chemically bound to the inner walls of the capillary or the microchip.[52] On the other hand, a further increase in silanisation reaction can cause a heterogeneous porous structure and form a less porous layer at the inner walls.[65]

The silanised capillary or microchip is filled with the polymerisation mixture, which commonly consists of monovinyl monomer, divinyl crosslinking monomer, porogenic solvents, and free radical initiator.[66] The polymerisation reaction consists of three steps; the first is the initiation step, when the initiator produces free radicals that will react with the monomer. Following initiation, the process continues with the successive addition of monomer units to the chains. This is known as propagation step. The last step is the termination step and this happens when two free radicals react together and are no longer available to catalyse polymerisation; as a result, the polymerisation reaction will stop.[42, 67]

Generally, the initiation of a polymerisation reaction can be performed by thermal initiation (heat), or photoinitiation (light), which can only be carried out in a transparent mould such as a glass tube, fused silica capillary, or glass microchip.[60] Thermally initiated polymerisation was a standard method for fabrication of the organic monolith in a completely filled closed column such as a column for HPLC.[68] However, adjustment of the length and position of the organic monolith is difficult to achieve using thermal initiation. Fabrication of organic monolithic material using photoinitiated polymerisation emerged in 1997 when Viklund *et al.*[69] fabricated a polymer-based monolith using glycidyl methacrylate and trimethylolpropane trimethacrylate inside a quartz tube (i.d. 2.4 mm). The results of this study showed that using a light initiated polymerisation process is faster than the thermally initiated polymerisation process. Photoinitiation has been used for fabrication of organic monoliths inside a capillary column or a microfluidic device for CEC, which requires

formation of the organic monolith in a specific location using a mask that prevents conversion of monomers to polymers in those areas that are not irradiated.[70]

After the polymerisation reaction, the organic monolithic material is washed in order to remove unreacted materials, such as residual monomers, the initiator, and porogenic solvents that remain in the pores of the monolith. Typically, the washing procedure is carried out using a mechanical pump or applying a voltage for a period of time.[71] After washing the monolithic material, it is ready to use. The scanning electron micrograph in figure 1.4 represents an example of the porous structure of a polymer-based monolith. The fundamental building units of this network are nuclei, which grow and agglomerate into globules, which will further agglomerate into larger clusters.[72]

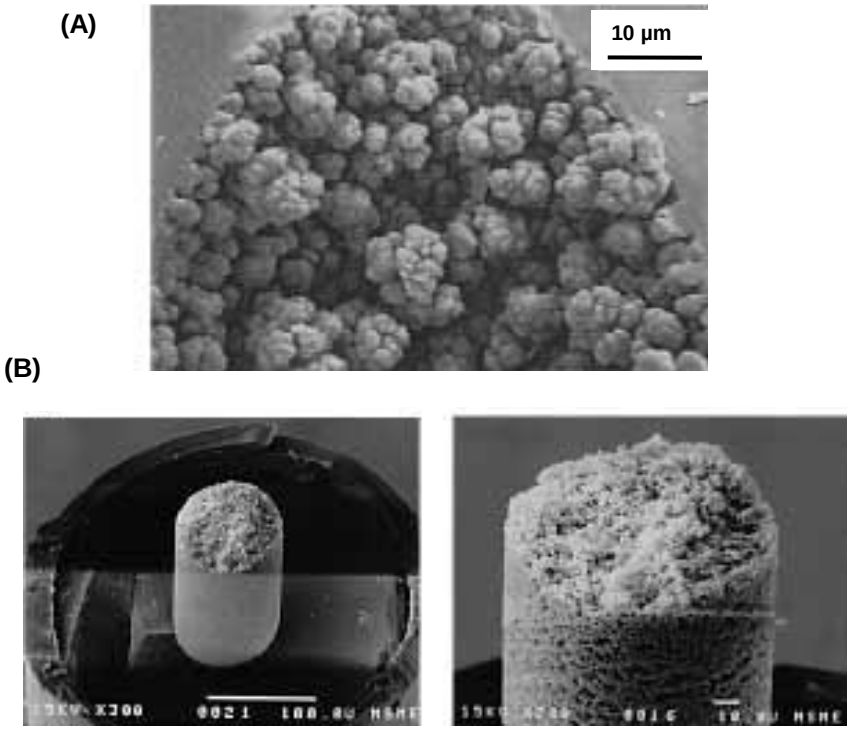

Figure 1.4 Scanning electron micrographs of polymer-based monoliths by (A) Horvath and coworkers,[73] and (B) Svec and coworkers [74] in 1999.

Polymeric monoliths can be fabricated by using a wide range of monomers and crosslinking agents enabling the porous properties of the monolith to be controlled; for

example, acrylate/methacrylate-, styrene-, and acrylamide-based stationary phases.[75] Figure 1.5 shows the common monomers and their crosslinking agents that have been used for fabrication of polymer-based monoliths. The monolith can be functionalised by co-polymerisation or post-polymerisation in order to convert it into a sorbent with the desired chromatographic binding properties.[73]

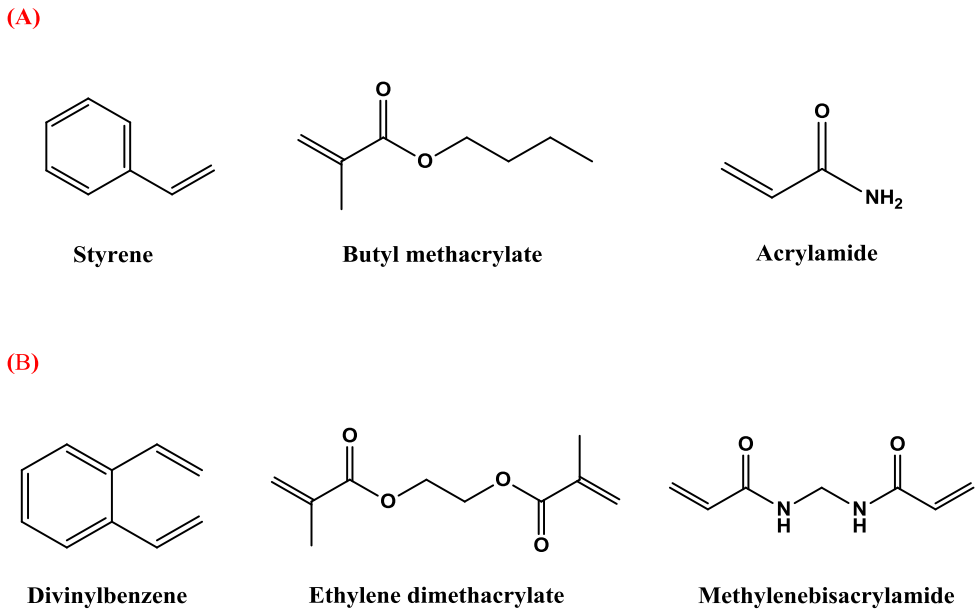

Figure 1.5 Examples of monomers (A), and their crosslinking agents (B) utilised for the fabrication of the polymer-based monoliths.

The important property of typical monolithic materials is high surface area, which can be increased by increasing the number of micropores. On the other hand, the permeability of the monolith requires macropores in order to allow liquid to flow through the monolith at a reasonable pressure.[70] Both the surface area and the hydrodynamic properties of the monolith depend on the pore size distribution of the monolith; therefore, a balance between the requirement of low flow resistance and high surface area must be found, and the ideal monolith should have both macropores in order to achieve sufficient permeability of the monolith, and micropores for high capacity.[60, 76] Many studies have been carried out to increase the surface area as well

as the permeability of flow through the monolith by optimising the composition of the polymerisation mixture and the reaction conditions.[77]

The most effective parameters in the fabrication of a polymer-based monolith that can affect its properties are the proportion of monomer to crosslinker, the polymerisation temperature or time of exposure to UV light, concentration of the initiator, and the percentage of the porogenic solvent system in the polymerisation mixture. The specific surface area and the pore size distribution are very sensitive to any variations of the listed parameters.[72]

Changing the ratio of monomer to crosslinker (monovinyl/divinyl monomer ratio) can be utilised to control the porous properties of the organic monolith. As the ratio of crosslinker to monomer increases, the monolith will be more dense and highly microporous, resulting in increase of the surface area of the monolith due to the shift of the pore size distribution to the small pore diameter as a result of early formation of highly cross-linked globules.[78, 79]

The polymerisation temperature can affect the kinetics of the polymerisation reaction, the pore size distribution, and the specific surface area. As the polymerisation temperature decreases, the reaction rate is slower and larger pores will be formed, resulting in a decrease in the surface area, while if the polymerisation temperature is increased, the reaction rate is quicker and smaller pores will be obtained, resulting in an increase in the surface area.[70]

Careful optimisation of the exposure to the UV light is required since the polymerisation time is responsible for conversion of monomers. As the polymerisation reaction continues, the degree of branching increases resulting in growing the polymer chains and making the monolith dense while reducing the irradiation time can lead to formation of less monolithic material in the capillary or the microchip, which can affect the performance of the fabricated monolith.[80] Figure 1.6 shows the effect of the irradiation time on the growth of the polymer chains. By increasing the irradiation time, the degree of branching increases resulting in forming a dense crosslinked polymer network.[81]

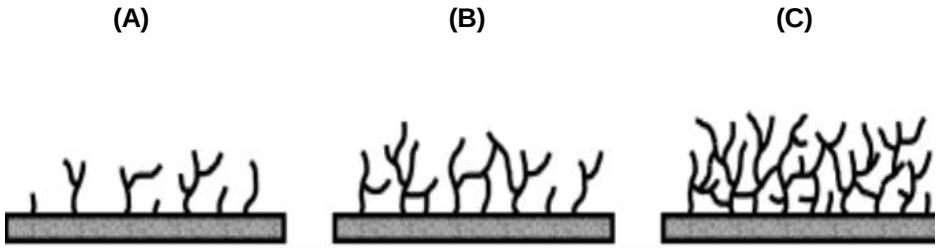

Figure 1.6 Schematic representation of the growing polymer chains during photografting with increasing irradiation time from (A) to (C).[81]

The effect of the concentration of initiator on the properties of the polymer-based monolith was firstly studied by Xie *et al*.[82], who mentioned that using a higher concentration of the initiator can increase the number of radicals resulting in an increase in the number of nuclei, which can lead to formation of small pores.

Increasing the percentage of the porogenic solvent system in the polymerisation mixture can lead to increase in pore volume, which can affect the rigidity of the polymer. A useful tool for preparation of a polymer-based monolith that can control the pore size without changing the chemical composition of the polymerisation mixture is the type and composition of the porogenic solvent system.[70] The polymerisation reaction starts from an initially homogeneous solution until the polymer precipitates, and further polymerisation and crosslinking continues both in the swollen nuclei and in solution.[83] As a rule, using a poorer solvent affects the solvation of the polymer chains leading to formation of large pores due to an earlier polymer phase separation,[60, 82] while if a good solvent is used, the phase separation happens later and this can lead to formation of small pores.[83]

There are many advantages of organic polymer-based monoliths since they contain micropores, which can provide the desired surface area, and macropores, which can allow a high flow rate at moderate pressures. Moreover, these polymeric monolithic materials are fritless, and they are covalently bonded to the inner walls of the capillary or microchip.[84] Another advantages of polymer-based monoliths are they can be

washed with caustic mobile phase, are stable over a wide range of pH values, and they are easy to prepare compared to silica-based monoliths because they are prepared in a single step by in situ polymerisation. Moreover, the desired length and shape to be exposed to the light source can be controlled easily by using electrical masking tape or foil, and this will help the fabrication of the monolith inside a microchip.[85]

However, it can be difficult to ensure the pores are large enough to reduce the backpressure, and that the mesopores are distributed over the desired size range. In addition, organic monolithic materials are not mechanically stable since they are affected by temperature and/or organic solvents causing shrinking or swelling and this can affect the performance of the monolith.[86, 87] Commonly, organic polymer-based monoliths are prepared on a small scale because the fabrication of a large size monolith is quite difficult. The reason for that is the unstirred nature of the polymerisation within the mould can cause a decrease in the capacity to dissipate the heat of polymerisation and creation of heterogeneity in the pore structure.[52, 88] Furthermore, polymer-based monoliths have low binding capacity, which is attributed to the low specific surface area. Although some attempts have been made to increase the surface area of organic monoliths, the fabricated monoliths in previous reports showed relatively low surface areas.[89, 90]

Porous polymer-based monoliths have found widespread use in many different applications such as liquid chromatography, solid phase extraction, and enzyme immobilisation in capillary and microfluidic chip formats.[65] This study will focus on the application of polymer-based monoliths in solid phase extraction. The history of using monolithic materials as sorbents is not very long. The first paper reporting the use of a porous polymer monolith for solid phase extraction was by Xie *et al*. in 1998.[89, 91] The porous poly (ethylstyrene-*co*-divinylbenzene) monolith was prepared using commercial 80 % divinylbenzene, 20 % ethylstyrene, and dodecanol with toluene as a porogenic solvent. The monolith was fabricated inside a threaded polyetheretherketone (PEEK) tube (20 mm × 1 mm i.d.) using thermal initiation at a temperature of 70 °C for 24 hours. The result showed that by increasing the percentage of divinylbenzene (crosslinking monomer) to ethylstyrene in the polymerisation mixture, the surface area was increased. Excellent properties of this fabricated monolith were demonstrated since it had excellent hydrodynamic properties (average

pore size of 6 µm) and a very high surface area (400 m^2 g^{-1}). Its performance was checked by preconcentration of polar organic compounds and quite high recoveries of about 85 % were achieved.

Lee *et al.* [92] have fabricated an organic monolith using glycidyl methacrylate (GMA), and trimethylolpropane trimethacrylate (TRIM). After fabrication of the poly (GMA-*co*-TRIM) monolith, protein G was immobilised on the monolith for preconcentration and capillary zone electrophoresis (CZE) of immunoglobulin G (IgG) from human serum. The monolithic material (1.5-2 cm) was fabricated inside the inlet end of a fused silica capillary (75 µm i.d. and 365 µm o.d.). The method was able to preconcentrate and clean up IgG from a human serum sample that was diluted to 500 and 65,000 times (figure 1.7). However, there was no true CZE separation since only one protein was investigated. The authors stressed that the fabricated organic polymeric monolith is applicable to preconcentrate any protein for which an antibody is available.

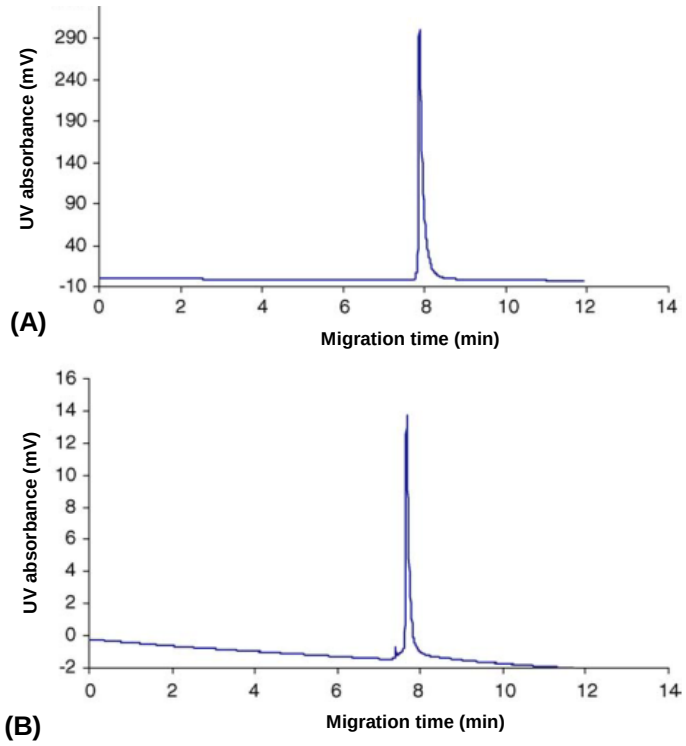

Figure 1.7 Electropherograms of on-line preconcentration-CE of IgG from human serum. Experimental conditions: 1.5 cm monolithic material inside a 64 cm (53 cm to detector) fused silica capillary (75 µm i.d.); 50 mM formic acid (elution buffer); 12.5 mM ammonium formate-formic acid (pH 7.6) separation buffer; 15 kV applied separation voltage; UV detection at 214 nm. (A) 500 times diluted human serum, and (B) 65,000 times diluted human serum.[92]

Later the same group fabricated a poly (butyl methacrylate-*co*-ethylene dimethacrylate) (BuMA-*co*-EDMA) monolith inside the inlet end of a polyvinyl alcohol-coated silica capillary, followed by coupling this hydrophobic monolith with the previous monolith via a zero dead volume union for on-line removal of IgG, extraction of standard proteins (lysozyme, cytochrome C, and trypsinogen A), and separation by CZE.[93] The coupled monoliths were equilibrated with 50 mM ammonium formate-formic acid (pH 7.6), followed by injection of the protein solution containing IgG for 50 min. The hydrophobic monolith was detached from the affinity

monolith (the protein G column) and mounted in the CE instrument. The monolith was washed with ammonium formate-formic acid buffer to remove unbound protein, and finally the preconcentrated proteins were eluted using 70 % ACN containing 0.1 % TFA. A good preconcentration and separation were obtained by this method, with RSD for peak area below 3 %, and 1 % for migration time. The authors suggested that this system could be a valuable means of sample preparation for preconcentration of low abundance proteins in a complex sample such as human serum and removal of high abundance proteins such as IgG, and human serum albumin (HSA). Although this work showed the possibility of coupling two types of organic polymeric monoliths (affinity and hydrophobic) for sample clean up and preconcentration, the technique required disconnection of the two monoliths before washing and elution of the preconcentrated proteins, which can cause loss of the preconcentrated proteins. Additionally, the technique would require affinity for a wide range of high abundance proteins.

Schley *et al.* [94] fabricated poly (styrene-*co*-divinylbenzene) (PS-*co*-DVB) monolith inside a fused silica capillary for both desalting and preconcentration of peptides and proteins (in 10 mm × 0.20 mm i.d. format), and for analytical separation (in 60 mm × 0.20 and 0.10 mm i.d. format). The fabricated monoliths were coupled with HPLC and the detection method was UV absorbance at 214 nm. The hydrophobic monolith showed its ability to preconcentrate and separate seven standard proteins, which were ribonuclease A, cytochrome C, lysozyme, transferrin, myoglobin, α-lactoglobulin B, and carbonic anhydrase. The effect of sample volume and concentration on the extraction recovery were investigated by injection of constant amounts of proteins dissolved in different volumes of water containing 0.050 % TFA (ranging from 1 to 100 µL). As can be seen in figure 1.8, reducing the concentration of the standard proteins by a factor of 100 accompanied with an increase in the injection of the sample volume did not affect protein recovery since there was no difference in the peak areas obtained for different concentrations and injection volumes.

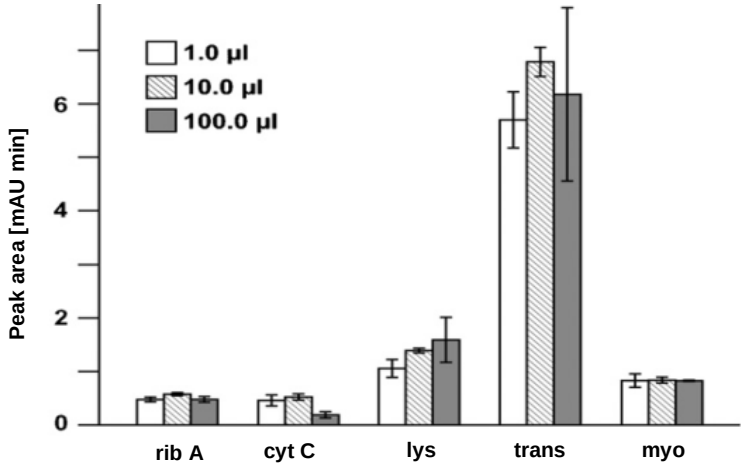

Figure 1.8 Preconcentration of a constant amount of proteins dissolved in different volumes of water containing 0.050 % TFA (1, 10, 100 µL). The plotted peak areas represent the average of two replicates.[94]

Extraction using organic monolithic material on a microfluidic device was first demonstrated by Yu *et al.*[95, 96] in 2001. The organic polymer monolith (7 mm long monolith) was fabricated within a simple straight microchannel (100 µm wide, 40 µm deep, and 6 cm long) of a glass microchip using photoinitiated polymerisation (UV irradiation at room temperature for 3 hours) in order to use it for on-chip solid phase extraction and preconcentration of small molecules, peptides, and proteins. Two types of organic polymer monolith were prepared in the chips. The first one was a hydrophobic monolith using butyl methacrylate with ethylene dimethacrylate, and the second one was ion-exchange (IE) using two monovinyl monomers, 2-hydroxyethyl methacrylate (HEMA) and [2-(methacryloyloxy)ethyl]trimethylammonium chloride (META) with ethylene dimethacrylate. Both polymeric monoliths were prepared using 2,2′-azobis(2-methylpropionitrile) (AIBN) as photoinitiator and a binary porogenic solvent, hexane and methanol. Both types of monoliths were able to preconcentrate a small organic acid (coumarin 519). Moreover, they were utilised to preconcentrate a recombinant green fluorescent protein (GFP), and a fluorescently labelled tetrapeptide. GFP was preconcentrated using the hydrophobic monolithic concentrator up to an enrichment factor of 1000 with elution of the protein using a 1:1 water/acetonitrile

mixture at a flow rate of 0.53 µL min^{-1} (figure 1.9). Although the fabricated hydrophobic and ion-exchange monoliths met the specific requirements for formation of macroporous monoliths (pore sizes were 19.5 and 13.2 µm, respectively), the specific surface areas of both fabricated monoliths were relatively low (0.7 and 1.3 m^2 g^{-1}, respectively).

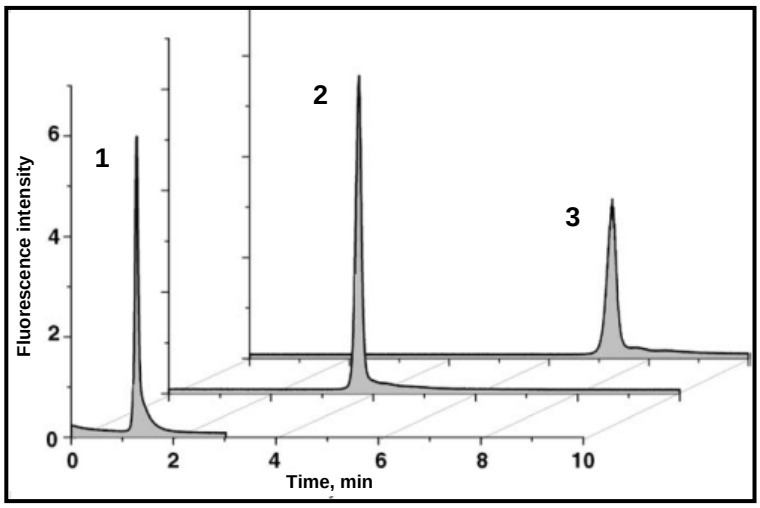

Figure 1.9 Elution of green fluorescent protein from hydrophobic monolithic concentrator. Conditions: loading 200 µL of protein solution in tris-HCl buffer solution (pH 8.0) containing 0.95 mol L^{-1} ammonium sulfate. The solution was pumped at a flow rate of 3 µL min^{-1}, elution with 1:1 acetonitrile/water at a flow rate of 3 (1), 1.03 (2), and 0.53 µL min^{-1} (3).[95]

Hua *et al.*[97] in 2011 fabricated a monolithic bed with two different surface chemistries by co-polymerisation of BuMA with META to form a monolith for solid phase extraction that supports anodal electroosmotic flow. The 1 mm long organic monolith (20 µm deep and 140 µm wide) was fabricated at the centre of a 3.5 cm long channel of a glass microchip, figure 1.10. The ends of the channel (20 µm deep and 56 µm wide) were sharp to reduce band-broadening effects. The microchip was coupled to electrospray mass spectrometry (ESI-MS) detection and its performance was checked by preconcentration of cytochrome C and myoglobin, as can be seen in figure 1.11,

which shows the ion electropherograms and mass spectra of the preconcentrated cytochrome C and myoglobin. However, the peak of the preconcentrated myoglobin was wider and significant tailing was observed, which required optimisation of the preconcentration procedure.

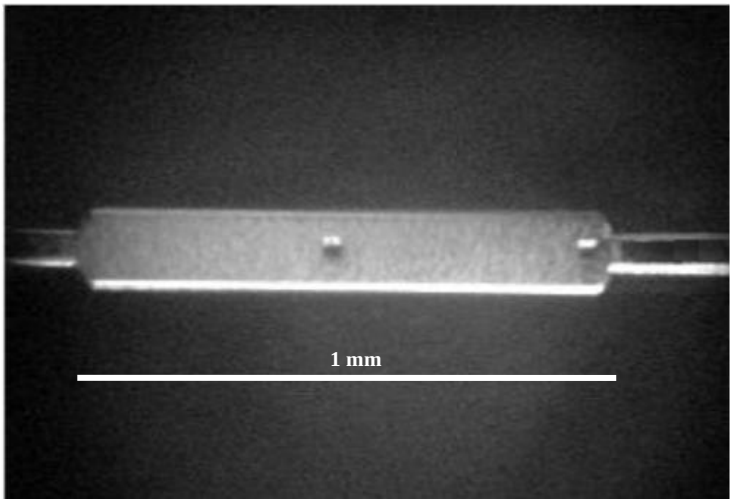

Figure 1.10 Optical micrograph of an enlarged monolith polymer bed (1 mm long), prepared in a 20 µm deep and 140 µm wide microchannel that has sharp edges.[97]

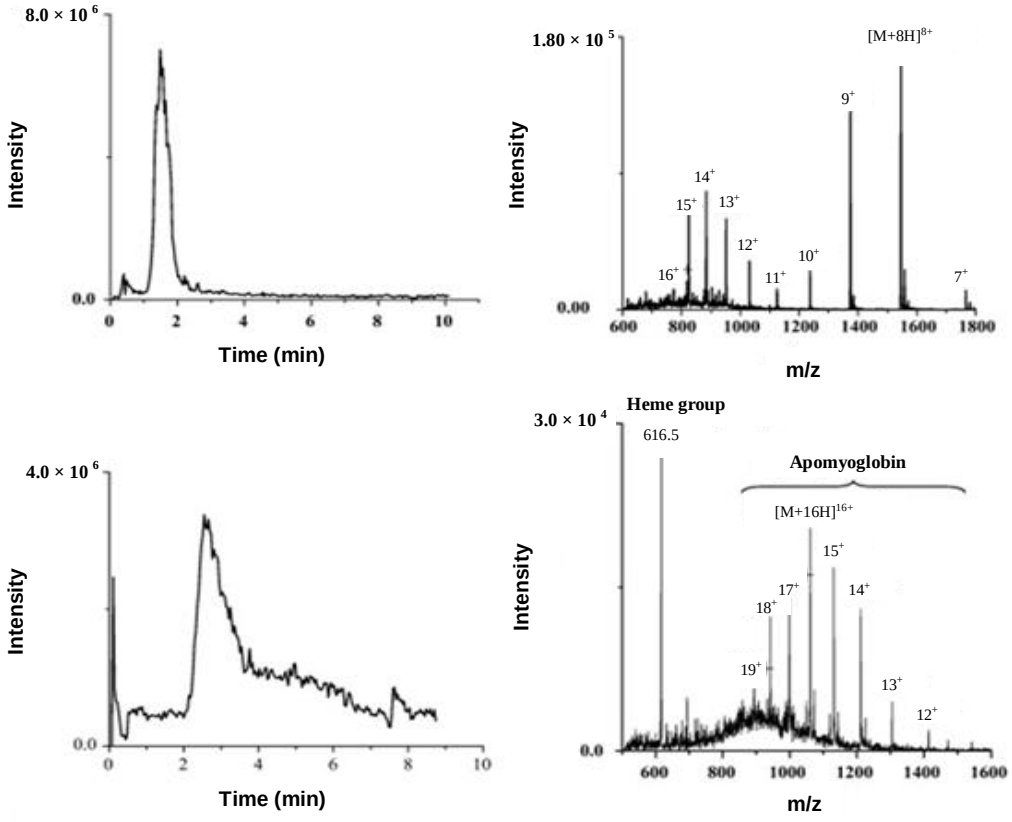

Figure 1.11 Total ion electropherograms and mass spectra of the preconcentrated cytochrome C (upper trace) and myoglobin (lower trace). Loading buffer (5 mM formic acid), and elution buffer (5 mM formic acid with 60% ACN). Samples were loaded and eluted electrokinetically with −2.5 kV at the sample reservoir and 3.2 kV on the electrospray tip.[97]

Li *et al.*[98] fabricated a poly (GMA-*co*-TRIM) monolith inside a channel of a glass microchip, which was fabricated using traditional photolithography and wet etching techniques. Figure 1.12 illustrates the extraction channel (2 cm long) containing the monolithic material and the injection arms (1.5 cm long). The width and depth of the channels were 100 µm and 25 µm, respectively. All flow in the microchip was carried out using a syringe pump (pressure driven).

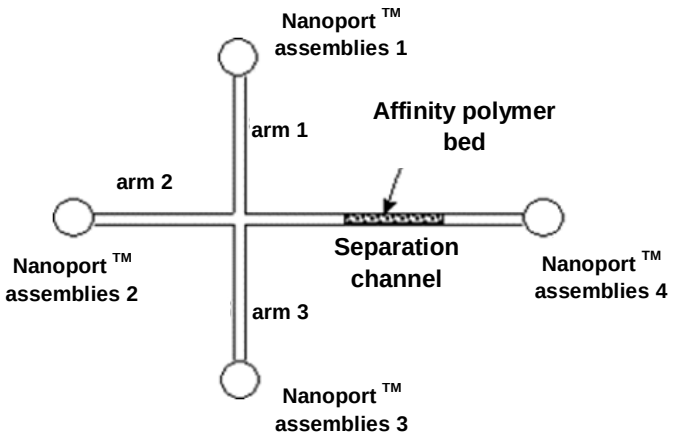

Figure 1.12 Schematic diagram of the glass microchip used for preconcentration of the protein, the extraction channel contained the polymeric bed, which was poly (GMA-*co*-TRIM) monolith.[98]

After fabrication of the monolith inside the extraction channel, it was derivatised with Cibacron-blue-3G-A, which is a triazine dye that has group specificity for some proteins such as albumin, dehydrogenase, interferon, lysozyme, and related proteins.[99] The extraction of proteins was carried out by injection of the protein sample solution using a syringe pump from nanoport assemblies 1 while the tubing connected to nanoport assemblies 3 was open and the others were closed. When the fluorescent sample was seen in arms 1 and 3 using a fluorescence microscope, nanoport assemblies 3 was closed while nanoport assemblies 4 was open. After preconcentration of the protein, the arms 1, 2, and 3 were flushed in order to wash the polymer bed. The fabricated Cibacron-blue-3G-A-modified polymeric monolith was tested to preconcentrate a standard protein (lysozyme). Cytochrome C and lysozyme were derivatised with fluorescein-5-isothiocyanate (FITC), and then the FITC-labelled lysozyme and FITC-labelled cytochrome C were preconcentrated individually using the fabricated device and fluorescence images were taken. Figure 1.13 (A) illustrates the fluorescence image of the preconcentrated FITC-labelled lysozyme, indicating the ability of the fabricated monolith to preconcentrate lysozyme, while figure 1.13 (B) shows no significant fluorescent signal was observed for preconcentration of FITC-labelled cytochrome C, which indicated that there was no significant adsorption of

cytochrome C. A mixture of unlabelled lysozyme and FITC-labelled cytochrome C was investigated and the fluorescence signal was similar to the detected fluorescent signal of FITC-labelled cytochrome C, figure 1.13 (C). The main drawback of this work is that the porous properties of the fabricated monolith were not reported. Furthermore, the fluorescent signal of the preconcentrated FITC-labelled lysozyme was high at the end of the polymer monolith, which indicates nonuniformity of the fabricated monolith. In addition, the benefit of the injection channel (arms 1 and 3) was not clear.

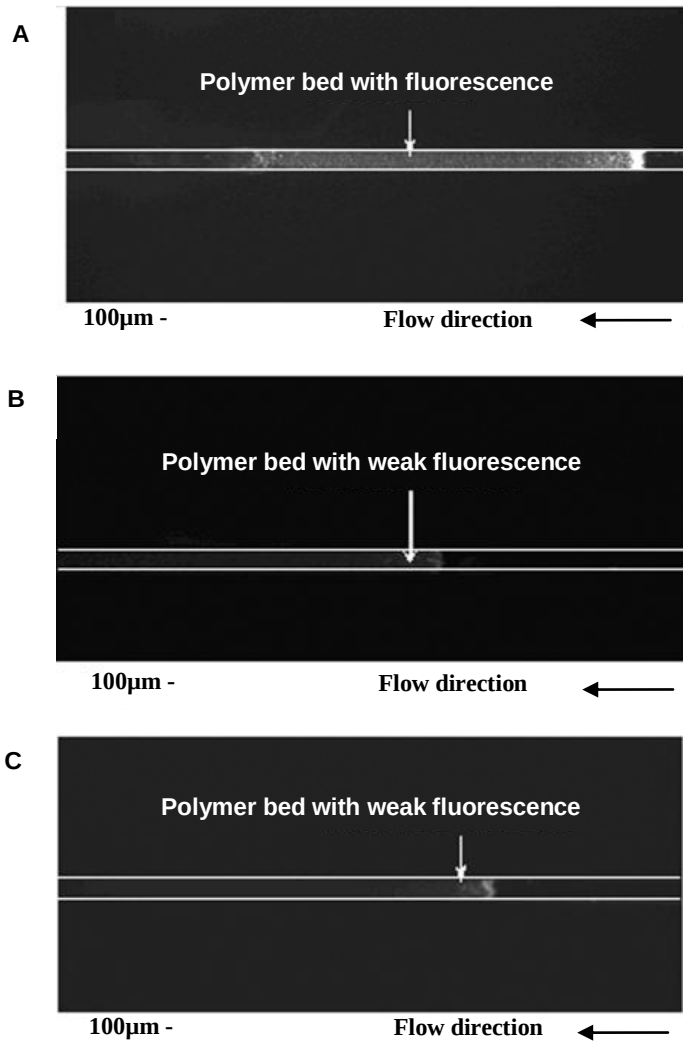

Figure 1.13 Fluorescence images of the polymer bed in a glass microchip: (A) the monolithic bed with captured FITC-labelled lysozyme, (B) capturing FITC-labelled cytochrome C, and (C) capturing unlabelled lysozyme and FITC-labelled cytochrome C mixture.[98]

1.4.2.2 Inorganic silica-based monoliths

Although polymer-based monoliths appeared earlier than silica-based monoliths, more research has been performed on the silica matrices.[100] So far, two methods have been used for fabrication of silica-based monoliths. The first method was introduced by Fields in 1996.[53] A fused silica column was filled with potassium silicate solution and heated at 100 ºC for 1 hour, followed by drying the column with helium for 24 hours at 120 ºC. The surface of silica-based monolith was modified using a 10 % solution of dimethyloctadecylchlorosilane in dried toluene, heated at 70 ºC for 5 hours. After modification, the column was rinsed and utilised for reversed-phase HPLC. Although this method can fabricate a continuous silica monolith, the morphology of the monolith is not homogeneous.[52] Another method for fabrication of silica-based monoliths is based on the sol-gel approach, as carried out by Minakuchi *et al*. [54] in the same year. This method can fabricate a silica-based monolith with a uniform structure high purity and better homogeneity.

The sol-gel approach involves fabrication of inorganic matrices through the formation of a sol, which is a colloidal suspension of solid species in a liquid and the gelation of the sol in order to form solid structures (wet gel) with spontaneous drying to remove the organic solvents and leave solid material.[100] Most sol-gel methods depend on using low molecular weight alkoxysilanes; for example, tetramethyl orthosilicate (TMOS), tetraethyl orthosilicate (TEOS), or methyltrimethoxysilane (MTMS).[101] Figure 1.14 shows the chemical structure of the common tetraalkoxysilanes used for the fabrication of silica-based monoliths.

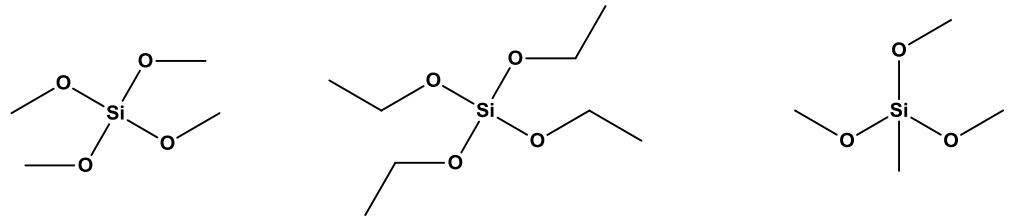

Figure 1.14 The chemical structure of the common tetraalkoxysilanes used for fabrication of silica-based monoliths.

The preparation of monolithic silica using the sol-gel approach involves three steps; the first step is hydrolysis of an alkoxysilane, followed by condensation of the hydrated silica, and finally the polycondensation reaction in order to form cyclic oligomers.[102] The preparation of the silica-based monolith is performed in the presence of a water-soluble polymer such as polyethylene oxide (PEO) acting as a porogen to form the macropores and micropores in the silica gel, and a catalyst, which can be an acid catalyst (such as acetic acid or nitric acid) [103] or a base catalyst (such as N-methylimidazole or dimethylaminopyridine) [104] or a binary catalyst, acid and base in sequence.[105,106] The hydrolysis of the alkoxysilane precursor (or its alkyl/aryl derivative) produces the silanol groups (Si-OH). This is followed by water or alcohol condensation to produce polycondensed species containing siloxane linkages (-Si-O-Si-) between two silane molecules, forming a three-dimensional network of sol-gel polymer.[107] The mixture is commonly stirred at 0 ºC for 30 min and then the homogeneous solution is poured into a mould and allowed to react at an elevated temperature.[108] A three-dimensional network will be created when the hydrolysis and polycondensation reactions are completed.[52] The resulting monolithic silica is treated with a basic environment, produced by thermal decomposition of urea or ammonium hydroxide solution at elevated temperature to tailor the mesopore structure. Figure 1.15 shows the SEM micrograph of the silica-based monolith showing the high porosity of the monolith. Silica-based monoliths consist of relatively large through-pores, which are important for fast flow and can provide high column efficiency, and small-sized skeletons, containing the mesopores which give high surface area.[109]

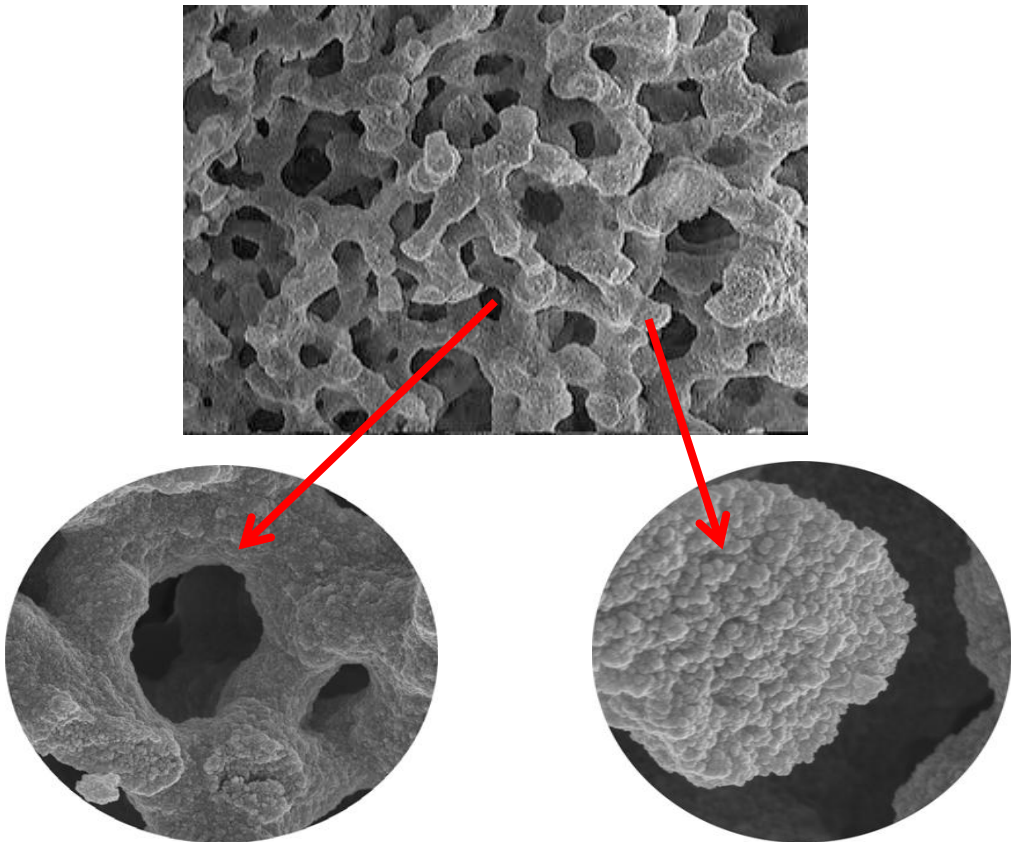

Figure 1.15 SEM micrograph of the porous structure of a silica-based monolith.[110]

The surface of the silica monolith can be easily derivatised with many functional moieties leading to additional efficiency and selectivity.[31] Modification of the surface of the silica-based monolith has been carried out by bonding the silica surface with another chemical species in order to get the desired selectivity for HPLC column or SPE sorbent. The most common reaction for derivatisation of the silica surface with chemical species is organosilanisation, which is based on using a derivatisation reagent.[111] The modification of the silica surface commonly occurs in the mesopores (2-50 nm) since the mesopores are more accessible for the derivatisation reagent as well as for the analytes. In contrast, micropores (>2 nm) are inaccessible and the silanol groups in these pores cannot be modified because they are blocked by the bonded moieties in the mesopores,[31] as can be seen in figure 1.16.

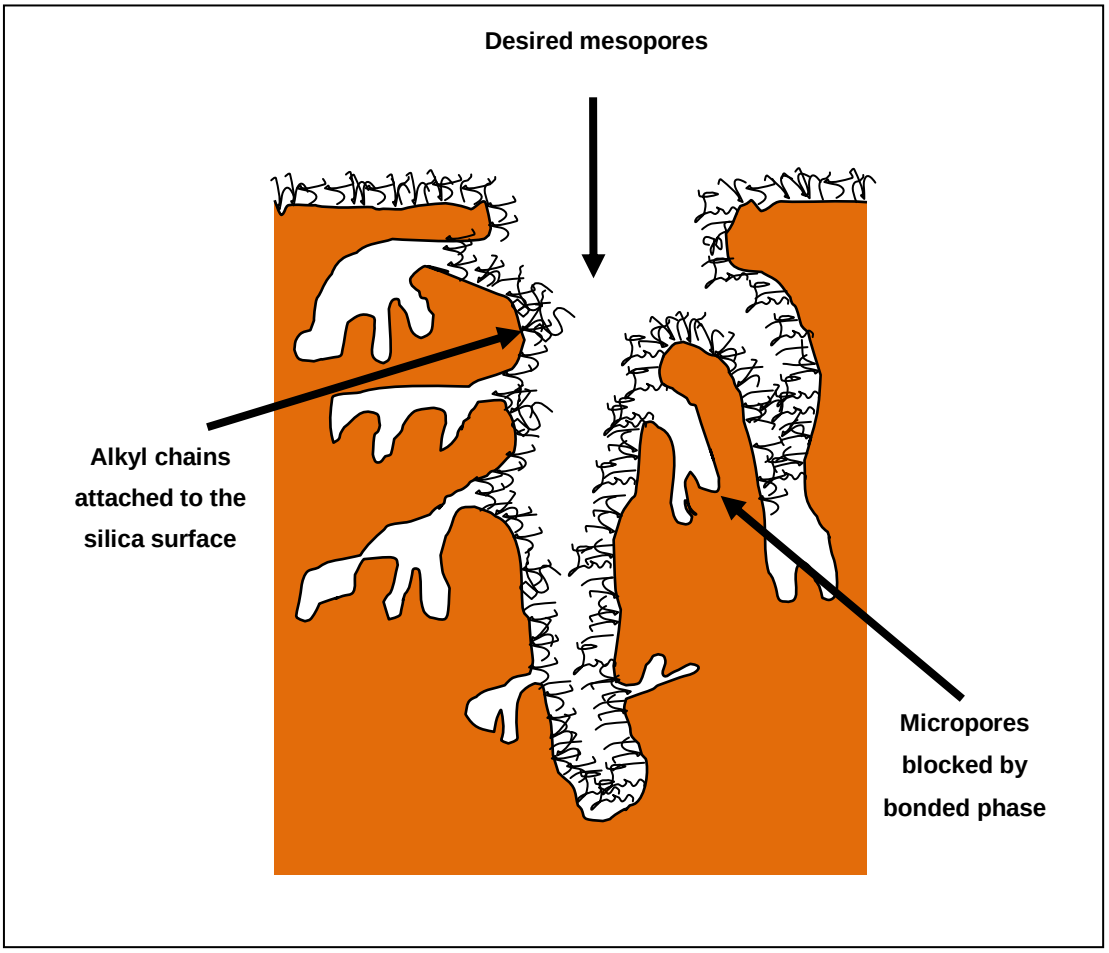

Figure 1.16 Schematic diagram shows the porous silica-based surface, showing the inaccessibility of some micropores.[31]

Some of the silanol groups in the mesopores stay without modification. If the attached organic moieties are small groups, their movement is restricted and the neighbouring silanol groups are not blocked, while if the attached organic moieties are large, such as octadecyl groups, then their movement blocks the neighbouring silanol groups and prevents other organic moieies from reaching these silanol groups thus having a number of free silanol groups.[31] These free silanol groups have a negative effect on separation and extraction because they can cause a second ion-exchange interaction between the free silanol groups and the analytes. In chromatography, this interaction can cause tailing peaks and decrease the resolution of separation, while the effect of the free silanol groups in SPE is that they can retain the polar functional groups and make elution more difficult.[112]

In order to decrease the effect of the secondary interaction, the number of free silanol groups needs to be decreased. This can be performed by using a second "end capping" reaction, which involves bonding smaller silane-type molecules such as trimethylchlorosilane (TMCS), or hexamethyldisilazane (HMDS) between the larger bonded moieties.[113]

Conditioning of the modified silica surface before loading the sample solution is important for many reasons. The most common bonded material is octadecylated silica sorbent, and before conditioning, the sorbent (in its dry form), the bonded moieties in the octadecyl bonded phase material are completely randomly oriented on the surface of the sorbent. If the sample solution is applied, the environment surrounding the bonded moieties would be highly polar and this environment is not compatible with octadecyl groups. As can be seen in figure 1.17 (A), if the octadecyl bonded phase sorbent is not conditioned, the alkyl groups will be aggregated between bonded groups in order to minimise exposure to the polar medium by forming clusters between them, and this can cause a decrease in the efficiency of the sorbent and decrease the extraction recovery of the target analytes. To solve this problem, the organic groups need to be conditioned with an organic solvent such as methanol. In this situation, the octadecyl bonded phase will be less aggregated, and ready for the interaction with the sample, figure 1.17 (B). The ideal situation happens when octadecyl bonded silica sorbent is treated with a solvent less polar than methanol such as acetonitrile or tetrahydrofuran, figure1.17 (C). In this case, the octadecyl bonded phase will be more opened and fully condititioned. Therefore, the selection of the conditioning solvent is important, which depends on the type of the bonded organic moiety.[28, 31, 114]

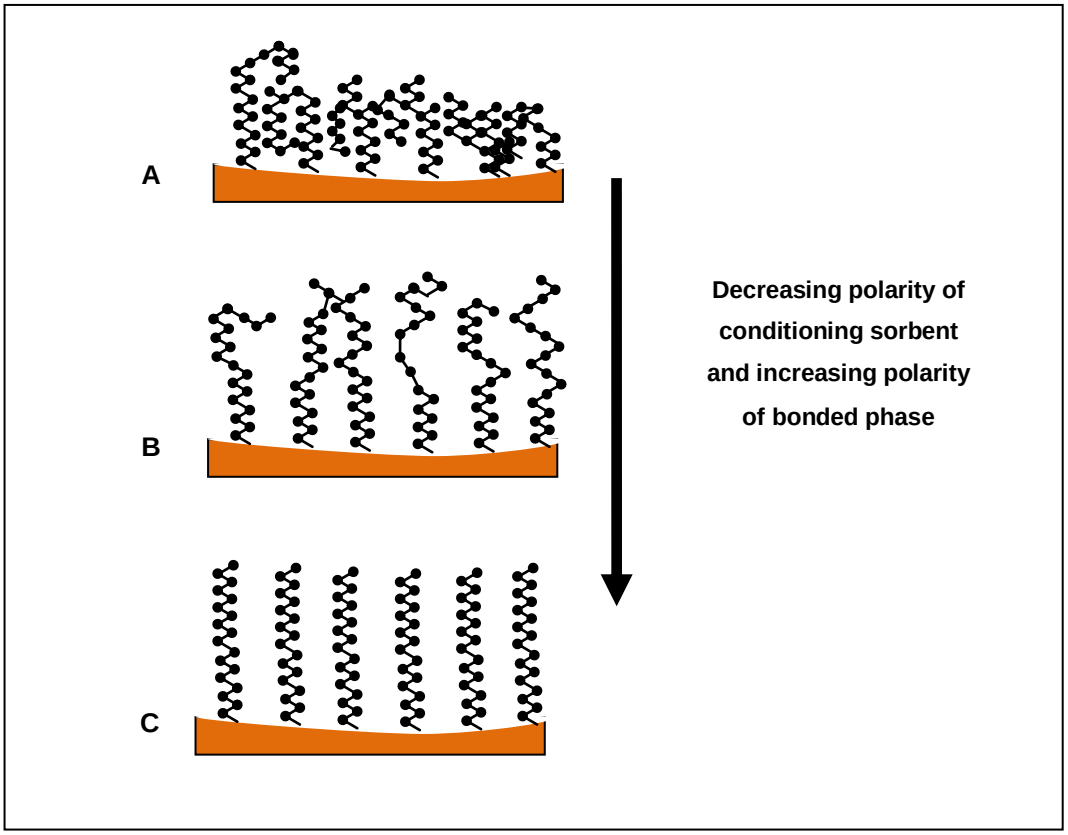

Figure 1.17 Schematic diagram showing the effect of conditioning step on octadecyl bonded silica: (A) without conditioning, (B) partially conditioned, and (C) fully conditioned.[31]

Porous inorganic silica-based monolithic materials can overcome the drawbacks of polymer-based monoliths since they have high mechanical strength, relatively high thermal stability, and high porosity.[115] Moreover, they are not affected by organic solvents in the same way as polymer-based monoliths, which can shrink or swell in the presence of organic solvents.[116, 117] Silica-based monoliths contain a distribution of both macropores that can increase the liquid flow through the monolith without increasing the backpressure, and mesopores that can increase the surface area giving a good interaction with analytes and maximising the loadability of the sorbent.[35, 118, 119] In addition, the surface of a silica-based monolith contains silanol groups (Si-OH) that can be used for immobilisation of different functional groups, and the attachment of groups on the silica surface is easier than on an organic polymer support since it has a high number of crosslinking bonds which require hours to reach equilibrium for surface activation.[120]

However, there are some disadvantages of silica-based monoliths; for example, the monolithic silica columns should be prepared and chemically modified independently, which means preparation of silica-based monoliths is time consuming and difficult to control, leading to poor reproducibility. Moreover, the monolithic silica rods need to be wrapped in column materials, such as PEEK, when they are prepared in a mould.[55] Additionally, fabrication of a sol-gel monolith directly inside a microchip is difficult because the location of the monolith inside the extraction chamber cannot be defined since the preparation of the silica-based monolith depends on using thermal initiation. Another negative aspect of the use of a sol-gel monolith in microchips is the shrinkage that happens as the monolith is formed during the condensation reaction, which can cause voids between the silica network and the microchip wall, resulting in a reduced surface area for sample adsorption and can cause the silica monolith to crack.[121, 103] The main problem with using silica-based monoliths is that silica is not stable at high pH values.[25]

Synthetic silica-based monolithic materials have been introduced as porous monolithic separation media in HPLC, GC, and CEC.[105, 122] In addition, they have been used as immobilised enzymatic reactors [123] and as sorbents in solid phase extraction.[49] Although silica-based monoliths are becoming increasingly popular as sorbents, there are few papers describing their use as materials for protein extraction; therefore, the use of the silica-based monolith as a sorbent in different applications will be reviewed.

In 2002, Landers *et al.* [124] fabricated different silica matrices onto a microchip for use as a sorbent for DNA. The silica matrix was fabricated using silica beads (15 µm), silica-based monolith using a sol-gel process, or a combination of silica beads and monolithic silica material, which was fabricated by adding the silica beads to the sol-gel precursor mixture before the condensation reaction. Figure 1.18 (A) and (B) shows images of the microchamber packed with silica beads. The extraction recovery of DNA using the silica beads was as high as 57.1 %; however, the DNA extraction was highly irreproducible (standard deviation 43.1 %). Figure 1.18 (C) shows the silica sol-gel monolith that was fabricated using TEOS, PEO, and an aqueous solution of nitric acid. The monolithic silica material was cracked and the extraction recovery of DNA was very low (33.2 %). The best extraction recovery of DNA was achieved

using the silica bead/sol-gel hybrid matrix (70.6 %), figure 1.18 (D) and (E), and with acceptable reproducibility (standard deviation < 3%).

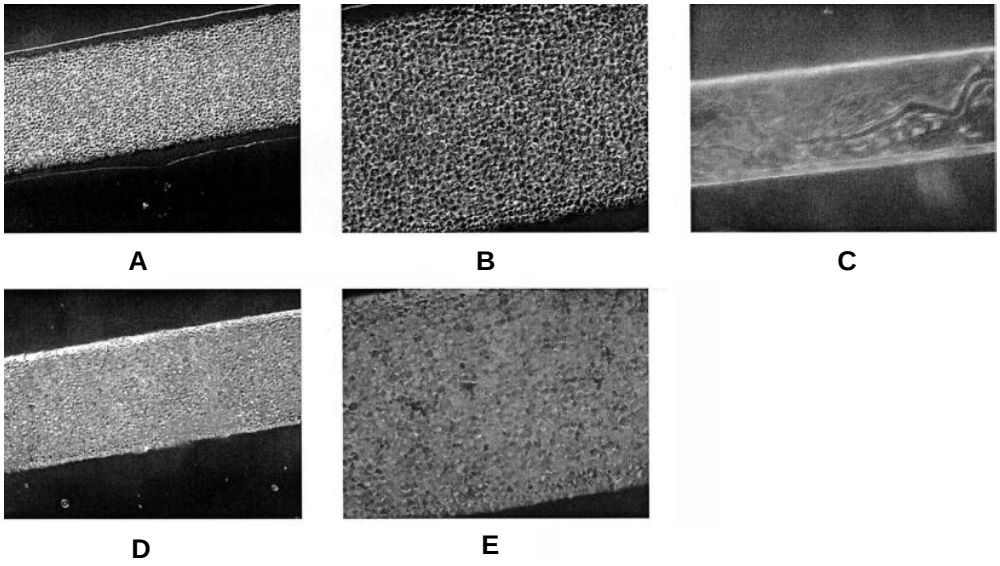

Figure 1.18 Silica materials in microfabricated chambers: (A) silica beads, (B) silica beads at 10× magnification, (C) silica-based monolith using sol-gel, (D) two-step silica beads and sol-gel, and (E) two-step silica beads and sol-gel at 10× magnification.[124]

Miyazaki *et al.* [125] in 2004 developed a monolithic silica extraction tip for the analysis of peptides and proteins. The silica-based monolith was fabricated using TEOS, PEO with average molecular mass 100,000 g mol^{-1} as a porogen, and an aqueous solution of nitric acid. After fabrication, the monolithic silica rod was cut and fixed inside a 200µL pipette tip using supersonic adhesion. Following this, the silica surface was chemically modified with either an octadecyl group in order to make it hydrophobic and enrich proteins, or the silica surface was coated with a titania phase and used for the concentration of phosphorylated peptides. The results show that the C_{18}-bonded monolithic silica extraction tip has the ability to purify different standard proteins varying in molecular weight up to 40000 Da; however, the extraction of proteins

decreased with increasing molecular weight of the proteins. In addition, the fabricated monolith was not optimised nor its porous structure characterised.

In 2006, Wu *et al*.[126] fabricated a glass microchip containing a TMOS-based silica-gel monolith for DNA extraction from clinical samples and from bacterial colonies. The problem of shrinkage of the inorganic monolithic material was minimised by treating the inner walls of the glass microchip with a 1 M sodium hydroxide solution (NaOH) for 12 hours to hydrolyse the walls of the glass microchip before fabrication of the monolith. This allowed the surface to participate in the condensation reaction resulting in the attachment of the silica skeleton to the glass walls. The average extraction recovery of DNA using the underivatised silica monolith was 85%. However, shrinkage of the silica monolith was not completely avoided and the monolith contained large interstitial voids. In addition, pore blockage of the monolithic material was observed during repeat extraction on a single device, as confirmed by a decrease in the extraction recovery.

In 2008, Xu and Lee [127] fabricated a hybrid organic-inorganic silica-based monolith using two monomers that were TMOS and 3-mercaptopropyltrimethoxysilane (MPTS) to yield thiol groups. This was followed by oxidation of the hybrid silica monolith using hydrogen peroxide (H_2O_2) for 24 hours at room temperature to derivatise mercapto groups into sulfonic acid groups for use in cation-exchange purification. The effect of the amount of PEO in the polymerisation mixture was investigated. Increasing the amount of PEO resulted in changing the final monolith from opaque to transparent, and the macropores of the monolith, which were studied by SEM observations, were decreased (figure 1.19). The performance of the mercapto-modified monoliths was tested for in-tube microextraction of four anaesthetics (procaine, lidocaine, tetracaine, and bupicaine) in spiked human urine, and the extraction recovery was greater than 92%.

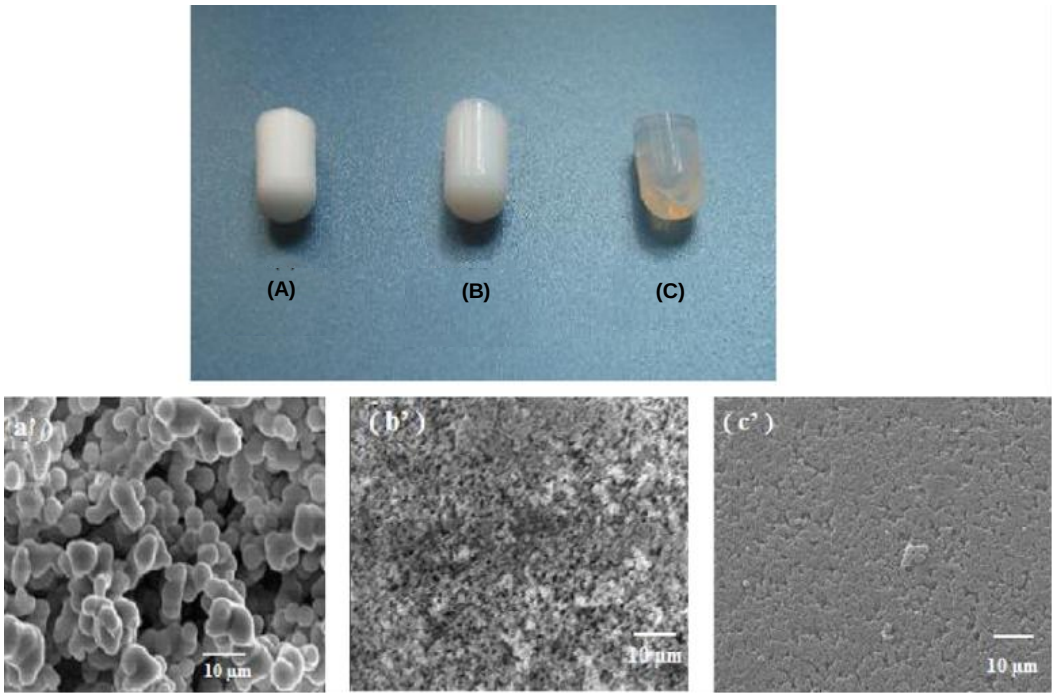

Figure 1.19 Photograph and SEM micrographs of silica-based monoliths prepared using different PEO content: (A) 0.1 g, (B) 0.2 g, and (C) 0.4 g.[127]

In 2010, Nema *et al.*[49] fabricated a silica-based monolith using TMOS and PEO (MW 10,000 g mol^{-1}) in the presence of 0.01M acetic acid as a catalyst. A monolithic silica rod was fixed in a 2 mL syringe installed in SPE vacuum manifold (figure 1.20). The unmodified silica-based monolith with ionisable silanol groups was used in off-line cation exchange for preconcentration of polar analytes (epinephrine, normetanephrine, and metanephrine) from a urine sample. The technique was simple and robust. Although the extraction recovery of metanephrine was approximately 105 %, the extraction recoveries of epinephrine and normetanephrine were approximately 60 % and further optimisation is required.

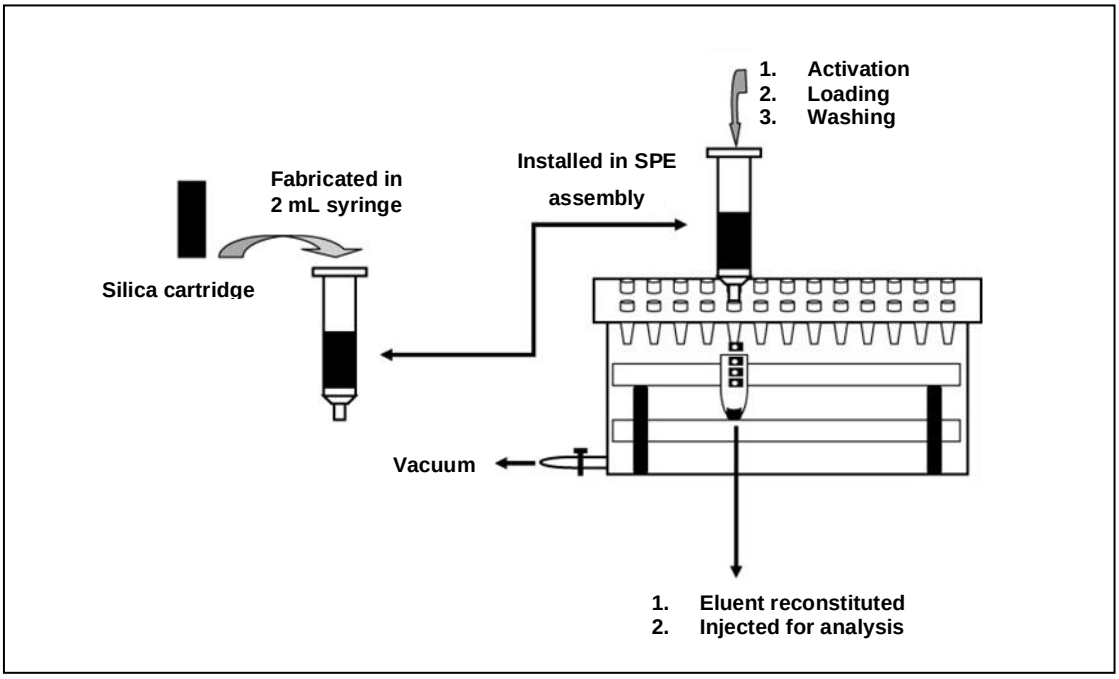

Figure 1.20 Extraction steps using non-modified silica monolith on SPE manifold.[49]

Based on the literature, each monolith has its own individual advantages and disadvantages, as indicated in the summary of previous monolith research in table 1.1, which shows comparison data for organic and inorganic monoliths.

Comparison	Organic monoliths	Inorganic monoliths
Simple preparation method	Yes.	Yes.
Preparation time	Short, since the fabrication of the organic monolith is a single-step process.[66, 67]	Long, since they should be prepared and chemically modified independently.[55]
Option for stationary phase	They can be fabricated by using a wide range of monomers and crosslinking agents enabling the porous properties of the monolith to be controlled.[75]	No.
Surface modification of the monolith	They have a high number of crosslinking bonds, which require hours to reach equilibrium for surface activation.[120]	They can be easily derivatised with many functional moieties leading to additional efficiency and selectivity.[31, 120]
Fabrication inside microchip	Easy, since the initiation of a polymerisation reaction can be performed by photoinitiation (light).[69, 70]	Difficult, since the location of the monolith inside the microchip cannot be defined because their fabrication depends on using thermal initiation.[103, 121]
Surface area	Although some attempts have been made to increase the surface area of organic monoliths, the fabricated monoliths in previous reports showed relatively low surface areas.[89, 90]	High.[35, 118, 119]
Permeability	Moderate.[86, 87]	High.[35, 118, 119]
Affected by temperature and/or solvents	They are affected by temperature and/or organic solvents causing shrinking or swelling.[86, 87]	They have high mechanical strength, and relatively high thermal stability.[115]
Stable over the whole pH range	They are stable over a wide range of pH values.[282]	They are not stable at high pH values.[25]
Use for protein extraction	They have found widespread use in protein extraction in capillary and microfluidic chip formats.[65]	Few papers describing their use as materials for extraction.[49]
Protein extraction efficiency	High.[93, 94]	The ability to purify different standard proteins varying in molecular weight up to 40 kDa.[125]

Table 1.1 Summary of the advantages and disadvantages of organic and inorganic monoliths based on literature review.

1.5 Reduction and alkylation of proteins

Disulphide bonds play an important role in the stabilisation of the structure of proteins, maintaining some three-dimensional structures, and have a protection role for bacteria.[128] At least 5 % of the known protein structures contain disulphide bonds between cysteine residues.[129] They are formed between the thiol groups of cysteine residues in the endoplasmic reticulum by oxidation.[128] There are two types of disulphide bonds; namely, intrachain disulphide bonds, which are formed between two cysteine residues within the same protein chain, and interchain disulphide bonds, which are formed between two cysteine residues of individual chains of the same protein or between two cysteine residues of distinct proteins.[130] Figure 1.21 shows a schematic representation of human insulin that contains three disulphide bonds, one intrachain [A6-A11], and two interchain [A7-B7] and [A20-B19].[131]

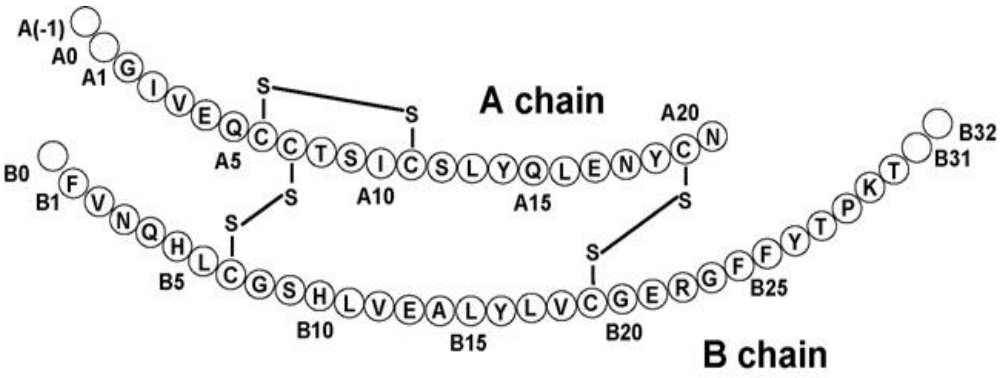

Figure 1.21 Schematic representation of human insulin where the A chain and B chain are joined by disulphide bonds.[131]

The structural analysis of proteins by mass spectrometry depends on the measurement of protein fragments produced by protein digestion, carried out by using proteolytic enzymes such as trypsin to cut proteins at specific locations. The ability of enzymes to digest proteins could be decreased if the protein contains disulphide bonds that can keep the protein folded, and hinder the digestion of proteins by blocking access of proteolytic enzymes.[132] Figure 1.22 illustrates the effect of disulphide bonds on the digestion of lysozyme, which contains four disulphide bonds, showing that the

peptides are still linked by the disulphide bonds and lysozyme is not digested completely, resulting in reducing the amount of protein sequence coverage that can be obtained.

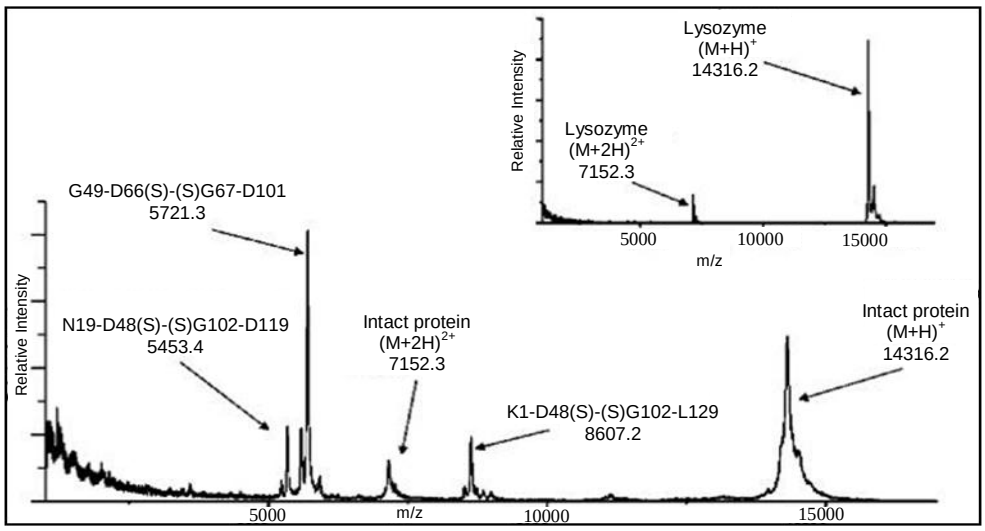

Figure 1.22 MALDI-TOF mass spectra of lysozyme before (inset) and after digestion. The detected peptides are attributed to peptides formed from digestion while the intrachain disulphide bonds are still intact.[133]

Breaking of the disulphide bonds can make a protein unfold and this results in improving the proteolytic digestion of proteins by making the specific location accessible to the enzyme. As a result, the protein sequence coverage will be increased and facilitate their identification by mass spectrometry. Therefore, it is important to assist the unfolding of polypeptides by reduction of disulphide bonds.[133, 134]

Cleavage of the disulphide bonds can be carried out by chemical reduction of the disulphide bonds by adding a reducing reagent to the protein. Common reducing reagents are dithiothreitol (DTT), 2-mercaptoethanol (BME), and several phosphines.[134] The reaction of the first two reagents depends on the thiol-disulphide exchange reaction, and the excess amount of these two reducing reagents should be

removed because they can react with many derivatisation reagents for thiol groups. On the other hand, phosphines are not stable in solution and they have an irritant odour.[134] Tris-(2-carboxyethyl)phosphine hydrochloride (TCEP) was used as a reducing reagent for disulphide bonds in 1969 by Levison *et al.* [135]; however, it was not used again until Burns and coworkers found a suitable synthetic procedure in 1991.[136]

Many studies have focused on using TCEP for reduction of the disulphide bonds in proteins because it has many advantages over other reducing reagents. For example, it has the advantages of being odourless, which eliminates the need to do the reaction within a fume hood, and safe to handle. In addition, it reacts quickly with disulphide bonds over a wider pH range (1.5-8.5) than DTT, it is highly stable in aqueous solution and buffers, it cannot form covalent interactions with cysteine residues, and it is more resistant to oxidation in air.[137, 138] Moreover, TCEP is water-soluble, not reactive to other functional groups in proteins, and thermostable at high temperature, while DTT could be oxidised within seconds.[139-141] Another major advantage of this reducing reagent is that it does not need to be removed before adding the alkylation reagents, since it does not react with them.[142, 143]

The free thiol groups are active and can be oxidised with other thiol groups resulting in reforming of the disulphide bonds; therefore, it is important to block them by an alkylation reaction.[133] Common suitable alkylating reagents are vinylpyridine (VP), iodoacetamide (IAA), iodoacetic acid (IA), and iodoethanol (IE). The most popular procedures have utilised IAA for the alkylation reaction since it is odourless and therefore not necessary to do the reaction in a fume hood, in contrast to other alkylation reagents, such as VP, that have a pungent odour and are air sensitive.[143, 144]

There are a multitude of procedures for reduction and alkylation of proteins, which are performed in two steps. The reduction reaction involves mixing the reducing reagent with the protein sample dissolved in an appropriate solvent in a container, which could be a test tube, and incubating at a specified temperature for a specified time in order to improve the reduction process. Commonly, the conditions for reduction of disulphide bonds range in time from 30 min to 24 hours, and the temperature of the solution ranges from 25 to 60 ºC.[133] This is followed by alkylation of the thiol groups with an alkylating reagent since they are highly reactive and can oxidise with other thiol

groups. The alkylation step involves adding the alkylating reagent to the reduced protein and incubating it at a specific temperature. In 2006, Hale *et al.*[145] invented a novel composition and method for reduction and alkylation of lysozyme in one step for one hour at 37 ºC. The composition of the mixture was a combination of a volatile reducing reagent (triethylphosphine), a volatile alkylating reagent (iodoethanol), and a volatile solvent (acetonitrile) to dissolve the reagents and lysozyme.

So far, there has been no work focusing on fabrication of monolithic materials (organic or inorganic) for the purpose of reduction of proteins. Therefore, the purpose of this work is to review recent research into reduction and alkylation of proteins inside a microfluidic device.Recently efforts have been made to fabricate microfluidic devices such as digital microfluidics for proteomic sample preparation. In 2009, Luk and Wheeler [146] fabricated a droplet-based (digital) microfluidic device for reduction,

alkylation, and enzymatic digestion of proteins. The digital microfluidic device consisted of two glass plates, an unpatterned indium tin oxide (ITO) coated glass (top plate) and a patterned bottom plate. The droplets were sandwiched between the two plates and actuated by applying electric potentials between the top electrode and sequential electrodes on the bottom plate. Figure 1.23 (A) shows the digital microchip used for reduction of the disulphide bonds, alkylation of the sulfhydryl groups, and digestion of the reduced and alkylated protein. A droplet of protein solution was dispensed and mixed with a droplet with the reducing reagent, which was 10 mM TCEP, followed by incubation for 30 min, figure 1.23 (B). The reduced protein was then reacted with a droplet of the alkylating reagent, 12 mM iodoacetamide for 2 min, figure 1.23 (C). The reduced and alkylated protein was merged with a droplet containing enzyme (trypsin) for protein digestion and the microchip was incubated for 60 min, figure 1.23 (D), and (E). All the incubation was carried out in room temperature.

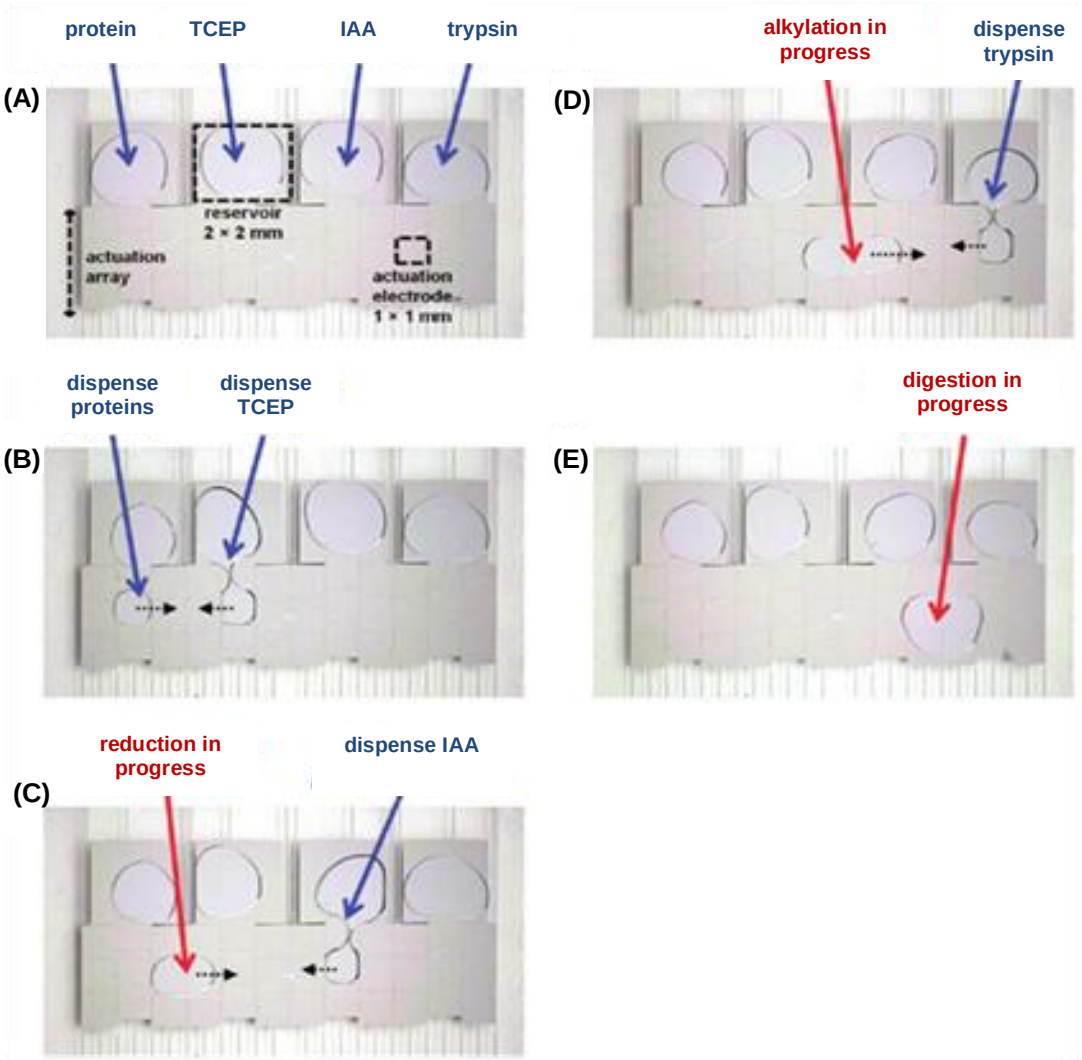

Figure 1.23 Digital microfluidic device used for proteomic sample processing (A). Droplets of protein and 10 mM TCEP are mixed and incubated (B). The sample droplet is mixed with a droplet of 12 mM IAA and incubated again (C). The sample droplet is mixed with a droplet of trypsin (1:5 enzyme to protein ratio w/w) (D), and then incubated a final time (E).[146]

The ability of the digital microfluidic device to reduce and alkylate protein was tested using insulin. Figure 1.24 shows a comparison between the MALDI-TOF mass spectra of the non-processed insulin, which shows the singly and doubly charged ions of insulin, figure 1.24 (A), reduced insulin in which the two chains are separated, figure 1.24 (B), and the reduced and alkylated insulin with iodoacetamide, which adds 57 Da

to each thiol group, 1.24 (C). In addition, the ability of the fabricated device to reduce, alkylate, and enable enzymatic digestion of proteins was checked using larger proteins (BSA), figure 1.24 (D), and lysozyme, figure 1.24 (E). The procedure was fast and easy to use; however, the main problems with this type of microfluidic device are droplet evaporation since the procedure involves multiple incubation steps, which was solved by incubation of the microchip in a humidified chamber during all incubation steps, and non-specific adsorption, which was solved by using adhesion-reducing additives.

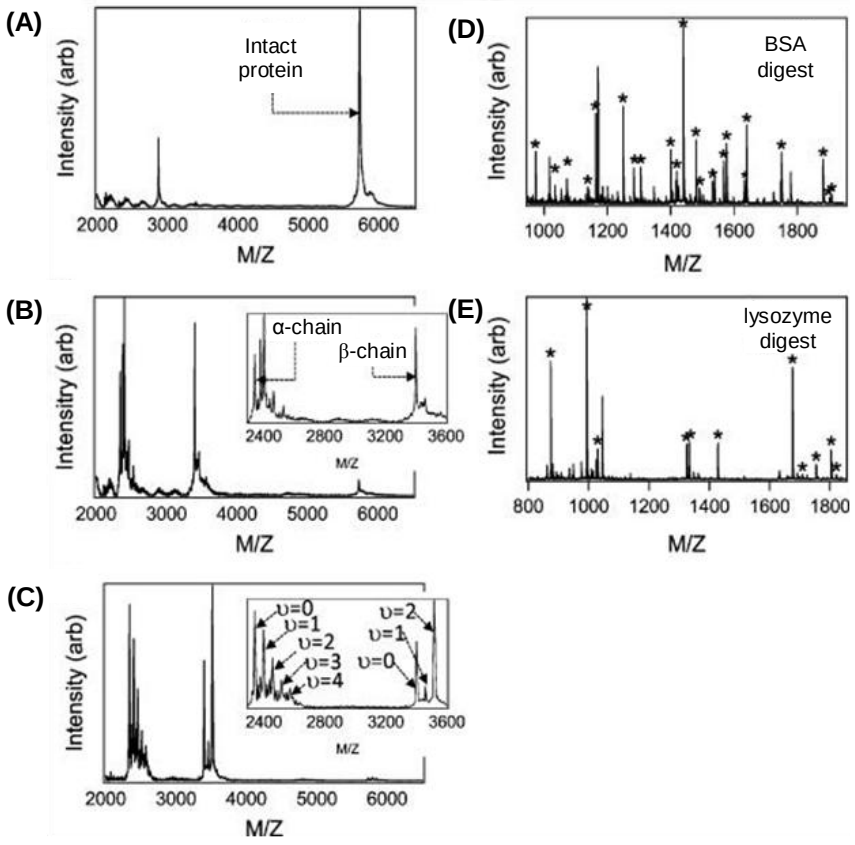

Figure 1.24 MALDI-TOF mass spectra of the samples prepared by DMF-driven processing: (A) non-processed insulin, (B) reduced insulin, (C) reduced and alkylated insulin, where *υ* means the number of the alkylated thiols, and (D, E) BSA and lysozyme after reduction, alkylation, and digestion. Asterisks denote peptides identified by Mascot.[146]

Following this work, Garrell *et al.*[147] in 2010 fabricated a droplet-based digital microchip for proteomic sample processing. The fabricated microchip was used for disulphide bond reduction, alkylation, enzymatic digestion, crystallisation with MALDI matrix, and in-situ MALDI-TOF analysis. The fabricated device (30×15×0.5 mm) was formed from two plates. The top plate had a single large electrode (ITO ground electrode) while the bottom plate has individually addressable electrodes, (figure 1.25). The droplets were sandwiched between the two plates and moved by applying potentials between the electrodes in the top and bottom plates.

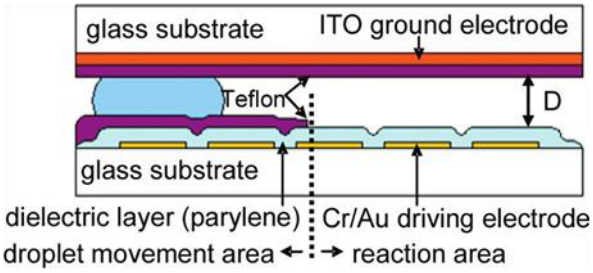

Figure 1.25 Schematic cross-section of a digital microfluidic device consisting of two plates. The top plate has a single ITO electrode and Teflon-AF coating while the bottom plate has an array of electrodes under a dielectric layer and Teflon-AF coating. The droplet is sandwiched between the two plates, which are separated by gap (D).[147]

Different proteins (carbonic anhydrase, cytochrome C, ubiquitin, insulin, lysozyme, and BSA) were utilised to test the performance of the fabricated device. A droplet of protein solution was mixed with the reducing reagent, 5 mM TCEP, and incubated for 5 min at room temperature. A third droplet containing the alkylating agent, 5 mM N-ethylmaleimide (NEM), was mixed with the reduced protein and incubated for 5 min at room temperature. A droplet of the reduced and alkylated protein was mixed with a droplet of 0.5 μM trypsin and incubated at 37 °C for 4 hours, followed by mixing with a droplet containing α-cyano-4-hydroxycinnamic acid as matrix, and the top plate was

removed manually to accelerate drying of the droplet in air. Finally, the bottom plate was placed into a MALDI target and inserted into a mass spectrometer for analysis. Generally, the method was fast, simple, and used smaller amounts of sample and reagents compared with conventional techniques for proteomic sample preparation. However, the main problem of this procedure is droplet evaporation, since the digestion process was performed at an elevated temperature (37 °C). Additionally, when the top plate was removed to expedite crystallisation, some of the droplets could cling to the top plate, which could cause partial loss of the sample.

Figeys *et al.*[148] in 2011 fabricated a polymer-based microfluidic proteomics reactor (figure 1.26). Three glass capillary tubes (365 µm o.d. and 200 µm i.d.) were assembled with a hard thermoplastic substrate and a soft elastomer layer. The reactor was filled with strong cation exchanger (SCX) beads that were kept in a microchannel (1 cm) by two integrated pillar frits (25 µm in diameter with an interstice of 8 µm between pillars). The device was utilised for the simultaneous processing of multiple samples on the same device, by preconcentration, reduction, alkylation, and digestion on the microfluidic device, followed by using the device for protein-protein interaction studies. The performance of the fabricated device was checked using immunoprecipitated samples from three yeast strains (control, Htz1-TAP, and Htz1-TAP swr1Δ). The sample was mixed with trypsin and then loaded into three separate channels using a pressurised vessel. The proteins were reduced using 100 mM DTT in 10 mM ammonium bicarbonate for 30 min at room temperature, followed by alkylation and digestion reactions. The alkylation reaction was carried out using 10 mM iodoacetamide in 100 mM tris-HCl (pH 8.0) and incubating the device for 1 hour at room temperature, and finally the resulting digested peptides were eluted and analysed by nano-HPLC-MS/MS system. The result showed the fabricated proteomic reactor was able to reduce, alkylate, and digest protein efficiently. Moreover, it did not contaminate the detection system, and was suitable for studies of protein-protein interactions.

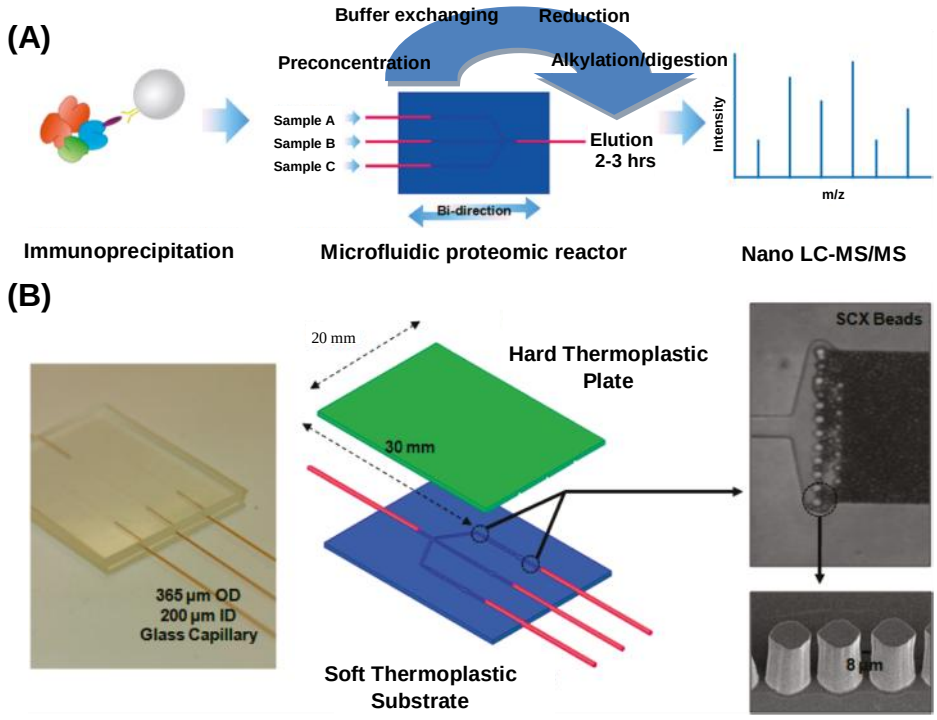

Figure 1.26 (A) Workflow of the microfluidic proteomic reactor for protein-protein interaction study, and (B) the design of the fabricated three-channel microfluidic proteomic reactor.[148]

1.6 Matrix-assisted laser desorption/ionisation time-of-flight mass spectrometry

Mass spectrometry (MS) is a powerful detection method that can be used to identify unknown compounds. It can measure the molecular mass of biomolecules with a very high accuracy.[149] By using mass spectrometers, the masses of peptides can be measured, sequence data for peptides can be obtained, and proteins identified.[12, 150]

Mass spectrometers consist of three main parts; the ionisation source, the analyser, and the detector. The ionisation source is employed to produce ions from the sample while the analyser separates the ions according to their mass (m) to charge (z) ratios (m/z) rather than the mass. Finally, the separated ions are detected by the detector. The mass analyser and the detector, and often the ionisation source, work only at high vacuum

because the ions cannot move from one part of the instrument to another without being under high vacuum; therefore, a vacuum pump system must be used.[6]

The biomolecules are very large and polar, and it is not easy to produce ions from these samples; therefore, they need an ionisation source. One method is inductively coupled plasma (ICP). However, ICP-MS is specific only to metalloproteins and it cannot be used if the protein does not contain metal atoms. In addition, it cannot give information about the molecular weight of the proteins. The most common approaches used to ionise protein samples are electrospray ionisation (ESI), and matrix-assisted laser desorption/ionisation (MALDI). These ionisation sources are "soft ionisation" methods because they import very little energy to the sample ions and can give information about the molecular mass of the analytes without causing significant fragmentation.[84, 151]

The MALDI technique was introduced in 1988 by Hillenkamp and Karas. It has become a standard tool to ionise peptides, proteins, and most other biomolecules (oligonucleotides, carbohydrates, and lipids).[152] The main advantages of using a MALDI source are ease of use, speed of analysis, robust instrumentation, high sensitivity, and tolerance to salts, detergents, and non-volatile buffers such as phosphate, sulfate, and citrate.[153, 154] Moreover, the data produced are not as complicated as an ESI mass spectrum because MALDI depends on producing mainly singly charged analyte ions rather than the multiply charged ions produced in electrospray.[155] However, the efficiency of MALDI analysis can be affected by the quality of the sample since contamination of the sample with significant levels of detergents, buffers, salts, and organic modifiers can inhibit sample ionisation in the MALDI source. Other disadvantages of MALDI analysis are low resolution and mass accuracy that are caused by factors related to sample preparation such as the choice of suitable matrices and solvents, and shot-to-shot reproducibility is relatively poor.[154, 156, 157]

This kind of ionisation source works under high vacuum (less than $3x10^{-6}$ torr). The sample is mixed with an excess of a solid matrix material**,** which is a small organic molecule containing a chromophore that is responsible for absorbing the light at the wavelength of the laser that is used. The choice of the matrix is important for success in MALDI experiments.[158] Typical matrix compounds that can be used for peptides

and proteins are α-cyano-4-hydroxycinnamic acid (4HCCA), 3,5-dimethoxy-4-hydroxycinnamic acid (sinapinic acid or SA), and 2,5-dihydroxybenzoic acid (DHB).[152] The sample/matrix admixture is spotted onto a MALDI target plate and left to evaporate to form crystals. The plate is then placed into the MALDI source. The admixture is irradiated by nanosecond laser pulses, commonly an ultraviolet (UV) laser with a wavelength of 337 nm.[159] The matrix will strongly absorb the laser light energy and becomes electronically excited. The excess energy is then transferred to the sample and resulting in ionisation.[152, 158] The matrix and analyte ions are ejected into the gas phase. Figure 1.27 shows the schematic diagram of the ion source (MALDI).

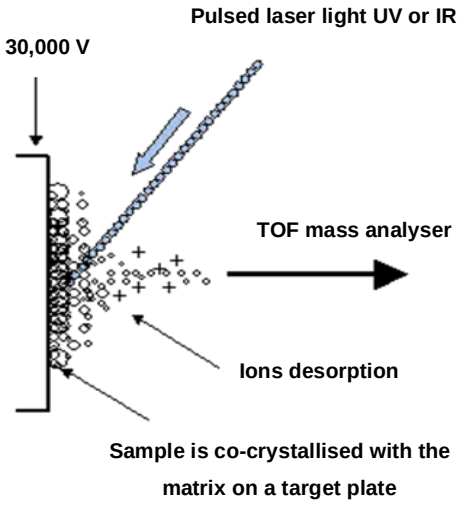

Figure 1.27 Schematic representation of matrix-assisted laser desorption/ ionisation (MALDI).[152]

The ionisation process can generate positive and negative ions, depending on the nature of the sample. If the sample has a functional group that will accept a proton then the positive ionisation mode is used and the formula for this mode will be $(M+H)^+$. The positive ionisation mode is commonly used for peptides and proteins. In negative ionisation mode, the sample has the ability to lose a proton and the formula $(M-H)^-$ will be dominant. The negative ionisation mode can be employed to ionise saccharides and oligonucleotides.[151, 160]

After the ions are formed in a MALDI ionisation source, they will be transferred to the mass analyser, which is commonly a time-of-flight (TOF) analyser. This analyser measures the time that the ions take to fly through the mass analyser to the detector. The TOF analyser can operate in linear or reflectron modes. The linear TOF mass analyser can be used for highest mass range with very fast scan speed. However, the resolution of the linear TOF mass analyser is very low and this is because the ions have different velocities for the same m/z ratio (small ions will travel faster from the TOF analyser to the detector than large ions). On the other hand, reflectron mode TOF depends on using a reflectron, which is a device located at the end of the flight tube to alter the paths of ions in order to make ions of the same m/z ratio reach the detector at the same time. As a result, the resolution will be enhanced; however, it has limited m/z range.[157] Figure 1.28 shows a schematic diagram of the TOF: (A) linear mass analyser, and (B) reflecting mass analyser.

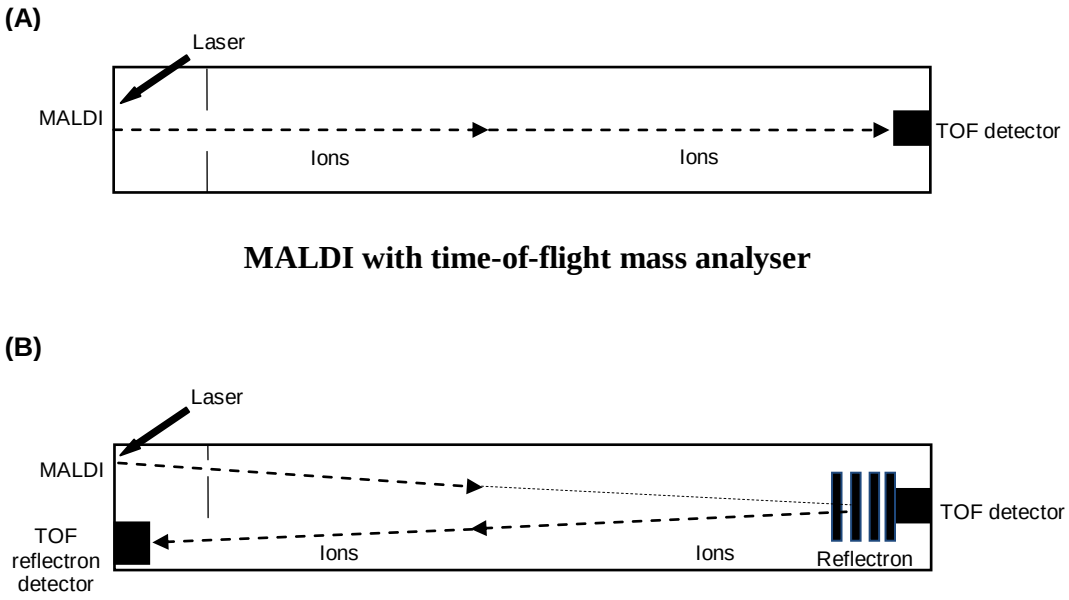

Figure 1.28 Schematic representation of MALDI-TOF mass spectrometry: (A) linear mode, and (B) reflecting mode.[152]

1.7 Microfluidics

Often current procedures are very time consuming and labour-intensive; therefore, there has been a trend to employ microfluidic devices in many fields; for example, diagnostics, pharmaceuticals, medical, food industry, biotechnology, process industry, and environmental technology. The performance of microfluidic devices is better than that of traditional devices; for example, reduced volumes of reagent, which could be expensive, and sample, which in some cases is not available in large amounts. Additionally, the reaction time can be reduced and reactions carried out more safely due to the size of the reactors. The use of microanalytical tools increases the performance of analytical devices in terms of detection limit, selectivity, reproducibility, and the ability to integrate multiple analytical processes into a single microfluidic device.[161, 162] Another advantage of microfluidic systems is that the ratio between the inner surface area of the channel to the volume occupied by the solution is higher than that of conventional systems, resulting in an increase of the interaction between the immobilised reactant used and the analyte, so the reaction will be more efficient in microfluidic systems than in the conventional systems.[163]

"Microfluidics", also called micro total analysis systems (μTAS) or "lab-on-a-chip" can be defined as an analytical technique which uses small volumes of fluids, micro-, nano-, pico- or femtolitre, driven in microstructured channels. The size of these microchannel dimensions could be between millimetres and micrometres. At these dimensions, the behaviour of fluids will be changed, and the flow in miniaturised systems is always laminar, providing well defined streamlines.[161, 164]

Common materials used for microfluidic devices are silicon and glass. The reason for the popularity of these materials is the ease of fabrication using the standard methods of microelectronics such as patterning and etching.[164] Moreover, silicon has high thermal conductivity resulting in fast temperature ramping while glass is optically transparent for detection and supports electro-osmotic flow (EOF).[165, 166] Fabrication of these materials depends on using protective photoreactive layers and masks that have the desired pattern. The substrate is covered with the protective photoresist and exposed to light through the mask. Then, the photoresist is removed and the whole device is etched by chemical agents, commonly hydrogen fluoride (HF), followed by bonding to close glass or silicon microstructures. The main disadvantages of silicon or

glass are low flexibility, the chemical etching depends on using harsh and dangerous chemical reagents (HF), and fabrication needs a clean room. Additionally, glass microchips can be broken easily and there is a high cost involved in processing glass.[163, 167]

Other materials that can be used for fabrication of microfluidic devices are thermoplastic polymer materials such as polymethylmethacrylate (PMMA), polydimethylsiloxane (PDMS), and polypropylene (PP). They are widely used because they have good mechanical flexibility, do not need clean room facilities, are not easily broken, can be easily processed, and can avoid the high cost of multistep wet fabrication by using inexpensive "dry" techniques such as injection moulding or hot embossing.[164] However, polymers have some limitations; for example, there can be interaction between the wall of the polymeric microchip and the analyte leading to adsorption of analyte on the surface of the microchips. Another disadvantage of polymeric microchips is the limited compatibility with organic solvents because they can absorb solvents and swell, which limits their use to aqueous solutions.[168] In addition, EOF can be poorly defined in polymeric michrochips.[169]

Pumping fluids in microfluidic systems can be achieved in two ways, either by mechanical micropumps, which can be displacement pumps or dynamic pumps, or by non-mechanical micropumps (electro-kinetic pumps). The advantage of mechanical micropumps is that it allows easy control of flow rate; however, they cause parabolic flow profile, and the signal of the mechanical pumps is low and long. In contrast, electro-kinetic pumps can provide a flat flow profile, and the signal is high and sharp. However, the choice of the kind of pump depends on the liquid because electro-kinetic pumps are not suitable for all liquids. Moreover, they require control of the microchannel wall surface charge, and the sample ionic strength, which can be a problem when dealing with a real sample. In addition, a slight difference in the solution levels in the reservoirs can induce a pressure-driven flow (PDF).[163, 170]

There has been a trend to use microfluidic devices in proteomics for tasks such as sample pretreatment, protein/peptide separation, immunoassays, chemical modification, digestion on chip, and interfacing of microfluidic devices with electrospray ionisation-mass spectrometry.[171, 172] Microfluidic sample preparation for proteomics is probably the most neglected step, as indicated by the number of

publications compared to those for protein separation and detection, yet it represents a hurdle on the way to a fully integrated proteomic platform.[163] The complexity of the real sample matrix, and the low concentrations of some proteins create challenges for the use of microfluidic devices for sample preparation.[173]

1.8 Proteins in milk and egg white

To our best knowledge, there has been no published data to date on the use of monolithic materials in the preconcentration of proteins from milk and egg white; therefore, this study will focus on the proteins present in these real samples.

Milk is a secretion of the mammary glands of mammals. It is important for infant nutrition since it is the only source of feeding for newborns and infants, but it is also a major nutritional source for all ages. A molecular understanding of the biological basis of milk function has emerged as a central theme in nutritional research. Milk is a complex fluid that consists of 88 % water and a number of different components including proteins, carbohydrates, fatty acids, minerals, and vitamins.[174, 175]

Proteins (3-3.5 %) in milk have received great attention since they are the main source of bioactive peptides for infants and babies.[174, 176] In addition, milk proteins have a high economic value since they are fundamental to the production of other foodstuffs such as yogurt, cheese, and drinks.[177, 178] The benefits of milk proteins are to defet against pathogenic bacteria, yeast, and viruses, improve the immune system, and maturate the gut. Milk proteins can be separated into two major protein fractions, which are 80 % caseins (insoluble) and 20 % serum or whey proteins (soluble). There are several different types of caseins including α_{s1}, α_{s2}, β and κ as well as γ_1, γ_2 and γ_3 that are fragments of β-casein.[174, 179] Most of these caseins are phosphorylated and can contain variable numbers of phosphate groups. They readily undergo proteolysis and diffuse faster in the milk micelle interfaces compared to serum proteins that comprise β-lactoglobulin and α-lactalbumin. Caseins and serum proteins differ in their molecular weight, hydrophobicity and abundance; caseins have a lipophilic character while serum proteins are amphiphilic.[177] In addition, proteins from both groups can be present in genetic variants. The proteins in a milk sample can be affected by a variety of factors such as the origin of the sample, the time lapse before analysis, and variation in the concentration of enzymes such as plasmin.[179]

Eggs consist of a protective eggshell, egg yolk, and egg white and play an important role as an inexpensive source of high quality protein in the human diet. The egg white or albumen represents an important material for the food industry because it has been used as an ingredient in food processing due to its unique functional properties, such as foaming, gelling, binding, thickening, and coating. Foaming ability is one of the most important properties of the egg white protein in manufacturing bakery products such as bread, cakes, ice cream, and cookies and it has been used as an ingredient in food processing. Therefore, much research has been conducted into its components, especially proteins.[180-182] Moreover, the egg white proteins are of medical interest as allergens causing food allergies.[183]

The egg white contains 9.7 to 12 % proteins that are known to be glycosylated and phosphorylated. It contains proteins that vary in molecular weight (12.7-8000 kDa), isoelectric point value (4-11), and some proteins are much more abundant than others.[184] There are five major proteins; firstly, ovalbumin, which is a phosphoglycoprotein and comprises 54 % of the total proteins in the egg white. The molecular weight of ovalbumin is 44500 Da, its isoelectric point is 4.5, and it has 385 amino acid residues, half of them hydrophobic. Secondly, ovotransferrin or conalbumin (77700 Da), which comprises 13 % of the total egg white protein and can bind to metal ions and form a protein-metal complex, which is resistant to denaturation by heat, pressure, or enzyme digestion. This is followed by ovomucoid (11 %), which is a glycoprotein bearing carbohydrate contents ranging from 20 to 25 %. The molecular weight of ovomucoid varies from 26100 to 28300 Da, and its isoelectric point lies between 3.9 and 4.3. Next is lysozyme, which is a glycoprotein and represents 3.5 % of the total egg white. Finally, ovomucin, which is a glycosulphoprotein that constitutes 2 % of the total egg white protein, and differs from other proteins because of its large molecular weight, which varies from 5.5 to 8.3 MDa.[181, 185]

1.9 Aims of the PhD project

Proteomics is increasingly important in the development of new medicines. Current procedures are very time consuming and labour-intensive. Decreasing the total analysis time is limited by the sample preparation. Therefore, the sample preparation

step is considered a bottleneck in a system for chemical analysis. The aim of the present study has been to develop a protein extraction microchip. This work should lead to a reduction in the amount of sample required and solvents used, leading to reduce waste, and decrease analysis time. In addition, the method should be fast, cheap, reproducible, and environmentally friendly. The previously completed literature review indicated that these objectives could best be met by the use of solid phase extraction (SPE) as a proteomic technique. This can be performed by fabrication of monolithic materials that are polymer- and silica-based monoliths, since there are many advantages of the monolithic materials compared with the conventional packed materials. The next step was optimisation of the porous properties of each monolith in order to maximise the extraction recovery of proteins. Then, evaluation of the optimised monolith for preconcentration/extraction purposes for proteins was carried out. Finally, fabrication of the monolithic materials inside a microchip device was performed. The suitable sorbent material should have the ability to preconcentrate several different standard proteins with high extraction recovery, remove interfering materials, improve the sensitivity of detection, and be reproducible.

In this study, the polymer-based monolithic materials using poly (butyl methacrylate-*co*-ethylene dimethacrylate) (BuMA-*co*-EDMA) stationary phase was of interest as an extraction sorbent for proteins because of its hydrophobicity and good solubility. Since adsorption of proteins occurs typically on the surface of the monolith, a very large surface area is a favorable feature of sorbent materials in order to increase the sorption capacity. In addition, it is important to control the hydrodynamic properties of the polymer-based monolith in order to decrease the resistance to flow through the monolithic material and decrease the backpressure during the experiments. In this study, the physical properties of the organic monolith were optimised by investigation of the energy of the UV light, time of exposure to the UV light, and the composition of the porogenic solvent system.

Fabrication of a reproducible crack-free inorganic silica-based monolith for preconcentration/extraction of proteins was also investigated. The negative aspect of the sol-gel monolith in microchips is the fact that the shrinkage of the monolith as the condensation reaction happens can cause voids between the silica network and the microchip wall resulting in a reduced surface area for protein adsorption, and can

cause the silica monolith to crack.[117, 186] Previous studies have minimised this problem, but the shrinkage could not be completely avoided during preparation of the silica-based monolith.[106, 187, 188]

Proteomics samples commonly are highly complex and many proteins are folded by disulphide bonds between cysteine residues within the amino acid chains. As a result, specific locations in the proteins are inaccessible to the proteolytic enzyme; therefore, reduction of the disulphide bonds in a protein assists with protein unfolding and allows better access by the proteolytic enzyme making protein identification more precise. Therefore, the second aim of this study was to fabricate a device with the ability to reduce and alkylate disulphide bonds in proteins.

Recently, there has been increasing attention on modifying the surface of the silica-based monolith with organic groups, which can be performed by co-condensation or a post-synthesis process.[189] The organic groups could be alkyl or aryl-, chloro-, thio-, amino- and other groups.[190] Immobilisation of the reducing reagent on the microchip-based silica sol-gel monolith can decrease the amount of protein sample and reagents, speed the reaction time, and facilitate integration with other microchips. To the best of our knowledge, immobilisation of a reducing reagent on the surface of monolithic materials has not been previously reported. Therefore, another objective of the present study was to develop a new method for immobilisation of the reducing reagent on the surface of a silica-based monolith in order to use it for reduction of the disulphide bonds in proteins before enzymatic digestion.

2.0 Experimental

This chapter describes the experimental setup and procedures utilised for the work in this thesis, detailing fabrication of the monolithic materials (2.1), characterisation of the monolithic materials (2.2), application of the polymer- and silica-based monolith in protein extraction, and application of the silica-based monolith in protein reduction and alkylation (2.3). All chemicals were utilised without further purification. Water used for preparing the solution was deionised in the laboratory using the Elgastat Prima 3 reverse osmosis water system [Elga Ltd., High Wycombe, UK].

2.1 Fabrication of the monolithic materials

2.1.1 Fabrication of the organic monolith

2.1.1.1 Pretreatment procedure

The polymer-based monolith was fabricated inside a borosilicate tube with an inner diameter of 2.10 mm, and an outer diameter of 3.90 mm [Smith Scientific, Kent, UK]. A straight/standard bore adapter [Kinesis, Cambs, UK] was used to connect the borosilicate tube with the polyetheretherketone (PEEK) tubing [Thames Restek Ltd., Saunderton, UK] while a microtight adapter [Kinesis, Cambs, UK] was used to connect the PEEK tubing to the disposable plastic syringe [Scientific Laboratory Supplies, Nottingham, UK]. All solutions were injected using a syringe pump [Bioanalytical System Inc., West Lafayette, USA]. Figure 2.1 shows a photograph of the experimental setup for fabrication of the polymer-based monolith.

Before fabrication of the organic polymer-based monolith inside the tube, the inner walls of the borosilicate tube were activated as previously reported.[191, 192] Firstly, the tube was washed with acetone [Fisher Scientific, Loughborough, UK], followed by washing with deionised water. Then, it was washed with 0.2 M sodium hydroxide solution (NaOH) [Fisher Scientific, Loughborough, UK] for 1 hour at a flow rate of 2 µL min^{-1} using a syringe pump, followed by washing with deionised water. To neutralise and remove alkali metal ions, the tube was washed with 0.2 M hydrochloric acid solution (HCl) [Fisher Scientific, Loughborough, UK], which was pumped through the tube for 1 hour at a flow rate of 2 µL min^{-1}, followed by washing with

deionised water, and finally the tube was rinsed with ethanol [Scientific Laboratory Supplies, Nottingham, UK].

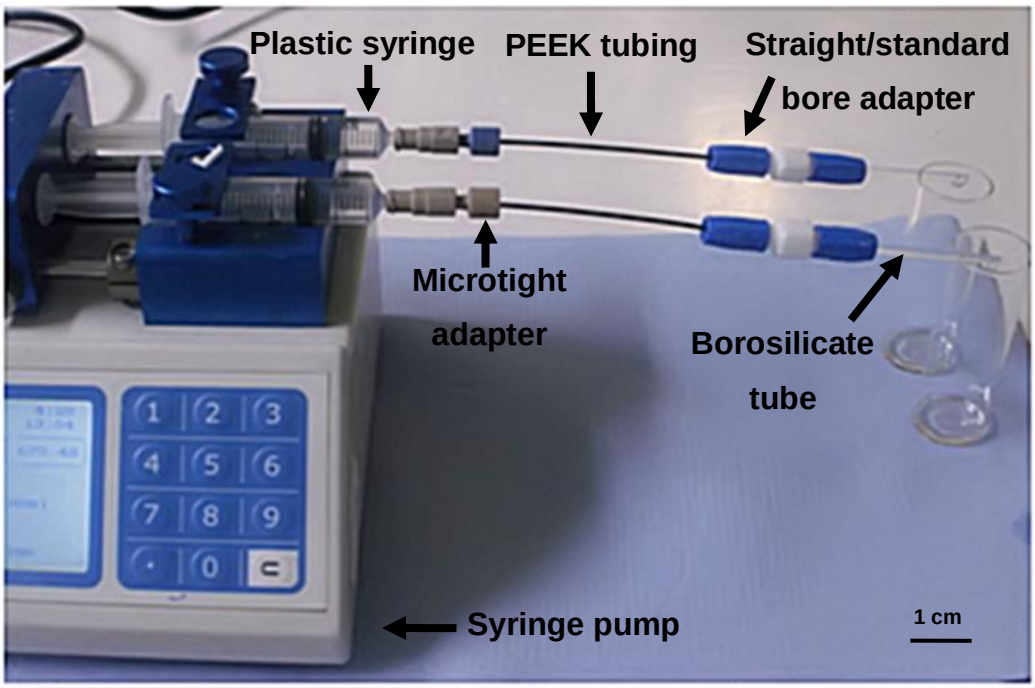

Figure 2.1 Photograph of the experimental setup for preparation of the polymer-based monolith.

The inner walls of the borosilicate tube were silanised with 3-(trimethoxysilyl) propyl methacrylate (γ-MAPS).[192] The surface silanisation was achieved by washing the tube with a solution consisting of 20 % (v/v) γ-MAPS [Sigma-Aldrich, Poole, UK] in 95 % ethanol adjusted to pH 5 with glacial acetic acid [Fisher Scientific, Loughborough, UK] using a pH meter [Fisherman hydrus 300, Thermo Orion, Beverly, MA, USA]. The solution was injected inside the tube using the syringe pump at a flow rate of 2 µL min^{-1} for 1 hour. After surface-vinylisation of the borosilicate tube, it was rinsed with acetone, dried under a stream of nitrogen gas and left overnight. After 24 hours, the tube was ready for the polymerisation reaction.

2.1.1.2 In-situ polymerisation of poly (BuMA-*co*-EDMA) monolith

Photoinitiated free radical polymerisation was utilised for the preparation of the polymer-based monolith within the borosilicate tube at room temperature under UV

irradiation. The polymer-based monolith was prepared as described by Frechet *et al*.[193] with some modifications. The polymerisation mixture consisted of a monovinyl monomer, butyl methacrylate 99 % (BuMA) [Sigma-Aldrich, Poole, UK], a crosslinker, ethylene dimethacrylate 98 % (EDMA) [Fisher Scientific, Loughborough, UK], the free radical photoinitiator, 2,2-dimethoxy-2-phenyl acetophenone 99 % (DMPA) [Sigma-Aldrich, Poole, UK], and the porogenic solvent system, which was a binary mixture of methanol [Scientific Laboratory Supplies, Nottingham, UK] and another solvent (50:50). The solvents that were investigated for fabrication of the organic monolith were ethanol, acetonitrile, chloroform, hexane, tetrahydrofuran, 1-propanol, ethyl acetate, and cyclohexanol [Scientific Laboratory Supplies, Nottingham, UK]. Table 2.1 shows the main components of the polymerisation mixture used for the preparation of the polymer-based monolith.

Type	**Chemical**	**Weight (g)**
Monomer	Butyl methacrylate (BuMA)	1.422
Crosslinker	Ethylene dimethacrylate (EDMA)	0.96
Porogenic solvent system	50:50 of main solvent (methanol) and other solvent (ethanol, acetonitrile, chloroform, hexane, tetrahydrofuran, 1-propanol, ethyl acetate, and cyclohexanol)	3.6
Photoinitiator	2,2-dimethoxy-2-phenyl acetophenone (DMPA)	0.024

Table 2.1 The composition of the polymerisation mixture used for the preparation of the polymer-based monolith.

The polymerisation mixture was sonicated for 10 min to dissolve the initiator and get a homogeneous solution using a sonicator [Ultrawave Sonicator U 300HD, Cardiff, UK] and purged with nitrogen gas for 10 min to remove oxygen. The surface-vinylised tube was rinsed with this polymerisation mixture solution for 2 min, and then completely

filled with the polymerisation mixture using a syringe pump and the ends of the tube were sealed with blu-tack [Lyreco, Telford, UK]. The tube filled with the polymerisation mixture was placed under the UV lamp [Spectronic Analytical Instruments, Leeds, UK] at 254 or 365 nm at room temperature. Different exposure times were investigated which were 8, 10, 12, 14, 16, 18, 20, and 22 min and the distance between the tube and the UV lamp was 5 cm. Only 1 cm of the borosilicate tube was exposed to UV radiation, while the rest of the tube was covered with electrical tape [Onecall, Leeds, UK] to prevent the monolith forming throughout the full length of the tube. After the polymerisation reaction, the monolithic tube was flushed with methanol by a syringe pump at a flow rate of 2 µL min^{-1} for 12 hours to clean the monolith of unreacted components and the porogenic solvents. The monolith was inspected under an optical microscope [Zeiss Axiovert S100, Jena, Germany] to check if the appearance of the monolith was satisfactory. Figure 2.2 depicts the polymer-based monolith inside the borosilicate tube used as extractor for protein extraction.

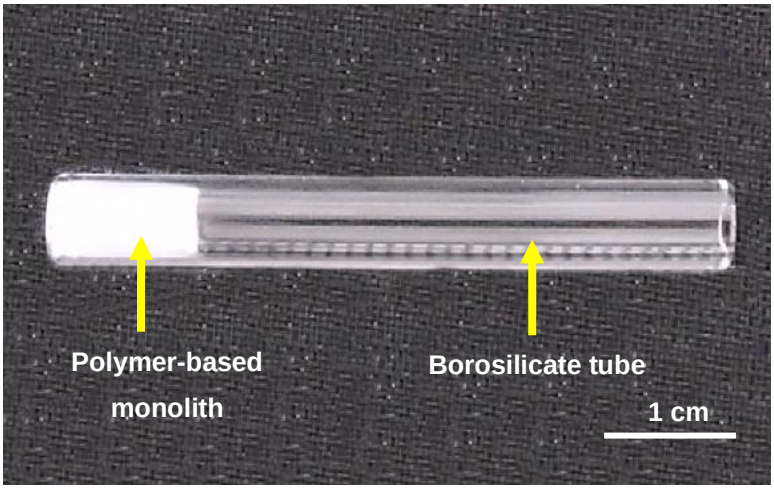

Figure 2.2 The BuMA-*co*-EDMA monolith was fabricated inside the borosilicate tube. The channel surface of tube was treated with γ-MAPS, followed by polymerisation reaction using the UV lamp (365 nm) at room temperature. The polymerisation mixture was BuMA (1.422 g), EDMA (0.96 g), DMPA (0.024 g), and the porogenic solvent (3.6 g) was 50:50 MeOH and 1-propanol.

2.1.1.3 Investigation of using tertiary porogenic solvent system

The same polymerisation mixture and experimental setup were used as previously described, except that the porogenic solvent system was changed from a binary to a tertiary mixture. The main solvent was methanol (MeOH) which constituted 50 % of the total amount of the solvent (3.6 g) and the other 50 % was a mixture of 1-propanol and ethanol (EtOH) in different ratios, as can be seen in table 2.2.

MeOH (%)	1-propanol (%)	EtOH (%)
50	40	10
50	30	20
50	25	25
50	20	30
50	10	40

Table 2.2 The composition of the tertiary porogenic solvent system used for the polymerisation mixture of the polymer-based monolith.

2.1.1.4 Fabrication of the organic monolith inside a glass microchip

A glass microchip was fabricated using standard photolithography technology followed by wet etching and thermal bonding.[194] Figure 2.3 shows a schematic diagram and a photograph of the glass microchip filled with blue food dye to facilitate visualisation. The glass microchip consisted of two plates and the thickness of both plates was 1 mm. The dimensions of the glass microchip were 32 mm length and width. All etching was on the upper surface of the base plate of the chip to a depth of 100 µm. The microchip consists of an inlet microchannel that connects to the extraction chamber and three outlet microchannels. The top and etched bottom plates were thermally bonded at 575 °C for 3 hours to produce the complete microfluidic device.

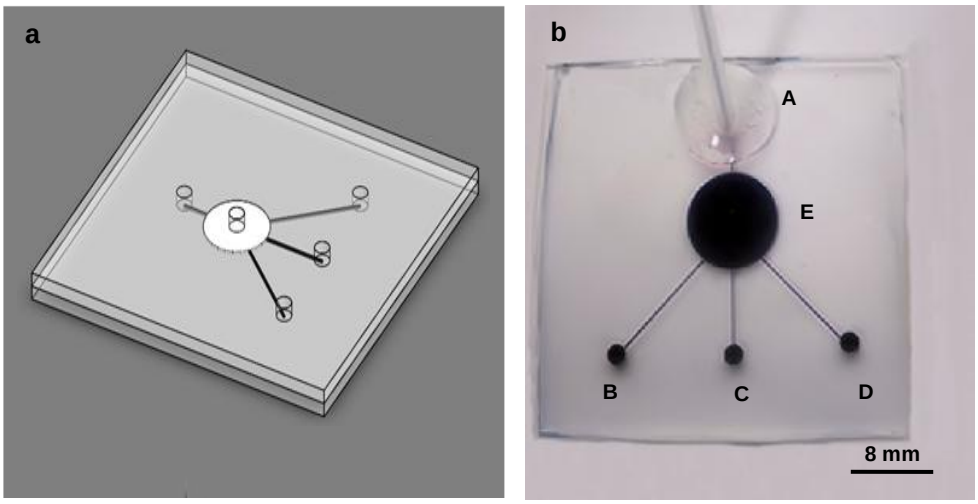

Figure 2.3 Schematic diagram (a) and photograph (b) of the glass microchip that was filled with blue food dye and used for fabrication of the polymer-based monolith. The dimensions of the glass microchip were 32 mm length and width. The top plate contains 1.5 mm (A-E) access holes for attachment of ETFE tubing. All etching was into the upper surface of the base plate of the chip to a depth of 100 µm.

The microchip had five access holes (1.5 mm) in the top plate produced using a diamond tipped drill. The ethylenetetrafluoroethylene (ETFE) tubing (1/16" x 0.17 mm i.d.) [Thames Restek Ltd, Saunderton, UK] was fixed into the access holes using Double Bubble Mix and Fix epoxy resin [Bondmaster limited, London, UK]. The ETFE tubing was connected to the inlet hole (A) for injection of the reagents and samples. The outlet hole was one of the access holes (B, C, or D) and the rest of the holes were blocked with epoxy resin. The extraction chamber contained an access hole (E) in the centre of the chamber to facilitate injection of the polymerisation mixture into the protein extraction chamber. A microtight adapter was utilised to connect the ETFE tubing to a 1 mL disposable plastic syringe, which was connected to the syringe pump to control the flow rates.

The polymer-based monolith was fabricated inside the extraction chamber of the glass microchip. The extraction chamber was cleaned and silanised as described before (section 2.1.1.1). This was followed by fabrication of the polymer-based monolith using the same procedure that was used to fabricate the polymer-based monolith inside

the borosilicate tube (section 2.1.1.2). After preparation of the polymerisation mixture, it was injected through the access hole (E).The surface of the chip was then covered with electrical tape, except for the extraction chamber. The exposure time was 20 min and the distance between the UV lamp (365 nm at room temperature) and the glass microchip filled with the polymerisation mixture was 5 cm. After formation of the white monolithic material inside the glass microchip, the microchip was washed with methanol for 12 hours at a flow rate of 2 µL min^{-1} to remove unreacted materials.

2.1.2 Fabrication of the inorganic monolith for protein extraction

2.1.2.1 Fabrication of the bare inorganic monolith

The silica-based monolihs were fabricated following the previously reported procedure [195] with some modifications in the fabrication conditions. The porous silica rods were fabricated inside a disposable plastic syringe (1 mL), which acted as a mould, by adding 0.282 g of polyethylene oxide (PEO) with average relative molecular mass MW=10,000 g mol^{-1} [Sigma-Aldrich, Poole, UK] to 2.537 mL of 1 M nitric acid [Fisher Scientific, Loughborough, UK] and 0.291 mL of distilled water. The solution was stirred using a stirrer [VWR International, West Chester, PA, USA] for 20 min while immersed in an ice bath to promote a hydrolytic reaction. Then, 2.256 mL of tetramethyl orthosilicate 99 % (TMOS) [Fisher Scientific, Loughborough, UK] was added to the cooled transparent solution and the solution was mixed for 30 min until the two-phase mixture gradually became a homogeneous solution. When the mixture was homogeneous, it was left to settle for 2 min to remove any bubbles that may have formed during mixing. The resulting homogeneous mixture was left in the ice and 0.4 mL was poured slowly down inside 1 mL disposable plastic syringes. When the mixture was in the syringe, it was shaken carefully to remove any air bubbles in the syringe. The thin end of the syringes was sealed using polytetrafluoroethylene (PTFE) thread seal tape [ARCO Ltd., Hull, UK]. The syringes were placed in an oven and the gelation happened within 2 hours. The gelled sample was aged to give white solid rods at different gelation times (1, 2, 3, and 4 days) and different gelation temperatures (40 and 50 °C). The monolithic silica rods were slowly tapped out of the plastic tube because they were quite brittle at this step. The monolithic silica rods were soaked in a water bath for 2 hours.

The monolithic silica rods were treated with the basic environment, which was introduced by thermal decomposition of 1 M aqueous ammonia solution [Fisher Scientific, Loughborough, UK], or 1 M aqueous urea solution [Sigma Aldrich, Poole, UK] at an elevated temperature of 85 °C for 24 hours to form mesopores. The rods were then washed with deionised water until a neutral pH was obtained. The monolithic silica rods were placed in the oven for 24 hours at 40 °C, followed by placing the rods in the oven for another 24 hours at 100 °C. For heat treatment, the rods were placed in an oven at 500 °C for 2 hours. After preparation, both ends of the rods were cut off, since they had large voids and the silica rods were cut to the desired length.

Before the monolithic silica rod was functionalised, it was connected to the borosilicate tube (o.d. 3.90 mm) via the heat shrinkable sleeving polytetrafluoroethylene (PTFE) tube, whose internal diameter shrinks from 4.8 mm to 2.8 mm [Adtech Polymer Engineering Ltd., Stroud, UK]. The monolithic silica rod and the borosilicate tube were placed inside the shrinkable tube and then placed in the furnace at 330 °C for 2 hours to seal the heat shrinkable tube around the borosilicate tube and monolithic silica rod. The resulting silica monolithic rod inside a heat shrinkable tube was ready to use for protein extraction or for modification of the surface of the silica-based monolith. Figure 2.4 shows the main components of the silica-based monolith extractor used for protein extraction.

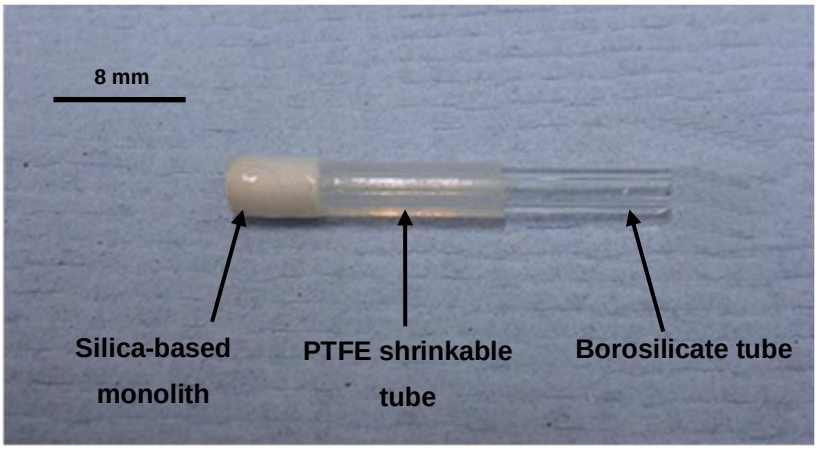

Figure 2.4 The fabricated silica-based monolith that was connected to the borosilicate tube using PTFE shrinkable tube.

2.1.2.2 Derivatisation of the inorganic monolith with C_{18} groups

The surface of the monolithic silica rod was chemically modified with octadecyl groups by a method similar to the one previously described.[196] The derivatisation reagent was 1 g chlorodimethyl octadecyl silane 95 % (CDMOS) [Sigma-Aldrich, Poole, UK] in 10 mL toluene [Fisher Scientific, Loughborough, UK] with 10 drops of 2,6-lutidine 98 % [Sigma-Aldrich, Poole, UK]. The derivatisation was carried out on column by continuous flow from the syringe pump at a flow rate of 30 µL min^{-1} for 6 hours at 80 °C. The end capping procedure used 1 g trimethylchlorosilane 95 % (TMCS) [Sigma-Aldrich, Poole, UK] in 10 mL toluene for another 6 hours in order to block unreacted silanol moieties. After derivatisation, the monolith was flushed with the same solvent and then with methanol using a syringe pump at a flow rate of 10 µL min^{-1} for 2 hours and finally the derivatised silica column was placed in an oven for 24 hours at 40 °C prior to use. Silanes used for the chemical modification step were handled with caution for safety.

2.1.2.3 Fabrication of the inorganic monolith inside the micropipette

Two methods were investigated to fabricate the silica-based monolith inside a micropipette (200 µm i.d.) [Thelabwarehouse, London, UK]. A microtight adapter was used to connect the micropipette to a 1 mL plastic syringe, which was connected to a syringe driver to control and adjust the flow rates. The silica-based monolith was fabricated inside the micropipette using the previous method (see section 2.1.2.1).

The second method was adopted from Wu *et al.*[126] The micropipette was continuously fed with 1 M sodium hydroxide solution (NaOH) for 12 hours using the syringe pump at a flow rate of 2 µL min^{-1}, followed with deionised water for 10 min, then with ethanol for 10 min, and air-dried. The sol-gel mixture was prepared by mixing 2 mL TMOS, 0.44 g PEO, and 10 mL 1 M nitric acid solution. The sol-gel mixture was stirred for 45 min while immersed in an ice bath. The hydrolysed sol mixture was injected into the micropipette, and sealed with PTFE thread seal tape and the micropipette was placed in the oven for 10 hours at 40 ºC. The sol-gel monolith was washed with ethanol using the syringe pump at a flow rate of 2 µL min^{-1} for 2 hours. The sol-gel monolith inside the micropipette was then treated with 1 M ammonia solution for 24 hours at 85 ºC, followed by washing with deionised water. The

derivatisation of the surface of the monolithic silica with octadecyl groups was performed as previously described (section 2.1.2.2).

2.1.2.4 Fabrication of the inorganic monolith inside the microfluidic device

Two types of microchip were investigated for fabrication of the silica-based monolith, namely polycarbonate microchips and glass microchips. The design of the polycarbonate microchip consisted of two plates, as can be seen in figure 2.5. The dimensions of the top plate were 13.5 mm length and width, and a thickness of 1 mm with an access hole (1.5 mm). The base plate had a length and width of 23.5 mm with a thickness of 2.8 mm, and contained the extraction chamber (6.5 mm width and 2 mm depth) that was milled using a CNC (computer numerical control) milling machine, and a 1.5 mm access hole in the centre of the chamber.

The same sol-gel mixture and experimental setup were used to fabricate the monolithic silica rod (2.1.2.1), except a 2 mL disposable plastic syringe was used rather than 1 mL. After fabrication of the monolithic silica rod, a silica monolith disk was cut to length 2 mm and then the diameter adjusted with a scalpel blade to provide a tight fit in the extraction chamber. It was placed inside the extraction chamber on the base plate of the polycarbonate microchip. The two plates were fixed together using epoxy resin and the ETFE tubing was fixed into the access holes drilled into the microfluidic device using epoxy resin. After bonding the two plates, the microchip was used for protein extraction.

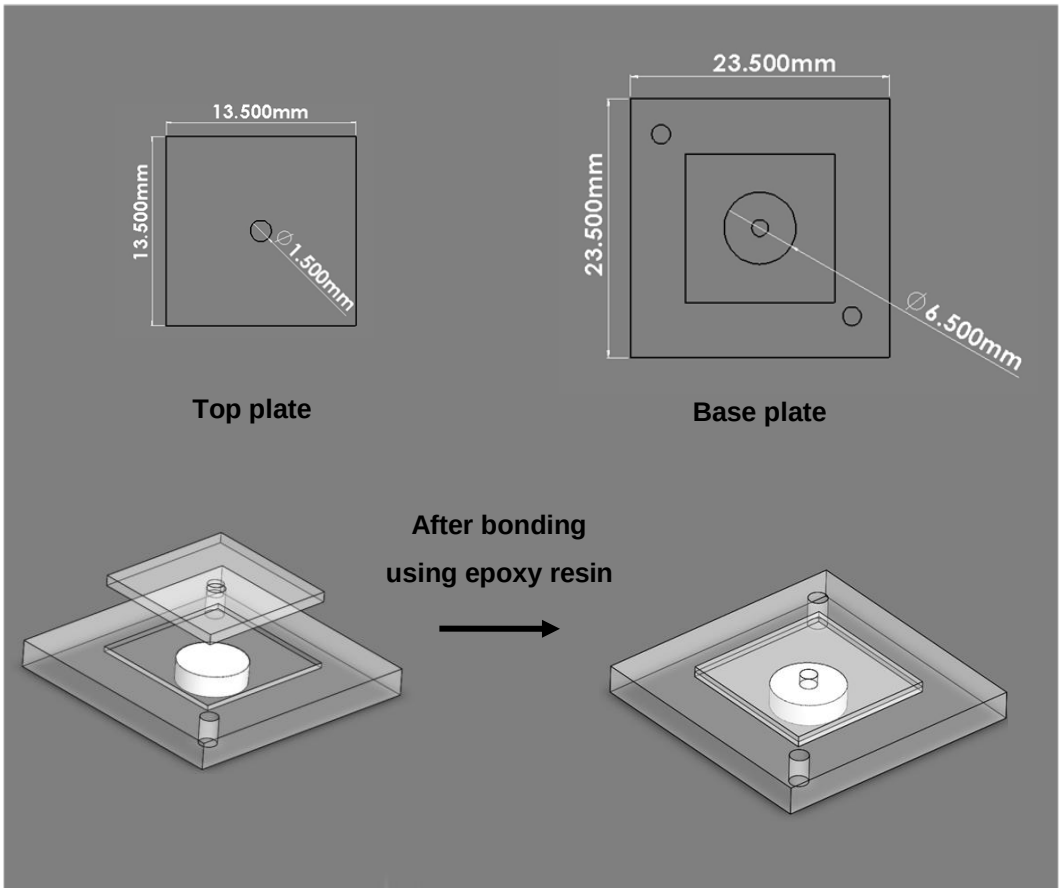

Figure 2.5 Schematic diagram of the polycarbonate microchip. The top plate was 13.5 mm in length and width, and the thickness was 1 mm. The base plate was 23.5 mm in length and width, the thickness was 2.8 mm, and contained the extraction chamber (6.5 mm width and 2 mm depth). Both plates contained an access hole (1.5 mm).

The second microchip was fabricated from glass. The main structure of the glass microchip was again composed of two plates, with a base plate of dimensions 16.5 mm length, 14 mm width and a thickness of 3 mm, and a top plate of 1 mm thickness with all other dimensions the same as the base plate. Both plates contained an access hole of 1.5 mm diameter, which was created using traditional glass drilling techniques. The base plate contained the extraction chamber (2 mm depth and 6.5 mm width) that was milled using a CNC (computer numerical control) milling machine. The diameter of the silica monolith disk (2 mm) was adjusted with a scalpel blade. After placing the monolithic silica disk inside the chamber, the two plates were thermally bonded by

placing them on a quartz plate inside a muffle furnace with a block of quartz (mass 70 g) placed on top. The oven temperature was then maintained at 575 °C for 3 hours. The ETFE tubing was fixed into the access holes using epoxy resin. A microtight adapter was used to connect the ETFE tubing to the plastic syringe, which was connected to a syringe pump. Figure 2.6 illustrates a schematic diagram and a photograph of the plates of the glass microchip.

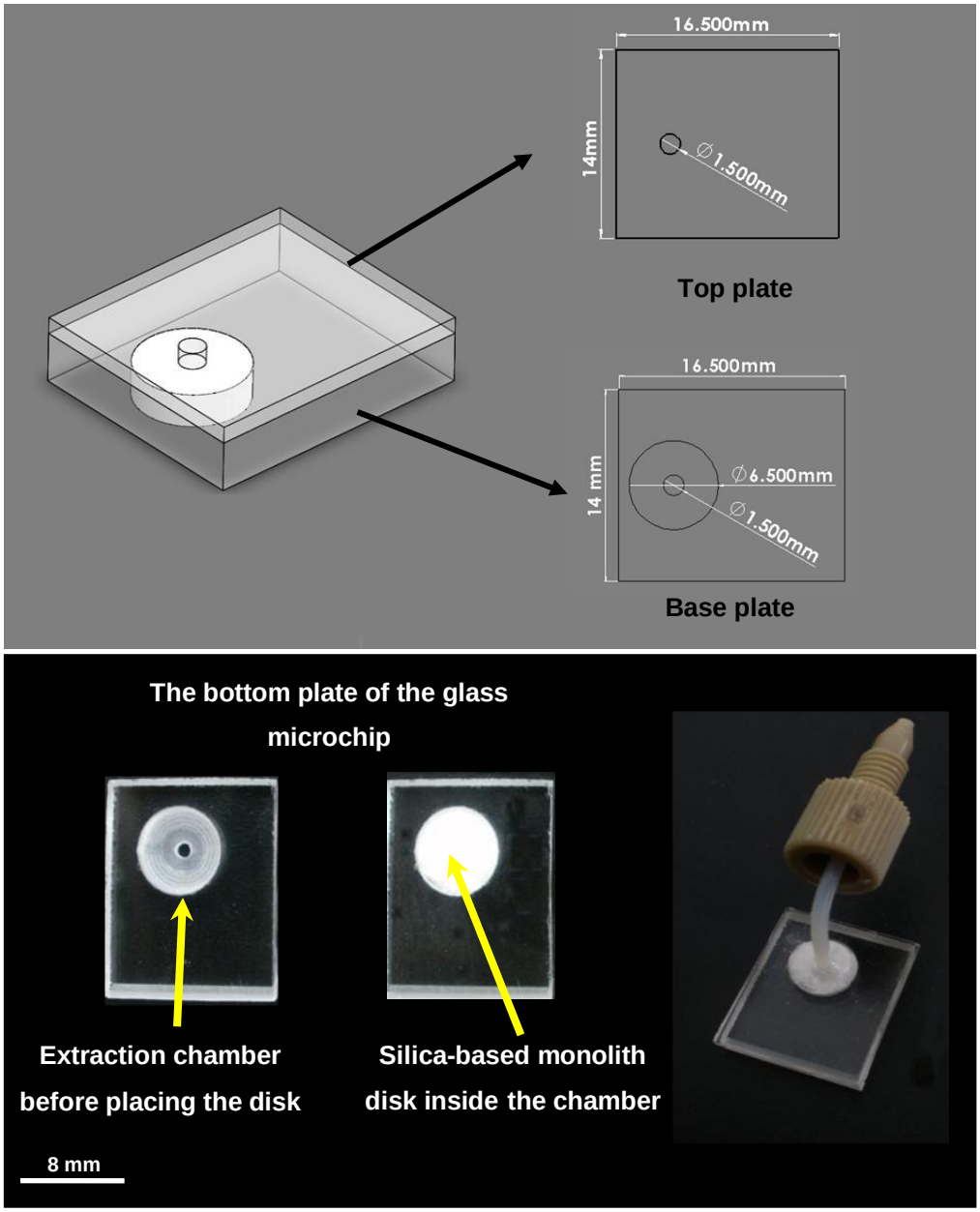

Figure 2.6 Schematic diagram (top) and photograph (bottom) of the glass microchip used for extraction of proteins. The access holes in the top and base plates were 1.5 mm for attachment of ETFE tubing. The photograph shows the base plate of the glass microchip showing the extraction chamber and the access hole before and after placing the monolithic silica disk inside the extraction chamber, and the final microfluidic device after thermal bonding of the top-plate and fixing the ETFE tubes in place.

2.1.3 Fabrication of the inorganic monolith for protein reduction

2.1.3.1 The design and fabrication of the reduction microchip

A glass microchip containing a silica-based monolith designed to carry out protein reduction was fabricated and utilised a similar design to the chip used for protein extraction except that the base plate of the microchip contained only the chamber (2 mm depth and 6.5 mm width) in which to place the monolithic silica disk with no access hole. In addition, the top plate contained two microchannels ending in access holes (1.5 mm). The microchannel length, width, and depth were 4 mm, 1 mm, and 1 mm, respectively. Figure 2.7 presents a schematic diagram and a photograph of the design of the microchip that was used for protein reduction. The reason for drilling the holes in the top plate only was that the fabricated microchip needed to be placed in the oven and incubated for the time of the reduction reaction. The monolithic silica disk was fabricated and placed within the chamber and the two plates were thermally bonded as previously described. The ETFE tubing were fixed in the access holes using epoxy resin.

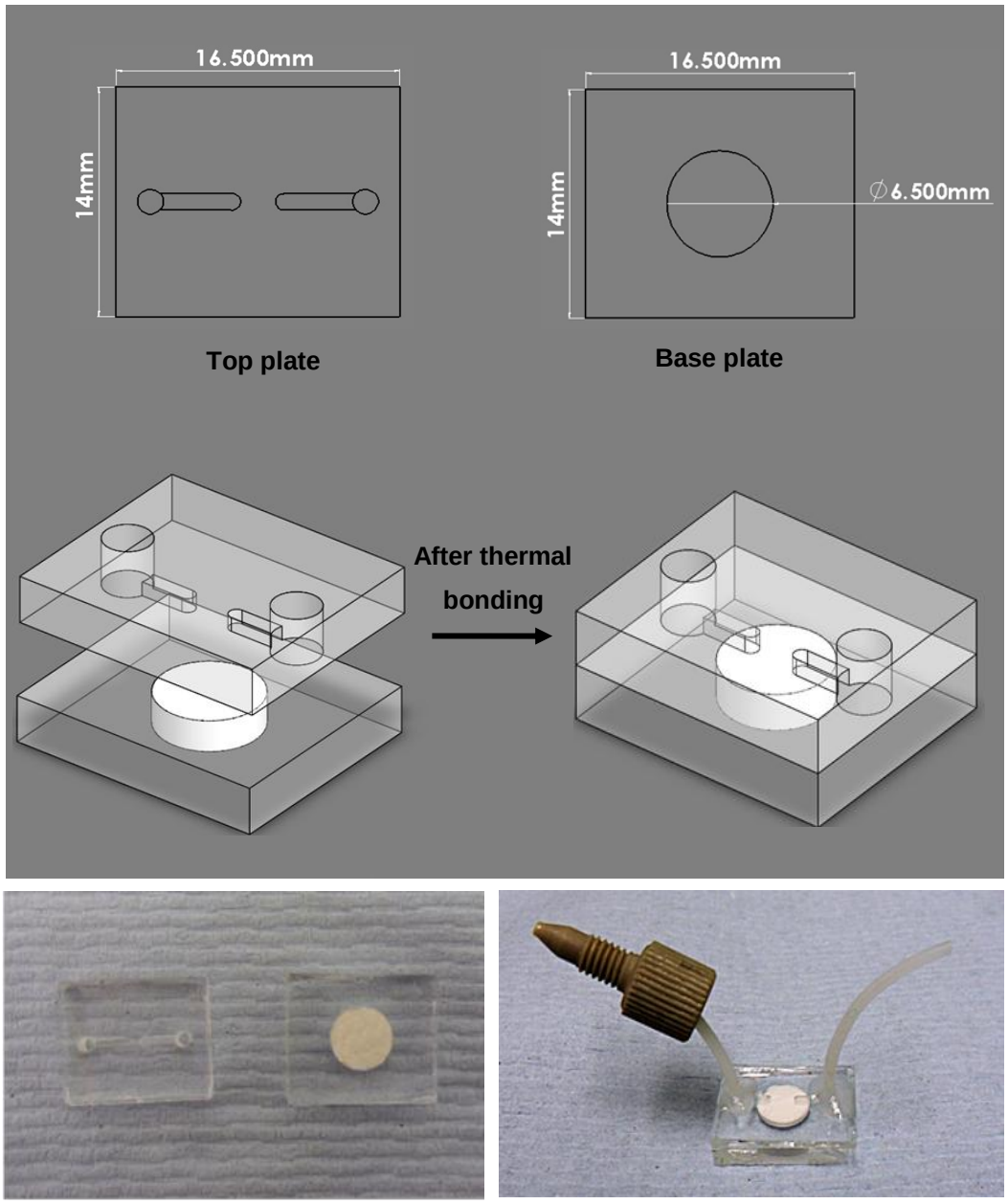

Figure 2.7 Schematic diagram (top) and photograph (bottom) of the design of the glass microchip used for reduction of the disulphide bonds in protein. The dimension of the glass microchip was 16.5 mm × 14 mm. The top plate contained microchannels (length 4 mm, width 1 mm, and depth 1 mm) and access holes (1.5 mm) for attachment of ETFE tubing. The base plate contained the chamber (6.5 mm width and 2 mm depth).

2.1.3.2 Preparation of the amino-modified silica monolith

The surface of the silica-based monolith disk inside the chamber of the glass microchip was chemically modified with amino groups via a reaction between silanol groups on the silica monolith and an organosilane reagent (3-aminopropyl)triethoxysilane (APTES).[197] This was carried out by continous feeding of the monolithic silica disk inside the microchip with a solution of 33 % (v/v) APTES 98 % [Sigma-Aldrich, Poole, UK] in the reaction medium (dried toluene) by injection of the mixture using a syringe pump at a flow rate of 7 µL min^{-1} for 24 hours at room temperature. After silanisation, the non-covalently bonded APTES solution was flushed out by washing the amino-bonded silica monolith with dried toluene for 1 hour, followed with methanol for 1 hour at a flow rate of 10 µL min^{-1}.

Chemical characterisation of the amino-modified silica monolith in terms of the amino groups attached to the surface of the silica monolith was achieved by washing the amino-modified silica monolith with 200 µL rhodamine B isothiocyanate (RBITC) (0.5 mg mL^{-1}) [Sigma-Aldrich, Poole, UK] in methanol to label the amino groups on the silica monolith. Then, the monolith was washed with methanol to remove the unbound dye (free RBITC). The fluorescence measurement was studied with an inverted light and fluorescence microscope [TE 2000, Nikon, Japan]. The excitation wavelength was 570 nm and the emission wavelength was 595 nm.

2.1.3.3 Immobilisation of TCEP on amino-modified silica monolith

The amino-modified silica monolith was utilised to prepare the reduction silica monolith. Immobilisation of the reducing reagent tris (2-carboxyethyl) phosphine hydrochloride (TCEP) on the surface of the amino-modified silica monolith in the glass microchip was chemically performed via the amino groups by the following procedure. Firstly, 0.3 g TCEP 98 % [Sigma-Aldrich, Poole, UK] was dissolved in 2.5 mL 0.1 M 4-morpholineethanesulfonic acid (MES) buffer solution (pH 6.5) [Sigma-Aldrich, Poole, UK], followed by adding 0.03 g N-(3-dimethylaminopropyl)-N′-ethylcarbodiimide hydrochloride (EDC) 98 % [Sigma-Aldrich, Poole, UK], and 0.015 g N-hydroxysulfosuccinimide sodium salt (Sulfo-NHS) 98.5 % [Sigma-Aldrich, Poole, UK]. The amount of Sulfo-NHS added was in the molar ratio 1:2 to EDC as described previously.[198] The mixture was stirred for 15 min to allow the activation of the carboxylic acid groups, and the mixture was pumped through the monolith for

immobilisation of TCEP onto the amino-modified silica monolith using a syringe pump at a flow rate of 1.5 µL min^{-1} for 24 hours at room temperature. After immobilisation, the microchip was washed with 0.1 M MES buffer solution (pH 6.5) for 1 hour at a flow rate of 10 µL min^{-1}, followed by washing with deionised water to remove unreacted materials.

2.2 Monolithic material characterisation

2.2.1 SEM analysis

The morphology of the dried monolith was characterised by scanning electron microscopy (SEM) using a Cambridge S360 scanning electron microscope [Cambridge Instruments, Cambridge, UK]. Images were obtained using an accelerating voltage of 20 kV and a probe current of 100 pA in high vacuum mode. The samples were coated with a thin layer of gold-platinum (thickness around 2 nm) using a SEMPREP 2 Sputter Coater [Nanotechnology Ltd., Sandy, UK].

2.2.2 BET analysis

The physical properties of the bulk monolith (surface area, average pore diameter, and the pore volume) were studied by the Brunauer-Emmett-Teller (BET) model using a Surface Area and Porosity Analyser [Micromeritics Ltd., Dunstable, UK]. The porous monolith was fabricated inside a 1 mL disposable plastic syringe using the same polymerisation mixture. Then, the monolithic rod was removed from the syringe and the unreacted materials were extracted via a Soxhlet extractor with methanol at 80 ºC for 24 hours. The monolith rod was dried using N_2 gas. The porous properties of the monoliths were determined using the BET isotherms of nitrogen adsorption and desorption at 77 K. The isotherms were analysed to get the surface area according to the BET model. The pore volume and pore size distribution of pores within the monoliths were measured from the nitrogen adsorption isotherm using the BJH (Barrett-Joyner-Halenda) model.

2.2.3 Measuring porosity

The total porosity $\emptyset_t$ equal to the volume fraction of both the micron-scale and nm scale pores of the cylindrical monolith samples was measured as described by Fletcher *et al.*[199] The porosity was measured by weighing the monolith when dried (i.e. with all pores containing only air) and when filled with deionised water**.**

$$\emptyset_t = \frac{W_M - W_T}{dLR^2\pi} \qquad (1)$$

Where W_T and W_M are the weights of the monolith when dried and when filled with water respectively, d is the density of water (at 23 ºC = 0.9975 g cm^{-3}), and L and R are the whole length and radius of the cylindrical monolith, respectively, which were measured using Draper 0-150 mm/0-6" Digital Vernier Caliper [Toolbox Ltd., Lincoln, UK]. The measurement was repeated five times and the average was taken.

2.2.4 Permeability of the monolith

The permeability of the organic monoliths was investigated by measuring the backpressure generated while pumping deionised water using an HPLC pump [Series 200 LC pump, PerkinElmer, California, USA] at different flow rates through the monolith.[200] Then, the value of the pressure in the system was recorded.

2.2.5 TEM analysis

The formation of mesopores in the silica-based monolith was confirmed by using transmission electron microscopy (TEM) [JEOL Ltd., Welwyn Garden City, UK]. The samples were crushed, mixed with 1 mL acetone and sonicated for 4 min. 5 µL aliquot was put onto lacy carbon coated 3 mm diameter copper grids. TEM images were acquired with a Gatan Ultrascan 4000 digital camera attached to a JEOL 2010 transmission electron microscope running at 20 kV.

2.2.6 EDX analysis

Energy dispersive X-ray (EDX) analysis was used to find the chemical composition of monolithic materials before and after modification of the surface of the silica-based

monolith. EDX analysis was performed using an INCA 350 EDX system [Oxford Instruments, Abingdon, UK].

2.2.7 Contact angle measurement

Contact angle measurement was used to verify chemical surface modification. After modification of the micropipettes using the same procedures that used before for fabrication of the amino-modified silica monolith, and immobilisation of TCEP on the amino-modified silica monolith, they were dried in the oven at 30 °C for 24 hours. Then, the deionised water contact angles for the empty micropipette, amino-modified micropipette, and TCEP-immobilised micropipette were measured by using Image J software for five different samples.

2.2.8 FT-IR spectroscopy

The FT-IR spectra were collected in the attenuated total reflectance (ATR) mode using a PerkinElmer RX FTIR ×2 with diamond ATR, DRIFT attachment [PerkinElmer, Buckinghamshire, UK] to compare the infrared spectra before and after modification of silica-based monoliths. The IR range was from 600 to 4000 cm^{-1}, six scans with resolution 4 cm^{-1} were taken.

2.2.9 Combustion elemental analysis

Combustion elemental analyses of silica monolith before and after derivatisation with APTES were performed using a Fisons instrument Carlo Erba 100 C H N S analyser [Carlo Erba Instruments, Wigan, UK]. Each analysis was repeated three times with three different samples. The surface coverage of aminopropyl ligands on the silica-based monolith was calculated from the carbon and nitrogen content as measured using elemental analysis of different parts of the amino-bonded silica monolith rod. The surface coverage of aminopropyl ligands (αNH_2) was calcuated using equation 2 [201]:

$$\alpha NH_2[\mu mol\ m^{-2}] = \frac{10^6}{S_{BET}\left[M_{Element} \times 100 \times \frac{n_c}{P_c} - M_{Ligand}\right]} \qquad (2)$$

Where S_{BET} is the surface area in m^2 g^{-1} of the bare silica-based monolith that was calculated using BET analysis, $M_{Element}$ is the mass of the calculated element while M_{Ligand} is the molecular mass of the attached ligand. n_c or n_N is the number of carbon or nitrogen atoms per bonded ligand, respectively, and P_c or P_N is the percentage of carbon or nitrogen in the aminopropyl ligands measured using elemental analysis.

2.3 Applications of the monolithic materials

2.3.1 Protein extraction using the organic monolith

2.3.1.1 Using organic monolith prepared in a borosilicate tube

After fabrication of the organic monolithic stationary phase, its performance was checked using eight standard proteins, which were bovine pancreas insulin, bovine heart cytochrome C, chicken egg white lysozyme, myoglobin from horse heart, β-lactoglobulin from bovine milk, ovalbumin from chicken egg white, human hemoglobin and bovine serum albumin [Sigma-Aldrich, Poole, UK]. The proteins (60 µM) were dissolved in 10 mM ammonium acetate buffer solution (pH 9.3) [Sigma-Aldrich, Poole, UK]. All experiments were carried out at an ambient temperature around 23 ºC. All solutions and the protein sample were injected using the syringe pump at a flow rate of 10 µL min^{-1} for all steps except for loading the sample (5µL min^{-1}). The proteins were extracted individually to calculate the extraction efficiency for each protein.

The steps of protein extraction were conditioning and equilibration of the sorbent, then loading the protein sample, washing the monolith, and finally elution of the protein. Table 2.3 illustrates the steps of protein extraction using the polymer-based monolith. The organic polymeric monolith was activated with 400 µL acetonitrile (ACN) and the solvent was discarded. Then, it was equilibrated with 400 µL 10 mM ammonium acetate buffer solution (pH 9.3) and the buffer solution was discarded. The protein sample (1000 µL) was loaded and then the sorbent was washed with 200 µL 10 mM ammonium acetate buffer solution (pH 9.3). Finally, 500 µL 20 % ACN containing 0.1% trifluoroacetic acid (TFA) [Fisher Scientific, Loughborough, UK] was injected via the sorbent and the eluent was collected into an Eppendorf tube.

Step	**Procedure**
Condition	Aspirate 400 µL ACN and discard it.
Equilibration	Aspirate 400 µL 10 mM ammonium acetate buffer solution (pH 9.3) and discard it.
Apply sample	Aspirate 1000 µL protein sample dissolved in 10 mM ammonium acetate buffer solution (pH 9.3).
Washing	Aspirate 200 µL 10 mM ammonium acetate buffer solution (pH 9.3) and discard it.
Elution	Aspirate 500 µL 20 % ACN (0.1 % TFA) and dispense into the Eppendorf tube.

Table 2.3 Purification profile of proteins on the polymer-based monolith.

A sample of the eluent was injected directly into the HPLC-UV detector using a PerkinElmer LC 200 series binary pump, Symmetry C_8 column, 4.6 mm × 250 mm packed with silica particles (size 5 µm) [Thermo Fisher Scientific, Loughborough, UK] and a PerkinElmer 785A UV/Visible Detector [PerkinElmer, California , USA]. The mobile phase was acetonitrile-purified water (50:50) in the presence of 0.1 % (TFA) under isocratic conditions. The sample injection volume was 20 µL. The flow rate was set at 1 mL min^{-1} and all experiments were performed at ambient temperature around 23 °C. Three different wavelengths were investigated which were 210, 254, and 280 nm.

The purpose of using HPLC-UV detection was to study the peak area obtained for the preconcentrated proteins and compare them with the peak areas of the non-processed protein standard solutions to calculate the extraction recovery (ER) that was calculated as given by Furuno *et al.*[202] using the following equation:

$$Extraction\ recovery\ (\%) = \frac{I_{elute}}{I_{total}} \times 100 \qquad (3)$$

Where I_{elute} is the amount eluted form the sorbent, and I_{total} is the amount of protein introduced to the sorbent.

2.3.1.2 Using organic monolith prepared in a glass microchip

The performance of the microfluidic device containing the polymer-based monolith was studied. The four standard proteins (insulin, cytochrome C, myoglobin, and hemoglobin) were dissolved in 10 mM ammonium acetate buffer solution (pH 9.3) and used in the extraction trials. The proteins were extracted using the polymer-based monolith prepared in the glass microchip using the same procedure previously employed with the polymer monolith prepared in the borosilicate tube, except the flow rates of all solutions and the protein sample were decreased to 3.5 µL min^{-1}. In addition, the amounts of the protein sample and reagents were decreased. The polymer-based monolith inside the microchip was activated with 100 µL ACN, and was equilibrated with 100 µL 10 mM ammonium acetate buffer solution (pH 9.3). The protein sample (800 µL) was applied to the monolithic microchip. After extraction, the microchip was washed with 50 µL 10 mM ammonium acetate buffer solution (pH 9.3).The elution of the proteins from the glass microchip was achieved using 150 µL 20 % ACN (0.1 % TFA) that was injected into the microchip and the eluent was collected into the Eppendorf tube and analysed using HPLC-UV detection. The extraction recovery was calculated using equation 3.

2.3.2 Protein extraction using the inorganic monolith

2.3.2.1 Using the inorganic monolith prepared in a shrinkable tube

The proteins were extracted following the procedure as described by Alzahrani and Welham.[203] The eight standard proteins; insulin, cytochrome C, lysozyme, myoglobin, β-lactoglobulin, ovalbumin, hemoglobin and bovine serum albumin were used at a concentration of 60 µM. The steps that were used for non-modified silica monolith are summarised in table 2.4 and for modified silica with octadecyl groups in table 2.5.

Step	Procedure
Condition	Aspirate 400 µL ACN and discard it.
Equilibration	Aspirate 400 µL 20 mM ammonium hydrogen carbonate buffer solution (pH 8.0) and discard it.
Apply sample	Aspirate 1000 µL protein sample dissolved in 20 mM ammonium hydrogen carbonate buffer solution (pH 8.0).
Washing	Aspirate 200 µL 20 mM ammonium hydrogen carbonate buffer solution (pH 8.0) and discard it.
Elution	Aspirate 500 µL 20 % ACN (0.1 % TFA) solution and dispense into the Eppendorf tube.

Table 2.4 Purification profile of proteins on the non-modified silica-based monolith.

Step	Procedure
Condition	Aspirate 400 µL ACN (0.1 % TFA) solution and discard it.
Equilibration	Aspirate 400 µL ACN and discard it.
Apply sample	Aspirate 1000 µL protein sample prepared in 50 mM tris-HCl buffer solution (pH 7.0) containing 10 mM NaCl and adjusted with 0.1 % TFA.
Washing	Aspirate 200 µL 50 mM tris-HCl buffer solution (pH 7.0) and discard it.
Elution	Aspirate 500 µL 60 % ACN (0.1 % TFA) solution and dispense into the Eppendorf tube.

Table 2.5 Purification profile of proteins on the C_{18}-bonded silica monolith.

The proteins were dissolved individually in 20 mM ammonium hydrogen carbonate buffer solution (pH 8.0) [Sigma-Aldrich, Poole, UK] for non-modified silica monolith and in 50 mM tris-HCl buffer solution (pH 7.0) containing 10 mM sodium chloride (NaCl) [Sigma-Aldrich, Poole, UK] and adjusted with 0.1 % TFA in case of the performance examination of C_{18}-bonded silica monolith. All experiments were carried out at an ambient temperature of around 23 ºC.

All solutions were injected using the syringe pump via the borosilicate tube at a flow rate of 10 µL min^{-1} for all steps except for loading the sample (5 µL min^{-1}). The proteins were extracted individually to calculate the extraction recovery for each protein. The non-modified sorbent was conditioned with 400 µL ACN. Then, the sorbent was equilibrated using 400 µL 20 mM ammonium hydrogen carbonate buffer solution (pH 8.0). After that, 1000 µL of the sample solution was applied. After loading the sample solution through the monolith, the sorbent was rinsed with the washing solvent, which was 200 µL 20 mM ammonium hydrogen carbonate buffer solution (pH 8.0). Finally, proteins were eluted from the sorbent using an eluting solvent, which was 500 µL 20 % ACN (0.1 % TFA) solution and collected into the Eppendorf tube.

For C_{18}-bonded modified silica monolith, the sample was adjusted with 0.1 % TFA before extraction. The sorbent was cleaned with 400 µL ACN (0.1 % TFA) solution and then equilibrated with 400 µL ACN. After the sample application (1000 µL sample), the monolith was washed with 200 µL 50 mM tris-HCl buffer solution (pH 7.0). Finally, the sample was eluted using 500 µL 60 % ACN (0.1 % TFA) solution and dispensed into the Eppendorf tube. The eluent was injected into the HPLC-UV instrument, and the extraction recovery was calculated as previously described.

2.3.2.2 Extraction of proteins from spiked sample

The performance of the octadecylated silica monolith microchip was checked using a spiked sample. The standard proteins were dissolved individually in a 5 mL mixture consisting of 1 mL phosphate-buffered saline (PBS) tablet [Sigma-Aldrich, Poole, UK] that was dissolved in 100 mL deionised water and yielded 137 mM NaCl, 2.7 mM KCl and 10 mM phosphate buffer solution (pH 7.4 at 25 °C), and 4 mL 50 mM tris-HCl buffer solution (pH 7.0) containing 10 mM sodium chloride (NaCl), 120 µM

3-[(3-cholamidopropyl) dimethylammonio]-1-propanesulfonate (CHAPS) [Sigma-Aldrich, Poole, UK], and 5 µL TFA.

The standard proteins were purified using the same procedure and experimental conditions used before to purify proteins using the octadecylated silica monolith in shrinkable tube (section 2.3.2.1), except the amounts of the sample and reagents were reduced. The sorbent inside the microchip was cleaned with 100 µL ACN (0.1 % TFA) solution, and then equilibrated with 100 µL ACN. After the sample application (500 µL), the impurities were washed out with 100 µL 50 mM tris-HCl buffer solution (pH 7.0). Finally, the protein was eluted using 150 µL 60 % ACN (0.1 % TFA) solution and dispensed into the Eppendorf tube. The efficiency of extraction was calculated as previously described. The mobile phase was acetonitrile-water (50:50) in the presence of 0.1 % (TFA) and the flow rate was 0.3 mL min^{-1}. The detection wavelength was adjusted to 210 nm.

The performance of the octadecylated silica monolith was compared with a commercial SPE cartridge, Discovery DSC-18 containing polymerically bonded silica particles (50 µm) octadecyl coated and endcapped, frit: polyethylene (PE) [Supelco Inc., Bellefonte, PA, USA] under the same conditions except all the solutions were processed using a vacuum rather than the syringe pump to pull the solutions through the cartridge.

2.3.2.3 Preconcentration of proteins from a real sample

Two different real samples were used to check the performance of the fabricated octadecylated silica monolith microchip. They were skimmed cows' milk, and hen egg white.

250 µL skimmed milk containing 0.5 % fat [local supermarket, Hull, UK] was diluted with 250 µL tris-HCl buffer solution (50 mM, pH 7.0) containing 10 mM NaCl and the sample acidified with 0.1 % TFA.

A fresh hen's egg [local supermarket, Hull, UK] was used and the egg white was manually separated from the egg yolk, then 150 µL of egg white was diluted with 350 µL tris-HCl buffer solution (50 mM, pH 7.0) containing 10 mM NaCl and then the pH of the sample solution was adjusted with 0.1 % TFA.

The proteins in the skimmed cows' milk and the hen egg white were preconcentrated using the same procedure that was used to preconcentrate standard proteins from spiked sample (section 2.3.2.2). The performance of the octadecyl-functionalised silica monolith was compared with that of the conventional cartridge. In addition, the performance of the octadecylated silica monolith microchip in preconcentration of real samples was studied using matrix-assisted laser desorption/ionisation time-of-flight mass spectrometry (MALDI-TOF-MS) using a ReflexIV instrument [Bruker Daltonics, Bremen, Germany].

Two MALDI sample preparation methods were investigated. The first method was carried out by mixing 0.5 µL of the eluent with 15 µL of the matrix solution that was prepared by dissolving 4-hydroxy-α-cyano cinnamic acid (4HCCA) [Sigma-Aldrich, Poole, UK] in 20 µL 2-propanol [Fisher Scientific, Loughborough, UK], followed by adding 30 µL purified water and 10 µL formic acid [Fisher Scientific, Loughborough, UK]. Then, the saturated matrix solution was vortexed followed by centrifuging for 5 min. 1 µL of the sample-matrix solution was placed onto the MALDI plate and left to dry at room temperature. When the crystal formed, 0.5 µL of cold water was spotted over the crystal.[204]

The second method was the two layer sample preparation method as previously reported.[205] The first layer was 6 mg mL^{-1} sinapinic acid (3,5-dimethoxy-4-hydroxycinnamic acid) [Sigma-Aldrich, Poole, UK] in 60 % methanol/acetone. 0.5 µL of the first layer was deposited on a MALDI target and allowed to dry in order to form a microcrystalline layer. The second layer solution was 1 µL sample solution and 9 µL saturated matrix solution of sinapinic acid in 25 % ACN in distilled water containing 0.1 % TFA. 0.5 µL of the second layer solution (sample/matrix) was placed on the microcrystalline first layer and allowed to dry.

After drying, the MALDI target was inserted into a mass spectrometer for analysis. The instrument was equipped with a pulsed nitrogen laser (337 nm, pulse width 4 ns), and operated at positive linear mode at accelerating voltages of 20-25 kV. All mass spectra were acquired in the linear positive ion mode. No baseline correction was applied to the mass spectra shown in the figures.

2.3.3 Reduction and alkylation of proteins

2.3.3.1 Two-step procedure

The activity of the glass microchip containing TCEP-immobilised silica monolith was evaluated for its efficiency in the reduction of the disulphide bonds in the proteins. The standard proteins that were used for studying the performance of the fabricated microchip were insulin and lysozyme. The concentration of the standard proteins was 60 µM. They were dissolved separately in 50 mM ammonium hydrogen carbonate buffer solution (pH 8.0). The buffer was prepared immediately before use by dissolving 98.8 mg in 25 mL of deionised water. Before reduction and alkylation of the proteins, protein denaturation was accomplished by mixing 100 µL of the protein sample with 100 µL 8 M urea solution (480.5 mg mL^{-1}) prepared in purified water in a 1 mL Eppendorf tube then placing it in the oven at 37 °C for 1 hour.[206] Subsequently, the denatured protein (100 µL) was injected inside the microchip using a syringe pump at a flow rate of 10 µL min^{-1}. Both ends of the ETFE tubes were sealed with blu-tak. The microchip was incubated at room temperature for 1 hour, or the microchip was kept in a humidified chamber (a petri dish partially filled with deionised water) in order to decrease evaporation of the solution in the oven at 60 ºC for 30 min.[146]

The reduced protein was eluted from the microchip using the alkylating reagent, which was 500 µL 15 mM iodoacetamide (IAA) solution [Sigma-Aldrich, Poole, UK] that was dissolved in 50 mM ammonium hydrogen carbonate buffer solution (pH 8.0). The alkylating reagent was prepared immediately before use, since IAA is unstable. The IAA solution was injected onto the microchip, which was covered with foil, at a flow rate of 10 µL min^{-1} and the reduced protein was collected into an Eppendorf tube, which was incubated at room temperature for 1 hour or in the oven at 60 ºC for 30 min.

2.3.3.2 One-step procedure

A mixture consists of 40 µL denatured protein and 60 µL 15 mM IAA solution was injected into the fabricated microchip at a flow rate 10 µL min^{-1}. During injection of the solution, the microchip was covered with foil. Both ends of the ETFE tubes were sealed and the microchip was placed in the oven at 60 °C for 30 min. The microchip was placed on a petri dish partially filled with deionised water. After incubation, the

reduced and alkylated protein was eluted from the microchip using 300 µL 50 mM ammonium hydrogen carbonate buffer solution (pH 8.0).

The performance of the glass microchip containing the TCEP-immobilised silica monolith was checked using MALDI-TOF-MS and the MALDI sample was prepared using the two-layer sample preparation method. The MALDI-TOF mass spectrum of the reduced and alkylated protein was compared with the MALDI-TOF mass spectrum of the non-processed protein.

3.0 Results and discussion: fabrication of monolithic materials

The main steps in proteomics are sample preparation, extraction, digestion, separation, and detection. Efficient extraction of proteins by removing interfering materials such as salts, buffer, and detergents is the most critical step in proteomics, and is necessary because most instruments cannot handle such contaminated sample matrices directly.[17, 163, 207] In addition, analysis of proteins at low concentrations in complex matrices requires an SPE technique to preconcentrate the sample, and improve the detection sensitivity.[208] As mentioned in the introduction, new materials that can be used as a sorbent are the recently invented monolithic materials. Based on the nature of materials used in their construction, these monolithic materials can be divided into polymer- and silica-based monoliths.[209, 210]

It is known from the literature that the reduction of the disulphide bonds in proteins can help the proteins unfold and this can improve the proteolytic digestion of proteins by making specific locations accessible to enzymes. Therefore, it is important to make polypeptides unfold by reduction of the disulphide bonds between cysteine residues within the amino acid chains.[134]

In this chapter, evaluation of the fabrication of polymer- and silica-based monoliths will be discussed. In addition, a new procedure used to immobilise the reducing reagent (TCEP) on the surface of the silica-based monolith will be assessed. Moreover, different characterisation tests of the monolithic materials will be discussed.

3.1 Fabrication of the organic monolith

The aim of this study was to fabricate an organic polymer-based monolith and evaluate it as an SPE sorbent for protein extraction. The reason for choosing this type of monolithic material is because the preparation of an organic polymer-based monolith is fast and simple. In addition, they are stable over a wide range of pH values, and can be washed without damage with caustic mobile phase.[211]

3.1.1 Pretreatment of the borosilicate tube

The first step in the creation of the organic polymer-based monolithic stationary phases inside the borosilicate tube was the pretreatment of the borosilicate tube, which was carried out in order to clean and activate the inner wall surface of the tube. This was performed by washing the borosilicate tube with acetone to clean out any organic materials and then it was rinsed with water to flush out any acetone remaining. Treatment with a basic solution such as potassium hydroxide solution (KOH) or sodium hydroxide solution (NaOH) can hydrolyse siloxane bridge and form silanol groups.[56, 212] In this work, 0.2 M sodium hydroxide solution (NaOH) was used to activate the surface of the tube. This was followed by washing the tube with deionised water to remove any remaining basic solution. Finally, the tube was washed with 0.2 M hydrochloric acid solution (HCl) to neutralise and remove alkali metal ions. The reaction of the surface of the borosilicate tube with the pretreatment chemicals is depicted schematically in figure 3.1.

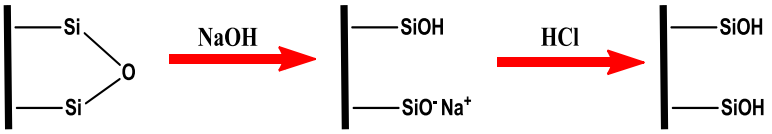

Figure 3.1 Schematic depiction of the reaction of the surface of the borosilicate tube with the pretreatment chemicals used for pretreatment of the borosilicate tube.[213]

After activation of the surface of the borosilicate tube, it was silanised before fabrication of a porous polymer monolith (PPM) inside the borosilicate tube. The benefit of the silanisation is to ensure covalent attachment of the monolith, to avoid the effect of shrinkage during the polymerisation reaction, and prevent the occurance of undesired interactions of the proteins with the silanol groups of the borosilicate tube.[214]

The silanisation of the surface of the tube was based on static coating using a silanising agent 3-(trimethoxysilyl) propyl methacrylate (γ-MAPS), which is a bifunctional agent and has the ability to covalently anchor trimethoxysilane functional groups of the silanising agent to some of the silanol (Si-OH) groups in the borosilicate tube. Subsequently, the methacrylate groups of the silanising agent will participate in the polymerisation reaction causing the porous continuous beds to be bound covalently to the inner wall of the tube.[215] Figure 3.2 illustrates schematically the reaction of the trimethoxysilane functional group of γ-MAPS, the silanising agent, in the presence of a catalyst, glacial acetic acid, with the silanol groups of the surface of the borosilicate tube.

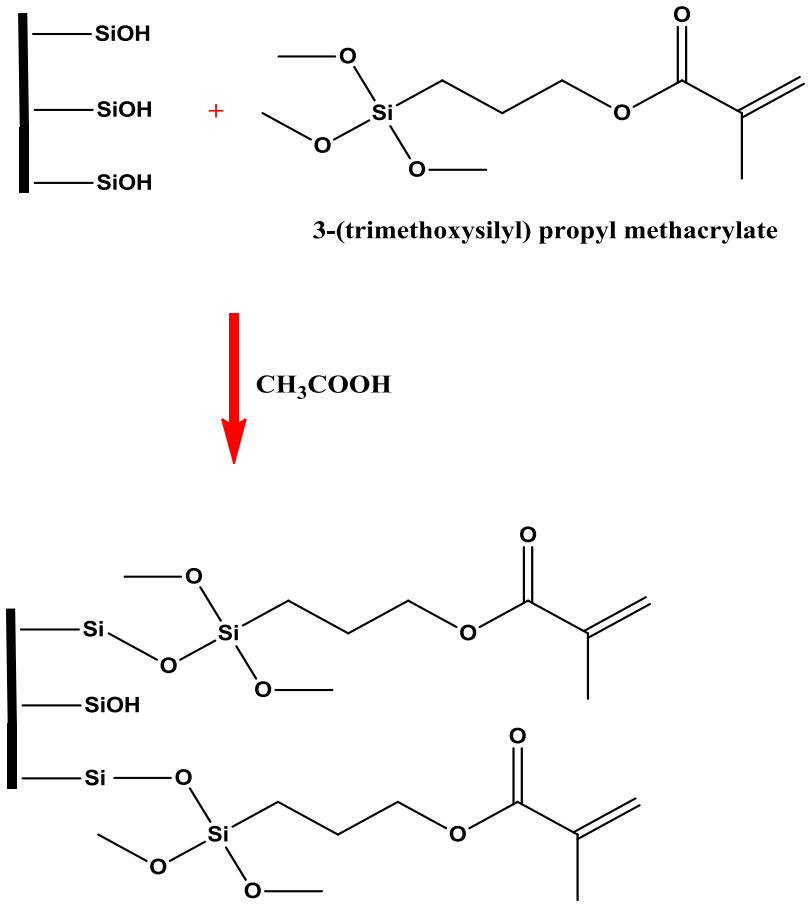

Figure 3.2 Schematic representation of silanising the surface of the borosilicate tube using 3-(trimethoxysilyl) propyl methacrylate.[84]

In order to study the effect of the silanisation step on the fabrication of the polymer-based monolith, two borosilicate tubes were filled with the monolithic materials; one of the tubes was silanised with γ-MAPS while the other tube was not silanised. After formation of the monolith inside the tubes, the appearance of the monolith was observed using scanning electron microscopy (SEM). The SEM micrograph in figure 3.3 (A) shows that part of the monolith does not anchor to the inner walls of the tube and this can affect the work of the monolith by resulting in the removal of the monolith from the tube, particularly under hydrodynamic flow conditions. Figure 3.3 (B) shows the covalent binding of the monolith to the inner walls of the tube, and the boundary between the monolithic polymer and the inner wall of the borosilicate tube appears smooth without any disconnection.

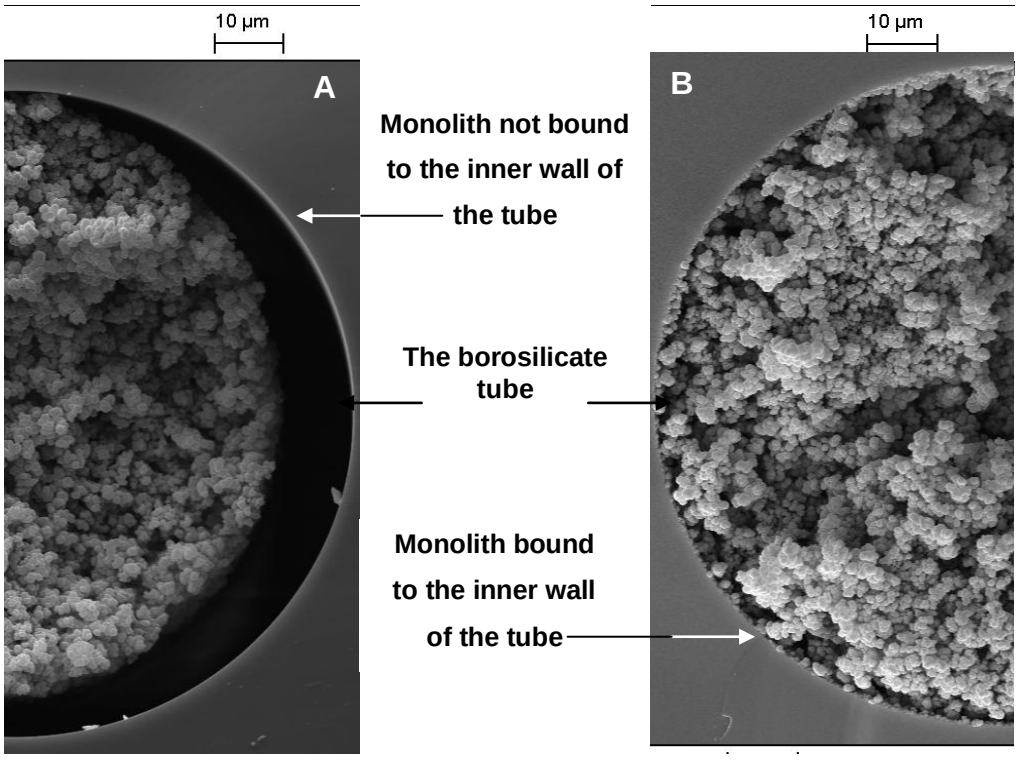

Figure 3.3 SEM images showing a part of the cross-section of the borosilicate tube: (A) without silanisation, and (B) with silanisation. The silanisation mixture was 20 % (v/v) 3-(trimethoxysilyl) propyl methacrylate in 95 % ethanol with its pH adjusted to 5 with glacial acetic acid, the mixture was injected through the tube using a syringe pump at a flow rate of 2 µL min^{-1} for 1 hour.

It was concluded that the silanisation step is necessary in order to bind the monolith covalently to the walls of the tube; otherwise, voids will be formed at the monolith wall interface.

3.1.2 Fabrication of poly (BuMA-*co*-EDMA) monolith

A methacrylate-based monolith was chosen for the organic polymer-based monolith in this study as this is widely used.[216] The polymerisation mixture consisted of the monovinyl (BuMA) and divinyl monomer (EDMA) in the presence of porogenic solvents and a free radical initiator (DMPA). Although use of long alkyl chain non-polar methacrylate monomers to prepare the methacrylate-based monolith can increase the hydrophobicity of the continuous bed, increasing the interaction between the bed and the protein during the extraction compared with the short alkyl chain monomer (BuMA), it is reported that they have limited solubility.[89] Therefore, BuMA was chosen as a monomer in this study.

The free radical polymerisation reaction was initiated using UV light (photoinitiation process) at room temperature rather than using a water bath (thermal initiation process). The reason for choosing the photoinitiation method for preparation of the organic monolith is because the desired length of the borosilicate tube to be exposed to the light source can be controlled easily by using electrical masking tape to cover the rest of the tube and this would help to facilitate fabrication of the polymer-based monolith inside the microfluidic device. Poly (butyl methacrylate-*co*-ethylene dimethacrylate) stationary phase was prepared as described by Frechet *et al.*[193] using the same polymerisation mixture except the photoinitator was changed from 2,2′-azobis(2-methylpropionitrile) (AIBN) to DMPA to avoid formation of voids during the polymerisation reaction. The voids reported are thought to be due to the generation of nitrogen gas during polymerisation.[217]

The mechanism of free radical polymerisation involves three steps: initiation, propagation, and termination.[218] Firstly, the initiator DMPA was decomposed by using UV light into inhibiting species (the acetal fragment), and the initiating species (the benzoyl fragment), which caused the free radical polymerisation reaction to start.[219] Figure 3.4 illustrates the decomposition of the initiator (DMPA). The electron pair in the bond of DMPA is broken, resulting in formation of two initiator fragments, acetal

and benzoyl fragments, each with one unpaired electron. These fragments with unpaired electrons are the free radicals.

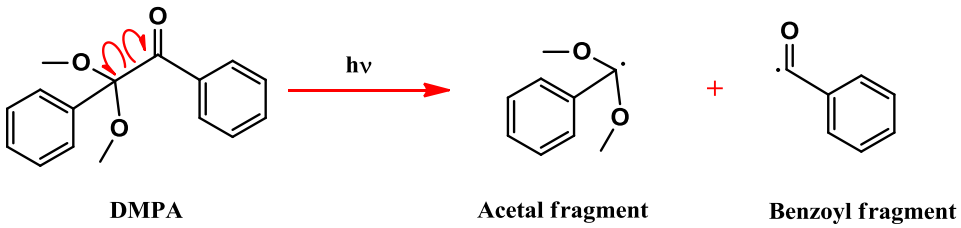

Figure 3.4 The UV induced decomposition of 2,2-dimethoxy-2-phenylacetophenone (DMPA) into passive initiating (acetal fragment), and active initiating (benzoyl fragment).

The active initiating (benzoyl fragment) will attack the carbon-carbon double bond in the monomer (BuMA). As a result, a new chemical bond will be formed between the initiator fragment and one of the double bond carbons. In addition, a new free radical will be formed on the carbon atom. The process of the reaction of the initiator fragment with the monomer molecule is called the initiation step of the free radical polymerisation, as illustrated by figure 3.5 (A). The next step involves adding further monomer molecules in order to the growing chains and this step is called the propagation step, as shown in figure 3.5 (B). The last step of the free radical polymerisation is the termination step that occurs when two free radicals react with each other, as shown in figure 3.5 (C).

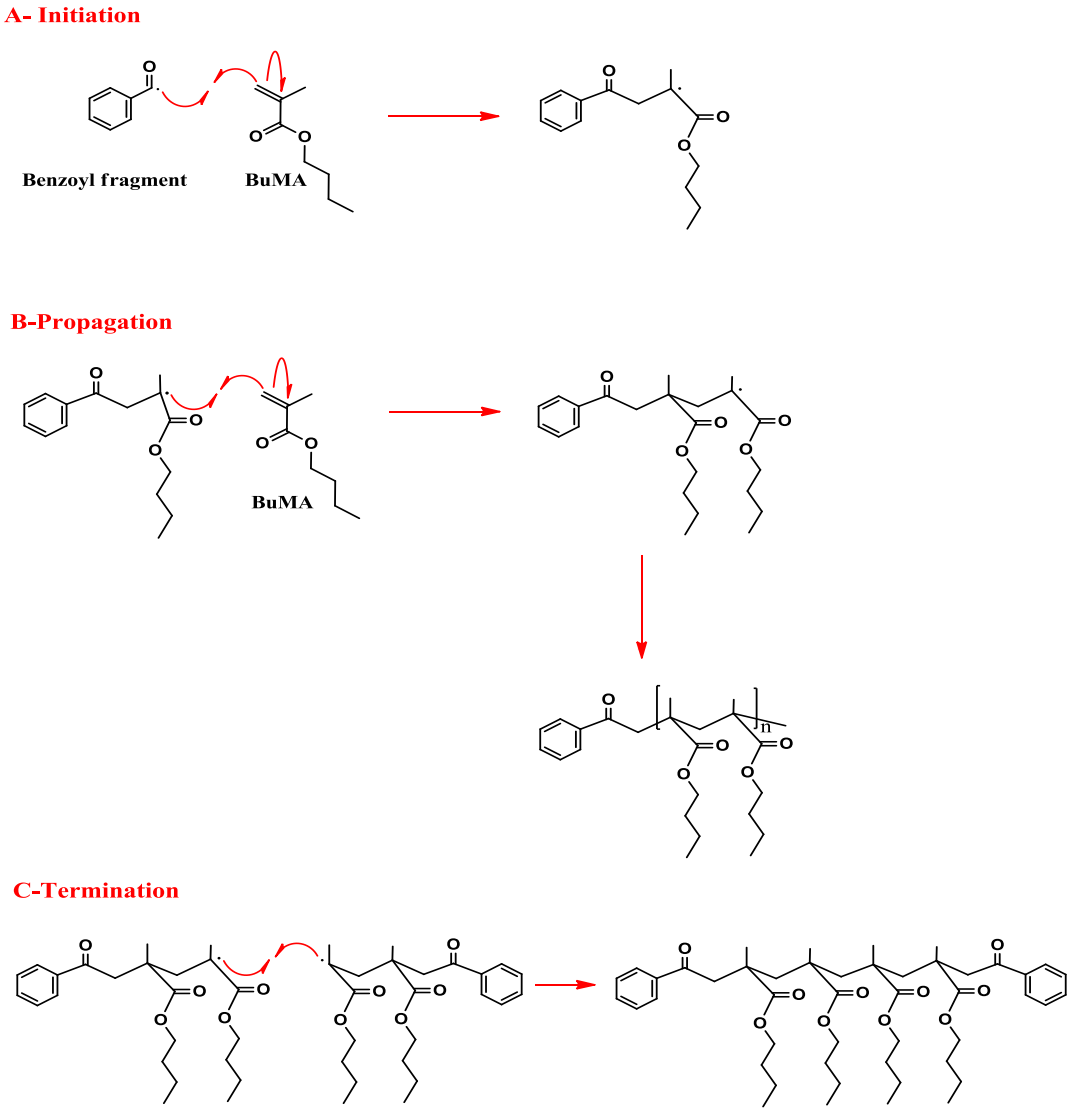

Figure 3.5 Reaction mechanism of the free radical polymerisation of BuMA initiated with benzoyl fragment.

After placing the tube filled with the polymerisation mixture under the UV lamp, the polymer started to form and precipitated. If the appearance of the polymer-based monolith was satisfactory (bright white material), then the monolithic tube was washed. The solvents, which formed the porogenic system, the unreacted monomeric materials, and soluble oligomers remaining in the pores were flushed away from the tube using a syringe pump (hydrodynamic approach) at a flow rate of 2 µL min^{-1} for

12 hours in order to prevent further polymerisation reaction, since the monomer and the crosslinker have the affinity to continue the polymerisation reaction.[220]

3.1.3 Optimisation of fabrication of the organic monolith

It was very important before using the prepared poly (BuMA-*co*-EDMA) monolith for protein extraction to optimise its physical properties in order to get an organic monolith with high mechanical stability and good permeability. Many factors can affect the porous properties of a polymer-based monolith, such as the polymerisation time, the UV lamp power, monomer to porogen ratio, monomer to crosslinker ratio, concentration of the photoinitiator, and composition and type of the porogenic solvent system.[81, 221]

Increasing the concentration of the initiator can cause an increase in the number of the free radicals and this can lead to large numbers of nuclei, which results in decreasing the size of the pores, forming a condensed monolith, while decreasing the amount of the initiator results in a long reaction time.[69] Therefore, the concentration of the initiator was not changed. Another factor that can be changed is the ratio of the total monomer to the porogenic solvent system ratio or crosslinker ratio, which can increase the permeability of the monolith, but this can affect the homogeneity and rigidity of the monolith, or decrease the median pore size and form highly crosslinked globules.[222] In this study, it was decided to investigate the energy of the UV light, time of exposure to the UV light, and the type of the porogenic solvent system.

3.1.3.1 Investigation of UV light energy and exposure time

Since the irradiation process was used to initiate the polymerisation reaction, the influence of the UV light energy on the preparation of the polymer-based monolith was investigated. The experiment was carried out by filling the borosilicate tube with the polymerisation mixture and performing the polymerisation reaction using UV light with different wavelengths, 254 and 365 nm. It was expected that using the short wavelength (254 nm) would be best for the polymerisation reaction because short wavelength light provides more energy than longer wavelength (365 nm), since the wavelength is inversely proportional to the energy and the reaction time could be reduced by increasing the light energy. However, it was observed that the photoinitiation reaction was faster and more polymerisation was obtained by using the

long wavelength, as was also observed by other groups.[223] The reason for that is acrylate monomers absorb the UV light in the range 200-300 nm, reducing "the energy dose" and decreasing the efficiency of the photoinitiator, when using UV light with a wavelength of 254 nm. Therefore, it was decided to use the longer wavelength (365 nm) for the polymerisation reaction in this study.

The effect of the duration of exposure to the UV light on the preparation of the polymer-based monolith was examined at eight different time-points in order to find the most suitable time to complete the polymerisation reaction. The different exposure times investigated were 8, 10, 12, 14, 16, 18, 20, and 22 min. A good indication of forming continuous beds was the appearance of the porous polymer monolith, which was a bright white material. It was found that the irradiation time was an important factor affecting the polymerisation reaction as evident from figure 3.6, which shows the difference in the appearance of the organic monoliths prepared in the sample vials. The first conclusion derived from the figure is related to the effect of the polymerisation time on the formation of the organic monolith. It was observed that the exposure time 8 min was not enough to fabricate the organic monolith in the sample vials. Therefore, the exposure time was increased by 2 min each time up to 20 min. It was observed that the white solid monolithic material was increased while the polymerisation mixture, which contained the unreacted monomeric materials and the casting solvents, was decreased. The polymerisation reaction was changed to 22 min, it was observed that there was no difference in the white solid monolithic material in the sample vial; however, it was found that the monolithic polymer tube could not be washed. The reason for that could be because increasing the duration of exposure to the UV light can generate smaller pores and this can decrease the permeability of the monolith.[200] It was concluded that the optimum irradiation time to get polymer-based monolith in the tube was 20 min because the appearance of the polymeric monolithic stationary phases was satisfactory compared with the other monoliths, and the monolithic tube was still washable.

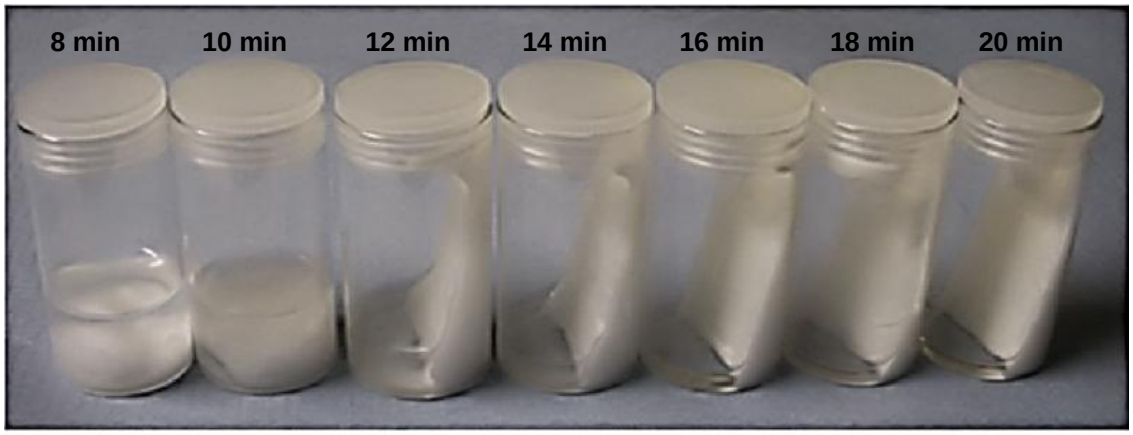

Figure 3.6 Effect of the duration of exposure to the UV lamp on the formation of the poly (BuMA-*co*-EDMA) monolith.

3.1.3.2 Investigation of binary porogenic solvent system

The purpose of using the porogenic solvent is to dissolve monomer, crosslinker, and photoinitiator without reacting during the polymerisation reaction in order to get a homogeneous solution. In addition, the benefit of the porogenic solvent is to form the pores since the monomer is soluble in the porogen while the polymer is insoluble; therefore, the fraction of the solvent in the polymerisation reaction is related to the fraction of the pores in the monolith.[224]

The composition of the binary porogenic solvent system was investigated to control the physical characteristics of the organic monolith. The purpose of changing the composition of the binary porogenic system was to find a porogenic solvent system that can offer a monolith with a high surface area.[87, 225] In addition, the chosen porogenic solvent system should offer macroporous materials, since the pore diameter can affect the permeability of the monolith. Therefore, the chosen porogenic solvent system should be a mixture of a good solvent that forms micropores due to the later phase separation and a poor solvent that forms macropores and results in good permeability.[193] Another important property of the prepared polymer-based monolith is that it does not shrink or swell when using organic solvents, because this can affect reproducibility and causes a deficiency in mechanical stability that would cause a short service life.[221]

A common solvent for the preparation of methacrylate-based monoliths is methanol (MeOH).[226] Therefore, it was used here as the main porogenic solvent with co-porogen that was one of ethanol, acetonitrile, chloroform, hexane, tetrahydrofuran, 1-propanol, ethyl acetate, or cyclohexanol. The effect of the porogenic solvent system on the properties of the organic monolith was studied by using the same polymerisation mixture, except the porogenic solvent was a mixture of methanol and co-porogen (50:50). The polymerisation mixture was placed in a 1 mL plastic disposable syringe and the polymerisation reaction was carried out under identical conditions. After the polymerisation reaction, samples of the monoliths were studied. Figure 3.7 shows the appearance of the poly (BuMA-*co*-EDMA) monoliths prepared using different porogenic solvent systems before washing them with methanol. The porogenic solvent systems that gave a bright white material besides methanol were MeOH/EtOH, MeOH/1-propanol, and MeOH/hexane.

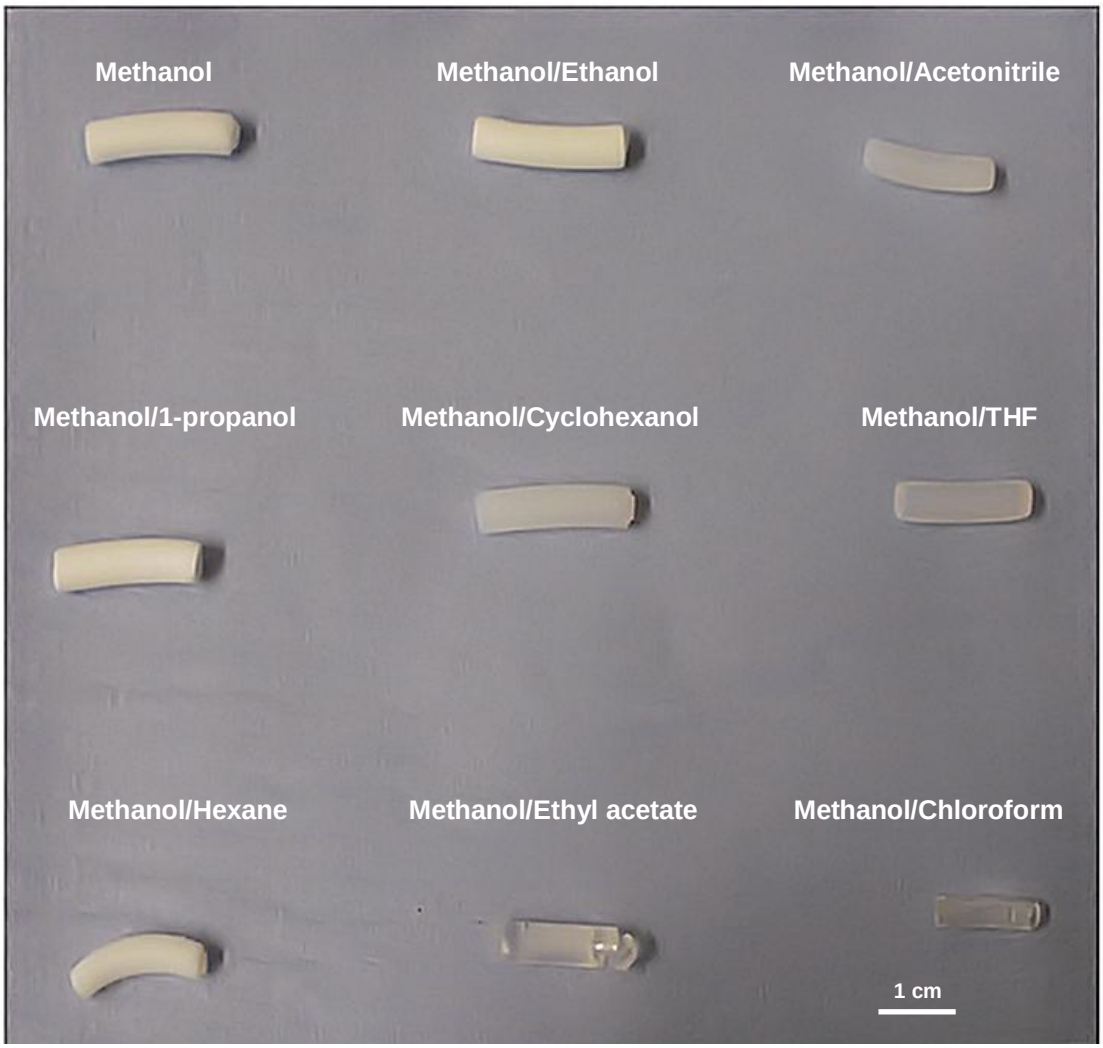

Figure 3.7 The appearance of the poly (BuMA-*co*-EDMA) monoliths prepared using different porogenic solvent systems before washing them with methanol. The polymerisation mixture was BuMA (1.422 g), EDMA (0.96 g), DMPA (0.024 g), and the porogenic solvent (3.6 g) was 50:50 MeOH and co-porogen.

After preparation of the monolithic polymer rod, it was washed by Soxhlet extraction using methanol at 80 ºC for 24 hours to remove the unreacted monomeric materials. The diameter of the cylindrical monolithic rod was measured using caliper to determine the degree of shrinkage in the prepared monolithic rod after washing with methanol. Figure 3.8 shows the difference in appearance of the poly (BuMA-*co*-EDMA) monoliths after washing with methanol. As can be seen in the figure, the monolithic polymer rods, which were not affected when they were washed with

methanol and were not shrunk or swollen compared with MeOH only (4.06 ± 0.07 mm), were the monolithic rods prepared using MeOH/EtOH (4.04 ± 0.16 mm) and MeOH/1-propanol (4.12 ± 0.05 mm) while the rest of the monoliths were shrunk significantly.

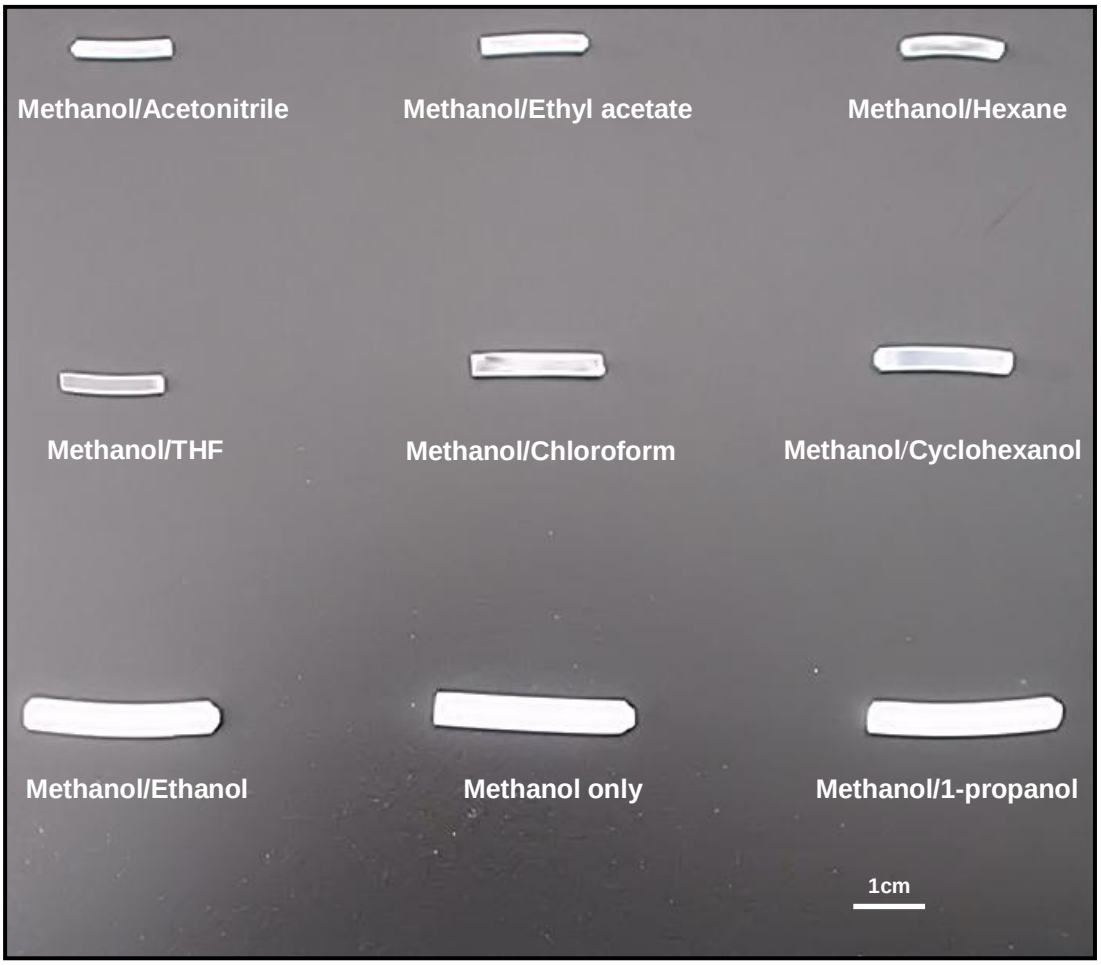

Figure 3.8 The appearance of the poly (BuMA-*co*-EDMA) monoliths prepared using different porogenic solvent systems after washing them with methanol to remove the unreacted monomeric materials using Soxhlet extraction with methanol at 80 ºC for 24 hours.

The effect of the solvent type on the bed structure of the fabricated polymer-based monolith was investigated by studying the morphology of the polymer-based monolith using SEM. It should be noted that the SEM analysis was performed on the dried sample while the polymer-based monolith was wet during the analysis; therefore, the

microglobular structure of the wet monolith could be slightly different.[214] However, studying the morphology of the monolithic material using SEM can give much information on surface area and permeability.[96] Figure 3.9 presents the SEM micrographs showing the morphology of the polymer-based monoliths fabricated using different porogenic solvent systems. Evaluation of the SEM micrographs shows that the structure of the fabricated monoliths was homogeneous and macroscopically uniform. In addition, the skeleton size of the fabricated polymer monolith was very small; therefore, it was expected that the physical strength of the fabricated polymer monolith was low.

From the SEM micrographs, it was observed that there is a clear effect of the porogenic solvent system on the morphology of the fabricated polymer-based monoliths since the size of globules and pores of the prepared monoliths were not similar. It can be seen that the morphology of the fabricated polymer monolith using MeOH/EtOH was similar to that of the polymer monolith fabricated using MeOH only and the fabricated polymer monoliths contained large globules and large pore size. This means using MeOH/EtOH as a porogenic solvent can offer an organic monolith with good hydrodynamic properties (high permeability) that allow using high flow rate velocities due to the large globules and large pore size. In contrast, the polymer-based monolith prepared using a porogenic solvent of MeOH/1-propanol resulted in small globules and small pores between them, which can provide an organic monolith with high surface area. The organic monolith that was fabricated using MeOH/cyclohexanol results in a condensed monolith contained large golubules and small pore size. The rest of the monoliths were very condensed (the SEM micrographs are not shown).

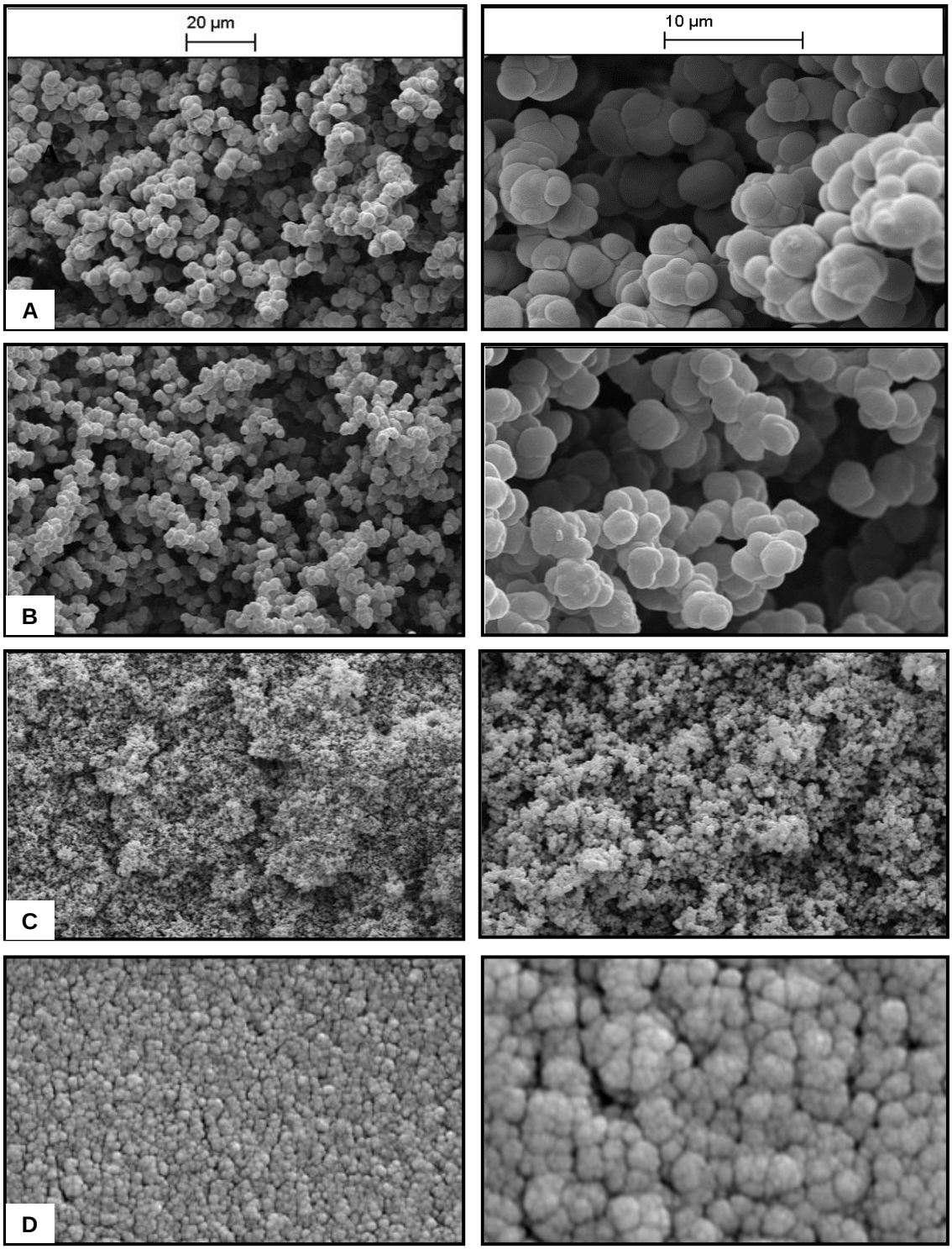

Figure 3.9 SEM micrographs of the poly (BuMA-*co*-EDMA) monoliths prepared using different porogenic solvent systems: (A) MeOH only, (B) MeOH/EtOH, (C) MeOH/1-propanol, and (D) MeOH/cyclohexanol.

The effect of the porogenic solvent type on the physical properties of the fabricated organic monoliths was investigated extensively. The important parameters that are sufficient for physical characterisation of the polymer-based monolith are the specific surface area (m^2 g^{-1}), and the pore size (nm).[120, 227] In this study, the surface area of the fabricated polymer-based monoliths and their pore size were measured using the BET analysis. It is important to emphasise that the measurement of the porous properties using BET analysis is always based on measuring the porous properties of the monoliths in their dry state, while the polymer-based monolith operates in a solvent, and this could result in shrinkage or swelling of the prepared monolith.[227-229] Therefore, the data shown in this study do not represent the actual surface area and pore size of the fabricated organic monolith during the extraction process. However, they allow a useful estimate of total surface area and the pore size of the polymer-based monoliths.

For studying the physical properties of the organic monoliths, they were prepared in 1 mL disposable plastic syringes and then washed by Soxhlet extraction using methanol at 80 ºC for 24 hours to remove unreacted monomeric materials. Finally, they were de-watered before BET analysis. A high surface area of the prepared polymer-based monolith is desired in order to increase the binding capacity of the monolith.[96] The bar chart 3.10 presents the surface areas of the polymer-based monoliths using different porogenic solvent systems. The result indicates that using MeOH/1-propanol as a porogenic solvent system resulted in a monolith with the largest surface area (56.89 m^2 g^{-1}). This result was expected since the SEM morphology of the monolith fabricated using this porogenic solvent system showed that it had small globules and pore size. The rest of the polymer-based monoliths prepared using different porogenic solvent systems had low surface areas, between 6.57 and 12.60 m^2 g^{-1}. In general, it was found that the surface areas of the prepared polymer-based monoliths were not very high.

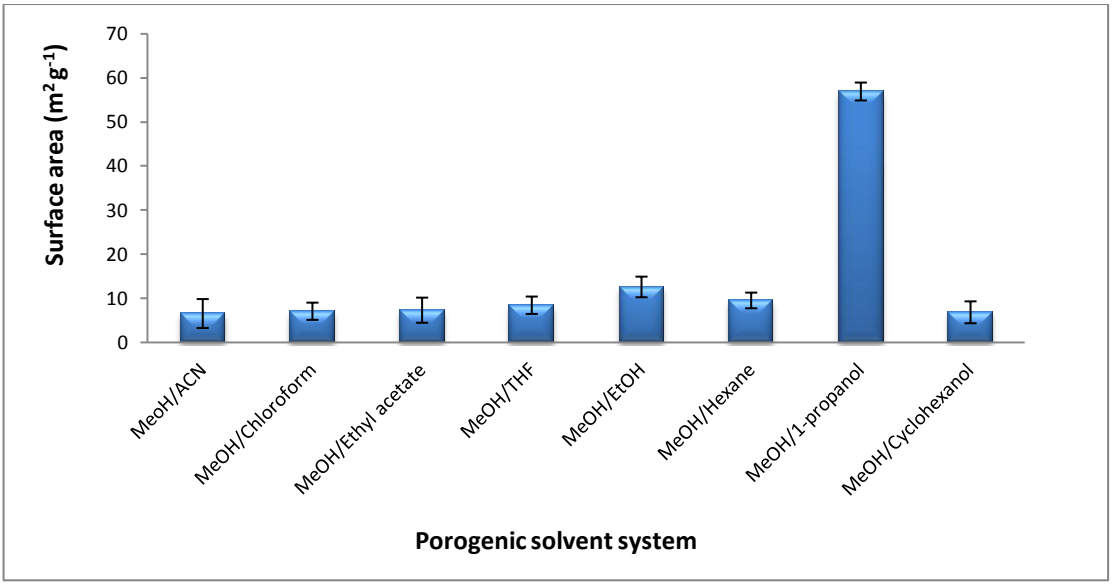

Figure 3.10 Effect of the composition of the porogenic solvent system on the total surface area of the prepared poly (BuMA-*co*-EDMA) monoliths using BET instrument, SD (n=3).

The size of the pores is a key factor for control of the hydrodynamic properties of the monolithic materials.[89] Large pore sizes within the monolithic material can lead to a decrease in the backpressure especially when the extraction is carried out in a microfluidic device. The pore size of the organic monoliths was also studied using the BET model. Figure 3.11 presents the effect of the porogenic solvent system on the pore size of the polymer-based monoliths. As can be seen in the figure, the diameter of the pores ranged between 4.73 and 12.93 nm, which places them in the mesopore range. It was found that the biggest pore size was obtained with the polymerisation mixture containing the porogenic solvent MeOH/EtOH (12.93 nm), followed by the organic monolith fabricated using MeOH/1-propanol (8.45 nm). The pore size of the rest of the polymer-based monoliths was low and this could cause a problem later when fabricating the organic monoliths inside the chamber of the microfluidic device.

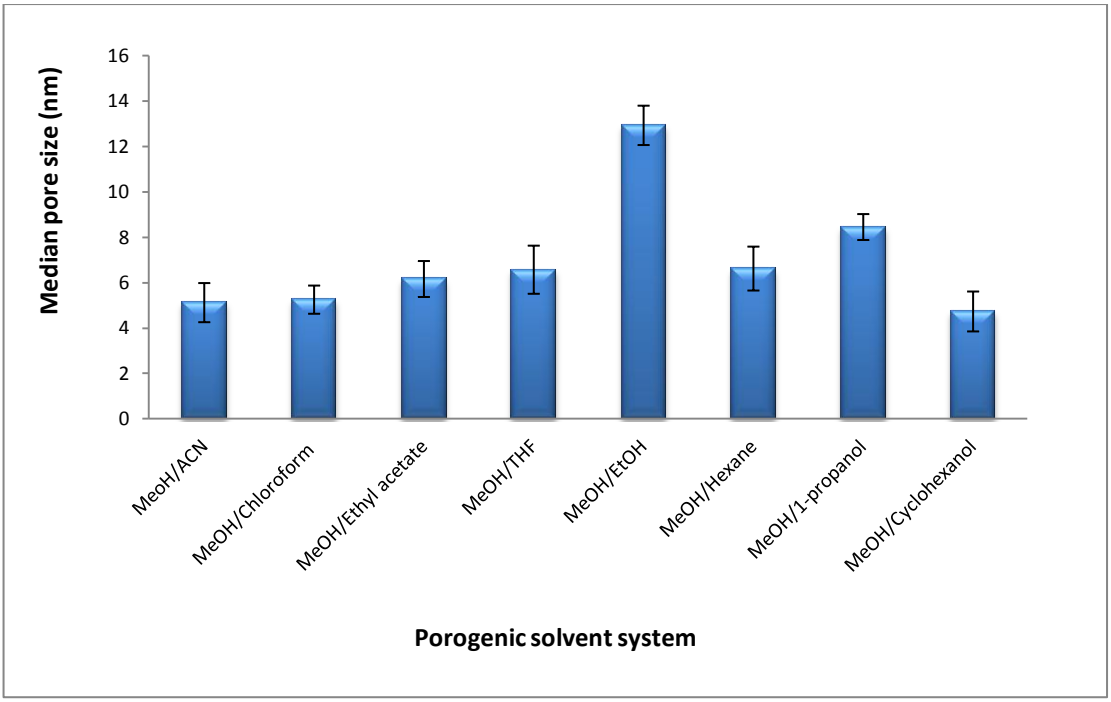

Figure 3.11 Effect of the porogenic solvent system on the median pore size of the prepared poly (BuMA-*co*-EDMA) monoliths using BET instrument, SD (n=3).

The porosity of the polymer-based monolith would be changed when it is exposed to organic solvents. Therefore, it is very important to study the effect of the porogenic solvent system on the porosity of the fabricated organic monolith, since there is a relation between the porosity of monolith and the backpressure; the higher the porosity, the lower the backpressure. The porosity of the polymer-based monoliths using different porogenic solvent systems was investigated, as described before (section 2.2.3). Figure 3.12 presents the effect of the porogenic solvents on the porosity of the prepared organic monolith. As can be seen from the figure, the highest-porosity monolith was obtained when using a polymerisation mixture containing MeOH/EtOH as a porogenic solvent system (porosity = 0.08), followed by the monolith fabricated using MeOH/1-propanol (porosity = 0.05) compared with the rest of the fabricated organic monoliths.

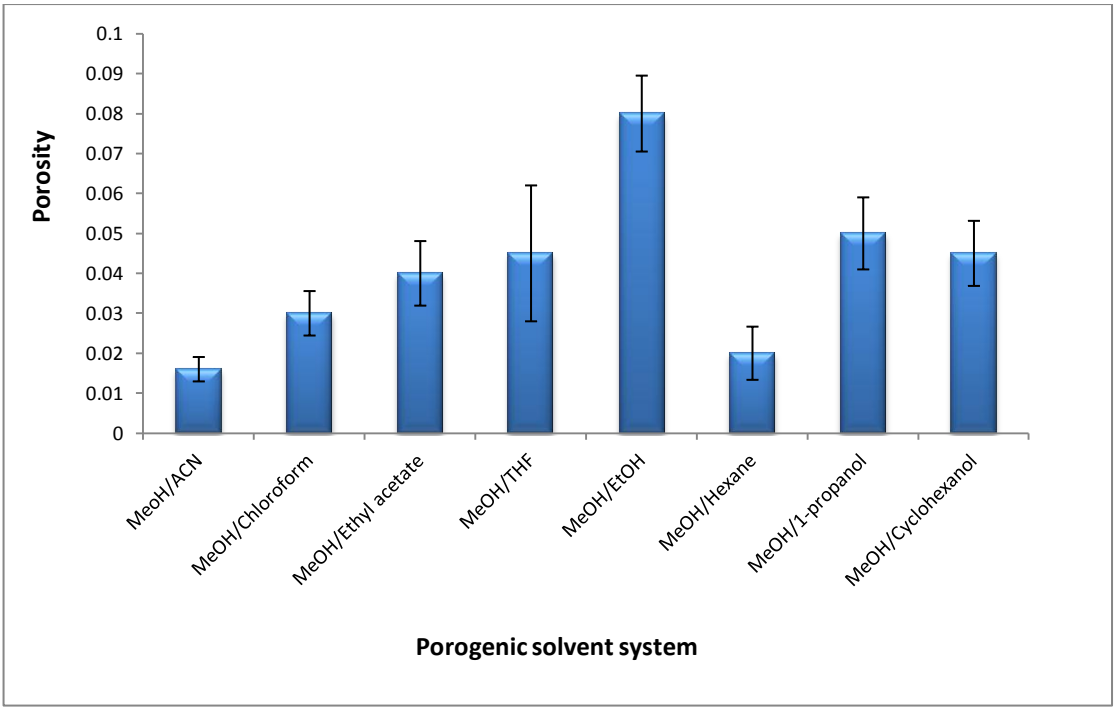

Figure 3.12 Effect of the porogenic solvent system on the porosity of the prepared poly (BuMA-*co*-EDMA) monoliths, SD (n=3). The porosity was calculated using equation 1, density of water at temperature 23 ºC = 0.9975 g cm^{-3}.

It is known that the porous polymer-based monoliths have a permeability to liquid flow through the network of canal-like pores within the monolith.[229, 230] The permeability of the monolith is an important factor since high permeability of the monolith means low backpressure, a higher flow rate, and consequently a shorter analysis time. However, an increase in the backpressure indicates that there is an interaction between the analyte and the surface of the monolith.

The flow resistance of the monolithic beds was measured using the liquid chromatography pump system by passing deionised water at different flow rates through the various monoliths. Since the level of the backpressure can give information about the permeability of the monolith, the value of the backpressure (flow resistance) in the system was recorded. Figure 3.13 shows the relationship between the backpressure and the flow rate of the deionised water through the organic monoliths prepared using different porogenic solvent systems, which were MeOH only, MeOH/EtOH, and MeOH/1-propanol. The linearity of the relation was found to be good, with a correlation R^2 = 0.998 for all the prepared organic monoliths. The

general conclusion that proceeds from measuring the backpressure is that the organic monoliths prepared using MeOH only, and MeOH/EtOH as porogenic solvent systems are characterised with low flow resistance and low backpressure for deionised water pumped through the monolith at different flow rates. The backpressure remains below a value of 350 psi at the high flow rate of 400 µL min^{-1}. The polymer-based monolith prepared using MeOH/1-propanol results in the same backpressure value but at a very low flow rate (19 µL min^{-1}). This result was expected since using MeOH/EtOH as a porogenic solvent system results in a monolith with high porosity, and large pore size. The permeability of the rest of the monoliths was not studied since the backpressures of these monoliths were too high and the experiment could not be completed.

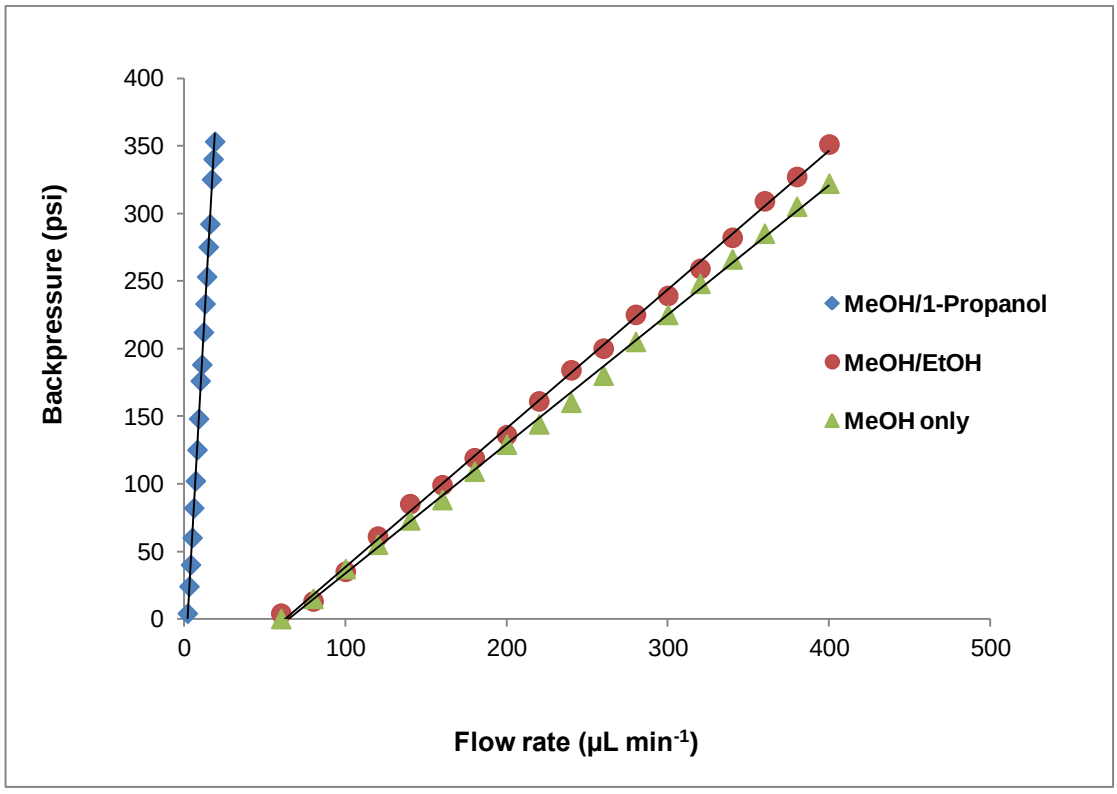

Figure 3.13 The relation between the backpressure and the flow rate of the deionised water through the poly (BuMA-*co*-EDMA) monoliths prepared using MeOH, MeOH/EtOH, and MeOH/1-propanol as porogenic solvent system.

The previous results confirm that the physical properties of the polymer-based monolith namely the surface area, pore size, porosity, and permeability can be substantially controlled by the porogenic solvent system. Based on the previous

experiments, it was found that the most suitable porogenic solvent systems to prepare the butyl methacrylate monolith were MeOH/1-propanol, since it can offer an organic monolith with a high surface area, and MeOH/EtOH, since it can offer an organic monolith with high porosity and permeability.

3.1.3.3 Investigation of tertiary porogenic solvent system

From investigating the effect of the binary porogenic solvent system, it was found that the porous properties of the polymer-based monolith were strongly affected by the porogenic solvent system. Further investigation was carried out in order to optimise further the physical properties of the prepared organic monolith in order to achieve a balance between the permeability and high surface area of the resulting monolith. To our knowledge, a tertiary porogenic solvent system consisting only of organic solvents has never been used for the preparation of organic monolithic sorbents. Therefore, it was decided to change the porogenic solvent system from a binary to a tertiary solvent system. The new porogenic solvent system consisted of 50 % the main solvent (MeOH) of the total amount of the porogenic solvent (3.6 g) and the other 50 % was a combination of 1-propanol and EtOH in various ratios: 40:10, 30:20, 25:25, 20:30, and 10:40. As mentioned before, the reason for choosing EtOH is because it was found that it can offer an organic monolith with high permeability and porosity while 1-propanol can offer an organic monolith with a high surface area.

The morphology of the organic monoliths fabricated using the tertiary porogenic solvent system at different ratios was examined using SEM, as can be seen in figure 3.14. In general, the structure of the fabricated organic monolith is characterised by homogeneity. The microglobular structure shows that by decreasing the amount of 1-propanol and increasing the amount of EtOH in the tertiary porogenic solvent system, the size of the globules and pores were increased slightly.

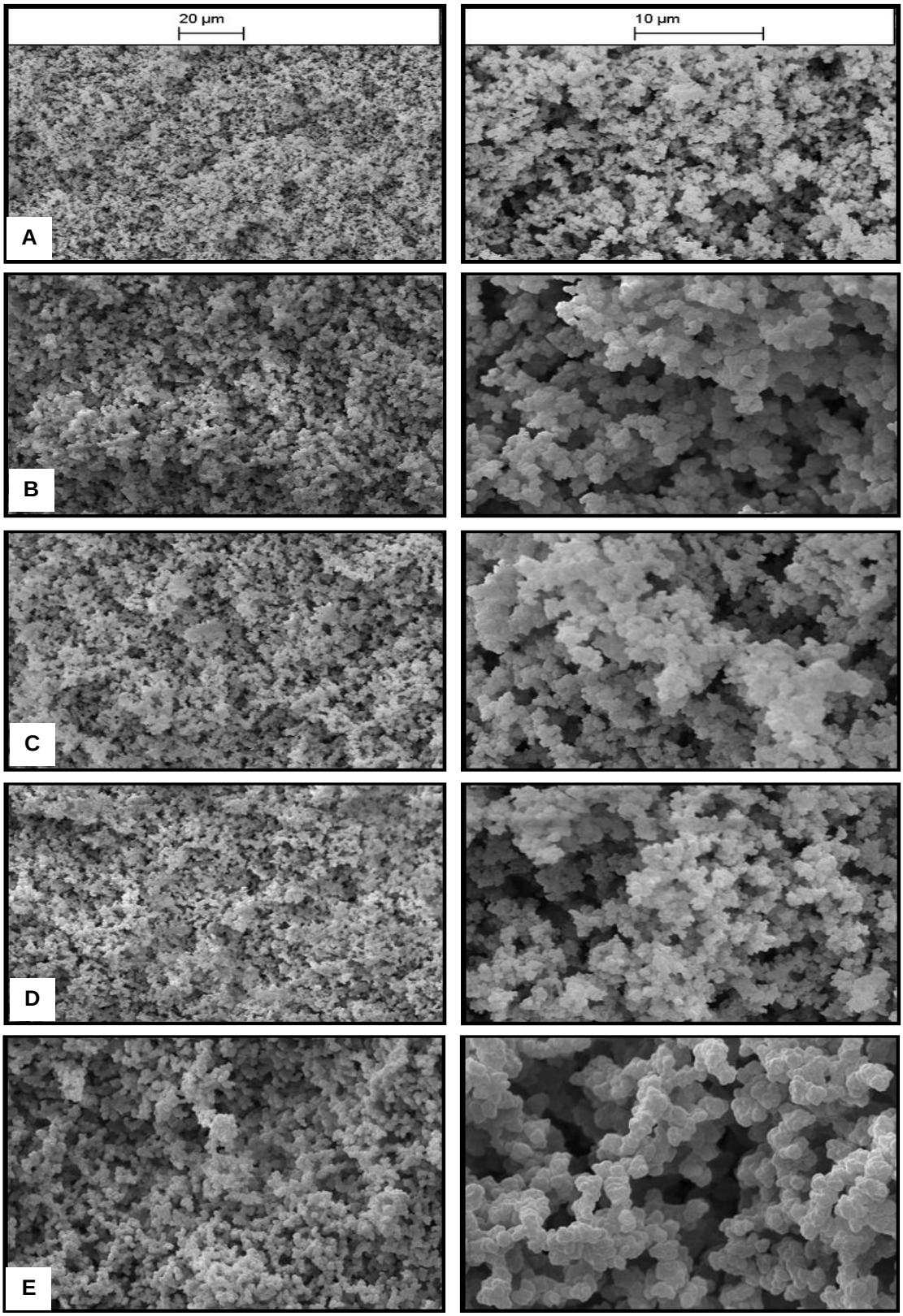

Figure 3.14 SEM micrographs of the fabricated poly (BuMA-*co*-EDMA) monoliths using different ratios of MeOH, 1-propanol, and EtOH: (A) 50:40:10, (B) 50:30:20, (C) 50:25:25, (D) 50:20:30, and (E) 50:10:40.

It was hard to see the differences in the physical properties of the prepared organic monoliths from the SEM micrographs; therefore, the surface area and the average pore size of the fabricated organic monoliths using tertiary porogenic solvent systems were investigated using the BET model. From the results in table 3.1, it can be seen that the surface area was decreased from 38.87 to 5.06 m^2 g^{-1} by decreasing the amount of 1-propanol and increasing the amount of EtOH in the porogenic tertiary solvent system, while the average pore diameter increased slightly from 4.41 to 11.90 nm. It was concluded that the surface area of the prepared organic monolith depends on the size of the pores: the surface area of the organic monoliths decreased as the size of pores increased. Therefore, small size pores give a larger suface area.[89]

Tertiary porogenic solvent system MeOH:1-propanol:EtOH	**BET surface area (m^2 g^{-1}) ± RSD**	**BET average pore size (nm) ± RSD**
50:40:10	38.87 ± 1.7	4.41 ± 3.0
50:30:20	15.65 ± 4.5	8.77 ± 4.8
50:25:25	13.21 ± 2.7	9.08 ± 2.9
50:20:30	9.18 ± 3.2	11.04 ± 5.0
50:10:40	5.06 ± 5.3	11.90 ± 3.6

Table 3.1 The effect of the tertiary porogenic solvent system (MeOH, EtOH, and 1-propanol) on the surface area and the average pore diameter of the prepared poly (BuMA-*co*-EDMA) monoliths.

3.1.4 Preparation of the organic monolith inside the glass microchip

The ultimate aim of this work was to fabricate a microfluidic device containing organic monolithic material for protein extraction. The reason for fabrication of the monolithic bed on microchip is for short analysis, and to decrease the volume of the sample and reagents. The glass microchip was fabricated as described before (section 2.1.1.4). It had five access holes. One of the access holes was used for injection of the

sample and reagents while the other access hole was drilled in the middle of the extraction chamber of the glass microchip in order to facilitate injection of the polymerisation mixture directly into the extraction chamber. The glass microchip contained two extra outlet holes to overcome any problems caused by the microchannel and the hole becoming blocked. The inner walls of the glass microchip were vinylised to attach the organic monolith covalently to the inner walls of the microchip. After silanisation, the monolithic poly (BuMA-*co*-EDMA) stationary phase was fabricated inside the glass microchip in order to use it as a sorbent for extraction and preconcentration of the proteins. The monolithic porous polymer was prepared by photoinitiation. It was found that the fabrication of the organic monolithic material within the extraction chamber of the microfluidic device was easy since the UV exposure could be confined to specific regions within the extraction chamber of the glass microchip.

3.1.5 Reproducibility of preparation of the organic monolith

The reproducibility of the fabrication of the polymer-based monolith is a significant factor in the effectiveness and practicality of the procedure. Since the fabrication of the polymer-based monolith is a single-step process, the number of parameters that can affect the reproducibility of the preparation of the organic polymer monolith is reduced. The reproducibility of the fabrication method was examined for three monoliths fabricated from three different polymerisation mixtures with the same composition. The reproducibility was assessed by checking the morphology shown by SEM for three different batches of the fabricated polymer-based monoliths. It was found that there was no visible difference in the morphology of the prepared monoliths.

3.2 Fabrication of inorganic monolith for protein extraction

The second type of monolithic material investigated for use in solid phase extraction was silica-based. These have a bimodal pore size distribution with µm-sized macropores and nm-sized mesopores. In this study, the monolithic silica rods were prepared by a sol-gel method, which has the ability to synthesise materials with high purity, and better homogeneity. In addition, it allows the porosity of the monolithic material to be controlled without affecting the surface area.[126, 231]

3.2.1 Fabrication of the monolithic silica rods

The macroporous wet silica gel was prepared inside a disposable plastic syringe (1 mL), which was used as a mould for preparation of the monolithic silica rod. The composition of the starting mixture was an alkoxy silicon derivative, tetramethyl orthosilicate (TMOS), undergoing a hydrolytic polymerisation reaction in the presence of a water-soluble organic polymer, polyethylene oxide (PEO). TMOS was chosen as the alkoxy silicon derivative because it undergoes more rapid hydrolysis than tetraethyl orthosilicate (TEOS).[109, 101] PEO was used as a porogen to promote the phase separation between silica and water and form the through-pores and the micropores in the silica gel.[109] Nitric acid was used as a catalyst to start the hydrolysis and condensation reactions. Water was used as a solvent because it is a good solvent for the reactants and non-toxic.[127] Moreover, it induced the hydrolysis of the alkoxide groups to produce the silanol groups (Si-OH) followed by water or alcohol condensation to produce polycondensed species containing siloxane linkages (-Si-O-Si-) between two silane molecules.[232]

Figure 3.15 presents the schematic reaction of the fabrication of the sol-gel silica-based monolith, which consists of two main reactions; hydrolysis and condensation reactions. The condensation reaction involves alcohol condensation or water condensation to form a dimer. After a polycondensation reaction, the gel will be formed. It was observed that the prepared monolithic silica rod was white and crack-free; however, it was found that the preparation of the silica-based monolith was accomplished with the volume reduction of the whole structure of the monolithic silica rod and shrinkage occurred during the gel formation without cracking in the monolith, as was also observed by other groups.[233-235]

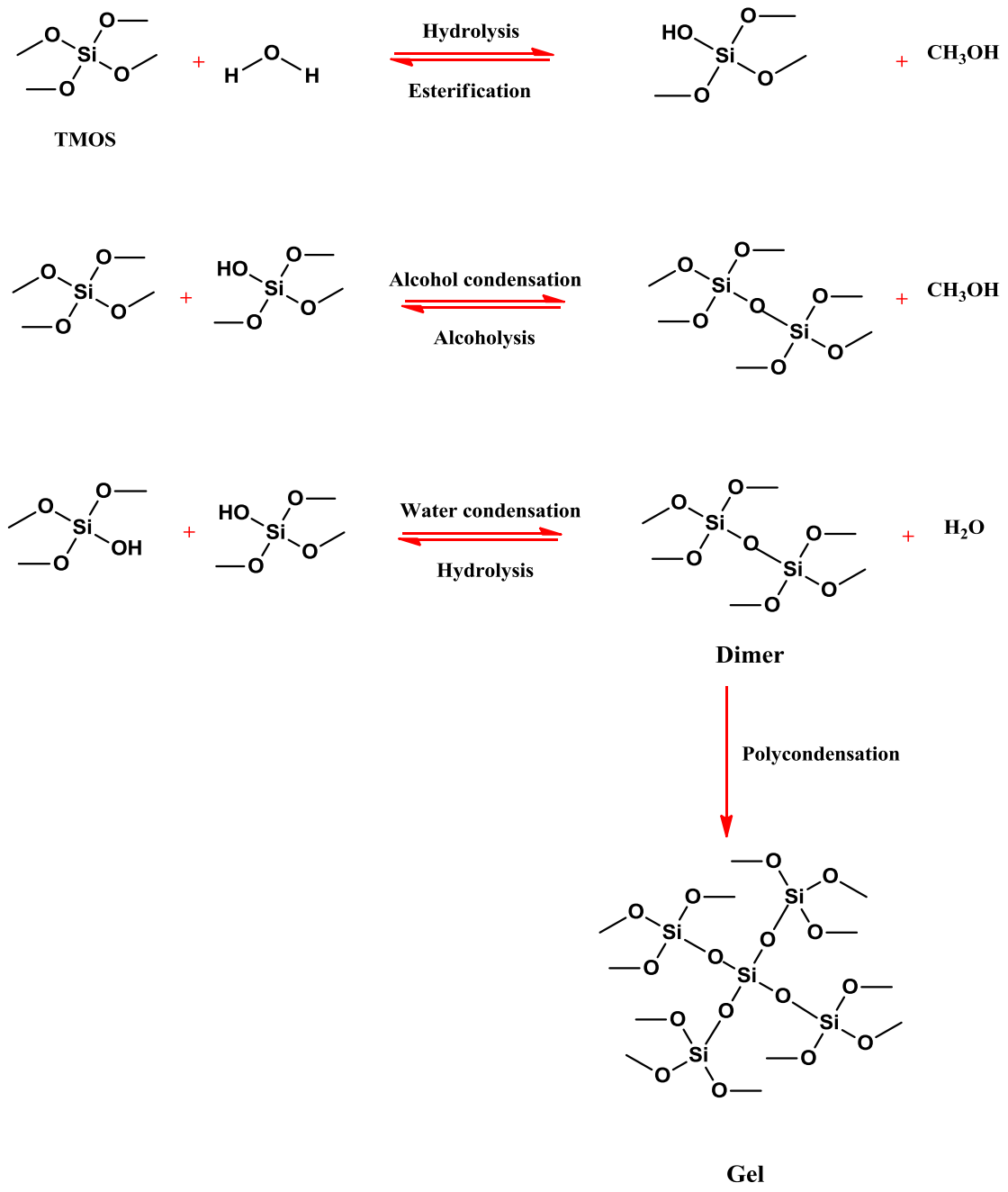

Figure 3.15 Hydrolysis and condensation reactions involved in the sol-gel process, as used for preparation of the silica-based monolith.

After formation of the network structure of the silica skeletons, the internal pore structure of the silica-based monolith was tailored while the monolith was in the wet state by the pore tailoring step.[218] The purpose of this step is to increase the surface

area of the silica-based monolith in order to increase the binding of proteins to the monolith by converting the micropores, which have a low surface area, to mesopores, which have a high surface area, without affecting the through-pores.[236]

The median size of the pores is based on the temperature and the pH of the pore tailoring medium, which should have a pH>8 such as ammonia.[196, 237, 238] Recently, urea has been utilised as a precursor of ammonia since it hydrolyses to ammonia at high temperature.[110] The benefit of using the pore tailoring medium is to produce an alkaline pH environment homogeneously around the whole monolithic structure at an elevated temperature. In this study, the formation of the mesopores on the silica skeletons was achieved by treating the aged wet gel with 1 M aqueous urea solution or 1 M aqueous ammonia solution. The time of the thermal decomposition was only 24 hours because a prolonged period of treatment can increase the pore size, resulting in a decrease in the surface area.[107]

In order to study the effect of the type of pore tailoring medium on fabrication of the silica-based monolith, two monolithic silica rods were fabricated; one of the rods was treated with 1 M aqueous urea solution while the other rod was treated with 1 M aqueous ammonia solution, and all other parameters involved in fabrication of the monolithic silica rods were kept identical. After calcination of the monolithic silica rods in the oven at 500 ºC for 2 hours, it was observed that the colour of the fabricated silica-based monolith treated with urea solution had changed from white to brown. Subsequently, the colour of the rod changed further from brown to black when washed with ACN in order to condition and prepare the monolith for protein extraction, as shown in figure 3.16. The reason for the colour change is unknown; however, it may be due to incomplete removal of the urea causing charring of the residual organic material in the oven. In contrast, the monolithic silica rod treated with ammonia solution was not affected and the colour of the monolith was not changed when it was placed in the oven or after washing it with ACN. Based on this experiment, it was decided to use ammonia solution as the pore tailoring medium to create the mesostructured silica monolith.

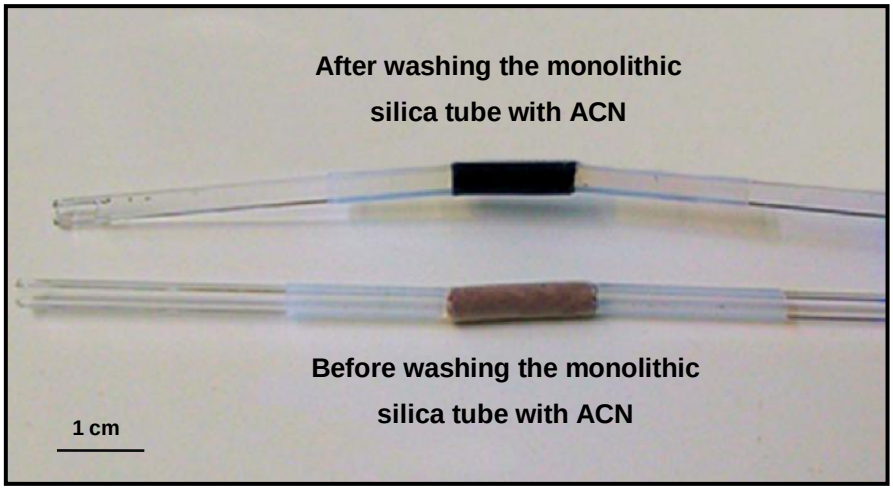

Figure 3.16 The appearance of the monolithic silica tubes after treating with 1 M aqueous urea solution and placing them in the oven at 500 ºC for 2 hours, before washing with ACN (brown material), and after (black material).

The presence of the mesopores in the monolithic structure was confirmed by transmission electron microscopy (TEM) analysis, which provides images of very small structures. Figure 3.17 shows the TEM micrographs of the silica-based monolith at different magnifications. The TEM images show the high homogeneity of the prepared silica-based monolith. The lower TEM micrograph shows the formation of the mesostructured silica monolith.

After formation of the mesopores in the silica skeletons, the monolithic silica rod was placed in the oven for 24 hours at 40 °C, the temperature was then increased to 100 °C for another 24 hours. Finally, the monolithic silica rod was calcinated at 500 °C for 2 hours. The purpose of the calcination step was to remove any remaining organic materials, and mechanically stabilise the double pore structure of the silica-based monoliths.[218, 239]

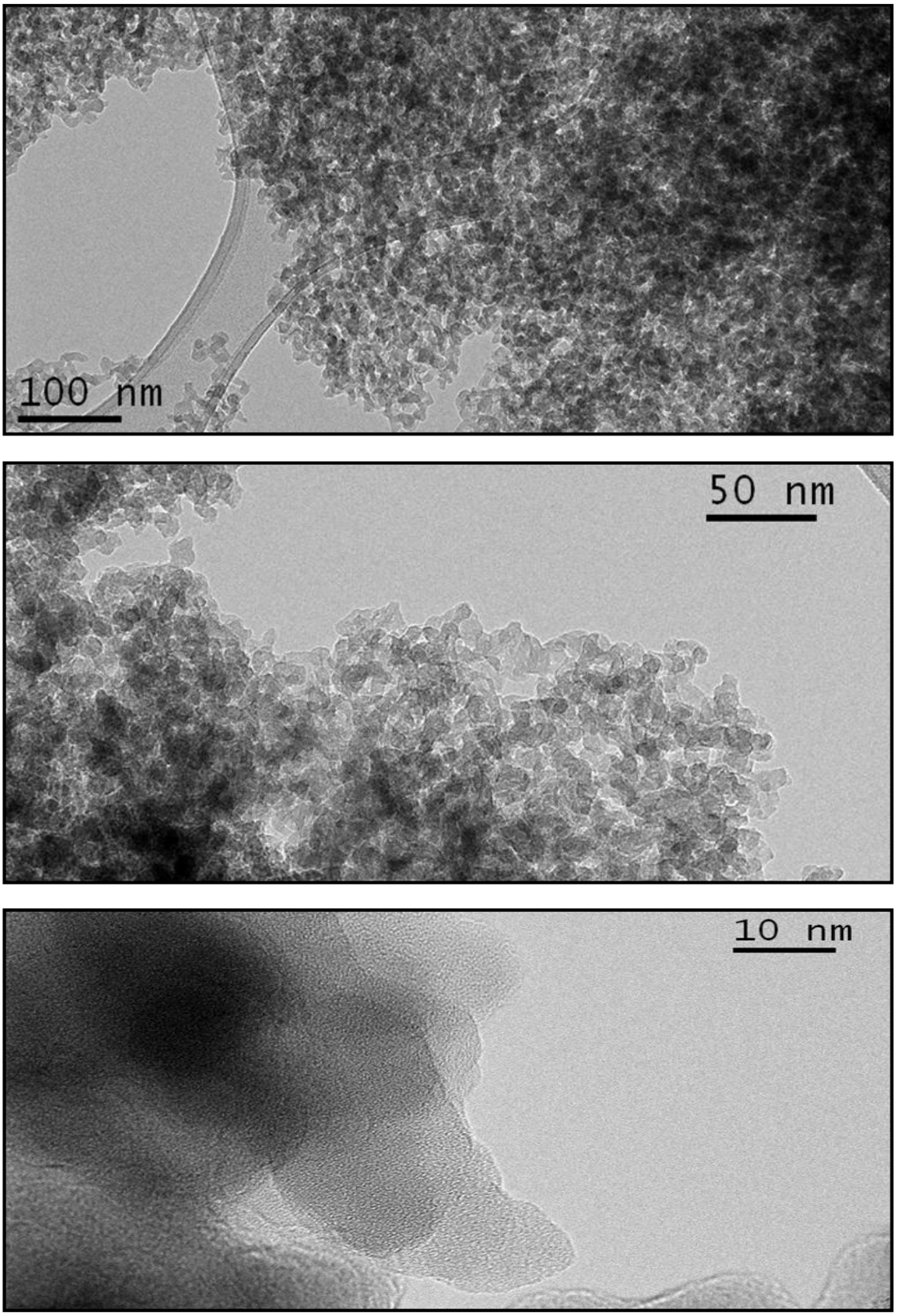

Figure 3.17 TEM images of the mesostructured silica film treated with 1 M aqueous ammonia solution at elevated temperature (85 °C) for 24 hours.

3.2.2 Effect of temperature and period of the gelation step

The silica-based monoliths are characterised by a bimodal pore structure with continuous macropores and mesopores.[240] The size of the macropores and mesopores can be independently controlled; as a result, the silica-based monolithic materials can offer high permeability and high surface area.[238] There are several experimental parameters that can affect the textural (skeleton and macropore size) properties of the silica-based monolith, such as pH, gelation temperature and period, and relative proportion of the precursors.[241] For optimising the structure of the prepared silica-based monolith, the effects of temperature and period of the gelation process on the properties of the silica-based monolith were studied. In this study, two different gelation temperatures were investigated (40 and 50 °C). In addition, different periods for the gelation process were studied (1, 2, 3, and 4 days).

The influence of the period of the gelation process on the structural morphology of the silica-based monolith was examined by SEM, since it can give an estimation of the size of the through-pores. Commonly, the micrographs of the silica-based monolith in the literature show a cross-section of the silica-based monolith, which does not give enough information on the homogeneity of the whole skeleton.[109] Therefore, longitudinal SEM micrographs of the prepared silica-based monolith were studied. Figure 3.18 shows the SEM micrographs of a longitudinal section of the monolithic silica rods prepared in the 1 mL disposable plastic syringe at 40 ºC for different periods of gelation (1, 2, 3, and 4 days). In general, the SEM micrographs show the continuous morphology of the silica gel skeletons having high homogeneity and a spongy structure characterised by large through-pores penetrating several layers of these skeletons and a network structure of skeletons of different sizes. The shape of the through-pores of the silica-based monoliths was relatively round. In addition, it was observed that the diameter of the through-pores was decreased as the period of the gelation process increased.

The effect of the gelation temperature on the structure of the silica-based monolith was investigated by fabrication of the bare silica-based monolith as before except with increased gelation temperature of 50 °C for different periods of the gelation process (1, 2, 3, and 4 days). The structural morphology of the silica-based monoliths was then studied using SEM analysis, as shown in figure 3.19.

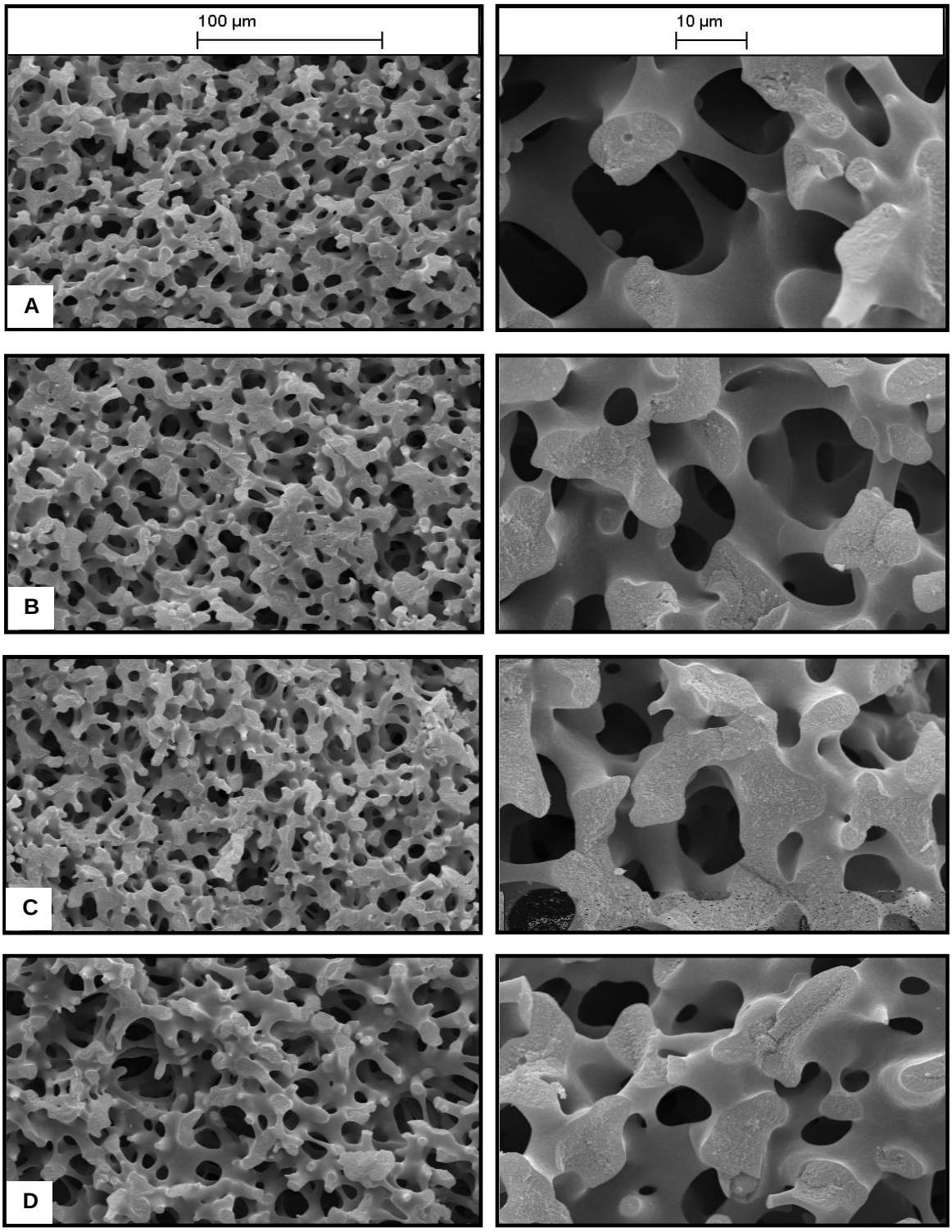

Figure 3.18 SEM micrographs of the bare monolithic silica rods prepared at 40 °C, showing the influence of the gelation period on the structure of the porous silica monolith: (A) 1 day, (B) 2 days, (C) 3 days, and (D) 4 days.

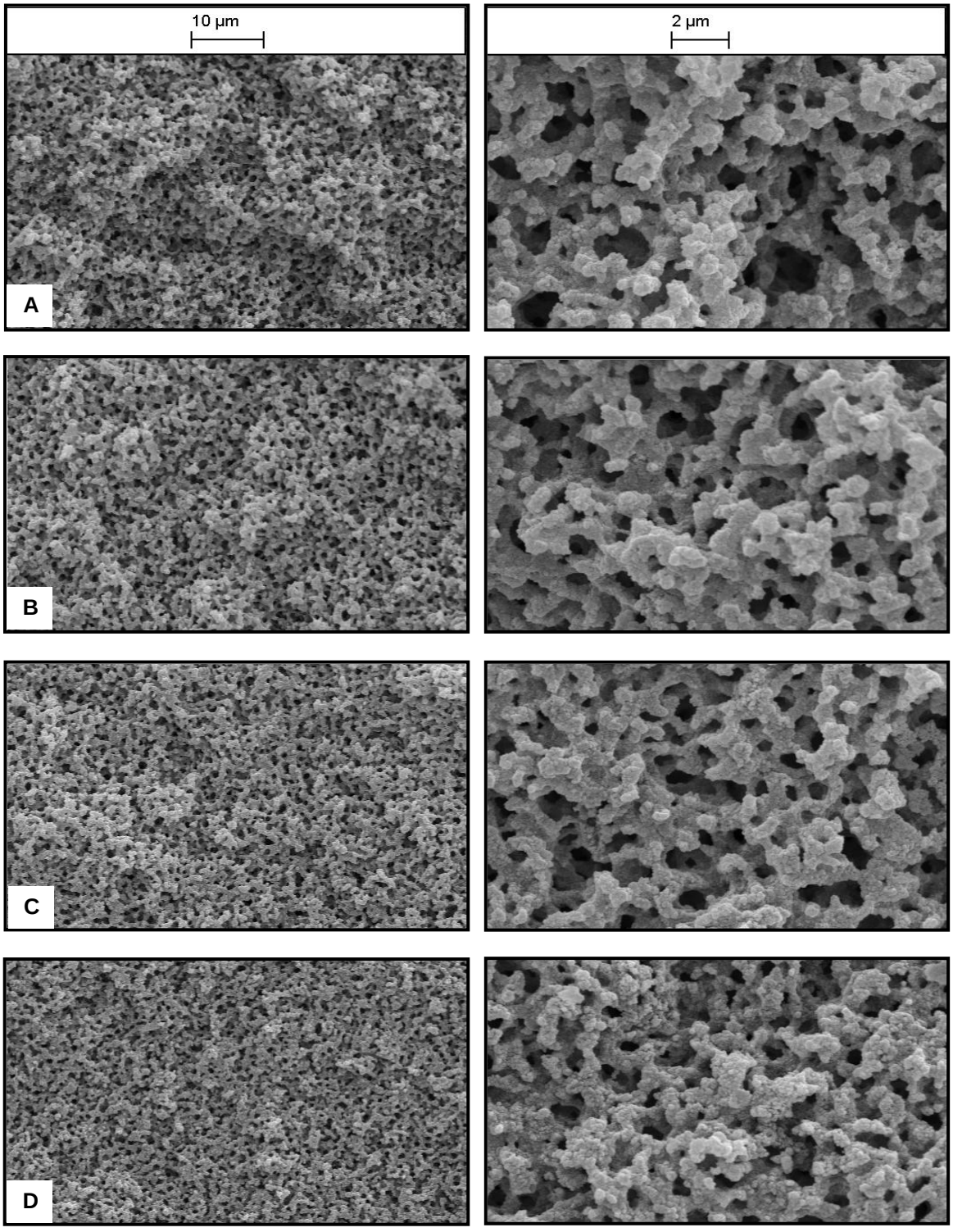

Figure 3.19 SEM micrographs of the bare monolithic silica rods prepared at 50 °C, showing the influence of the gelation period on the structure of the porous silica monolith: (A) 1 day, (B) 2 days, (C) 3 days, and (D) 4 days.

Comparison between figures 3.18 and 3.19 indicates that there was a huge effect due to the temperature of the gelation process on the structural morphology of the continuous silica rods. It was observed that the monolithic silica rods prepared at 40 ºC had high through-pore size/skeleton size ratios compared with the monolithic silica rods prepared at 50 ºC. In addition, the through-pore size of the silica-based monolith was generally decreased by increasing the period of the gelation step from 1 to 4 days.

Studying the size of the macropores (interaggregate voids) and the diameter of the monolithic silica rod can determine the hydrodynamic properties and mechanical strength of the prepared monolithic silica rods. Therefore, the influence of period and temperature of the gelation process on the textural properties of the silica-based monolith were investigated by measuring the size of the macropores and the diameter of the monolithic silica rods. The sizes of the macropores were measured using the SEM micrographs [242], while the diameter of the monolithic silica rods was measured using a caliper. Table 3.2 shows the size of macropores, and the diameter of the monolithic silica rods prepared at 40 and 50 ºC for 1, 2, 3, and 4 days.

Day (24 hours)	**Size of macropores (µm) (Average ± RSD)**		**Diameter of monolithic silica rods (mm) (Average ± RSD)**	
	40 ºC	**50 ºC**	**40 ºC**	**50 ºC**
1	2.2 ± 5.2	1.0 ± 3.2	3.9 ± 5.3	3.5 ± 1.1
2	2.0 ± 5.5	0.9 ± 2.5	3.8 ± 4.5	3.4 ± 3.5
3	1.6 ± 4.6	0.8 ± 2.1	3.6 ± 2.4	3.3 ± 1.5
4	1.4 ± 3.6	0.6 ± 3.0	3.3 ± 3.2	2.6 ± 2.5

Table 3.2 Size of macropores measured using SEM micrographs for 20 different macropores, and diameters of monolithic silica rods measured using caliper for three different batches.

From the table, it was found that although the variation in the size of macropores of the silica-based monoliths prepared at the same temperature was not very large, the size of the macropores of the fabricated silica-based monoliths was gradually decreased by increasing the gelation period. The size of the macropores of the silica-based monoliths prepared at 40 °C was decreased from 2.2 to 1.4 µm by increasing the gelation period from 1 to 4 days, while the size of the macropores of the silica-based monolith prepared at 50 °C was decreased from 1.0 to 0.6 µm. In addition, a significant change was found in the size of macropores of the monolithic silica rods prepared at different temperatures under the same gelation period, and the size of macropores was reduced to approximately half by increasing the gelation temperature from 40 to 50 °C.

It was found that the degree of shrinkage in the diameter of the monolithic silica rods was increased slightly by increase of the gelation temperature and period. The diameter of the monolithic silica rods prepared at 40 °C was decreased from 3.9 to 3.3 mm, while the diameter of the monolithic silica rods prepared at 50 °C was decreased from 3.5 to 2.6 mm. These results could be because the rate of hydrolysis and condensation of TMOS reactions were increased by elevating the gelation temperature or increasing the period of the gelation process, resulting in increase in the kinetics of the condensation reaction. As a result, the size of the macropores and the diameter of the silica-based monoliths will be decreased.

The prepared silica-based monoliths were characterised physically to relate these characteristics to their extraction behaviour. The influence of period and temperature of the gelation process on the physical properties of the silica-based monoliths was examined. The surface area, pore size, volume of the pores, and the porosity were all studied.

The impact of temperature and period of the gelation process on the surface area of the silica-based monolith was measured by BET analysis. Figure 3.20 presents the BET surface areas of the silica-based monoliths prepared at different gelation temperature (40 and 50 ºC), and at different periods of the gelation process (1, 2, 3, and 4 days). It was found that the silica-based monoliths prepared at 40 °C possessed higher surface areas (170.23-173.31 $m^2 g^{-1}$) compared to those prepared at 50 °C (155.97-160.03 m^2

g^{-1}). In addition, it was found that there was not a huge difference in the total surface areas of the silica-based monoliths prepared at different periods of the gelation process from 1 day to 4 days at the same temperature.

Generally, it was found that the total surface areas of the prepared silica-based monoliths were higher than those of the polymer-based monoliths (figure 3.10). This is a good indication that the silica-based monolith would be a suitable monolithic bed for protein extraction since a key characteristic of a good sorbent is a large surface area. Unfortunately, it was found that the total surface areas of the fabricated silica-based monoliths were somewhat lower than that in literature that were fabricated using the same sol-gel precoursor (195 m^2 g^{-1}).[243]

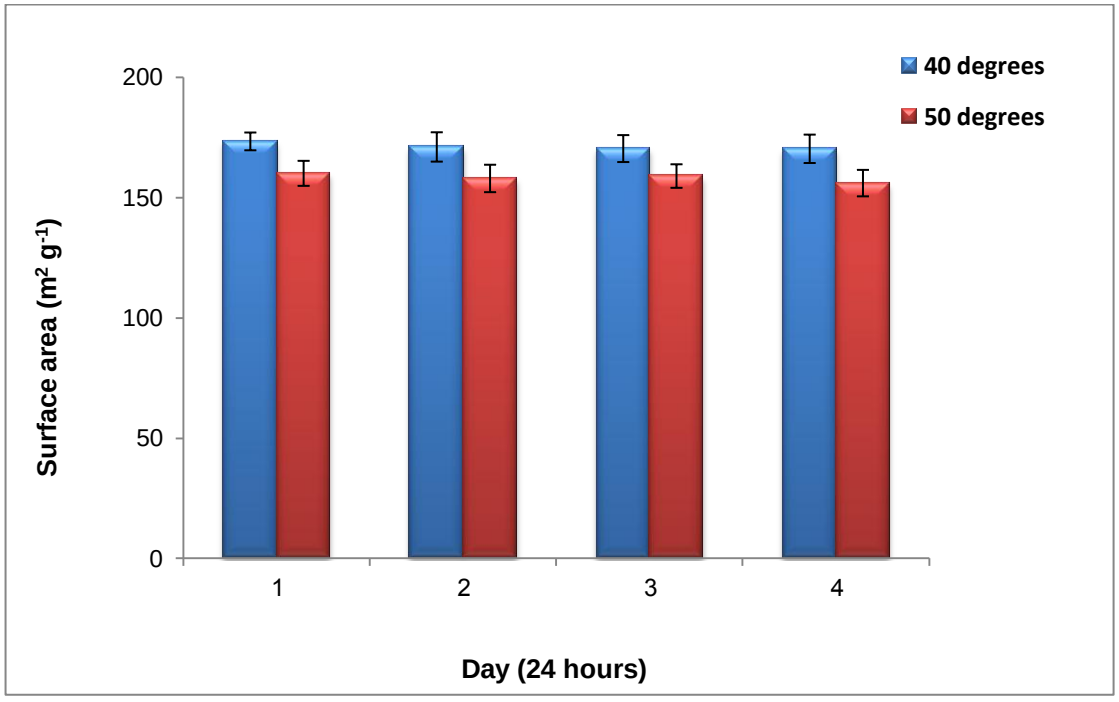

Figure 3.20 The BET surface areas of the bare silica-based monoliths prepared at 40 and 50 °C for 1, 2, 3, and 4 days, RSD (n=3).

The overall pore size distributions of the silica-based monoliths were calculated using the BJH method. Figure 3.21 shows the overall pore size distributions of the silica-based monoliths prepared at 40 °C at different periods of the gelation process (1, 2, 3,

and 4 days). From the figure, it can be seen that the average pore sizes of the silica gel monoliths were in the mesopores range (11.56 - 13.90 nm). It was found that the pore sizes of the fabricated silica-based monoliths were higher than those of the fabricated polymer-based monoliths (4.73-12.93 nm). The presence of large size mesopores is highly desirable, since large mesopores have been found to increase the loading of the macromolecules in the monolithic materials.[244] The total pore volumes of the prepared silica-based monoliths were between 0.46 and 0.66 cm^3 g^{-1}.

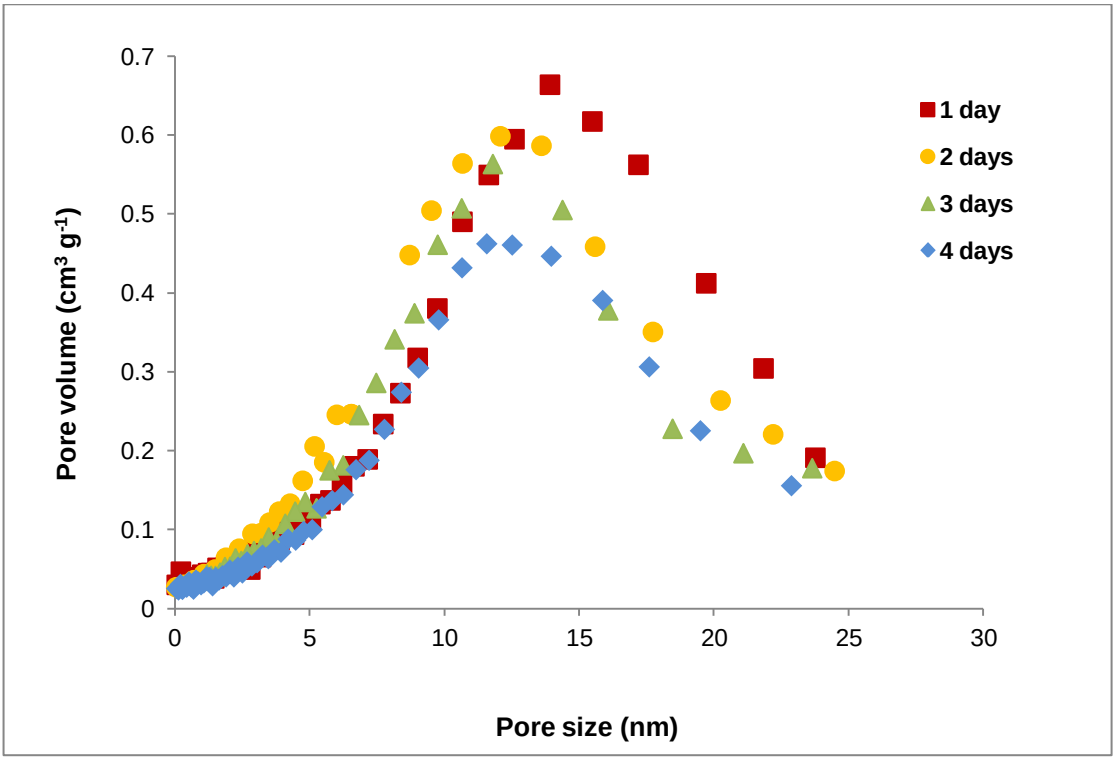

Figure 3.21 The overall pore size distributions of the bare silica-based monoliths prepared at 40 °C for 1, 2, 3, and 4 days, calculated by the BJH method.

The overall pore size distributions of the bare silica-based monoliths prepared at 50 °C at different periods of the gelation process (1, 2, 3, and 4 days) were calculated, as shown in figure 3.22. The average pore sizes of the silica-based monoliths prepared at 50 °C were also in the mesopores range (10.50 - 12.06 nm), and the total pore volumes of these monoliths were between 0.46 and 0.59 cm^3 g^{-1}.

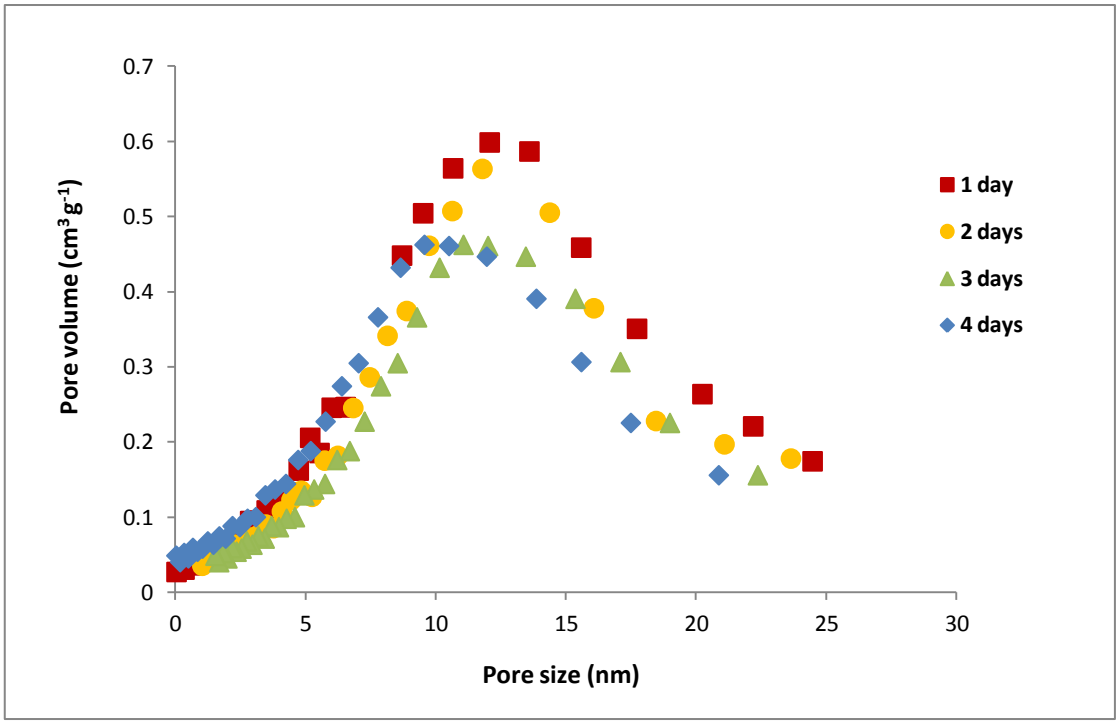

Figure 3.22 The overall pore size distributions of the bare silica-based monoliths prepared at 50 ºC for 1, 2, 3, and 4 days, calculated by the BJH method.

By comparing the results presented in figures 3.21 and 3.22, it was found that the sizes of the mesopores and the total pore volumes of the silica-based monoliths prepared at different periods and temperature of the gelation process were decreased slightly by increasing the temperature of the gelation process. However, the variation in the pore size and volume was not significantly different. This observation could be because the mesopores in the silica skeletons, which were created by the pore tailoring step, would not be affected because the concentration of the ammonia solution and the temperature of the reaction were constant for all the prepared monoliths.

The porosity of the silica-based monoliths prepared at 40 and 50 ºC at different times of the gelation process was measured, as can be seen in figure 3.23. It was found that the porosity of the silica-based monoliths was decreased gradually by increasing the temperature and period of the gelation process. The porosity of the monoliths prepared at 40 ºC was in the range (0.43 - 0.51), while the porosity of the silica-based monoliths prepared at 50 °C was in the range (0.24 - 0.44). This result was expected, since it was found that the size of the macropores of the silica-based monoliths was decreased by increasing the temperature and period of the gelation process. In general, it was found

that the porosity of the silica-based monoliths was much greater than that of the polymer-based monoliths (0.01- 0.08), which confirmed that the silica-based monolith is a highly porous material.

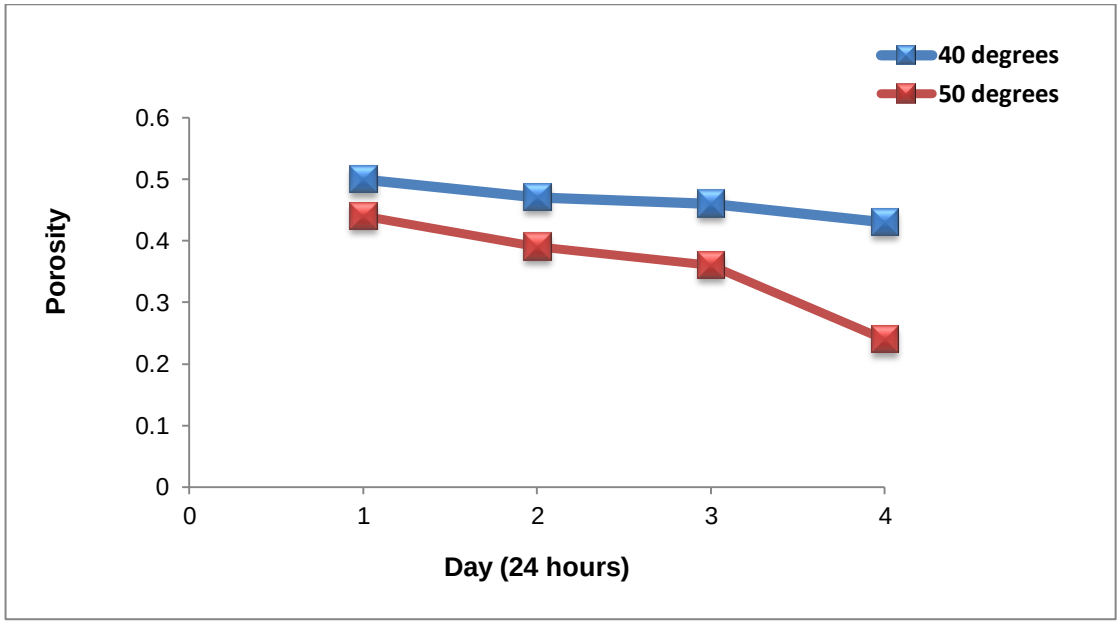

Figure 3.23 The porosity of the silica-based monoliths prepared at 40 and 50 °C at different times (1, 2, 3, and 4 days). The porosity was calculated using equation 1, density of water at temperature 23 °C = 0.9975 g cm^{-3}.

It is evident from the results that the gelation temperature has an effect on the structural morphology and the physical properties of the silica-based monolith. Since gelation at 40 °C can offer monolithic silica materials with a large macropore diameter, high porosity, and high total surface area, it was decided to use 40 °C as the temperature of the gelation process. Further investigation of the period of the gelation process was carried out in order to further optimise the physical properties of the silica-based monolith.

3.2.3 Surface modification of the inorganic monolith with C_{18} groups

The surface of the monolithic silica rod was chemically modified with long alkyl chain ligands in order to make the sorbent hydrophobic. The reason for choosing a long

alkyl chain is that the hydrophobicity of the silica-based monolith will be increased by increasing the n-alkyl chain length. As a result, the strength of the hydrophobic interaction between the sorbent and the proteins will be increased.[216]

Surface modification of the silica-based monolith was carried out on-column by continuously flowing through the porous monolithic silica rod inside the heat shrinkable tube with chlorodimethyl octadecyl silane (CDMOS) to produce an octadecyl-silica (C_{18}-silica) using a syringe pump at the flow rate of 30 μL min^{-1} for 6 hours at 80 °C. The modification reaction was carried out in the presence of 2,6-lutidine as catalyst in order to increase the reactivity of the derivatisation reagent.[107, 238] Figure 3.24 (A) shows the reaction of the silanol groups of the monolithic silica rods with CDMOS to derivatise the surface of the silica-based monolith with octadecyl groups. After the derivatisation step, the end capping process was carried out using trimethylchlorosilane (TMCS). The purpose of the end capping process is not only to increase the hydrophobic nature of the octadecylated silica monolith, but also to prevent non-specific adsorption by blocking the unreacted silanol groups, since the silanol groups can interact with proteins, especially at high pH.[122] Figure 3.24 (B) illustrates the further reaction of the octadecylated silica monolith with TMCS in order to block any unreacted silanol groups.

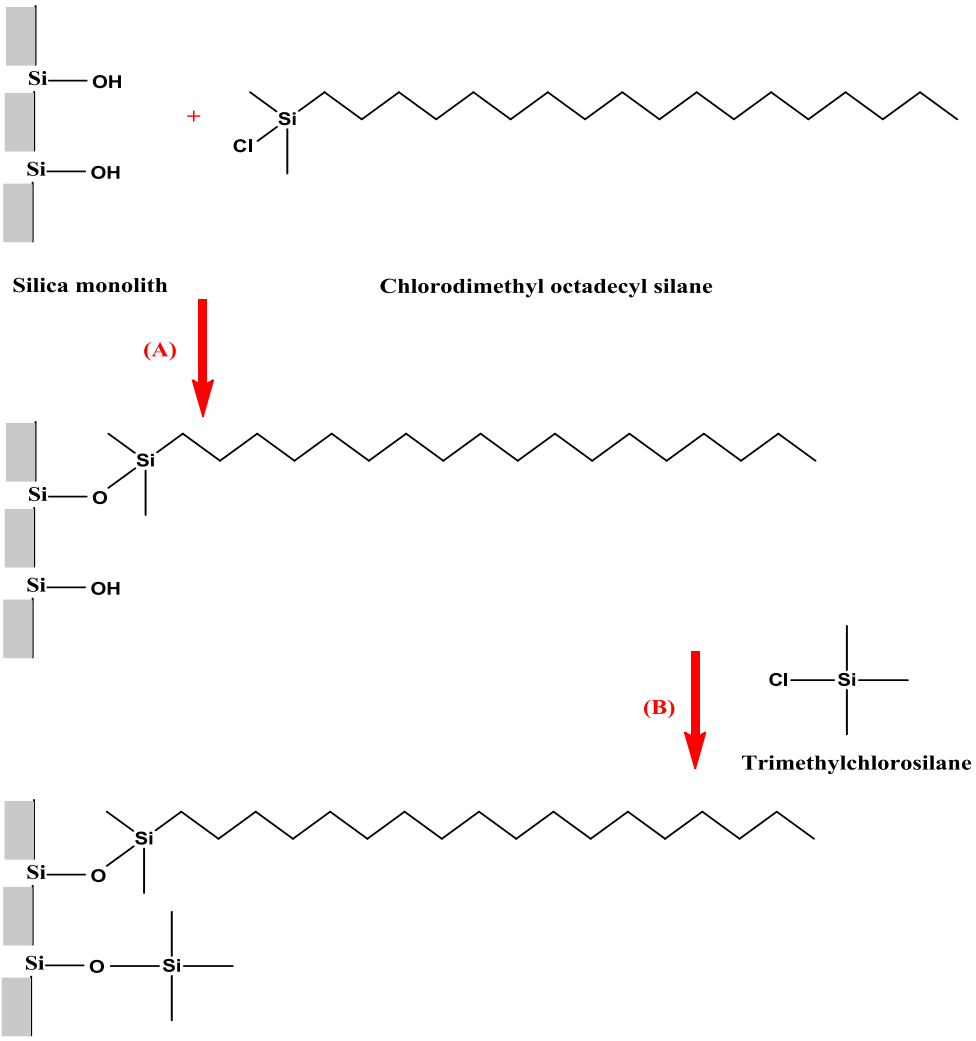

Figure 3.24 Formation of the bonded-phase silica: (A) monomeric octadecyl bonded phase, and (B) end capping of the residual silanol group.

It was observed that the colour of the non-modified monolithic silica rod was bright white while the octadecylated silica monolith rod was translucent as can be seen in figure 3.25, which shows the monolithic silica rods before and after modification with octadecyl ligands and end capping process.

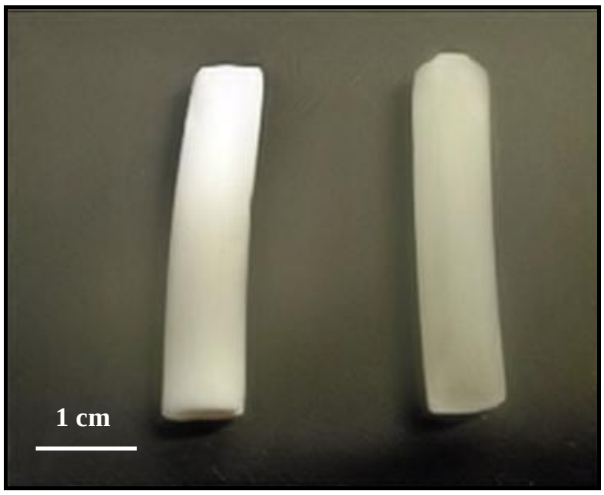

Figure 3.25 The silica-based monolith before (left) and after modification with octadecyl groups (right). The colour of the monolithic silica rod was changed from bright white to translucent. The sol-gel precursor was 2.256 mL TMOS, 0.282 g PEO, 2.537 mL 1 M HNO_3 solution, and 0.291 mL distilled H_2O. The derivatisation reagent was 1 g CDMOS in 10 mL toluene and 10 drops 2,6-lutidine, and the end capping reagent was 1 g TMCS in 10 mL toluene.

In order to use the fabricated octadecylated silica rod as a sorbent, it was placed inside the heat shrinkable polytetrafluoroethylene (PTFE) tube and placed in the oven. The temperature of the oven was increased from room temperature to 330 °C for 2 hours to shrink the tube around the monolithic silica rod. Surface modification of the silica-based monolith with octadecyl groups was carried out after placing the monolithic silica rod inside the heat shrinkable tube. The reason for that is because it was observed that if the monolithic silica rod was covered with the tube after the surface derivatisation reaction, the colour of the octadecylated silica monolith and the heat shrinkable tube changed to black, as can be seen in figure 3.26. This could be because of burning and decomposition of the alkyl chain groups when using a very high temperature (330 ºC) for sealing the monolithic silica rod with the heat shrinkable tube. Therefore, it was decided to seal the monolithic silica rod with the heat shrinkable tube before modification of the surface of the silica-based monolith with octadecyl groups.

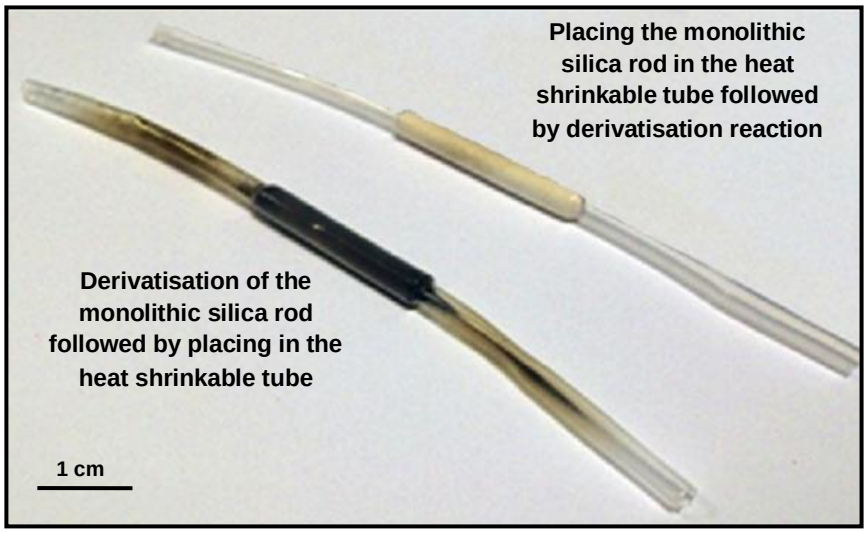

Figure 3.26 The effect of high temperature (330 °C for 2 hours) on the appearance of the octadecylated silica monolithic rods after placing them inside the heat shrinkable tube.

The structural morphology of the octadecylated silica monolith was examined by SEM analysis in order to investigate the effect of the surface derivatisation of the silica-based monolith with octadecyl groups on the morphology of the silica-based monolith. Figure 3.27 shows the SEM micrographs of the silica-based monoliths after modification with octadecyl groups prepared at different gelation times (1, 2, 3, and 4 days). The SEM micrographs show that the shape of the through-pores of the octadecylated silica monolith was relatively round and the size of the through-pores of the octadecylated silica monolith was smaller than that of the non-modified silica-based monoliths. Moreover, it was found that the size of the macropores was decreased by increasing the period of the gelation step from 1 day to 4 days.

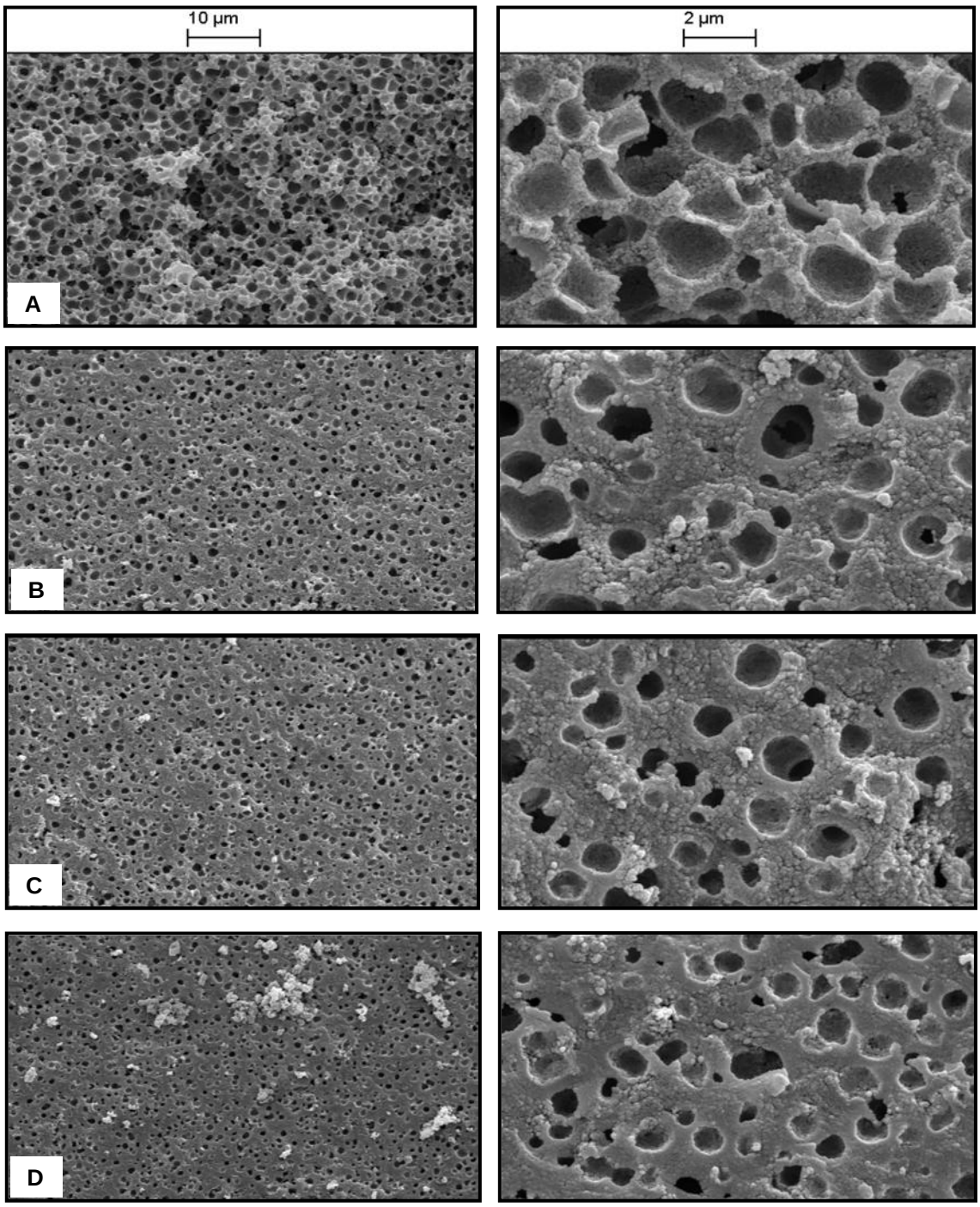

Figure 3.27 SEM micrographs of the silica-based monoliths prepared at 40 °C for different gelation periods: (A) 1 day, (B) 2 days, (C) 3 days, and (D) 4 days, followed by surface modification of the silica-based monoliths with octadecyl groups.

Besides the analysis of the octadecylated silica monolith with SEM analysis, the derivatisation of the silica-based monolith with octadecyl groups was confirmed by using energy dispersive X-ray (EDX) analysis. Figure 3.28 shows a comparison between the EDX spectra of the bare silica-based monolith and the octadecylated silica monolith. The result shows that following derivatisation of the surface of the silica-based monolith, new peaks for carbon (C) and chlorine (Cl) were observed as expected, since the modification reagent was chlorodimethyl octadecyl silane, while these peaks were absent in the bare silica-based monolith. This spectrum reveals the presence of octadecyl groups on the surface of the silica-based monolith.

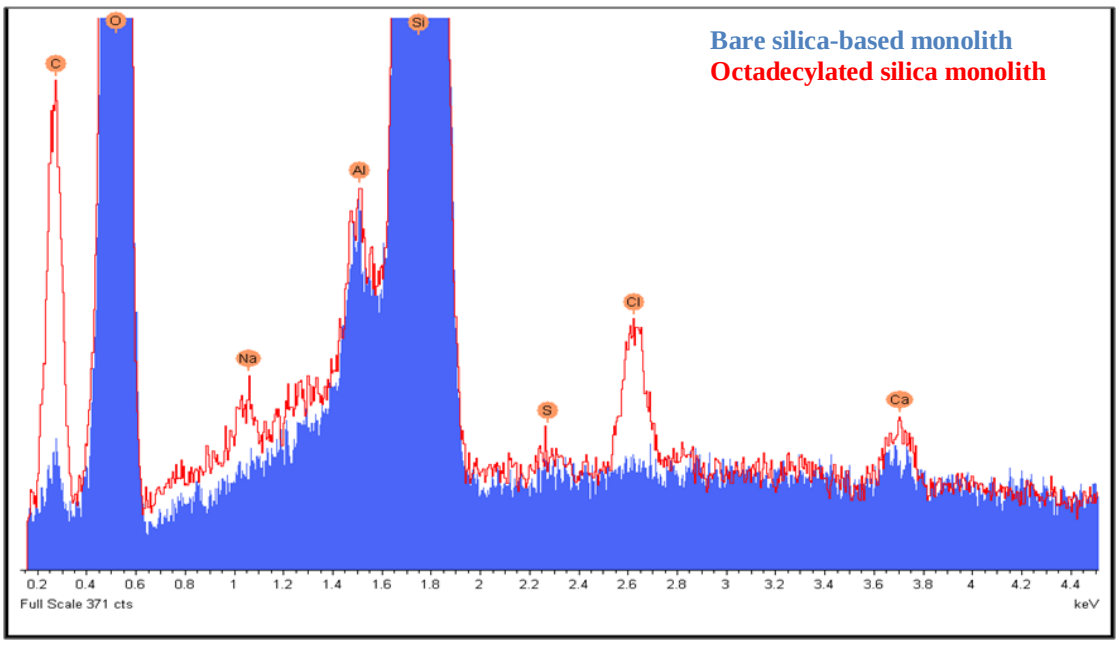

Figure 3.28 EDX spectra showing comparison between the bare silica-based monolith (blue spectrum), and octadecylated silica monolith (red spectrum).

The physical properties of the octadecylated silica monolith were studied using BET measurement in order to investigate the effect of the surface derivatisation on the total surface area, the average pore size, the total pore volume, and the porosity. Figure 3.29 shows the BET surface areas of the octadecylated silica monoliths that vary in the period of the gelation process (1, 2, 3, and 4 days). The figure shows that the BET surface areas of the silica-based monoliths were decreased after derivatisation with alkyl chains (C_{18}) compared with the non-modified silica monolith, as expected. The reason for this is blocking of the micropores in the silica-based monolith by the

bonded phase (the alkyl chains attached to the silica surface).[31, 245] In addition, it was found that the BET surface areas of the octadecylated silica monoliths were decreased from 154.29 to 96.21 m^2 g^{-1} by increasing the gelation period from 1 to 4 days.

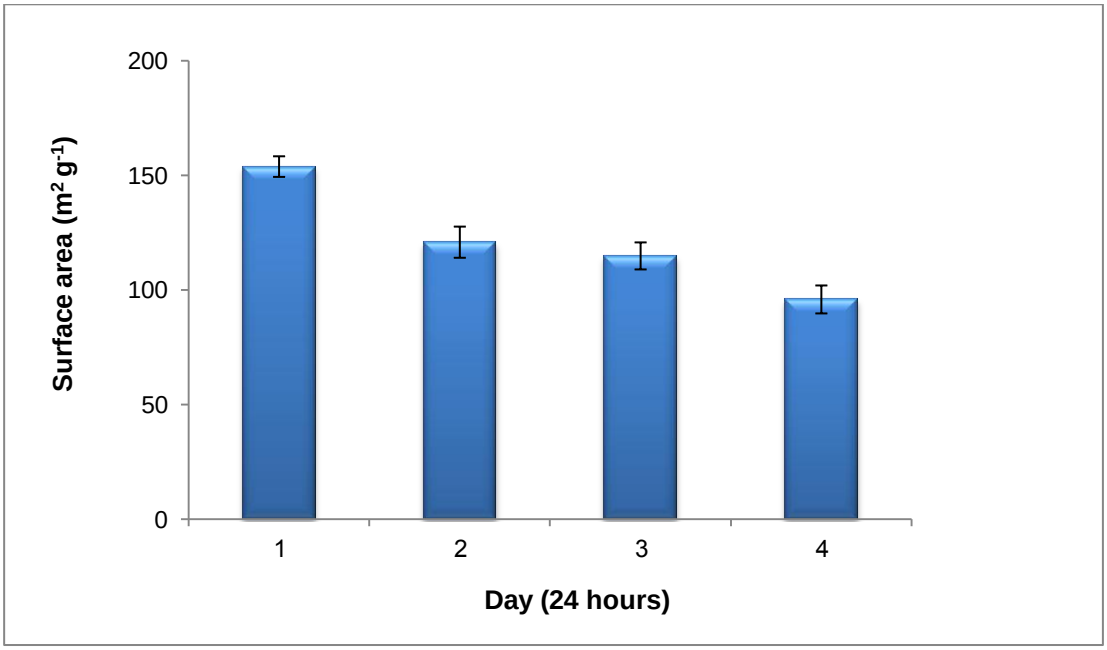

Figure 3.29 The BET surface area of the octadecylated silica monoliths prepared at different periods of the gelation process (1, 2, 3, and 4 days), RSD (n=3).

The overall pore size distributions of the octadecylated silica monoliths prepared at different gelation times (1, 2, 3, and 4 days) were calculated using the BJH method, figure 3.30. It was found that the average pore sizes of the prepared octadecylated silica monoliths were in the mesopore range (9.36-12.51 nm); however, they were smaller than the pore sizes of the non-modified silica-based monoliths, as expected. The reason for that could be because the surface silanol groups on the silica-based monolith are replaced by larger chemical ligands, resulting in a decrease in the pore size.[31, 245] In addition, it was found that the total pore volumes of these monoliths were between 0.27 and 0.37 cm^3 g^{-1}. The total pore volume of the silica-based monolith was decreased after surface derivatisation with octadecyl ligands. The reduction of the void space is due to the presence of the grafted moieties on the inner surface of the pore.

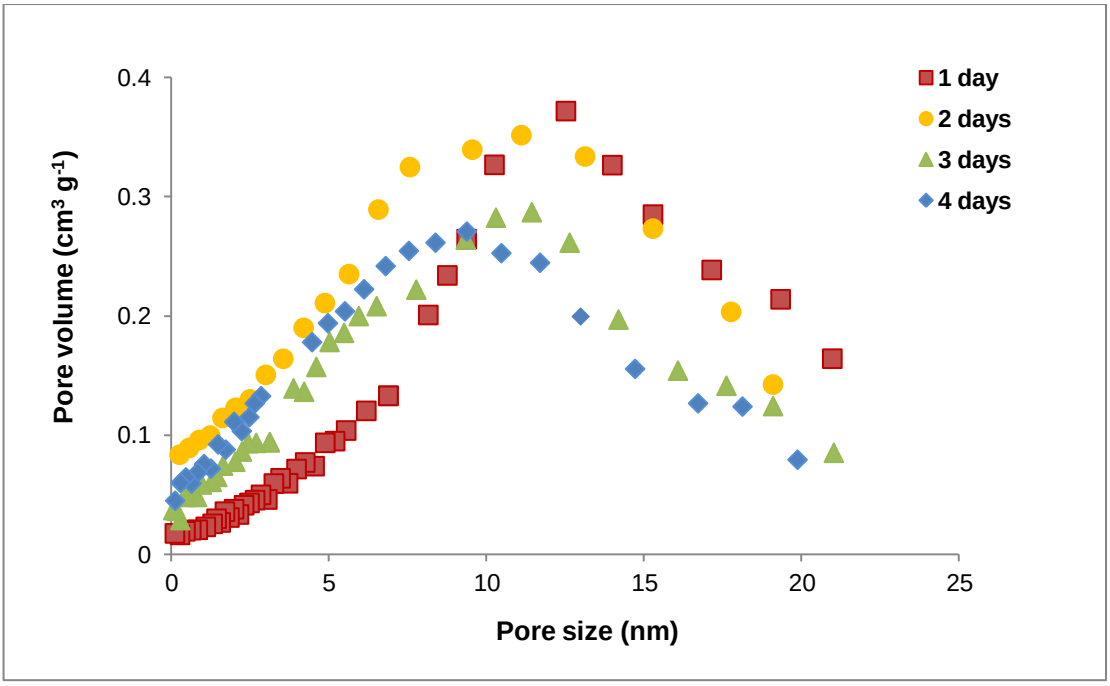

Figure 3.30 The overall pore size distributions of the octadecylated silica monoliths prepared at different gelation times (1, 2, 3, and 4 days), calculated by the BJH method.

The porosity of the octadecylated silica monoliths prepared at different periods of the gelation process was investigated. Figure 3.31 presents the effect of the gelation period on the porosity of the silica-based monolith modified with octadecyl groups. As can be seen from the figure, although the variation in the porosity of the prepared octadecylated silica monoliths was not very large, the porosity was gradually decreased by increasing the gelation period and the highest-porosity monolith was obtained when the gelation period was 1 day (porosity = 0.23).

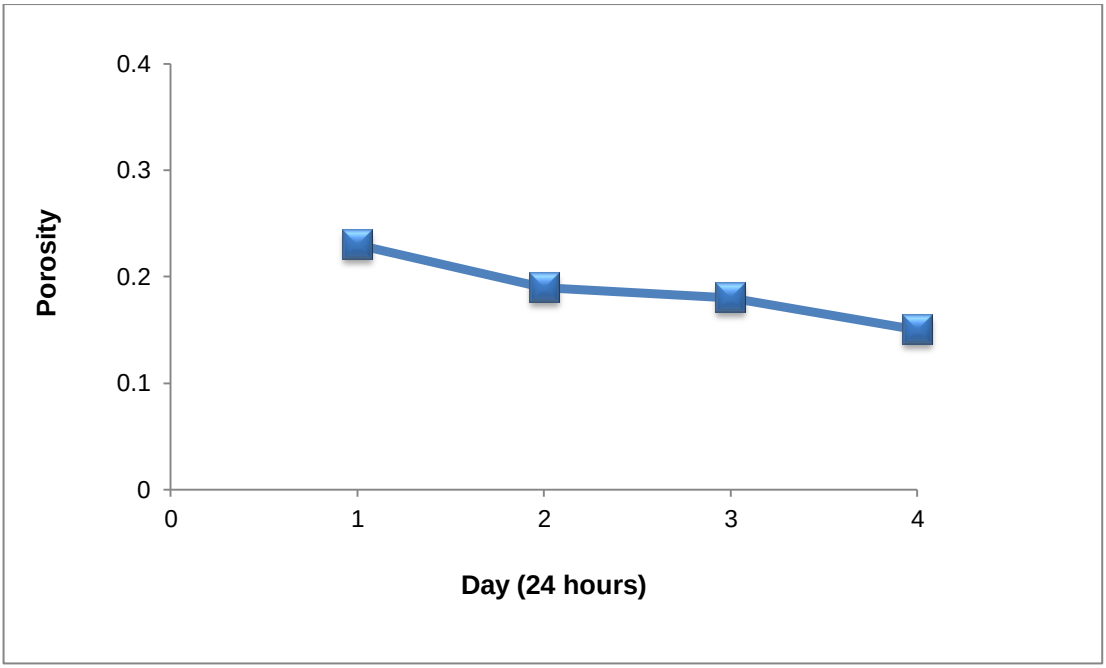

Figure 3.31 The porosity of the octadecylated silica monoliths prepared at different gelation times (1, 2, 3, and 4 days). The porosity was calculated using equation 1, density of water at temperature 23 ºC = 0.9975 g cm^{-3}.

It was found that the period of the gelation process has an effect on the structural morphology and the physical properties of the octadecylated silica monolith. It was found that by increasing the time of the gelation process from 1 day to 4 days, the BET surface area, the mean pore size, the total pore volume, and the porosity of the octadecylated silica monolith were decreased, which could affect the performance of the fabricated monolith. Therefore, it was decided to make the gelation time 1 day for fabrication of the silica-based monolith in this study, although the commonly reported gelation time for preparation of the silica-based monolith is 3 days.[246, 247]

3.2.4 Fabrication of the inorganic monolith inside the micropipette

It was preferred to fabricate the silica-based monolith inside a microchip rather than the heat shrinkable tube in order to speed the analysis, and reduce the volume of the analyte and the reagents. It is known that the preparation of the silica-based monolith inside a microchip is a challenging process, since the location of the monolith inside

the extraction chamber cannot be defined because the preparation of the silica-based monolith depends on using thermal initiation. Therefore, fabrication of the monolithic sol-gel matrix in the microchip must be addressed.

Before fabrication of the silica-based monolith inside the microchip, it was decided to fabricate it inside a 25 µL-sized micropipette, since it is cheaper than the microchip. Two trials were performed to prepare the sol-gel silica-based monolith. The first attempt was performed by using the same sol-gel mixture and procedure that were used before for fabrication of the silica-based monolith inside the heat shrinkable tube. The length of the monolith inside the micropipette was around (4-5) cm to give a clear picture of the homogeneity of the fabricated silica-based monolith inside the micropipette. After fabrication of the inorganic monolith inside the micropipette, it was observed that the inorganic monolith had shrunk during preparation and the monolith contained cracks, as can be seen in figure 3.32. Surface cracking can be a direct result of the shrinkage of the silica-based monolith inside the micropipette that is associated with the gelation process and large shrinkage of the monolith occurs during the drying stage.

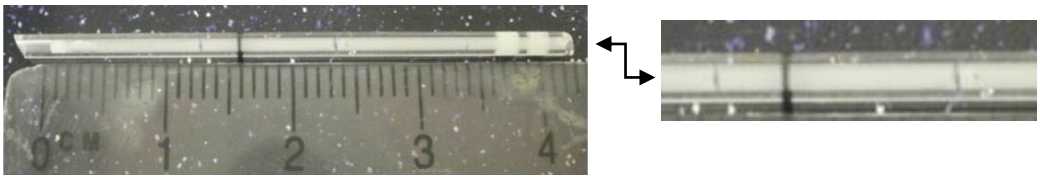

Figure 3.32 The shrinkage phenomena in the silica-based monolith prepared inside the micropipette. The sol-gel precursor was 2.256 mL TMOS, 0.282 g PEO, 2.537 mL 1M HNO_3 solution, and 0.291 mL distilled H_2O.

Although the previous procedure was successful in the fabrication of the inorganic monolith inside the heat shrinkable tube with a high surface area, preparation of the silica-based monolith inside the micropipette was unacceptable, since the shrinkage and the cracking in the monolith could affect the reproducibility of fabrication and protein extraction efficiency. Therefore, another sol-gel mixture and procedure were investigated for fabrication of the silica-based monolith inside the micropipette.

The second trial to fabricate the silica-based monolith inside the micropipette was adapted from Wu *et al.*[126] To eliminate the problem of shrinkage of the silica-based monolith inside the micropipette, the micropipette was washed with 1 M sodium hydroxide solution (NaOH) for 12 hours to generate free silanol groups on the surface of the micropipette, which participate in the condensation reaction. After activation of the inner surface of the micropipette, it was injected with the sol-gel mixture consisting of 2 mL TMOS (monomer), 0.44 g PEO (porogen), and 10 mL 1 M HNO_3 solution (catalyst), followed by surface modification with the octadecylated ligands. As can be seen in figure 3.33, the octadecylated silica monolith was anchored to the walls of the micropipette without shrinkage or voids at the interface monolith-walls of the micropipette. Moreover, this method of fabrication was faster compared with the previous procedure.

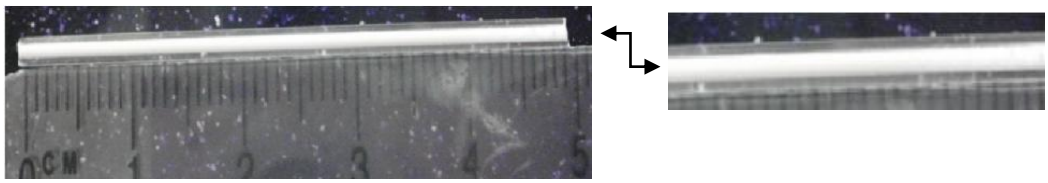

Figure 3.33 Fabrication of the octadecylated silica monolith inside the micropipette, which was activated by rinsing with 1M NaOH solution for 12 hours. The sol-gel precursor was 2 mL TMOS, 0.44 g PEO, and 10 mL 1 M HNO_3 solution.

The total surface area and the pore size of the fabricated octadecylated silica monolith were measured, and it was found that the BET surface area was 107.25 $m^2 g^{-1}$, and the pore size was 10.37 nm. Both surface area and the pore size of the octadecylated silica monolith prepared using this procedure were lower than that of the octadecylated silica monolith fabricated using the previous procedure.

3.2.5 Fabrication of the inorganic monolith inside the microfluidic device

The previous attempts to fabricate the silica-based monolith inside the micropipette were not satisfactory in terms of its performance in protein extraction, which will be discussed later in the section on application of the silica-based monolith in protein extraction. It was decided to fabricate the silica-based monolith as a rod using a mould (disposable plastic syringe) as performed before, then cut a monolithic silica disk and place it inside the extraction chamber of the base plate of the microchip. In this study, two types of microchips were investigated, fabricated from polycarbonate and glass.

The design of the extraction chamber (2 mm depth and 6.5 mm width) of both microchips was circular rather than a channel. The purpose of using the wider diameter of the extraction chamber is to get a faster flow that decreases the analysis time while keeping good contact between the monolith (the sorbent bed) and the sample solution.[31]

The first microchip investigated was made from polycarbonate. The reason for using the polycarbonate microchip is low cost.[248] After placing the monolithic silica disk inside the extraction chamber of the polycarbonate microchip, the base plate (23.5 mm length and width, and a thickness of 2.8 mm), and the cover plate (13.5 mm length and width, and a thickness of 1 mm) were bound using epoxy resin. Both plates contained an access hole (1.5 mm) for use as inlet and outlet holes. After bonding the two plates, the monolithic silica disk was modified with octadecyl ligands. However, it was found that the polycarbonate microchip was affected by the modification reagents and the high temperature. Therefore, it was decided to perform the modification reaction before placing the monolithic silica disk inside the extraction chamber, then the top and the base plates were sealed together.

The second microchip investigated was made from glass, since it is more resistant to reagents, organic solvents, and high temperature. After placing the monolithic silica disk into the extraction chamber of the base plate of the microchip, the top and base plates (16.5 mm length and 14 mm width) were thermally bonded together at 575 °C for 3 hours. The derivatisation of the surface of the silica-based monolith was carried out after the bonding step, since the organic moieties could be affected by the high temperature of the bonding step (575 °C). Another advantage of derivatisation of the

silica-based monolith with octadecyl groups after bonding is to coat the walls of the glass microchip with octadecyl groups. As a result, the undesired interaction of the protein with the surface of the glass microchip will be minimised. It was found that although the monolithic silica disk inside the microchip was not chemically anchored to the inner walls of the microchip, which was checked using an optical microscope, it was not affected by the thermal bonding step and the shrinkage of the disk was completely avoided.

3.2.6 Reproducibility of preparation of the inorganic monolith

The reproducibility of fabrication of the monolithic silica materials is an important parameter, since it is a multi-step procedure. Moreover, the reproducibility of the surface modification of the silica-based monolith is an important requirement for acceptance of the utilised preparation method, especially in industrial laboratories.[249] In order to check if the multi-step preparation of the silica-based monolith was reproducible sufficiently, the SEM morphology for three different batches of the silica-based monolith before and after modification with octadecyl ligands was assessed. It was found that there was no difference in the morphology of the prepared monoliths.

The reproducibility of preparation of the monolithic silica rod was also evaluated by measuring the relative standard deviations (RSDs) of the size of the macropores (20 different macropores) and the diameter of the monolithic silica rods (three different batches). As shown in table 3.2, the RSDs value of the macropores size and the diameter of the monolithic silica rods prepared at 40 °C for different periods of the gelation process were in the range 3.6-5.5 %, and 2.4-5.3 %, respectively. These results showed that the reproducibility of the preparation procedure of the silica-based monolith is acceptable.

The RSDs of the physical properties (the specific surface area, the pore size, the pore volume, and the porosity) of three different batches of the silica-based monolith before and after modification were calculated. The experimental results (table 3.3) indicate that the reproducibility of the fabrication procedure of the bare silica-based monolith and the surface modification procedure is acceptable.

Type of silica monolith	Surface area (m^2 g^{-1}) ± RSD (%)	Average pore size (nm) ± RSD (%)	Total pore volume (cm^3 g^{-1}) ± RSD (%)	Porosity ± RSD (%)
Non-modified	173.31 ± 3.7	13.58 ± 3.8	0.63 ± 4.7	0.51 ± 3.9
Modified with octadecyl group	154.29 ± 5.2	12.22 ± 4.2	0.38 ± 6.5	0.23 ± 3.1

Table 3.3 The physical properties of the silica-based monolith (the gelation process was at 40 °C for 1 day) before and after modification with octadecyl groups, and RSD (n = 3).

3.3 Fabrication of the inorganic monolith for protein reduction

Study of proteins usually involves digestion of the proteins using enzymes to produce peptides that are subsequently studied by mass spectrometry. Many proteins such as insulin, lysozyme, and bovine serum albumin are formed from folded polypeptides, containing disulphide bonds, which link the folds. If the proteins are folded, specific locations in the proteins are inaccessible to the proteolytic enzyme. Therefore, reduction and alkylation of proteins before proteolytic digestion can facilitate protein unfolding and increase the efficiency of enzymes in digesting the proteins.[250]

The aim of the present study was to develop a new method for immobilisation of the reducing reagent on the surface of a silica-based monolith for use in the reduction of disulphide bonds in proteins before enzymatic digestion. Although it is possible to immobilise the reducing reagent on the surface of the channel walls of a glass microchip, in this case, the overall surface-to-volume ratio is very small. Therefore, it was preferred to immobilise the reducing reagent on the surface of the silica-based monolith since the surface-to-volume ratio can be increased by filling the microchip with a solid phase.[193] As a result, loading of TCEP on the surface of the silica-based monolith will be increased and the interaction between the proteins having disulphide bonds and the immobilised TCEP on the surface of the silica-based monolith would be increased, which could improve the reduction of the disulphide bonds.

To achieve this objective, the silica-based monolith was fabricated through the sol-gel process as before, and then the monolithic silica disk was placed in the chamber (2 mm depth and 6.5 mm width) of the base plate, followed by thermal bonding of the top and base plates of the glass microchip. In order to use the silica-based monolith as a support for the immobilisation of the reducing reagent, the surface of the silica-based monolith was chemically modified with (3-aminopropyl)triethoxysilane (APTES), $NH_2(CH_2)_3Si(OC_2H_5)_3$, followed by immobilisation of the reducing reagent (TCEP) on the amino-bonded silica monolith. The fabricated amino-modified silica monolith and the TCEP-immobilised silica monolith were characterised using different techniques such as measuring the water contact angle, SEM analysis, EDX analysis, FT-IR spectroscopy, and BET analysis.

3.3.1 Surface modification of the inorganic monolith with APTES

As mentioned before, a silica-based monolith was used as a matrix for immobilisation of the reducing reagent. The silica-based monolith is an inorganic polymer having siloxane (Si-O-Si) groups in the bulk and its surface covered with silanol (Si-OH) groups that theoretically can be utilised as anchors for the organic groups.[251] However, it is unlikely that all the silanol groups are derivatised due to steric hindrance.[252] Therefore, silanisation with silane compounds has been utilised for surface modification of silica-based monoliths. The silane compounds commonly used for surface modification are aminosilanes because of the significant advances in the understanding of this kind of surface modification reagent.[253, 254] In this study, the surface of the silica-based monolith was modified with APTES, which contains two functional groups, triethoxysilane and amino groups. The triethoxysilane group can react with the silanol groups (Si-OH) on the surface of the silica-based monolith, while the amino functional groups are highly reactive to many functional groups and can offer the necessary active sites for other components to be futher immobilised.[255, 256] Figure 3.34 shows the chemical reaction of the silanisation reagent (APTES) with the surface silanol groups on the silica-based monolith. The derivatisation reaction occurs by condensation of the silanol group to produce siloxane bonds (Si-O-Si), and loss of ethanol (C_2H_5OH), as a by-product of the condensation reaction.[257]

In this study, surface functionalisation of the silica-based monolith with the amino groups was performed by continous feeding of the microchip-based silica monolith

with 33 % (v/v) APTES solution in dried toluene for 24 hours at room temperature using a syringe pump at a flow rate of 7 µL min^{-1}, followed by washing the amino-bonded silica monolith with dried toluene and methanol.

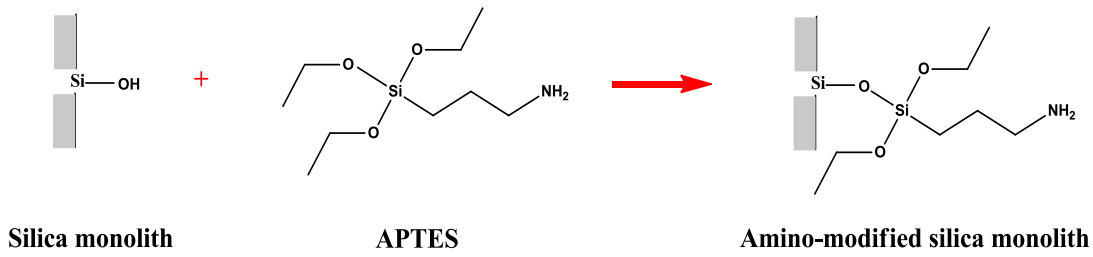

Figure 3.34 Schematic representation of the mechanism of reaction of the surface silanol groups on the silica-based monolith with the silanisation reagent that was (3-aminopropyl)triethoxysilane (APTES).

Surface modification of the silica-based monolith inside the glass microchip with APTES was performed after thermal bonding of the two plates of the glass microchip in order to modify not only the monolithic silica disk, but also the inner walls of the glass microchip, and thereby minimise the uncontrolled non-specific adsorption of proteins on the glass microchip. Another reason was to avoid burning and decomposition of the organic moieties when using a high temperature for the bonding step (575 °C for 3 hours).

It was very important to make sure that the surface of the silica-based monolith was coated with the amino groups before introducing the reducing reagent. The grafted monolith with APTES was qualitatively tested by a fluorescent dye, rhodamine B isothiocyanate (RBITC), since the isothiocyanate group (-N=C=S) in RBITC can react with the NH_2 terminal groups on the surface of the silica-based monolith, resulting in a covalent coupling of RBITC on the surface of the amino-bonded silica monolith, which cannot be washed out.[255] This was performed by flushing the specimen with RBITC dissolved in methanol at a concentration of 0.5 mg mL^{-1}, and then the

monolith was washed with methanol to remove unanchored dye. Figure 3.35 (A) shows the appearance of the amino-bonded silica monolith before and after washing it with RBITC. From the figure, it can be seen that the appearance of the amino-modifed silica monolith was white, then turned to pink after washing it with RBITC due to labelling of the amino groups on the surface of the silica-based monolith with RBITC. This result confirms of the functionalisation of the surface of the silica monolith with amino groups.

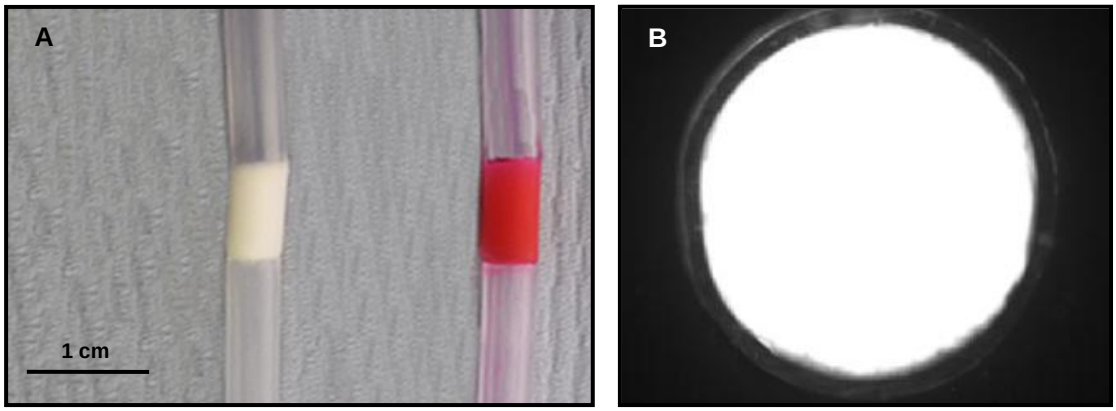

Figure 3.35 (A) The appearance of the amino-modified silica monolith before (white material), and after washing it with rhodamine B isothiocyanate (RBITC) dissolved in methanol at a concentration of 0.5 mg mL^{-1} (pink material). (B) Cross-section of the RBITC labelled amino-modified silica monolith using florescent microscope. The excitation wavelength was 570 nm and the emission wavelength was 595 nm.

It was important to make sure that not only the outer surface but also the inner surface of the silica-based monolith was modified with the amino groups; therefore, a cross-section of the modified silica monolith with the amino groups was examined under a fluorescent microscope. Figure 3.35 (B) shows a cross-section of the amino-bonded silica monolith that was labelled with RBITC using fluorescence microscope. From the figure, it can be seen that the surface of the silica-based monolith was modified equally with the amino groups since equal fluorescence signal intensity was obtained.

Another method to confirm surface derivatisation of the silica-based monolith with the amino groups was measuring the contact angle with deionised water, since this method is commonly utilised to give information about the surface of materials and show the variation of solid surface chemical composition.[258] In addition, the relative hydrophilicity or hydrophobicity of the sample can be easily obtained by measuring the contact angle.[259] However, measuring the contact angle directly on the surface of the silica-based monolith was not easy, since it is a very porous material and has the ability to absorb deionised water quickly; therefore, the contact angle measurement was performed in an empty micropipette (200 µm i.d.), since it contains silanol groups (Si-OH) similar to the surface of the silica-based monolith. After modification of the inner surface of the micropipette with APTES, the contact angle of the deionised water on the surface of the amino-modified micropipette was captured using an optical microscope with a charge-coupled device (CCD) camera, and compared with the contact angle of the deionised water on the surface of the non-functionlised micropipette for five replicate measurements for each specimen. Figure 3.36 shows microscope images of the water contact angles for the unmodified micropipette and the amino-modified micropipette. The water contact angle for the unmodified micropipette was hydrophilic with a measured contact angle of 37.0±1.6 º because of the presence of silanol groups (Si-OH) on the surface of the micropipette, which are largely dissociated to $Si\text{-}O^-$ at neutral pH.[212]

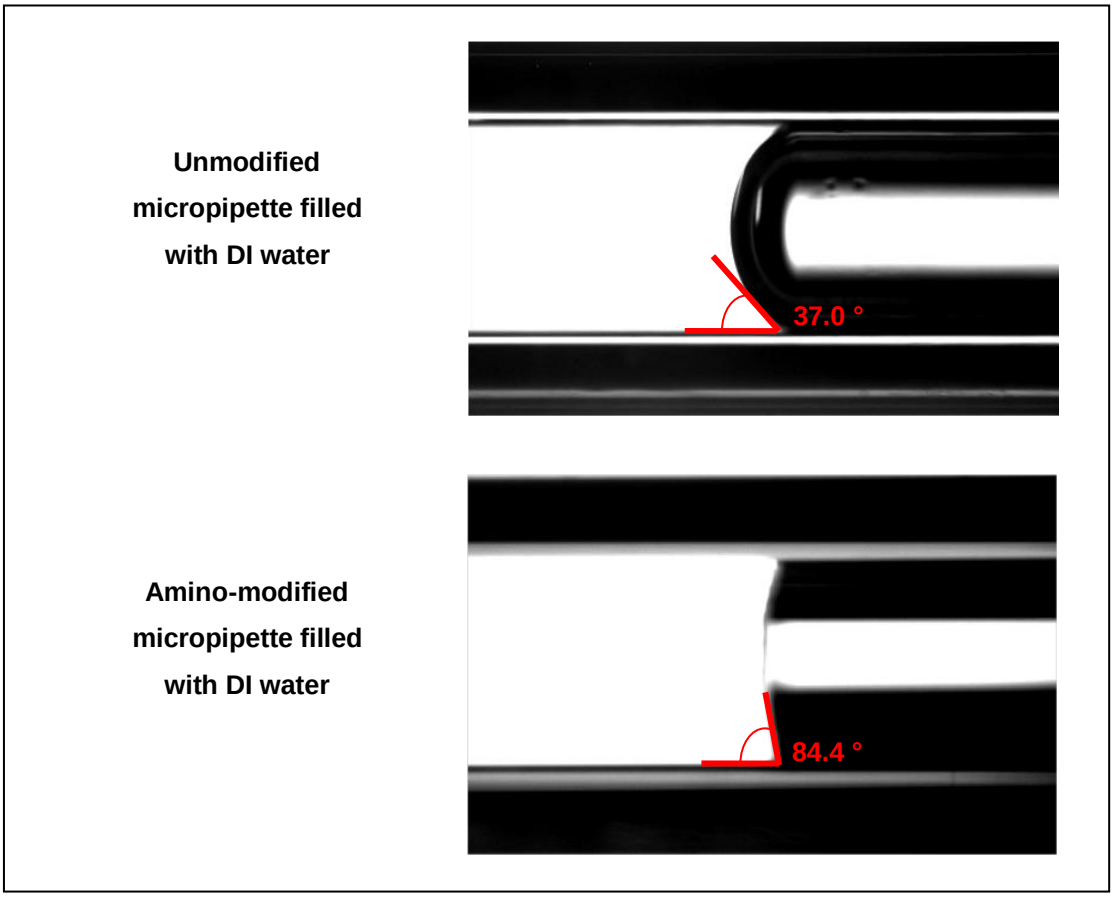

Figure 3.36 Comparison between the contact angles of the deionised water on the bare micropipette and the silanised micropipette with APTES, captured by an optical microscope with a CCD camera at magnification 10 ×.

Due to attachment of the amino groups on the surface of the micropipette, there was an increase in the surface hydrophobicity (i.e., higher contact angle = more hydrophobic) and the water contact angle increased from 37.0±1.6 º to 84.4±2.2 º. The increment of water contact angle value confirmed the successful functionalisation of the surface of the micropipette with the amino segments via covalent bonding. However, the value of the contact angle of the micropipette treated with APTES was slightly lower than that of the previous contact angle of the glass slide treated with APTES at room temperature for 24 hours; the contact angle increased from 8.0 º to 69.9±1.2 º.[260]

The surface of the bare silica-based monolith and the amino-functionalised silica monolith were examined by SEM analysis since SEM images are able to show whether or not there is a difference in the structural morphology of the prepared monoliths. Figure 3.37 presents SEM micrographs of the surface of the silica-based monolith before and after derivatisation with APTES. It can be seen that the SEM microrgraphs of the non-modified silica monolith, figure 3.37 (A), and the amino-bonded silica monolith, figure 3.37 (B) were homogeneous.

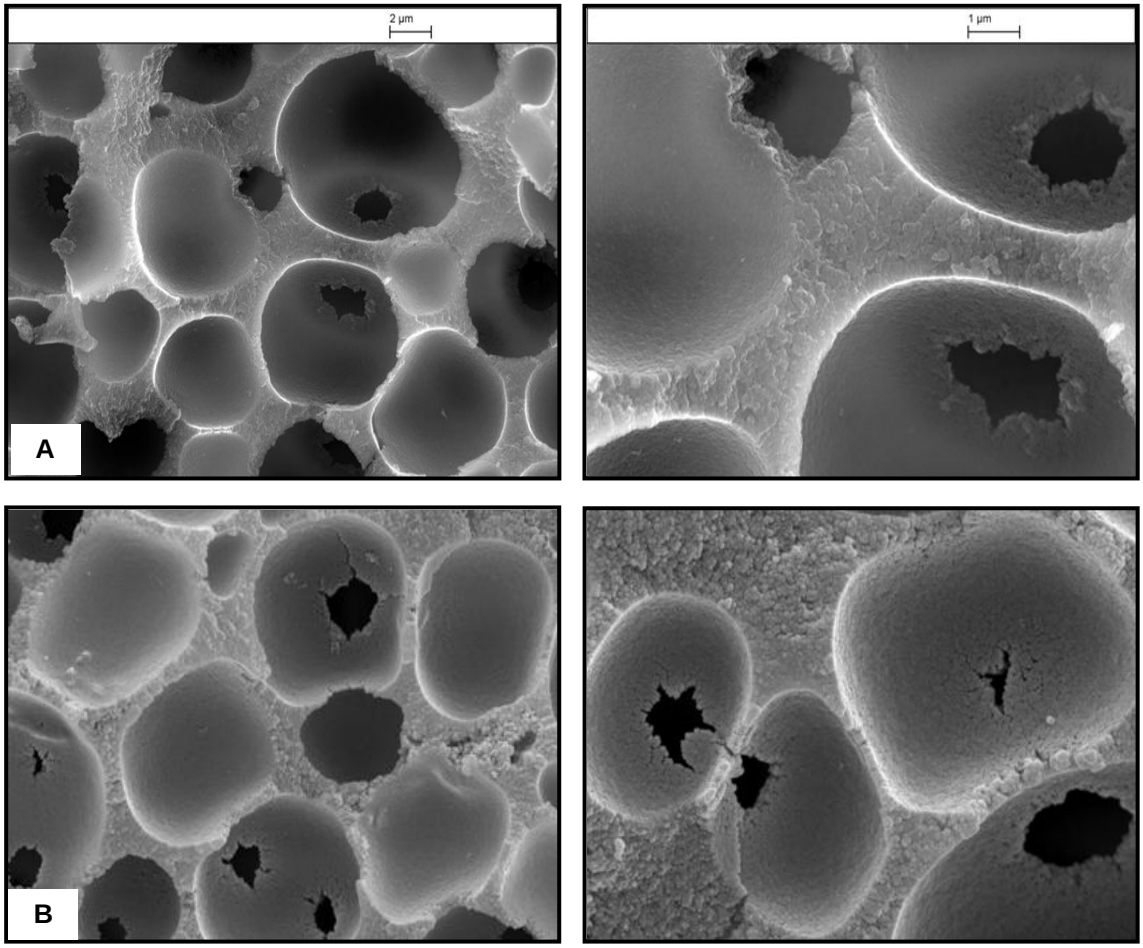

Figure 3.37 SEM images of the silica-based monolith before (A), and after modification of the surface of the monolith with amino groups (B).

It was expected that the size of the pores of the amino-functionalised silica monolith would be decreased due to anchoring of organic moieties on the inner surface of the pores; however, it was observed that the structural morphology of both samples was similar, and there were no noticeable differences in the diameter of the pore before and after the modification process. It was concluded that the amino layer on the surface of the silica-based monolith was not visible in the SEM micrograph, probably due to the

low density of the organic moieties compared to the silica monolith matrix or the low sensitivity of the characterisation method.

The chemical composition of the amino-bonded silica monolith was investigated by EDX analysis. Figure 3.38 shows the EDX spectrum of the derivatised silica-based monolith with APTES. In addition to silicon (Si) and oxygen (O), which are the main components of the bare silica-based monolith, carbon (C) and nitrogen (N) elements, which were from APTES, were found in the EDX spectrum. The amount of N is quite small; therefore, the EDX spectrum was expanded.

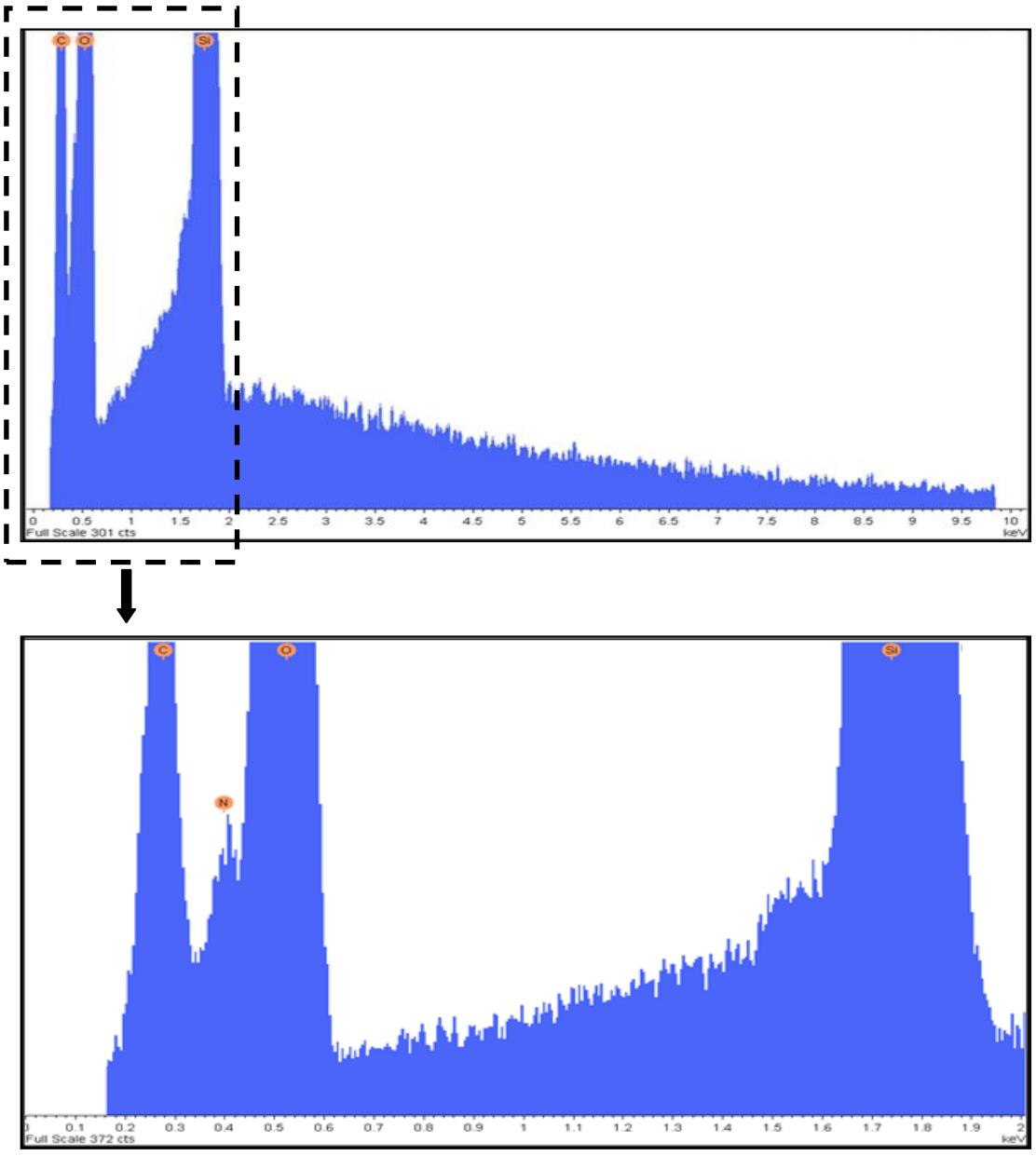

Figure 3.38 The EDX spectrum of the amino-modified silica monolith.

To further investigate the changes of the chemical structure between the unmodified and modified silica-based monolith with APTES and confirm the grafting of amino moieties on the surface of the silica-based monolith, Fourier transform infrared (FT-IR) spectroscopy was used, since this technique has the ability to follow structural changes that happen at the surface and in the network of the silica-based monolith.[261] Figure 3.39 displays the FT-IR spectra of the bare silica-based monolith (blue spectrum) and after modification the surface of the silica-based monolith with APTES (red spectrum). As can be seen from the figure, a strong band located at around 1075 cm^{-1} corresponded to asymmetric stretching vibration of Si-O-Si, indicating a strong cross-linked framework.[261] The band around 784 cm^{-1} resulted from symmetric stretching vibration of Si-O-Si.[262, 263] Both these bands of the inorganic frameworks were observed for both samples.

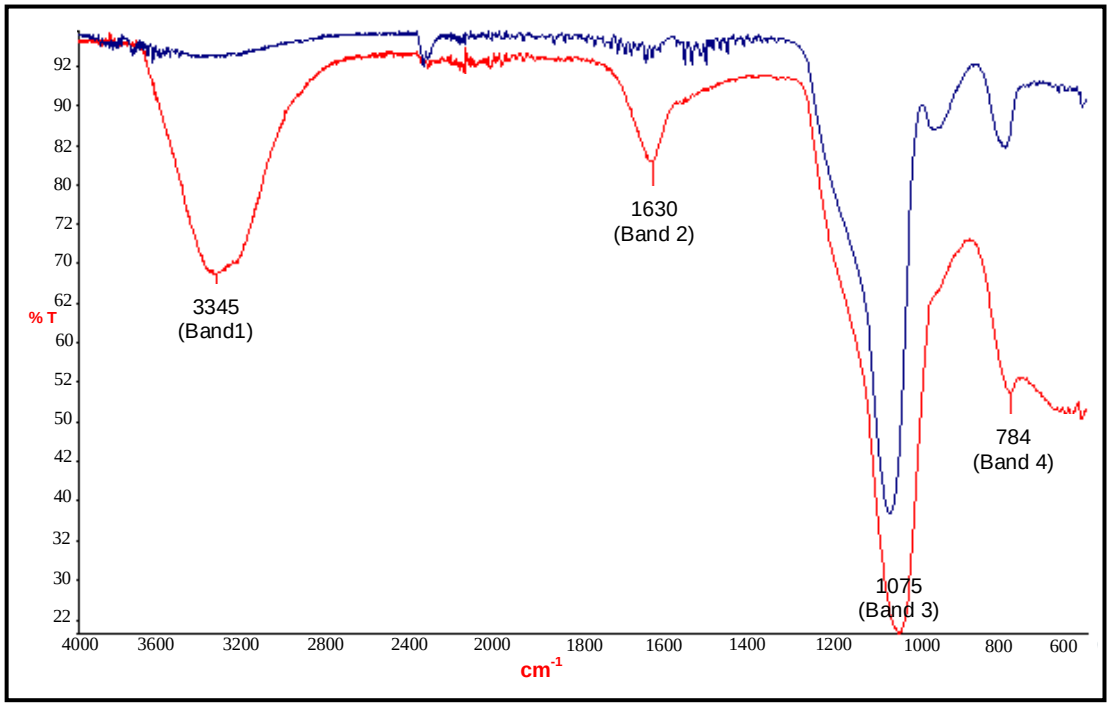

Figure 3.39 FT-IR spectra of the bare silica-based monolith (blue spectrum), and the amino-modified silica monolith (red spectrum). The IR range was in the middle infrared range (600-4000 cm^{-1}) using 6 scans at a resolution of 4 cm^{-1}.

In the FT-IR spectrum of the amino-bonded silica monolith, two new bands were observed. The broad band at 3345 cm^{-1} corresponded to the N-H stretching vibration, and the other band, observed at 1630 cm^{-1}, could be related to the bending vibration of

water molecules.[264] However, because the reaction medium of the silanisation reaction was dried toluene, this band is more likely related to the bending mode of free NH_2 groups.[265, 266] Since neither of these bands was observed in the spectrum of the bare silica-based monolith, this result was sufficient to give clear evidence that organic moieties (amino groups) were successfully grafted onto the surface of the silica network. The assignment of the IR bands is shown in table 3.4, which presents the experimental wavenumbers, their assignments, and the wavenumber limits for integration.

Band number	**Experimental wavenumber (cm^{-1})**	**Assignment**	**Range (cm^{-1}) [261, 263-265]**
1	3345	NH stretching vibration	3400-2700
2	1630	Bending vibration of free NH_2 group	1630-1625
3	1075	Asymmetric Si-O-Si stretching vibration	1130-1000
4	784	Symmetric Si-O-Si stretching vibration	860-730

Table 3.4 Assignment of bands observed in the FT-IR spectrum of the amino-modified silica monolith.

One question that remains is whether the surface of the silica-based monolith was coated with the amino groups equally or not. To address this, the surface coverage of the amino moieties on the silica-based monolith was calculated using equation (2) in order to check the homogeneity of modification of the silica surface with amino ligands throughout the entire silica-based monolith. The specific surface area of unmodified silica-based monolith, which was measured using BET analysis, was 173.31 m^2 g^{-1}. The percentage of carbon or nitrogen in the aminopropyl ligands bonded to the surface was measured by carbon and nitrogen content, which was measured using elemental analysis of different parts of the monolithic silica rod

treated with APTES (top, middle, and bottom). Table 3.5 presents evaluation of carbon and nitrogen in different parts of the amino-bonded silica monolith. The table shows the highest surface coverage of the organic moieties was in the top part of the monolith, as expected. It was found that the lowest surface coverage of the organic moieties was in the middle part of the monolith. This could be beause the core of the middle of the monolith is less exposed to the modification solution (33 % APTES in dried toluene) compared with the top and the bottom of the monolith. It was found that the surface coverage of the silica-based monolith with aminopropyl ligands was slightly higher than previously reported by another group.[211] Therefore, a satisfactory homogeneous surface coverage of the silica-based monolith with aminopropyl ligands was achieved.

Part of the monolith	**(% N = α NH_2)**	**(% C = α NH_2)**
Top	1.3% = 6.74 µmol m^{-2}	6.5% = 4.00 µmol m^{-2}
Middle	0.9% = 4.32 µmol m^{-2}	5.8% = 3.51 µmol m^{-2}
Bottom	1.1% = 5.48 µmol m^{-2}	6.4% = 3.93 µmol m^{-2}

Table 3.5 Evaluation of the concentration of carbon and nitrogen in different parts of the silica-based monolith treated with APTES.

3.3.2 Immobilisation of TCEP on the amino-bonded silica monolith

The amino groups introduced then were utilised for immobilisation of the non-thiol disulphide-reducing reagent (TCEP). This can be performed by formation of an amide bond (-CONH-) between the amino group on the surface of the silica-based monolith and the carboxyl group in TCEP. The reason for choosing TCEP as a reducing reagent is because it has many advantages compared with other conventional reducing reagents such as dithiothreitol (DTT) and 2-mercaptoethanol (BME), as discussed in the introduction section (1.5).

A key step in the immobilisation of TCEP on the surface of the amino-modified silica monolith is the formation of the amide bond; therefore, a peptide coupling reagent needs to be used in order to activate the carboxyl functional group of TCEP. The most common coupling reagents are carbodiimides, such as N,N'-dicyclohexylcarbodiimide (DCC) and N-(3-dimethylaminopropyl)-N′-ethylcarbodiimide hydrochloride (EDC). They have been widely utilised in peptide synthesis because they are relatively cheap.[267] In this study, EDC was used as a coupling reagent for immobilisation of TCEP on the surface of the amino-bonded silica monolith because it has many advantages over DCC; for example, it is water-soluble and it is soluble in different types of organic solvents, such as tetrahydrofuran and dimethyl formamide, while DCC is a waxy solid that is difficult to remove from the bottle and has to be handled in a fume hood. In addition, the by-product of EDC, which is isourea, can be removed easily while the by-product of DCC, which is dicyclohexyl urea (DCU), is insoluble in most solvents and needs to be removed from the reaction by using multiple filtrations.[268]

The coupling reagent (EDC) was mixed with the reducing reagent (TCEP) to activate the carboxyl functional group of TCEP. The coupling reagent is temporarily attached to the former carboxylate group forming an amine-reactive O-acylisourea intermediate for spontaneous reaction with the primary amino groups on the surface of the silica-based monolith to form an amide bond. However, when the reaction is carried out in an aqueous solution, O-acylisourea ester is an unstable complex and could undergo a rearrangement to form unreactive species that can significantly limit the yield.[269] Therefore, N-hydroxysulfosuccinimide sodium salt (Sulfo-NHS) was used as a coupling enhancer in order to increase the stability of the amine-reactive intermediate by reacting with O-acylisourea ester (an unstable reactive) to form the more stable succinimidyl activated ester, which readily undergoes nucleophilic substitution with the primary amine groups on the surface of the silica-based monolith and forms amide linkages.[270] The reason for choosing Sulfo-NHS ester is that it is unlike non-sulfonated NHS ester, since it is water soluble and does not need to be dissolved in organic solvent before being added to aqueous solution.

Figure 3.40 presents the reaction mechanism of immobilisation of TCEP on the surface of the silica-based monolith via the amino group using the coupling reagent

(EDC) in the presence of Sulfo-NHS in order to increase the efficiency of the conjugation reaction.

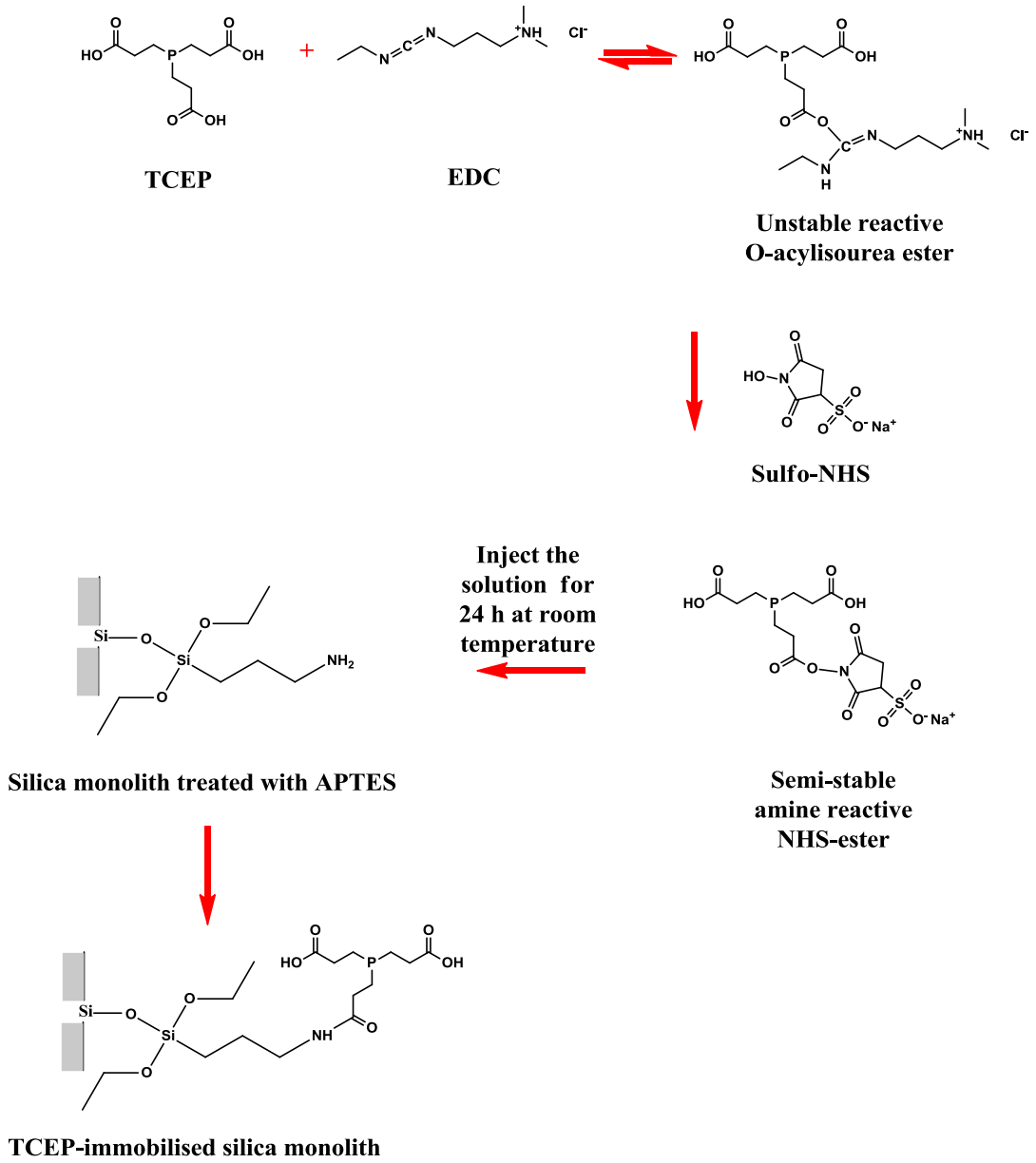

Figure 3.40 Reaction mechanism of the EDC/Sulfo-NHS conjugation reaction for coupling TCEP with the amino-bonded silica monolith. The efficiency of the conjugation reaction will be increased through the formation of succinimidyl activated ester, which is more effective in reaction with the amino groups coating the surface of the silica-based monolith, resulting in high yield of the amide bond formation.

The amidation reaction was performed under slightly acidic condition using 0.1 M MES buffer solution (pH 6.5) because EDC is more reactive under this condition.[198] After the amidation reaction, the by-product and unreacted materials were removed easily from the fabricated monolith by washing with 0.1 M MES buffer solution (pH 6.5) followed by deionised water for 1 hour at a flow rate of 10 µL min^{-1}.

It was important to make sure that the reducing reagent was immobilised onto the surface of the monolithic silica because if the reducing reagent was not immobilised, the proteins would pass through without reaction. Therefore, after immobilisation of the reducing reagent on the surface of the amino-functionalised silica monolith, it was characterised by measuring the water contact angle. Figure 3.41 shows the contact angle of the deionised water on the TCEP-immobilised micropipette. It was found that the water contact angle value of the TCEP-immobilised micropipette was decreased to 45.1±4.2° in comparison to the amino-bonded micropipette. The reason for that could be because the carboxyl group (-COOH) is more hydrophilic compared with the amino group ($-NH_2$), according to the work of Toworfe.[271] This confirms that the hydrophobic surface of the amino-modifed micropipette was hydrophilised by the immobilisation of TCEP on the surface of the amino-modifed micropipette, indicating that TCEP was successfully immobilised on the surface of the micropipette.

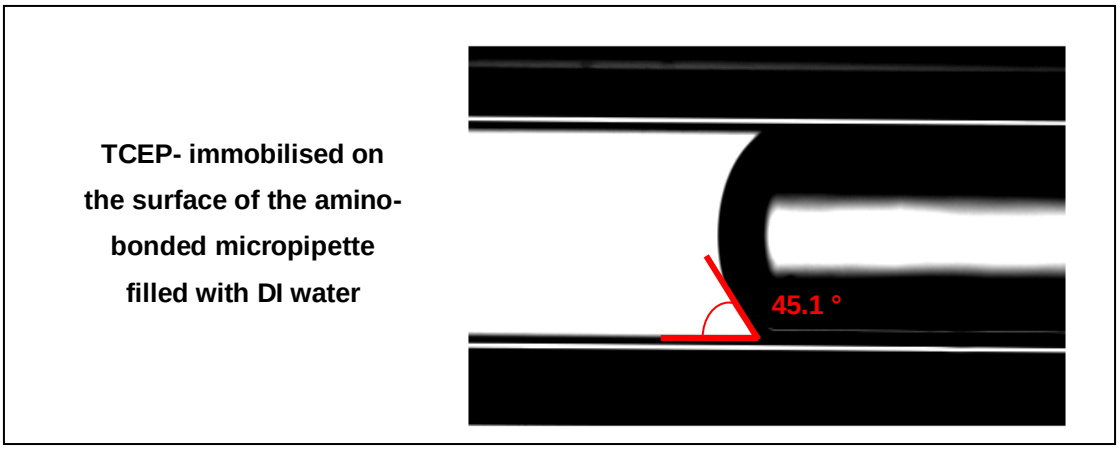

Figure 3.41 The contact angle of the deionised water on the TCEP-immobilised micropipette, captured by the optical microscope with a CCD camera at magnification 10 ×.

The structural morphology of the TCEP-immobilised silica monolith was examined using SEM analysis, as can be seen in figure 3.42; however, the SEM images did not obviously confirm the bonding of carboxyl groups of reducing reagent with amino groups on the silica-based monolith.

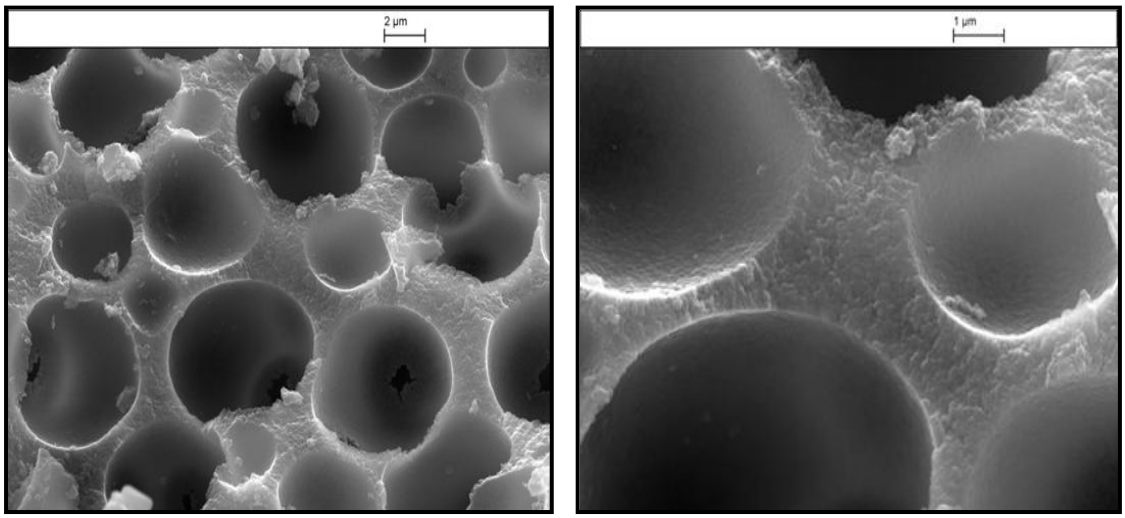

Figure 3.42 SEM images of the silica-based monolith coated with the reducing reagent (TCEP) via the amidation reaction. The mixture was 0.3 g TCEP, 0.03 g EDC, and 0.015 g sulfo-NHS dissolved in 2.5 mL 0.1 M MES buffer solution (pH 6.5) and injected into the amino-modified silica monolith using a syringe pump at a flow rate of 1.5 µL min^{-1} for 24 hours at room temperature.

The TCEP-immobilised silica monolith was further studied by EDX analysis, which was used to confirm immobilisation of the reducing reagent on the surface of the amino-functionalised silica monolith. As can be seen in figure 3.43, the EDX analysis of TCEP-immobilised silica monolith produced silicon (Si), oxygen (O), carbon (C), phosphorus (P) and chlorine (Cl) signals. Neither the P peak at 2.1 keV nor the Cl peak at 2.7 keV were observed in the EDX spectrum of the amino-bonded silica monolith (figure 3.38). The presence of these peaks indicates that the immobilisation of TCEP on the surface of the amino-bonded silica monolith was successfully performed.

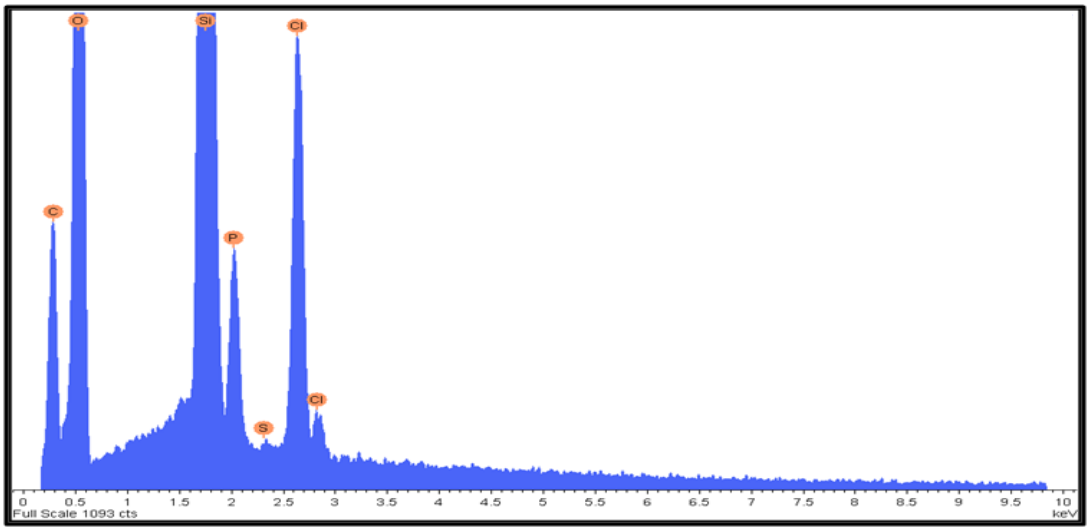

Figure 3.43 EDX analysis of the coating amino-bonded silica monolith with TCEP, containing detectable C, O, Si, P, and Cl.

The elemental compositions of the fabricated amino-bonded silica monolith and TCEP-immobilised silica monolith, which were obtained from EDX analysis, were compared (table 3.6). The most abundant elements were found to be oxygen and silicon in both samples. Significant oxygen and silicon content came from the precursor silica-based monolith. The presence of phosphorus and chlorine and increase of carbon content confirm the bonding of the reducing reagent to the amino-modified silica monolith.

Sample	**Chemical composition of the fabricated monolith determined by EDX analysis (atom %)**							
	C	**N**	**O**	**Si**	**P**	**S**	**Cl**	**Total**
Amino-bonded silica monolith	9.7	3.0	47.7	39.6	0.0	0.0	0.0	100.0
TCEP-immobilised silica monolith	21.0	3.9	45.3	24.3	1.7	0.1	3.7	100.0

Table 3.6 Summary of the chemical composition of the amino-bonded silica monolith, and the TCEP-immobilised silica monolith.

The TCEP-immobilised silica monolith was further characterised by FT-IR spectroscopy in order to assess the attachement of the carboxyl groups of the reducing reagent with the amino groups on the surface of the silica-based monolith. Figure 3.44 shows the FT-IR spectrum of the TCEP-immobilised silica monolith (blue spectrum), which was compared with the spectrum of the APTES silylated silica monolith (red spectrum). The strong band at 1050 cm^{-1} is attributed to asymmetric Si-O-Si stretching vibration, while the band at 796 cm^{-1} is attributed to symmetric Si-O-Si stretching vibration. Both these bands of the inorganic frameworks were observed for both samples. The FT-IR spectrum of the TCEP-immobilised silica monolith shows the formation of the amide bond in the monolith, which was confirmed by the N–H stretching vibration at 3330 cm^{-1}. In addition, new bands were observed at around 1617 cm^{-1} and 1569 cm^{-1} arising from the amide N-H bending vibration. A new band appears around 1718 cm^{-1}, which is the characteristic band of the carboxyl group (C=O stretching mode).[272, 273] The band at around 2969 cm^{-1} corresponded to alkyl (C-H) stretching vibration.[274] The comparison between the FT-IR spectra confirms that the reducing reagent was immobilised on the surface of the amino-bonded silica monolith via the amide bond. Band assignments are provided in table 3.7, which presents the experimental wavenumber, their assignments, and the wavenumber limits for the integration.

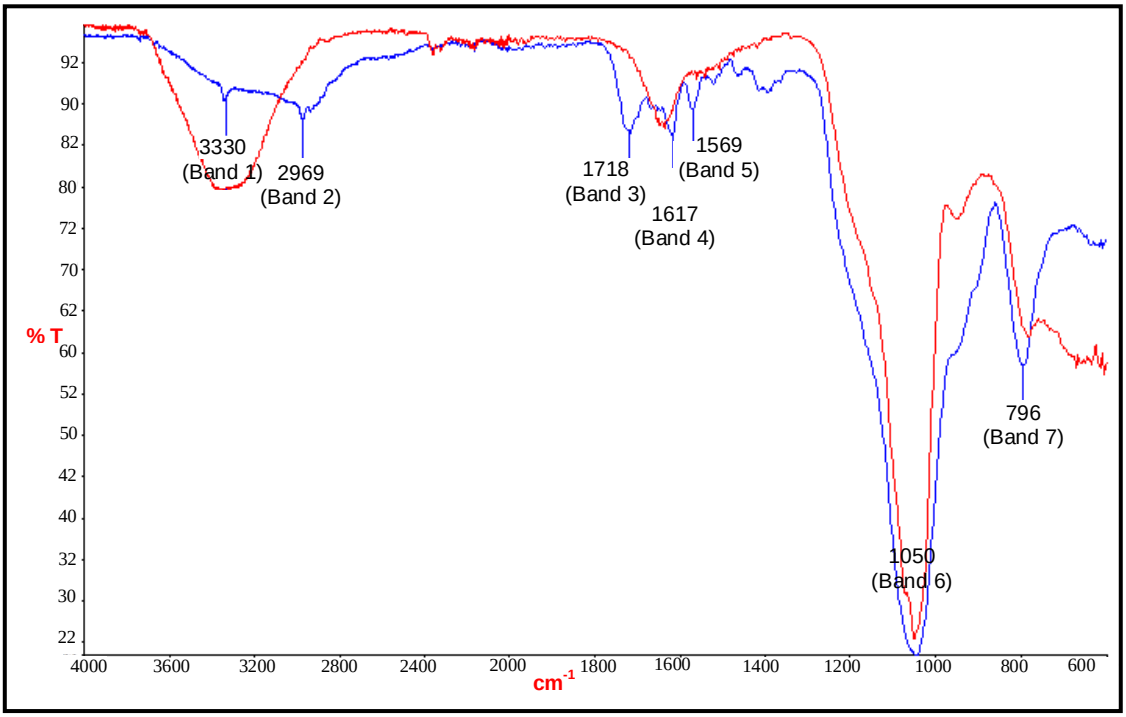

Figure 3.44 FT-IR spectrum of amino-modified silica monolith (red spectrum), and after coupling the amino-bonded silica monolith with TCEP (blue spectrum). The IR range was in the middle infrared range (600-4000 cm^{-1}) using 6 scans at a resolution of 4 cm^{-1}.

Band number	Experimental wavenumber (cm^{-1})	Assignment	Range (cm^{-1}) [263, 274, 275]
1	3330	N-H stretching vibration	3500-3180
2	2969	C-H stretching vibration	3300-2500
3	1718	C=O stretching vibration	1730-1700
4	1617	N-H bending vibration	1640-1550
5	1569	N-H bending vibration	1570-1515
6	1050	Asymmetric Si-O-Si stretching vibration	1130-1000
7	796	Symmetric Si-O-Si stretching vibration	860-730

Table 3.7 Assignment of bands observed in the FT-IR spectrum of the TCEP-immobilised silica monolith.

The physical properties of the amino-bonded silica monolith and the TCEP-immobilised silica monolith were studied using the BET instrument, as shown in table 3.8. The BET surface area, the total pore volume, and the mean pore diameter of the amino-modified silica monolith were 165.08 $m^2 g^{-1}$, 0.37 $cm^3 g^{-1}$, and 12.32 nm, respectively. The result shows that the surface area, the pore volume, and the pore size of the silica monolith silyated by APTES were lower than those for the starting silica-based monolith. The reason for this is the presence of organic groups (amino groups) on the surface occupied a volume inside the pores and prevented N_2 adsorption, resulting in a decrease in the original pore volume of the silica as well as a decrease in the surface area.[120]

Sample	**Specific surface area ($m^2 g^{-1}$) ± RSD (%)**	**Total pore volume ($cm^3 g^{-1}$) ± RSD (%)**	**Average pore size (nm) ± RSD (%)**
Bare silica	173.31 ± 3.7	0.63 ± 4.7	13.58 ± 3.8
Amino-bonded silica monolith	165.08 ± 4.1	0.37 ± 5.5	12.32 ± 5.2
TCEP-immobilised silica monolith	150.36 ± 6.5	0.35 ± 5.8	11.35 ± 4.8

Table 3.8 The physical properties of the bare silica-based monolith, amino-bonded silica monolith, and TCEP-immobilised silica monolith, calculated using the BJH method, RSD (n= 3).

From the table, it was found that the BET surface area of the TCEP-immobilised silica monolith was 150.36 $m^2 g^{-1}$. The total pore volume and the mean pore diameter of the TCEP-immobilised silica monolith were calculated to be 0.35 $cm^3 g^{-1}$, and 11.35 nm, respectively. It was found that after immobilisation of TCEP on the surface of the amino-functionalised silica monotlih, the specific surface area, the total pore volume, and the mean pore diameter were further decreased compared with the bare silica-based monolith, and the amino-modified silica monolith, as expected, since the pore

volume was decreased by the presence of the grafted organic groups on the surface and at the pore walls. These data lead to the conclusion that the amino-functionalised silica monolith was coated with TCEP.

3.3.3 Reproducibility of preparation of the TCEP-immobilised silica monolith

The reproducibility of synthesis of the fabricated monolithic materials is an important factor in order to guarantee constant reduction of the disulphide bonds in the proteins. Since the reproducibility of the bare silica-based monolith was evaluated before (section 3.2.6), the reproducibility of preparation of the amino-modified silica monolith and after immobilisation of the reducing reagent on the surface of the silica-based monolith were evaluated.

It was found that the anchoring of the amino groups on the surface of the silica-based monolith and immobilisation of TCEP on the amino-modified silica monolith was not strongly confirmed with SEM analysis; therefore, BET data were used for reproducibility purposes. The RSDs value of the physical properties of the fabricated amino-functionalised monolith and the TCEP-immobilised silica monolith measured using the BET instrument were in the range 4.1-5.5 %, and 4.8-6.5 %, respectively (table 3.8).

4.0 Results and discussion: applications of monolithic materials in proteomic analysis

This chapter discusses the performance of the prepared monolithic materials in proteomic analysis, specifically protein extraction and reduction of the disulphide bonds in proteins. The reason for choosing protein extraction in this study was that efficient extraction of proteins is the most critical step for proteomics because it can remove interfering materials and lower detection limits by preconcentration of the proteins. Therefore, the overall goal of this study was to find an appropriate SPE extraction sorbent for protein extraction. Another aim of this study was to develop a novel solid-phase reducing reagent for use in reduction of protein disulphide bonds as disulphide-reduced species can give more structural information than native proteins.[132]

This chapter will be divided into three main sections. The first section contains an evaluation of the use of fabricated polymer-based monoliths for performing solid-phase protein extraction (4.1). The second section concerns the performance of the fabricated silica-based monolith in protein extraction, and includes comparison between the extraction recovery of the non-modified silica and the C_{18} stationary phase (4.2). Finally, a new application of a monolithic sol-gel bed within a microchip for reduction and alkylation of proteins will be investigated (4.3).

4.1 Evaluation of organic monoliths for protein extraction

4.1.1 Selection of the UV wavelength for protein detection

Many different kinds of detectors have been used for protein analysis, such as fluorescence spectroscopy, mass spectrometry, and ultraviolet (UV) detector.[276] In this study, UV detector was used. Although it suffers from low concentration sensitivity, as a result of its short optical path length and small injection volume, it is simple, rapid, and does not need derivatisation of proteins because proteins always contain UV active groups.[277] It was decided to investigate the UV wavelength for protein detection before using the polymer-based monolith as a solid phase extraction sorbent. The overall goal of doing this was to find the UV wavelength that gives the highest signal

intensity for proteins and with minimal interference. The UV wavelength was investigated using standard proteins varying in molecular weight and isoelectric point, namely insulin, cytochrome C, lysozyme, myoglobin, β-lactoglobulin, ovalbumin, and bovine serum albumin. They were dissolved individually in the eluting solution, which was 20 % acetonitrile containing 0.1 % trifluoroacetic acid (TFA). The sample solution was injected directly into the HPLC-UV detector in order to study the UV chromatograms of the standard proteins.

Commonly, proteins absorb UV light in the wavelength range of 190-220 nm and 250-280 nm.[278] In this study, the signal intensities of the standard proteins were investigated at three different wavelengths: 210, 254, and 280 nm, since they are the common UV wavelengths used for proteins.[279] The mobile phase was acetonitrile-purified water (50:50) in the presence of 0.1 % TFA under isocratic conditions. Figure 4.1 shows a comparison between the UV chromatograms of lysozyme (100 µM) using three different UV wavelengths. It was found that lysozyme (retention time =1.63 min) had the strongest maximum at 210 nm. Detection of lysozyme at 254 and 280 nm shows significantly reduced signal intensity for lysozyme although the background was also reduced. The reason for that could be because the protein chromophore at 210 nm is the peptide bonds while detection at 254 and 280 nm is useful only for proteins containing aromatic amino acids, such as phenylalanine, tyrosine, and tryptophan.[280] Therefore, the ideal UV detection wavelength varies according to the structure of the proteins.

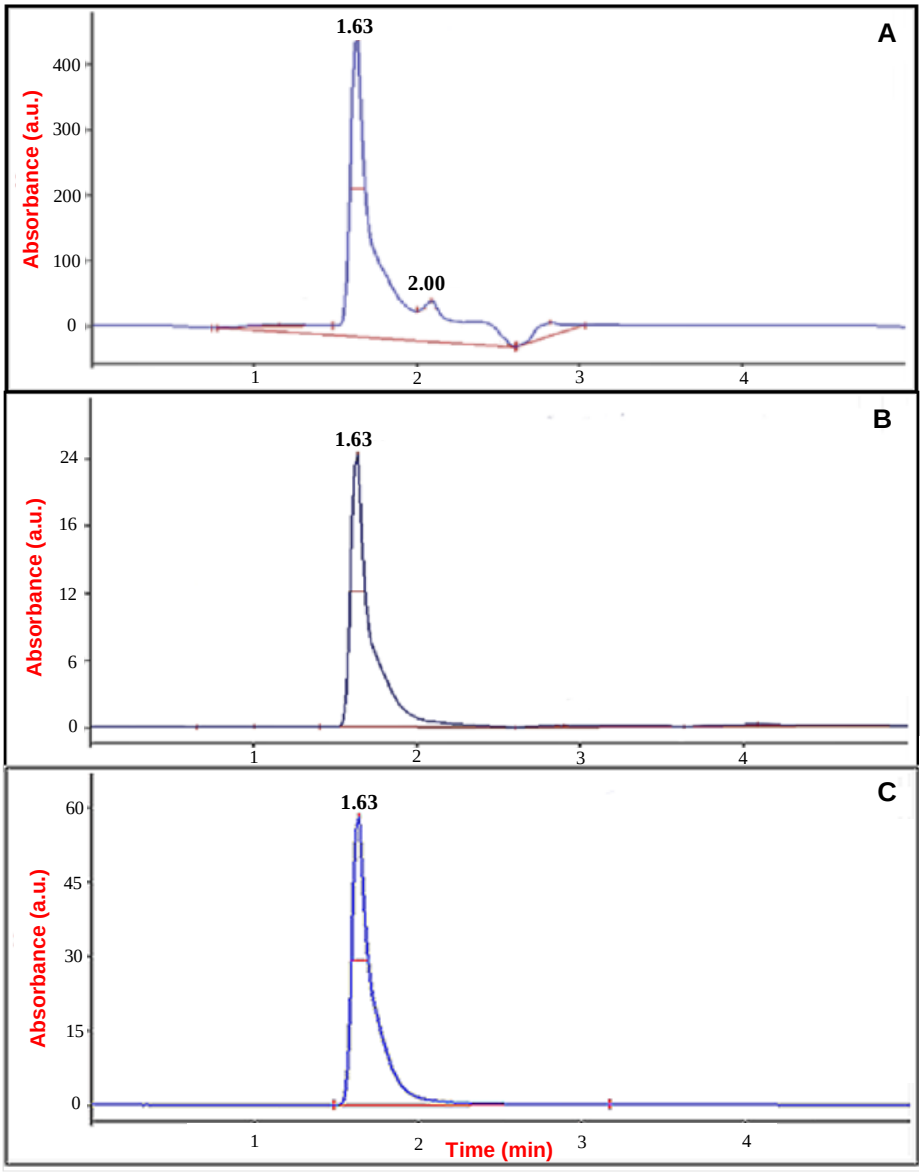

Figure 4.1 The UV chromatograms of lysozyme using three different UV wavelengths: (A) 210 nm, (B) 254 nm, and (C) 280 nm show different signal intensity. Experimental conditions: the mobile phase was composed of acetonitrile and purified water (50:50) containing 0.1 % TFA under isocratic conditions, flow rate was 1 mL min^{-1}, injection volume was 20 µL. The separation column was Symmetry C_8, 4.6 mm × 250 mm packed with silica particles (size 5 µm). All experiments were performed at ambient temperature around 23 °C.

The peak areas of the standard proteins were studied in order to compare the detection sensitivity of the standard proteins at 210, 254, and 280 nm. Table 4.1 presents the peak areas of all investigated standard proteins at the three different wavelengths of 210, 254, and 280 nm. It was found that the highest peak areas of the standard proteins were obtained when the UV detection wavelength was set at 210 nm, as expected, while the lowest peak areas were obtained when the UV detection wavelength was set at 254 nm.

Standard protein	**Peak area using UV detection**		
	210 (nm)	**254 (nm)**	**280 (nm)**
Insulin	1737	35	49
Cytochrome C	2569	236	294
Lysozyme	5205	205	505
Myoglobin	3561	145	173
β-lactoglobulin	6023	156	331
Ovalbumin	1053	12	18
Bovine serum albumin	8419	241	460

Table 4.1 Peak areas of the standard proteins at the three different UV detection wavelengths of 210, 254, and 280 nm.

Based on these results, it was concluded that the UV detection wavelength 210 nm was estimated as the optimal UV wavelength for studying the extraction of proteins, which provides the maximal sensitivity that would suffice for detection of most proteins.

4.1.2 Protein extraction using the organic monolith prepared using binary porogenic solvent system

Organic monolithic materials have been regarded as suitable sorbent materials since they are easy to prepare, and do not need frit fabrication and packing.[281] As mentioned before, the pore-forming solvent is an important factor since it can control the porous properties of the organic monolith without changing the chemical composition of the final fabricated organic monolith. Therefore, different porogenic solvent systems were studied in order to optimise the porous properties of the polymer-based monolith. From characterisation of the porous properties of the prepared poly (BuMA-*co*-EDMA) monoliths, it was found that the most suitable binary porogenic solvent systems to fabricate the organic polymer monolith were MeOH/EtOH and MeOH/1-propanol. The performance of both these monoliths was investigated in order to find which polymer-based monolith gives more efficient extraction of proteins.

In order to study the performance of the fabricated rigid porous polymeric monolith, it was fabricated using the UV initiated polymerisation inside a borosilicate tube (i.d. 2.10 mm and o.d. 3.90 mm) with length around 1 cm while the rest of the tube was covered with electrical tape. The performance of the fabricated organic SPE tube was examined using a standard protein, cytochrome C (12327 Da), since it is red in colour, which would facilitate visualisation of the change in the colour of the monolith if the protein was retained onto the surface of the monolith.

It is known that the main advantage of organic polymer monoliths is that they do not suffer from the problems associated with residual silanol interactions; therefore, they can be used over a wide pH range.[282] The chosen buffer for sample preparation should encourage the sorption of the proteins while preventing sorption of the interfering compounds.[96] Based on the literature, it was found that the most commonly used buffer for sample preparation in order to extract the target analyte from the polymer-based monolith is 10 mM ammonium acetate buffer solution (pH 9.3) [283]; therefore, this was used here to prepare the sample solution.

The organic monolithic stationary phase exhibited reversed phase chromatographic behaviour since the butyl methacrylate monolith contains butyl groups (hydrophobic moieties); therefore, the mechanism of protein extraction and preconcentration with

the butyl methacrylate monolith is based on hydrophobic interaction between the proteins and the butyl groups. The extraction of protein was carried out by off-line SPE since it is simple and highly flexible in comparison with on-line SPE.[284]

A hydrodynamic method was used to inject all solutions. Since the prepared organic monolith exhibited high mechanical robustness and was covalently attached to the walls of the borosilicate tube, a high flow rate of 10 µL min^{-1} could be used in order to inject the solution through the monolith without causing mechanical breakage of the monolith or leaking during the experiment. This is important especially in a situation where it is necessary to pass a large volume of the solution through the monolith within a short period of time. Although the easiest way to decrease the extraction time would be to increase the flow rate for injection of the sample solution, it was preferred to decrease the flow rate to 5 µL min^{-1} in order to increase the interaction time for binding proteins to the surface of the monolith.

The protein was extracted using a five step procedure consisting of activation and equilibration of the sorbent, loading of the sample solution, washing of the sorbent, and elution of the protein. Firstly, the monolith was exposed to a preconditioning solution, 400 µL acetonitrile (ACN), in order to activate the monolith, following which it was equilibrated with 400 µL 10 mM ammonium acetate buffer solution (pH 9.3). After loading the sample solution (1 mL), the sorbent was washed with 200 µL 10 mM ammonium acetate buffer solution (pH 9.3) to remove unwanted materials from the sorbent. Finally, the extracted protein was eluted using the eluting solution, which should be able to desorp the extracted protein rapidly and completely. In this study, 500 µL 20 % ACN (0.1 % TFA) solution was chosen as the eluting solution to elute the protein from the fabricated organic polymer monolith. The preconcentrated protein was collected into an Eppendorf tube, then the eluent was analysed using the HPLC-UV detector in order to calculate the extraction recovery of the preconcentrated protein.

The first organic polymer-based monolith investigated was prepared using MeOH/ EtOH as a porogenic solvent. It was found that the polymer-based monolith prepared using MeOH/EtOH had good hydrodynamic properties for easy pumping of the solvent through the monolith without any visible damage to the monolith. However, it

was observed that during the loading step, cytochrome C was not retained onto the surface of the organic monolithic stationary phase, as shown in figure 4.2. It was concluded that the organic polymer monolith prepared using MeOH/EtOH was not a suitable SPE extraction sorbent for protein extraction since very little amount of cytochrome C was retained, as confirmed from the colour of the monolithic material inside the borosilicate tube, and the extraction recovery of cytochrome C was calculated to be 17 %. This could be attributed to the relatively low surface area (12.6 m^2 g^{-1}) of the organic monolith prepared using MeOH/EtOH. Although this monolith was characterised by the lowest backpressure and high permeability, unsatisfactory preconcentration of cytochrome C was obtained; therefore, no further study was carried out using this type of organic polymer-based monolith.

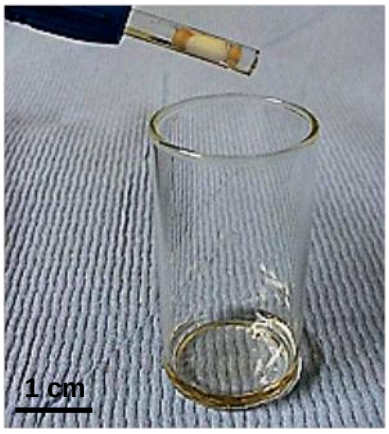

Figure 4.2 Washing the monolithic SPE tube with 200 µL 10 mM ammonium acetate buffer solution (pH 9.3) after loading of cytochrome C (60 µM) onto the poly (BuMA-*co*-EDMA) monolith prepared using MeOH/EtOH (50:50) as a porogenic solvent.

The second organic polymer-based monolith investigated was prepared using MeOH/1-propanol as a porogenic solvent. Its performance for protein extraction was checked using the same procedure that was used for protein extraction with the polymer-based monolith prepared using MeOH/EtOH and all reagents were injected using the same flow rate (10 µL min^{-1}), and for loading the sample solution was 5 µL min^{-1}.

Three different coloured proteins, cytochrome C (12327 Da, red colour), myoglobin (16951 Da, brown colour), and hemoglobin (64500 Da, brown colour) were used to investigate the performance of the organic monolith prepared using MeOH/1-propanol in the protein extraction. Figures 4.3 (A), (D), and (G) show cytochrome C, hemoglobin, and myoglobin, respectively, were retained onto the surface of the organic polymer monolith, as confirmed by the change in colour of the monolith, while excess proteins were not bound to the monolith. Figures 4.3 (B), (E), and (H) show the washing of the organic polymer monoliths inside the borosilicate tube with 10 mM ammonium acetate buffer solution (pH 9.3) in order to remove unbound protein. It was found that the retained proteins were not affected by the washing step, which was confirmed by checking the UV chromatogram of the collected solution during washing the sorbent. This was very important to make sure that the retained proteins would not be affected by washing away the interfering compounds, especially in preconcentration of proteins from a real sample. Figures 4.3 (C), (F), and (I) show the elution of the standard proteins from the organic polymer monolith that was achieved using 20 % ACN containing 0.1 % TFA. The protein desorption was efficient, as confirmed by the colour of the monolith, which turned to white. It was concluded that a porogenic mixture of MeOH and 1-propanol was suitable for the fabrication of the poly (BuMA-*co*-EDMA) monolith in order to use it as solid phase extraction sorbent, since the standard proteins were preconcentrated successfully, and enables a reasonably high flow rate to be used without sacrificing adsorption of proteins or decreasing the efficiency of protein desorption.

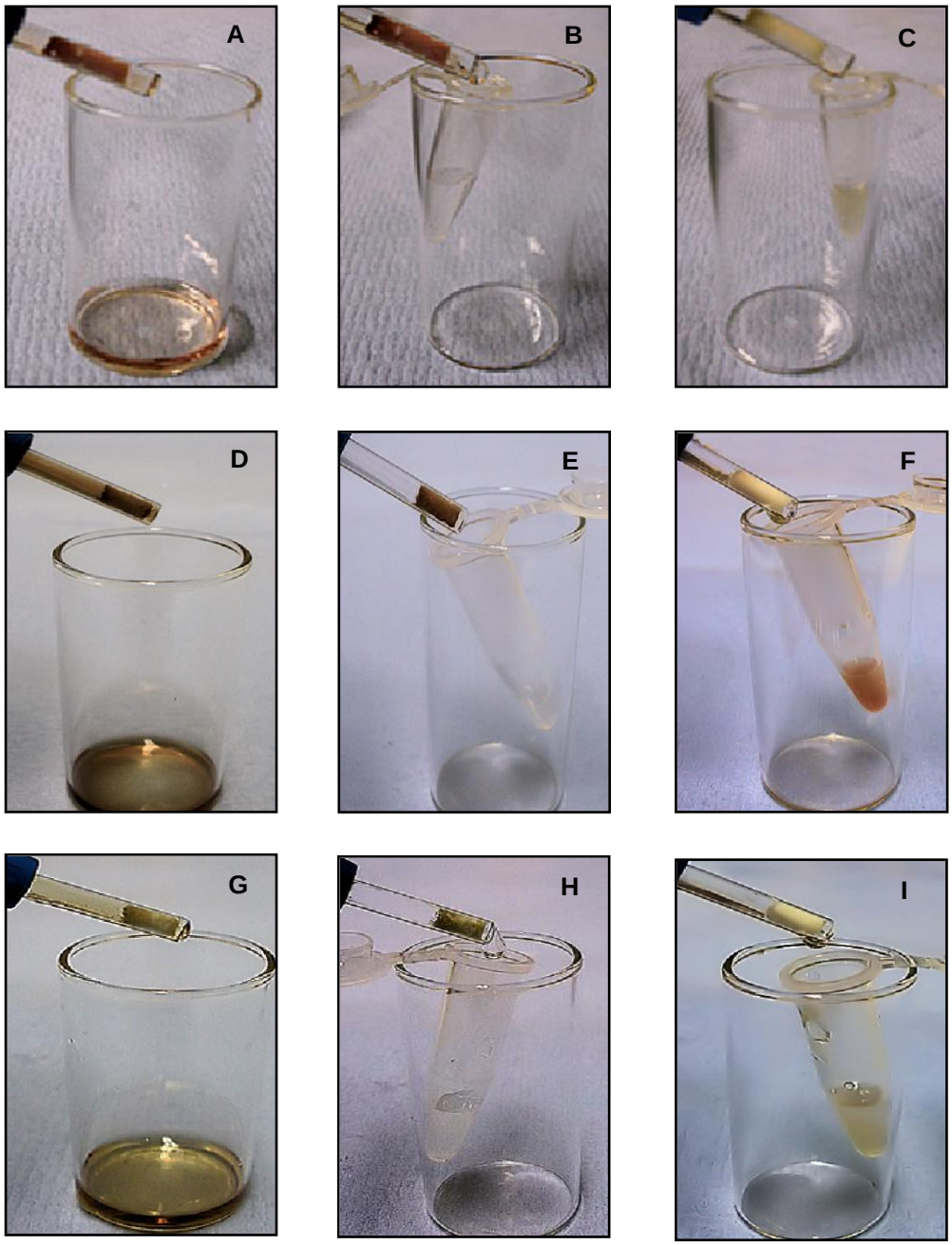

Figure 4.3 The steps of preconcentration of the standard proteins (60 µM) using poly (BuMA-*co*-EDMA) monolith prepared using MeOH/1-propanol (50:50) as a porogenic solvent. Cytochrome C: (A) loading, (B) washing, and (C) elution. Hemoglobin: (D) loading, (E) washing, and (F) elution. Myoglobin: (G) loading, (H) washing, and (I) elution. Volume of proteins was 1 mL, the washing solution was 200 µL 10 mM ammonium acetate buffer solution (pH 9.3), and the eluting solution was 500 µL 20 % ACN (0.1 % TFA).

After extraction of the standard proteins, the performance of the fabricated polymer monolith was checked using the HPLC-UV detector by comparing the peak area of each protein before and after preconcentration. Figure 4.4 shows the UV chromatogram of cytochrome C, which shows the difference in the peak areas of cytochrome C for the direct injection of a non-processed sample, and after preconcentration using the polymer-based monolith prepared using MeOH/1-propanol. The figure shows an increase in the peak area after purification of cytochrome C, which confirms that the sorbent organic polymer-based monolith has the ability to purify and preconcentrate cytochrome C.

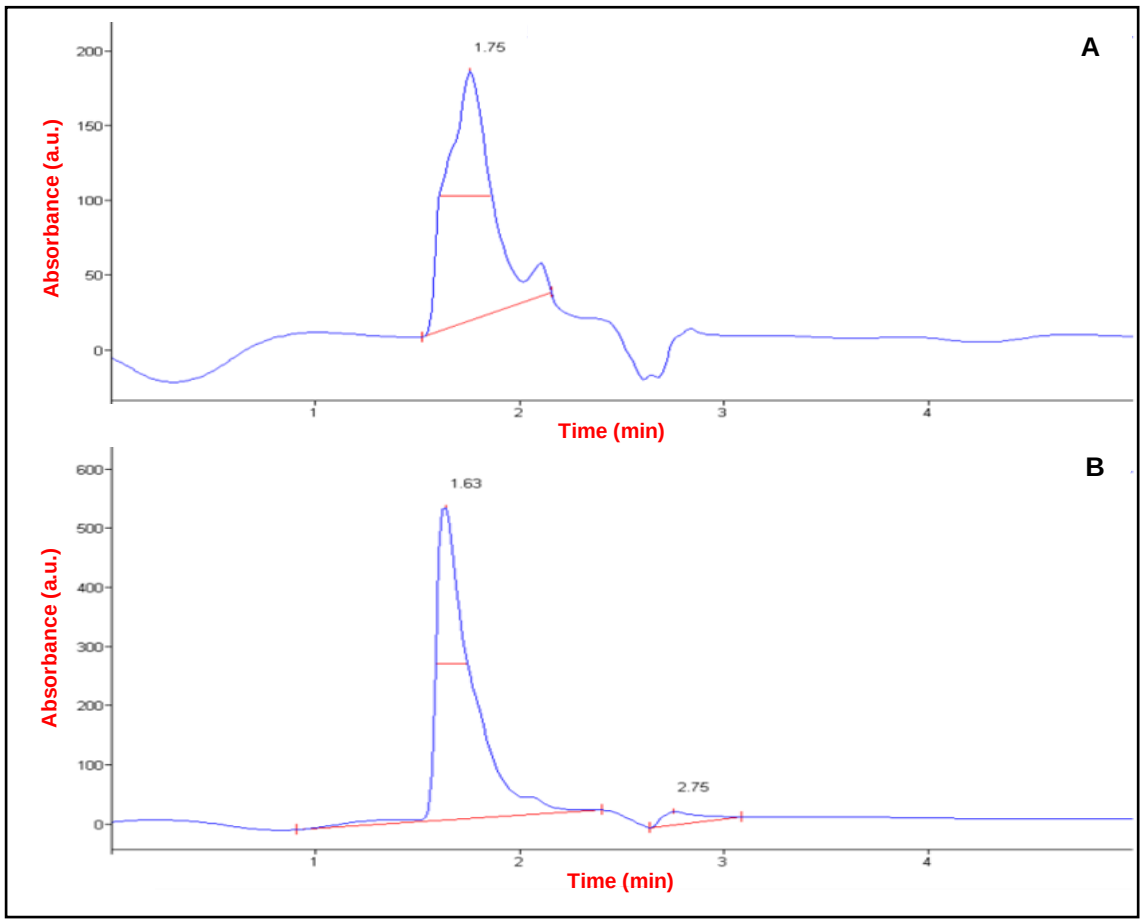

Figure 4.4 The difference in the peak areas of cytochrome C: (A) before, and (B) after extraction using the polymer-based monolith prepared using MeOH/1-propanol (50:50).

Many extractions were carried out with the same organic monolithic stationary phase using the same extraction procedure, as described earlier. The performance of the

polymer-based monolith prepared using MeOH/1-propanol was also investigated using non-coloured standard proteins, insulin (5700 Da), lysozyme (14300 Da), β-lactoglobulin (36000 Da), ovalbumin (44287 Da), and bovine serum albumin (BSA) (66382 Da). It was found that the extraction recovery of some standard proteins such as BSA was low as confirmed from comparing the peak area of BSA before and after extraction. Figure 4.5 shows a comparison of the peak areas before and after extraction using the polymer-based monolith, which indicates that BSA was preconcentrated with low extraction recovery.

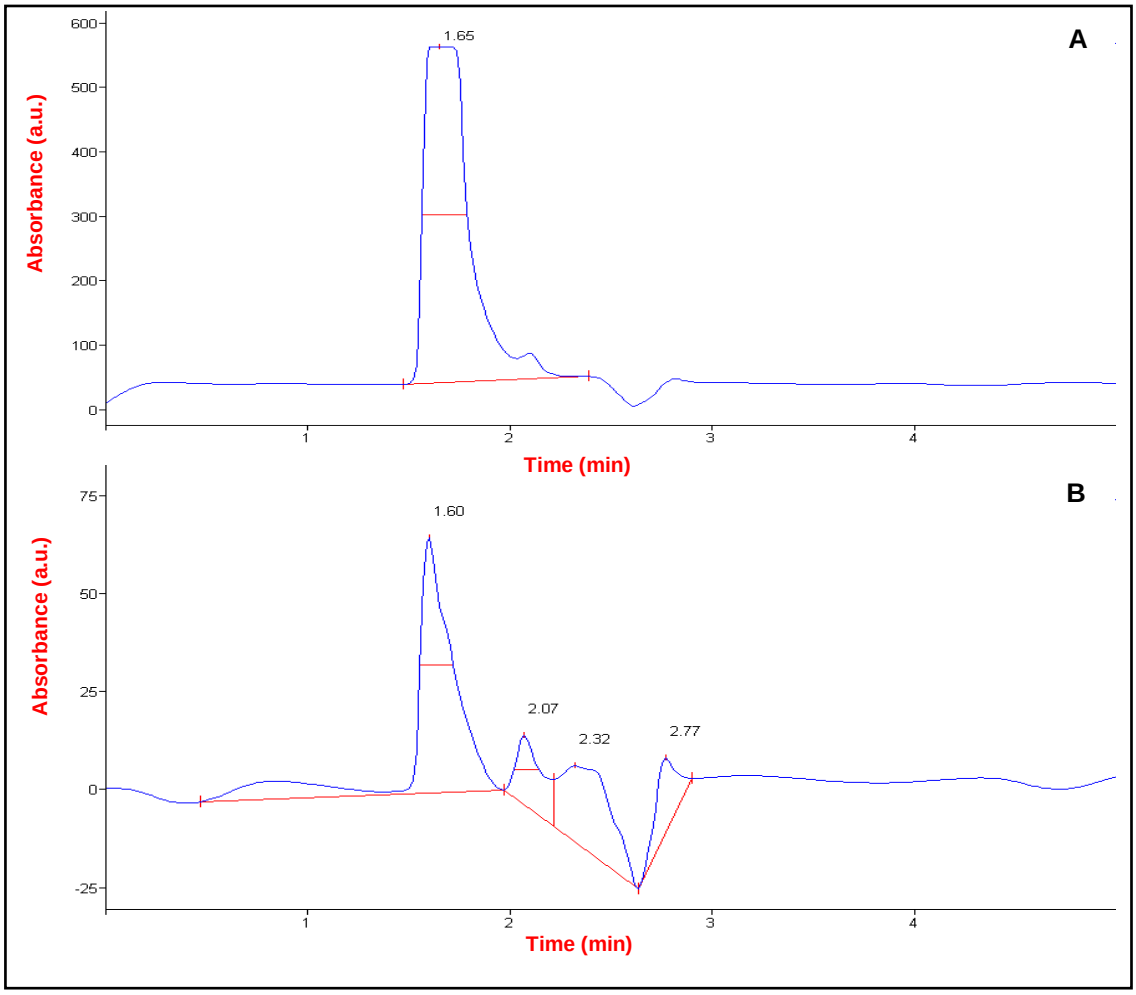

Figure 4.5 The difference in the peak areas of bovine serum albumin (BSA): (A) before, and (B) after extraction using the polymer-based monolith prepared using MeOH/1-propanol (50:50).

The extraction recoveries (ER) of the proteins preconcentrated using the polymeric SPE tube were calculated using the HPLC-UV detector. Table 4.2 shows the extraction recoveries of different standard proteins purified with the polymer-based monolith, calculated using equation 3. Each value represents the mean of three measurements. It was found that the extraction recoveries of the standard proteins ranged from 23.4 to 95.7% and the relative standard deviations (RSDs) for peak area counts were calculated to be between 3.3 to 6.4%. Generally, it was found that the fabricated organic monolithic material offered a fairly good extraction recovery and good reproducibility of some proteins such as insulin, cytochrome C, myoglobin, and hemoglobin. However, it was found that the extraction recoveries of some standard proteins, such as β-lactoglobulin, ovalbumin, and BSA, were very low.

Standard protein	**Molecular weight (M.W) (Da)**	**Isoelectric point (*pI*)**	**Extraction recovery (ER) (%)**	**RSD (%) (n=3)**
Insulin	5700	5.6	88.2	4.0
Cytochrome C	12327	10.0	95.7	3.3
Lysozyme	14300	11.0	41.1	5.7
Myoglobin	16951	6.8	75.3	4.2
β-lactoglobulin	36000	5.2	24.7	6.4
Ovalbumin	44287	4.6	23.4	4.7
Hemoglobin	64500	7.4	82.5	6.2
BSA	66382	4.7	25.0	5.1

Table 4.2 The extraction recoveries of the standard proteins purified with polymer-based monolith prepared using a binary solvent consisting of MeOH/1-propanol (50:50). The extraction recovery was calculated using equation 3.

4.1.3 Protein extraction using the organic monolith prepared using tertiary porogenic solvent system

Five organic polymer-based monoliths were fabricated inside borosilicate tubes using different ratios of the tertiary porogenic solvents consisting of methanol (MeOH), which formed 50 % of the total amount of the porogenic solvent (3.6 g) and a combination of 1-propanol and EtOH in various ratios: 40:10, 30:20, 25:25, 20:30, and 10:40. Their protein extraction performance was investigated using cytochrome C. Figure 4.6 shows the loading of cytochrome C onto the the surface of the five organic polymer-based monolithic stationary phases inside borosilicate tubes prepared using different ratios of MeOH, EtOH, and 1-propanol. As can be seen in the figure, the binding of cytochrome C was increased by increasing the ratio of 1-propanol in the porogenic solvent, as confirmed from the change in colour of the monolithic materials from white to red.

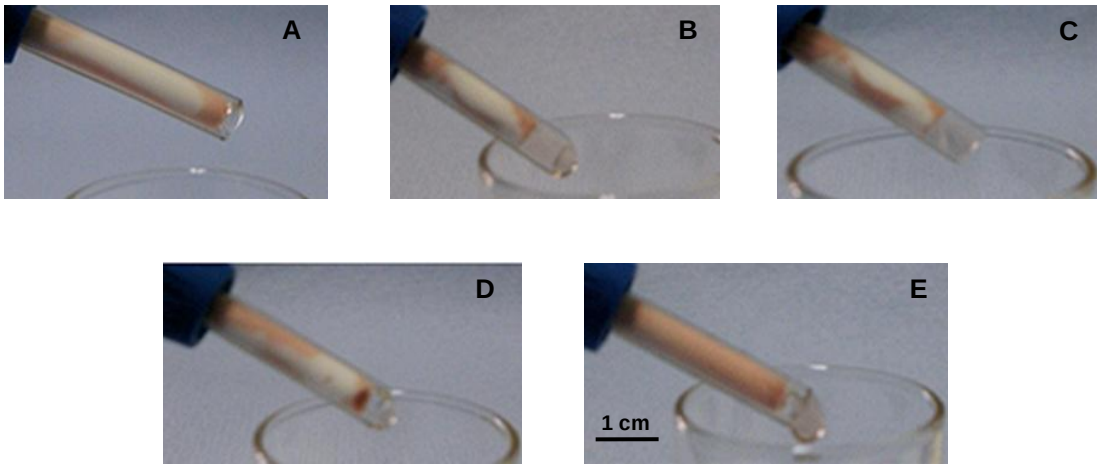

Figure 4.6 Preconcentration of cytochrome C (during loading step) using poly (BuMA-*co*-EDMA) monoliths prepared using different ratios of the tertiary porogenic solvent system consisting of MeOH, EtOH, and 1-propanol: (A) 50:40:10, (B) 50:30:20, (C) 50:25:25, (D) 50:20:30, and (E) 50:10:40.

The extraction recovery of cytochrome C preconcentrated using the polymer-based monolith prepared with different ratios of MeOH, EtOH, and 1-propanol was calculated (table 4.3). It was found that preconcentration of cytochrome C using the

organic polymer monolith prepared using a tertiary porogenic solvent system was achieved with RSD of below 7% (n=3); however, the extraction recovery of cytochrome C was not high (25.3 - 60.7 %). The reason for this could be due to the low surface area of these prepared monoliths, compared with the surface area of the organic polymer monolith prepared using the binary porogenic solvent consisting of MeOH and 1-propanol (50:50). Since the extraction recovery of cytochrome C was not satisfactory using organic polymer monoliths prepared using a tertiary porogenic solvent**,** no further work was undertaken.

Tertiary porogenic solvent MeOH:EtOH:1-propanol	**Extraction recovery of cytochrome C (%)**	**RSD (%) (n=3)**
50:40:10	25.3	3.4
50:30:20	30.7	4.4
50:25:25	48.5	5.7
50:20:30	52.1	6.8
50:10:40	60.7	4.3

Table 4.3 Extraction recovery of cytochrome C using poly (BuMA-*co*-EDMA) monolith prepared using a tertiary porogenic solvent system consisting of different ratios of MeOH, EtOH, and 1-propanol.

4.1.4 Protein extraction using the microchip-based polymer monolith

The ultimate motivation for transfer of protein extraction from the SPE tube to the microchip-based monolith is to decrease the amount of the protein samples required and to reduce the amount of solvents used leading to reduced waste. In addition, using a microfluidic device can speed the analysis. Therefore, it was decided to fabricate the organic polymer monolith inside a glass microchip in order to use it for protein extraction. The previous results showed that the porogenic solvent system can significantly affect the performance of the organic monolith in terms of using it as a

SPE sorbent for protein extraction. Based on previous results, it was found that the optimum solvent system for fabrication of the organic monolith in order to use it as a SPE sorbent was MeOH/1-propanol (50:50), since the fabricated organic polymer monolith has the ability to preconcentrate some standard proteins with good reproducibility. Therefore, it was chosen to fabricate the organic monolith inside the glass microchip.

After fabrication of the monolithic bed inside the extraction chamber of the glass microchip, its performance was tested. The standard proteins investigated were insulin, cytochrome C, myoglobin, and hemoglobin. The reason for choosing these proteins was because they were extracted with high extraction recovery. The amounts of the protein sample and reagents were decreased. The monolith bed inside the microchip was activated with 100 µL ACN, and was equilibrated with 100 µL 10 mM ammonium acetate buffer solution (pH 9.3). The protein sample (800 µL) was applied to the monolithic microchip. After extraction, the microchip was washed with 50 µL 10 mM ammonium acetate buffer solution (pH 9.3).The elution of the proteins from the glass microchip was achieved using 150 µL 20 % ACN (0.1 % TFA).

All solutions were injected using the hydrodynamic method using a syringe pump attached to the microfluidic device by ETFE tubing. The flow rate of the solutions was set at 10 µL min^{-1}, the same as previously with the organic monolithic tube. However, the fabricated polymer-based microchip showed somewhat disappointing results. Its main drawback was the high resistance of the monolith to the solutions, although this problem was not noticed when using the fabricated organic monolith inside a borosilicate tube using the same porogenic solvent system. The high flow resistance of the monolith was confirmed by the leaking of reagents from the holes and the experiment could not be completed. It is known that a large surface area is not accompanied by good permeability and large pore size of the monolith, resulting in an increase in the backpressure, which appears a significant disadvantage of the organic polymer monolith. In addition, the packpressure was generated due to using smaller dimensions of the channel on the glass microchip compared with the dimension of the organic monolithic tube. Therefore, it was decided to optimse the flow rate of the solutions in order to find the optimum flow rate that does not cause leaking of the

reagents from the holes or damage to the monolith inside the glass microchip. Different flow rates were investigated and it was found that the optimum flow rate that could be used without causing mechanical breakage of the monolith or the connecting tubes was 3.5 μL min^{-1}. This was then selected to inject all reagents and sample solutions inside the fabricated glass microchip.

Figure 4.7 (A) shows a photograph of the set-up of the microfluidic device and control apparatus for hydrodynamic pumping to perform the protein extraction. Since the UV light was used to fabricate the organic monolith, precise control over the location of the monolith within the extraction chamber was possible. Figure 4.7 (B) and (C) show the appearance of the polymer-based monolith inside the extraction chamber of the glass microchip before and during loading cytochrome C. The colour of the monolithic bed inside the extraction chamber was changed from white to red, which confirmed that cytochrome C was retained on the surface of the monolith.

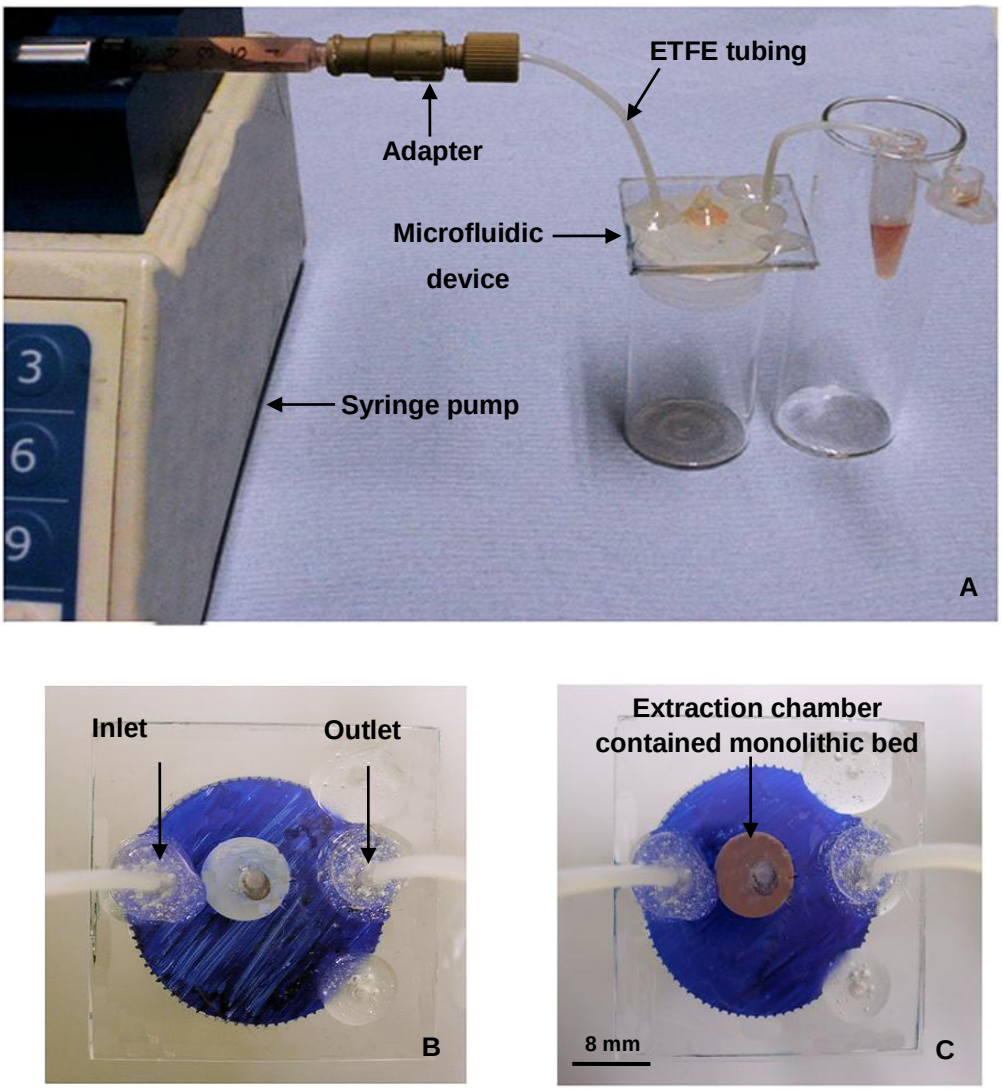

Figure 4.7 (A) Photograph showing the set-up of the solid phase organic polymer microchip, (B) the glass microchip during activation step, and (C) during loading cytochrome C (60 µM) showing change in the colour of the monolithic bed inside the extraction chamber due to the binding of cytochrome C. The flow rate was 3.5 µL min^{-1} for all reagents and protein sample solution.

It was noticed that the volume of the sample needed to be decreased since fabrication of the monolithic polymeric materials inside the microfluidic device leads to a decrease in the volume of the sorbent bed, which necessitate reduction of the volume of the sample and reagents. Therefore, different volumes of the protein sample

solution, 100, 200, 400, 600 µL, were investigated and the experiment was performed using the same procedure as before. In order to find out the maximum volume of the protein sample solution, the collected solution during the loading step was collected into an Eppendorf tube and studied using the HPLC-UV detector. It was found that the maximum sample volume that could be loaded without losing the sample was 200 µL, which indicates that the fabricated microchip has low sample capacity.

The extraction recoveries of the standard proteins (insulin, cytochrome C, myoglobin, and hemoglobin) using the microchip-based polymer monolith were calculated (figure 4.8), ranged between 79.1 and 98.4 %, which were slightly higher than the extraction recoveries of the same proteins using the polymeric monolith tube (75.3 - 95.7 %). Good extraction capability was achieved and the microchip-based polymer monolith is applicable to the preconcentration of proteins

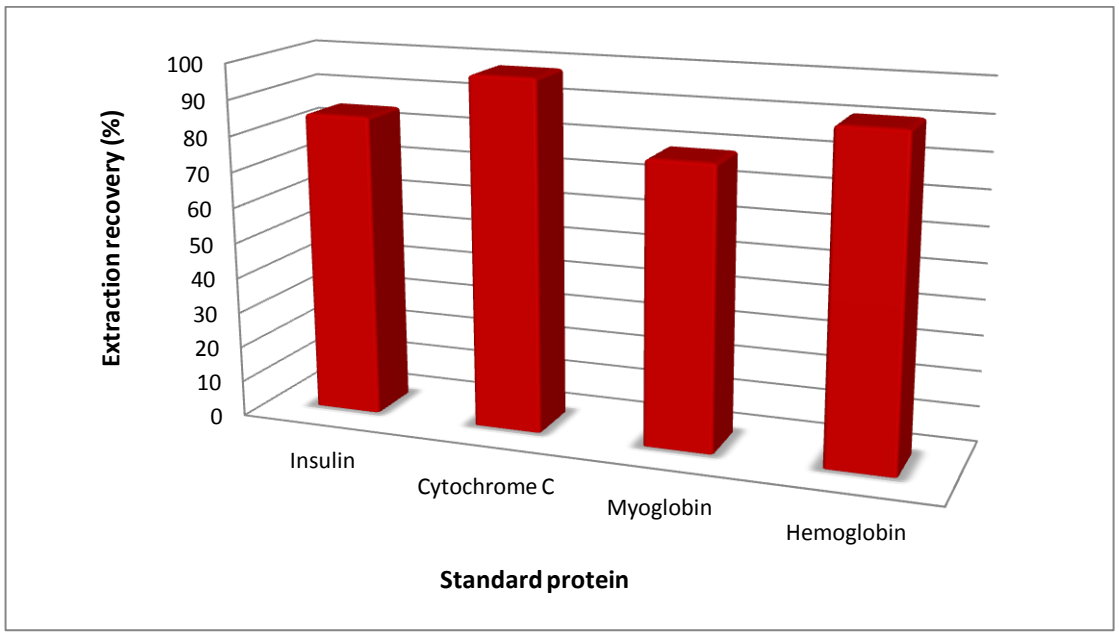

Figure 4.8 The extraction recovery of the standard proteins purified with organic monolith fabricated inside the glass microchip.

4.1.5 Reproducibility and stability of the fabricated device

In order to guarantee consistent extraction performance, the long-term stability and reproducibility of the performance of the monolithic microchip in the extraction of proteins were checked. The run-to-run reproducibility of the extraction of the proteins on the same microchip was investigated for extraction of the four standard proteins (insulin, cytochrome C, myoglobin, and hemoglobin). Between two analyses, the microchip was washed with the eluting solution and then with the washing solution in order to avoid any memory effect. In addition, to check the batch-to-batch reproducibility, extraction of the four standard proteins was investigated using three different fabricated microchips containing the organic polymer monolith. The data shown in table 4.4 show good reproducibility was achieved with intra-chip (run-to-run) and inter-chip (chip-to-chip) RSDs in the ranges of 3.4-5.6 % (n=4) and 4.2-7.1 % (n=3), respectively.

Precision (RSD %)	Insulin	Cytochrome C	Myoglobin	Hemoglobin
Intra-batch (n=4)	3.4	3.8	5.6	4.7
Inter-batch (n=3)	4.6	4.2	7.1	6.3

Table 4.4 RSD's of the extraction recoveries showing the intra-chip (run-to-run) and inter-chip (chip-to-chip) reproducibility of the fabricated organic polymer microchip.

The monolithic microchips were stable and reusable several times (15 times reuse). The extraction efficiency of the standard proteins was not affected and no changes were found in the backpressure. However, it was found that the lifetime of this type of monolithic material was not very long since the monolithic matrix tended to crack on drying. It is known that any degradation or deterioration of the monolithic bed can affect the extraction efficiency; therefore, it was found that it is very important to keep the monolithic materials in a solution of distilled water and ACN (50:50) to prevent drying of the organic polymer monolith and minimise cracking. This means a careful storage is required in order to use the monolith for protein extraction over a prolonged period.

4.2 Evaluation of the inorganic monolith for protein extraction

The second type of monolithic materials investigated were silica-based monoliths. After identify the optimal conditions for fabrication of the silica-based monolith, as described in the previous chapter (3.2), a monolithic silica rod was connected to a borosilicate tube via a heat shrinkable tube to evaluate their use in performing solid phase extraction (SPE) for preconcentration/extraction of proteins.

4.2.1 Performance comparison between bare silica-based monolith and C_{18}-bonded silica monolith

The objective of this study was to compare the performance of bare silica-based monolith with an octadecylated silica monolith for use in protein extraction in order to identify which one is more effective for use as a solid phase extraction (SPE) sorbent. It is known that the surface of a non-modified silica-based monolith consists of siloxane groups and the silanol groups.[285] The mechanism of extraction depends on the nature of the monolithic materials and the analyte of interest.[286] In the case of using bare (unbounded) silica-based monolith, the mechanism of extraction is normal-phase (NP) extraction and the retention of proteins under the normal-phase condition is due to the interaction between the polar functional groups in the proteins and the polar groups, which are hydrophilic silanol groups on the surface of the silica-based monolith.

A monolithic silica tube was used for off-line preconcentration of proteins, and the standard proteins were extracted using the same procedure that was used before for preconcentration of standard proteins using the polymer-based monolith except the type of buffer solution. Although the silica-based monolith can give good organic solvent resistance and mechanical stability, it can work only within a limited pH range (2-8). Therefore, it was decided to change the buffer solution from 10 mM ammonium acetate buffer solution (pH 9.3) to 20 mM ammonium hydrogen carbonate buffer solution (pH 8.0).[125]

The standard proteins were extracted individually to calculate the extraction recovery for each protein. The concentration of the standard proteins was 60 µM and they were dissolved in 20 mM ammonium hydrogen carbonate buffer solution (pH 8.0). The

non-modified silica monolith with polar functional groups was conditioned with 400 µL ACN to remove impurities and then it was displaced with 400 µL 20 mM ammonium hydrogen carbonate buffer solution (pH 8.0) to equilibrate the monolith. Although the permeability of silica-based monoliths is high and a high flow rate (30 µL min^{-1}) can be used without leakage, all solutions were injected using a syringe pump at a flow rate of 10 µL min^{-1} for all steps through the monolithic silica tube, except applying the sample solution. After equilibrating the sorbent (silica-based monolith), the sample solution was applied at a lower flow rate (5 µL min^{-1}) in order to obtain good percolation between the proteins and the sorbent. After loading the sample solution through the sorbent, it was rinsed with a washing solution, 200 µL 20 mM ammonium hydrogen carbonate buffer solution (pH 8.0), to remove interferences without losing the analyte. In order to elute the adsorbed protein from the sorbent, polar solvent (500 µL 20 % ACN containing 0.1 % TFA solution) was used, and the eluent was collected into an Eppendorf tube. In order to check the performance of the sorbent, an aliquot of the eluent was injected into the HPLC-UV detector.

The utility of the bare silica-based monolith for protein extraction was tested with cytochrome C. Figure 4.9 shows the steps of extraction of cytochrome C using the bare silica-based monolith inside the heat shrinkable tube. Figure 4.9 (A) shows the activation of the silica-based monolith inside the heat shrinkable tube, followed by loading of cytochrome C, which was retained in the non-modified silica monolith as confirmed by the change in colour of the sorbent from white to red, figure 4.9 (B), and finally, cytochrome C was eluted from the sorbent, figure 4.9 (C).

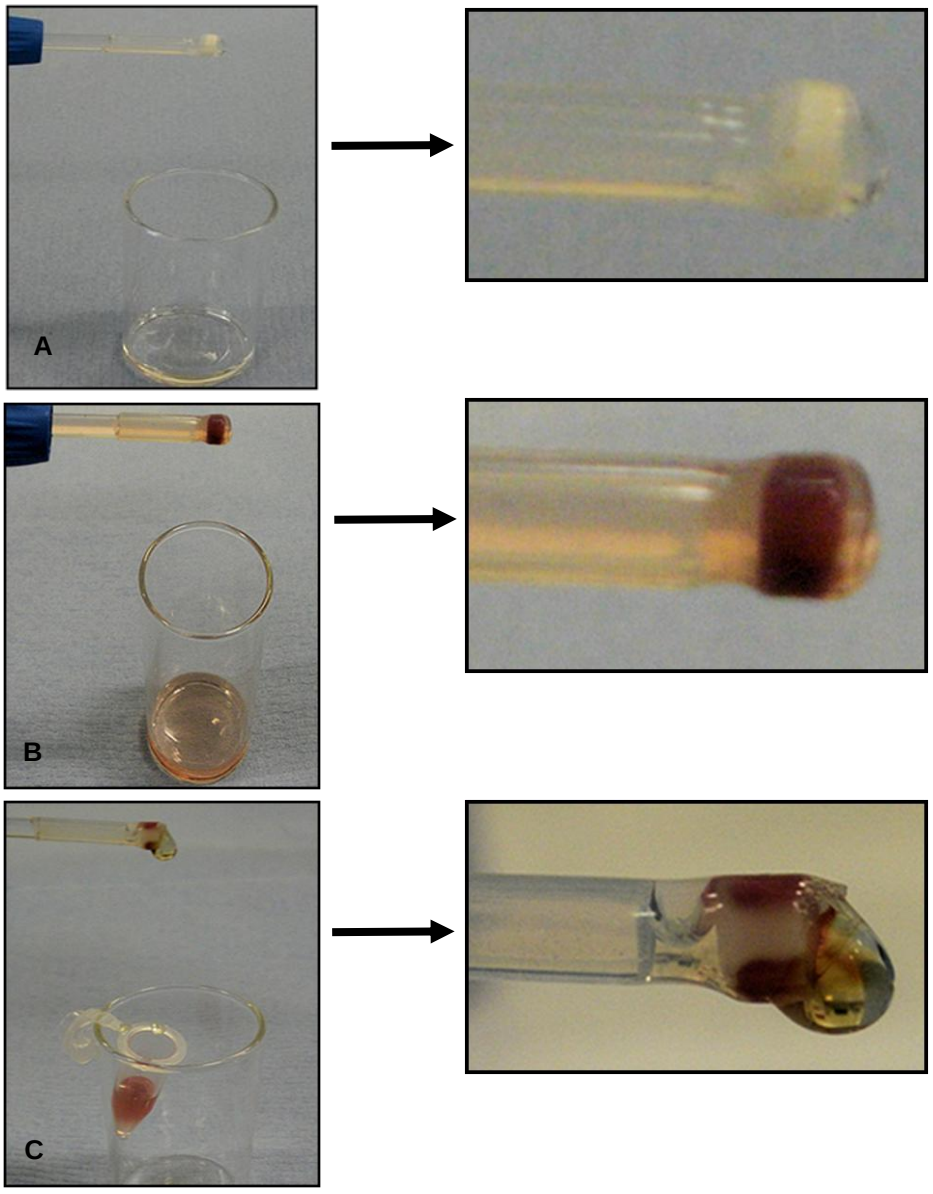

Figure 4.9 The main steps that were used for protein extraction using the bare silica-based monolith inside the heat shrinkable tube. The sample was 1 mL cytochrome C (60 µM), which is red in colour. All reagents were injected using a syringe pump at 10 µL min^{-1}. (A) Activation and equilibration of the monolith, (B) loading of cytochrome C at 5 µL min^{-1}, and (C) during elution of cytochrome C from the monolith using 500 µL 20 % ACN (0.1 % TFA) solution.

From this experiment, it was concluded that the bare silica-based monolith has the ability to preconcentrate cytochrome C with high extraction recovery (97.9 %) calculated using a HPLC-UV detector. After investigating the performance of the bare

silica-based monolith, the performance of the octadecylated silica monolith was tested. The retention of the proteins under reversed-phase (RP) conditions is primarily due to the interaction between the octadecyl functional groups on the surface of the silica-based monolith and the non-polar hydrophobic functional groups of the proteins.

It might be assumed that the performance of the bare silica-based monolith should be compared with the octadecylated silica monolith under the same conditions; however, it was preferred not to use identical conditions because the retention mechanisms of the non-modified silica monolith (normal-phase, hydrophilic interaction) and the octadecylated silica monolith (reversed-phase, hydrophobic interaction) are not the same. Therefore, different reagents for the conditioning, equilibration, washing, and elution steps and different matrices (buffer systems) were used based on the type of sorbent used. It is known that a suitable pH for the bonded phase is in the pH range of 2 to 7.5 because at pH levels above and below this range the bonded phase can be hydrolysed and cleaved off the silica surface. Since the buffering range of ammonium hydrogen carbonate buffer is between 8 and 11.3, it was decided to use a different buffer solution, 50 mM tris-HCl buffer solution (pH 7.0), which has an effective pH range between 7.0 and 9.5.[287]

The performance of the monolithic octadecyl-bonded silica (ODS) tube was examined using the same standard protein (cytochrome C). It was conditioned with 400 µL ACN (0.1 % TFA), then equilibrated using 400 µL ACN to ensure optimum binding of proteins. 1 mL protein sample solution was loaded, followed by rinsing the monolithic ODS tube with 200 µL 50 mM tris-HCl buffer solution (pH 7.0). The protein was eluted using a non-polar solvent, 500 µL 60 % ACN (0.1 % TFA) solution, in order to disrupt the forces that bind the protein to the sorbent. The eluent was dispensed into an Eppendorf tube then injected into the HPLC-UV instrument to calculate the extraction recovery. From the previous experiment, it was found that the octadecylated silica monolith has the ability to preconcentrate cytochrome C with high extraction recovery (109.7 %). Even if the concentration of cytochrome C was decreased from 60 to 10 µM, the extraction recovery of cytochrome C was not decreased. Figure 4.10 illustrates the main steps of preconcentration of cytochrome C (10 µM) using the octadecylated silica monolith. Figure 4.10 (A) shows binding of cytochrome C to the monolithic ODS tube, as confirmed from the change in colour of the monolith. The

monolithic ODS tube was washed with 200 µL 50 mM tris-HCl buffer solution (pH 7.0) without affecting the retained cytochrome C, as confirmed from the colour of the collected solution during the washing step and studying it with the HPLC-UV instrument, figure 4.10 (B). Finally, the preconcentrated cytochrome C was eluted successfully from the monolithic ODS tube, figure 4.10 (C).

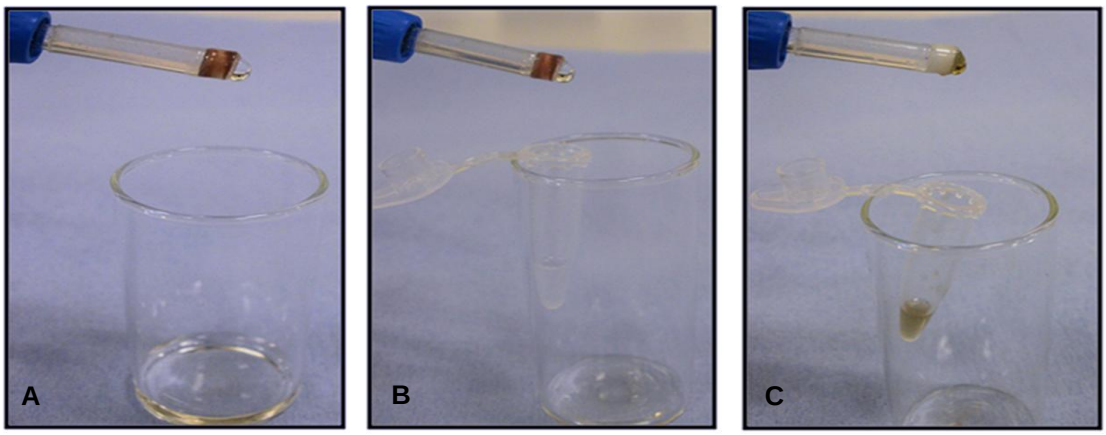

Figure 4.10 Steps of extraction of cytochrome C (10 µM) using the modified silica monolith with octadecyl groups. (A) Application of the sample solution, which was cytochrome C dissolved in 50 mM tris-HCl buffer solution (pH 7.0) containing 10 mM NaCl and adjusted with 0.1 % TFA, (B) washing the monolithic ODS tube using 200 µL 50 mM tris-HCl buffer solution (pH 7.0), and (C) elution of preconcentrated cytochrome C using 500 µL 60 % ACN (0.1 % TFA) solution.

Other coloured standard proteins that were used to investigate the performance of the octadecylated silica monolith were myoglobin and hemoglobin at a concentration of 60 µM. The same procedure that was used for preconcentration of cytochrome C was used to preconcentrate myoglobin and hemoglobin. Figure 4.11 illustrates the main steps of preconcentration of myoglobin using the monolithic ODS tube. Figure 4.11 (A) shows the retained myoglobin on the octadecylated silica monolith, as confirmed from the change in the colour of the octadecylated silica monolith from white to brown. Figure 4.11 (B) illustrates washing the monolithic ODS tube in order to

remove impurities without affecting the retained myoglobin, and finally the preconcentrated myoglobin was eluted from the monolithic ODS tube, figure 4.11 (C).

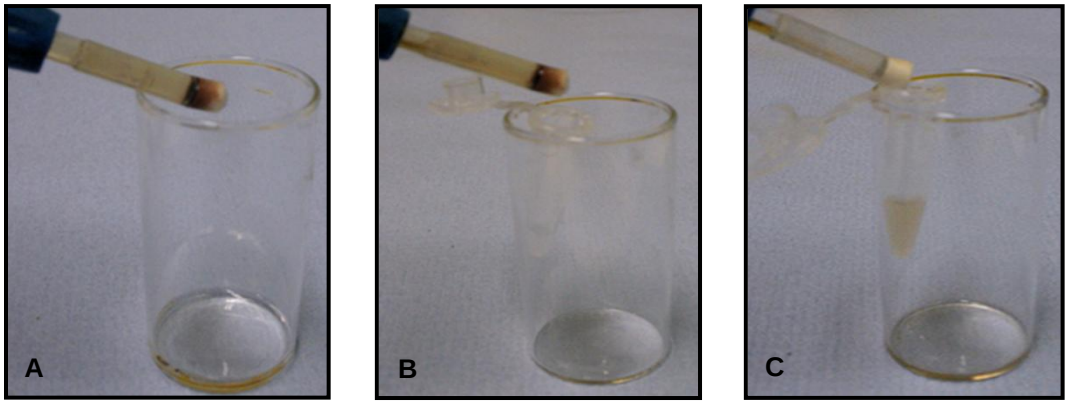

Figure 4.11 Steps of extraction of myoglobin (60 µM) using octadecylated silica monolith. (A) Loading myoglobin dissolved in 50 mM tris-HCl buffer solution (pH 7.0) containing 10 mM NaCl and adjusted with 0.1 % TFA, (B) washing the monolithic ODS tube with 200 µL 50 mM tris-HCl buffer solution (pH 7.0), and (C) elution of preconcentrated myoglobin using 500 µL 60 % ACN (0.1 % TFA) solution.

The comparison between the performance of the non-modified silica-based monolith and the octadecylated silica monolith shows that the octadecylated silica monolith has the ability to purify and preconcentrate both myoglobin and hemoglobin better than the bare silica-based monolith, as confirmed by figure 4.12, which shows myoglobin and hemoglobin during the loading step using bare silica-based monolith and octadecylated silica monolith. The figure shows that myoglobin, figure 4.12 (B), and hemoglobin, figure 4.12 (D), were retained strongly on the octadecylated silica monolith compared with the bare silica-based monolith.

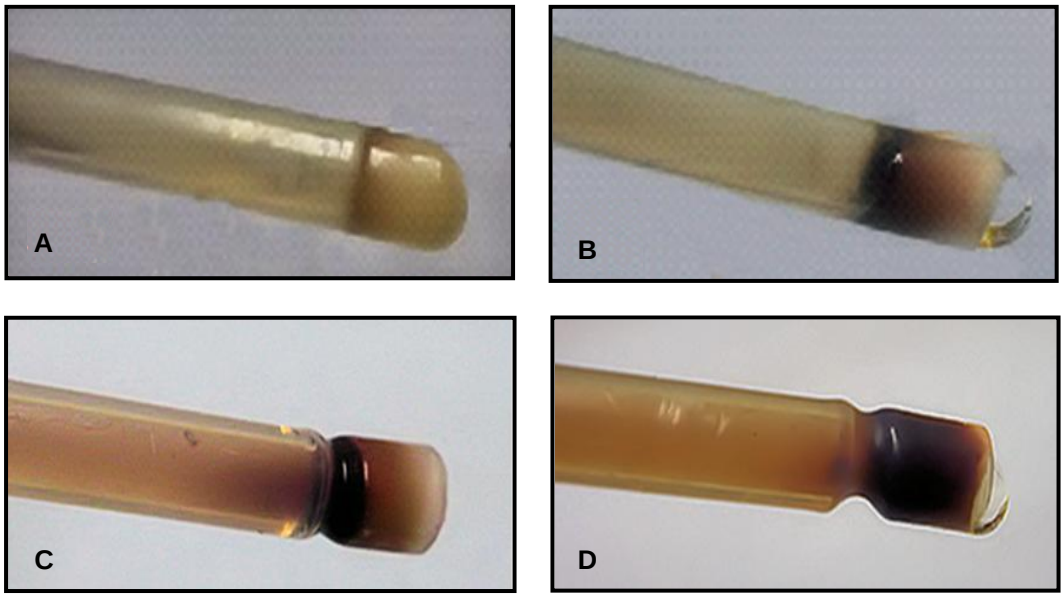

Figure 4.12 Loading myoglobin using non-modified silica-based monolith (A), and using octadecylated silica monolith (B). Loading hemoglobin using non-modified silica-based monolith (C), and using octadecylated silica monolith (D). The protein sample solution was injected using a syringe pump at flow rate 5 µL min^{-1}.

Another standard protein investigated for comparison of the performance of the non-modified silica-based monolith and octadecylated silica monolith was lysozyme. Figure 4.13 shows a comparison of the peak areas of lysozyme purified with bare silica-based monolith and with octadecylated silica-based monolith. From the figure, it can be seen that a huge difference in the peak areas of lysozyme purified with the octadecylated silica monolith compared with the bare silica-based monolith. As a result, the sensitivity of the analysis was enhanced.

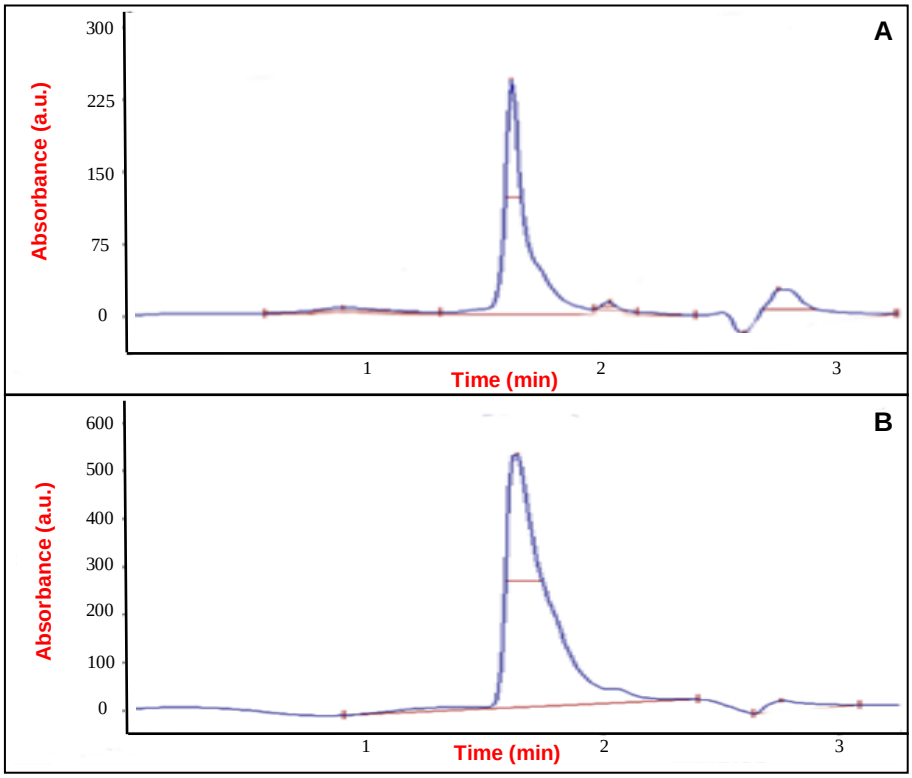

Figure 4.13 The difference in the peak area of lysozyme purified using (A) the bare silica-based monolith, and (B) the chemically modified silica monolith with octadecyl groups.

Different standard proteins (insulin, β-lactoglobulin, ovalbumin, and BSA) were also preconcentrated using the bare silica-based monolith and octadecylated silica monolith, and the extraction recoveries of the purified proteins were calculated. Table 4.5 presents a comparison of the extraction recoveries of all standard proteins preconcentrated in this study with the non-modified silica monolith and the octadecylated silica monolith. The comparison in the table indicates a huge increase in the extraction recoveries of the standard proteins when using the octadecylated silica monolith, ranging from 92.7 to 109.7 % while the range of extraction recovery of the standard proteins using the bare silica-based monolith was 25.5-97.9 %. The significant conclusion of this table is that efficient protein extraction was achieved using the octadecylated silica monolith. The reproducibility of the performance of the bare silica and modified silica monolith with octadecyl groups was evaluated by

calculating the RSD of the peak areas, which were calculated to be 2.9-7.4 % for the bare silica-based monolith and 2.0-6.1 % for the octadecylated silica monolith.

Standard protein	Bare silica monolith		Octadecylated silica monolith	
	(ER) (%)	RSD (%)	(ER) (%)	RSD (%)
Insulin	88.2	6.1	105.2	6.1
Cytochrome C	97.9	2.9	109.7	2.0
Lysozyme	75.3	6.9	96.9	3.8
Myoglobin	65.2	4.6	95.6	4.5
β-lactoglobulin	29.4	7.4	94.8	5.4
Ovalbumin	45.9	4.7	92.7	5.7
Hemoglobin	96.8	5.3	99.6	3.7
BSA	25.5	3.1	95.4	2.1

Table 4.5 Comparison of the extraction recovery of standard proteins purified with bare silica-based monolith, and with C_{18}-bonded silica monolith, where ER = extraction recovery.

Although the surface area of the octadecylated silica monolith (154.29 m^2 g^{-1}) was lower than that of the bare silica-based monolith (173.31 m^2 g^{-1}) due to the attachment of the octadecyl groups to the silica surface and blocking of the micropores by the bonded phase, this study shows that the octadecylsilylated monolithic silica rod was much better for preconcentration of eight standard proteins varying in molecular weights and isoelectric points compared with the bare silica-based monolith. It was concluded that although a high surface area of sorbent is desired to increase the loadability of the sorbent, the property of the sorbent is more important as the extraction recovery depends on the target analyte, the matrix, and the type of sorbent. Since satisfactory extraction recoveries of the standard proteins with a good

reproducibility were achieved using C_{18}-bonded monolithic silica, it was chosen for further study.

4.2.2 Protein extraction using the C_{18}-bonded silica monolith microchip

Before fabrication of the monolith inside the microchip, it was decided to fabricate the sol-gel silica-based monolith inside a 25 µL-sized micropipette, since it is cheaper than the microchip. Two trials were performed to prepare the silica-based monolith inside the micropipette. The first attempt was performed using the same sol-gel mixture and procedure; however, it was found that the sol-gel silica skeleton shrank during the preparation and there were cracks in the monolith inside the micropipette. Due to the shrinkage and the cracking in the monolith, its performance for protein extraction was not investigated.

The second attempt to fabricate the silica-based monolith inside the micropipette was based on washing the inner walls of the micropipette with 1 M NaOH solution in order to generate free silanol groups on the surface of the micropipette, which would take part in the sol-gel process. As a result, the silica skeleton monolith would be chemically anchored to the micropipette walls. After the micropipette treatment, the sol-gel mixture was injected into the micropipette to form the monolith, followed by surface modification of the silica-based monolith with octadecyl groups. Since the second attempt to fabricate the octadecylated silica monolith inside the micropipette was successful, it was decided to use it for protein extraction. The performance of the octadecylated silica monolith inside the micropipette was examined using cytochrome C. Figure 4.14 shows the steps of preconcentration of cytochrome C using the same procedure as used before for extraction the standard proteins with the octadecylated silica monolith inside the heat shrinkable tube.

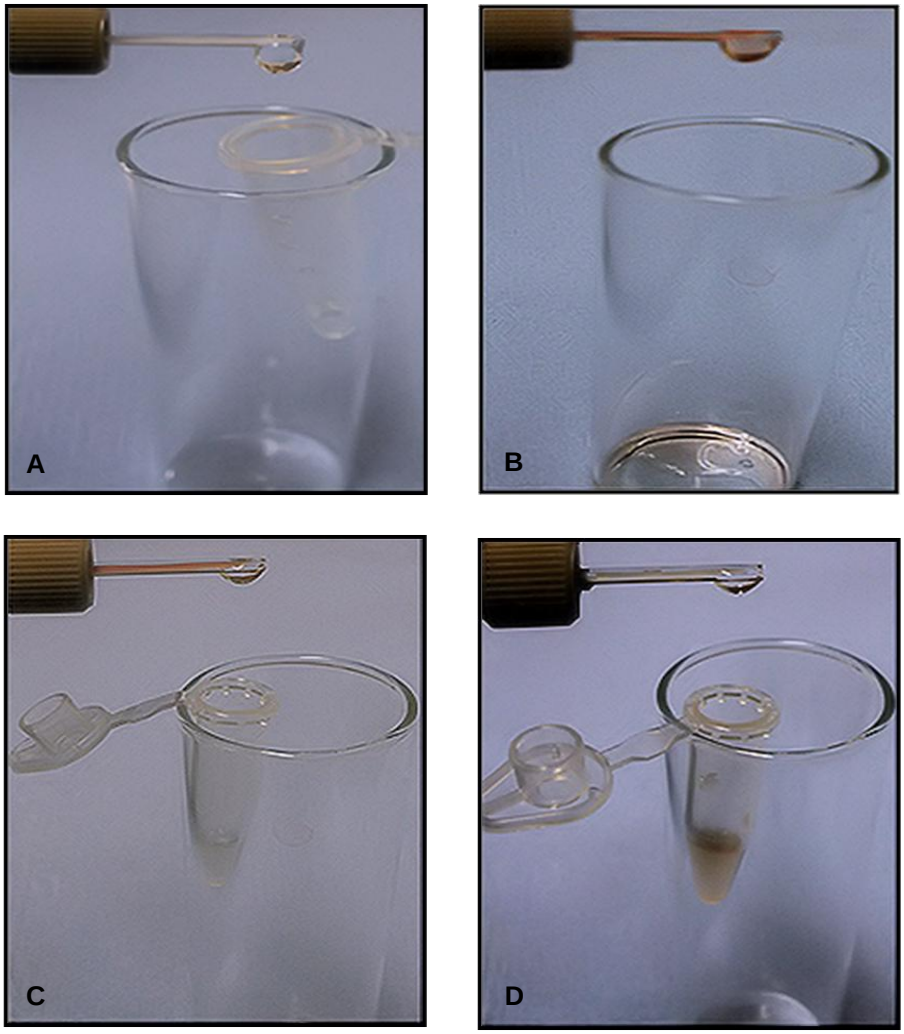

Figure 4.14 Steps of preconcentration of cytochrome C using crack-free octadecylsilyl-silica sol-gel monolith inside the 25 µL-sized micropipette. (A) Activation of the monolithic octadecylsilyl-silica gel micropipette, (B) loading of the protein sample solution, (C) washing the monolith, and (D) elution of the preconcentrated cytochrome C.

It was found that this method was successful in fabricating the octadecylated silica monolith inside the micropipette without any cracks or voids in the monolith, and the monolith was anchored to the walls of the micropipette. In addition, this method of fabrication was faster compared with the previous procedure. Moreover, it was found that the octadecylated silica monolith inside the micropipette was stable during the

experiment, and had excellent hydrodynamic properties. However, the result indicated that the extraction recovery of cytochrome C using the octadecylated silica monolith inside the micropipette was decreased to 70 %. This could be because of the lower surface area (107.25 m^2 g^{-1}) of the octadecylated silica monolith prepared using the second procedure compared with the octadecylated silica-based monolith prepared using the first procedure (154.29 m^2 g^{-1}). Since the extraction recovery of cytochrome C was not satisfactory, no further work was undertaken with the micropipette.

It was decided to use the same sol-gel mixture and procedure as used before for fabrication of the monolithic silica inside the heat shrinkable tube to fabricate the silica-based monolith inside a microchip. This was performed by fabrication of a monolithic silica rod as done before, followed by cutting of the rod to form a monolithic silica disk. The disk was placed inside the extraction chamber of the base plate for both polycarbonate and glass microchips.

The polycarbonate microchip containing the octadecylated silica monolith was used for extraction of cytochrome C using the same procedure used before to preconcentrate the standard proteins using the octadecylated silica monolith inside the heat shrinkable tube. Figure 4.15 shows the steps for extraction of cytochrome C using the polycarbonate microchip containing the octadecylated silica monolith. Figure 4.15 (A) shows the appearance of the top plate of the polycarbonate microchip containing the octadecylated silica monolith after loading of cytochrome C, which confirmed that cytochrome C was bound to the monolith and concentrated as is apparent from the change in the colour of the monolith from white to red. Figure 4.15 (B) shows the set-up of the polycarbonate microchip during washing the monolithic octadecylated silica disk without affecting the retained cytochrome C, as confirmed from the colour of the collected solution during the washing step. The preconcentrated cytochrome C was eluted successfully from the polycarbonate microchip, as can be seen in figure 4.15 (C), and (D).

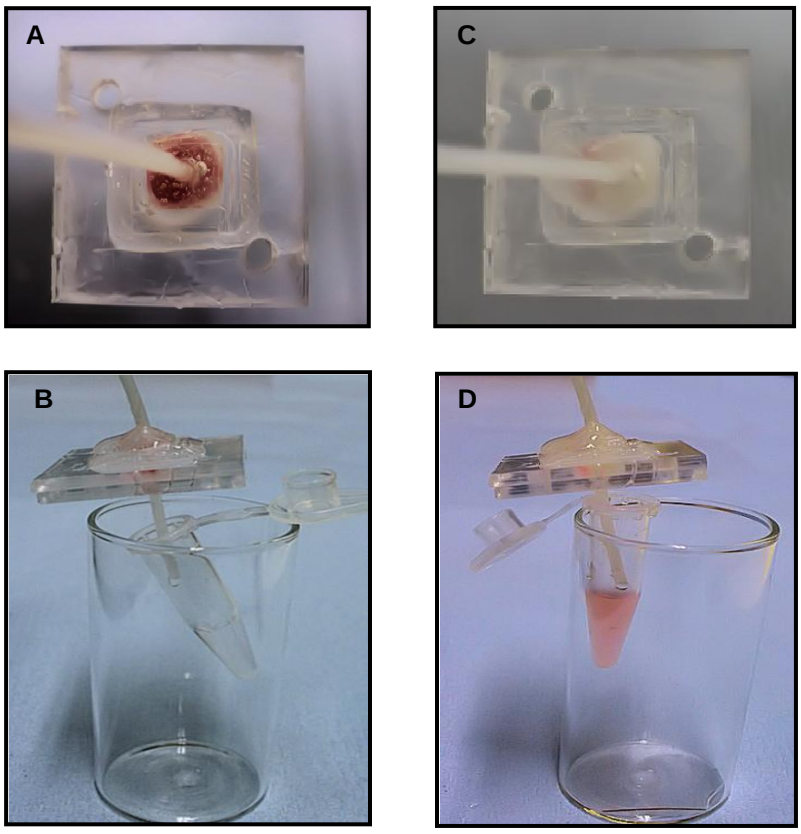

Figure 4.15 Photograph of the polycarbonate microchip containing the octadecylated silica monolith during preconcentration of cytochrome C. (A) Loading the protein, (B) washing step, (C) and (D) elution of cytochrome C from the microchip.

It was found that the permeability of the octadecylated silica monolith inside the extraction chamber was high and a high flow rate (10 µL min^{-1}) could be used without leakage. In addition, the extraction recovery of cytochrome C was not decreased, as expected, since the preparation procedure of the octadecylated silica monolith was not changed. However, it was found that the polycarbonate microchip was affected by the solvents and reagents. Moreover, the two plates of the microchip need to be fixed every time before the experiment, since they were fixed together by using epoxy resin. Therefore, it was necessary to investigate a different type of microchip, which was a glass microchip to overcome these issues. Although glass microchip is expensive

compared with the polycarbonate microchip, it is more resistant to reagents, organic solvents, and high temperature.

Detergents such as sodium dodecyl sulphate (SDS), 3-([3-cholamidopropyl] dimethylammonio)-1-propane sulfonate (CHAPS), cholate, and tween are commonly used to separate proteins from lipids.[288] They are added to the buffer for extraction of membrane proteins, which are usually insoluble in an aqueous buffer. However, increasing salt or detergent concentration can mask the signal of proteins especially the low abundance proteins and further complicate analysis by mass spectrometry.[28, 289] Therefore, the performance of the octadecylated silica glass microchip was checked by extraction of the standard proteins in the presence of the detergents and buffer, since they are usually used in protein analysis. This was performed by mixing the standard proteins (60 µM) with a double concentration of detergent (CHAPS) dissolved in a mixture consisting of 1 mL phosphate-buffered saline (PBS), and 4 mL 50 mM tris-HCl buffer solution (pH 7.0) containing 10 mM NaCl, and 5 µL TFA.

The octadecylated silica monolith inside the glass microchip was cleaned with 100 µL ACN (0.1 % TFA) to remove impurities and then equilibrated with 100 µL ACN to ensure optimum binding of proteins. The permeability of the octadecylated silica monolith inside the glass microchip is high and flow rates up to 10 µL min^{-1} could be used without leakage. After loading the sample solution through the monolith, the fabricated microchip was rinsed to remove interferences without losing the preconcentrated protein. Finally, the preconcentrated proteins were eluted from the sorbent using 150 µL 60 % ACN (0.1 % TFA), and collected into an Eppendorf tube. Figure 4.16 (A) shows the set-up of the fabricated glass microchip containing the octadecyated silica monolith during loading of cytochrome C, and (B) after elution of cytochrome C.

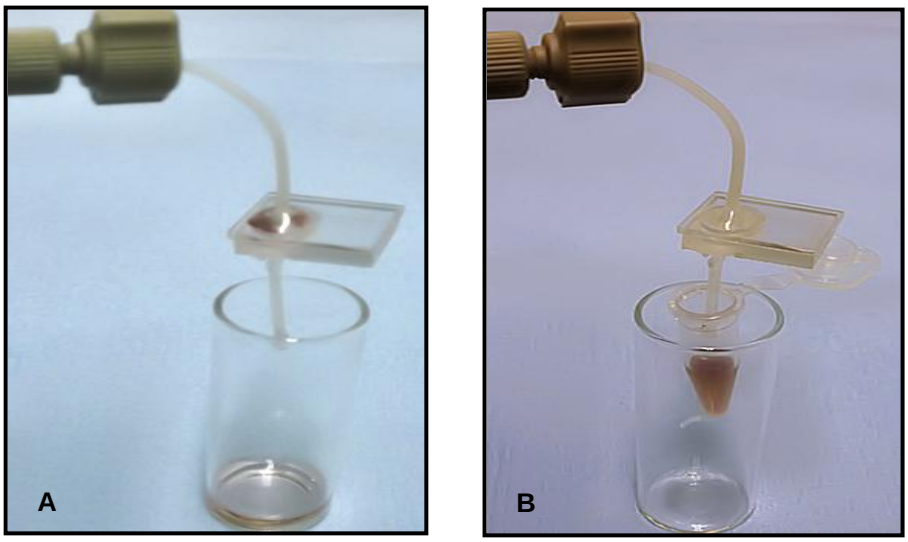

Figure 4.16 (A) The set-up of the glass microchip containing the octadecylated silica monolithic disk during loading cytochrome C, and (B) after elution of cytochrome C from the fabricated device.

Figure 4.17 (A) shows the appearance of the top plate of the octadecylated silica monolith inside the extraction chamber of the glass microchip before using the fabricated microchip for protein extraction, after binding of cytochrome C, figure 4.17 (B), and hemoglobin, figure 4.17 (C). Figure 4.17 (D) shows a cross-section of the glass microchip containing octadecylated silica monolith during loading of myoglobin. This confirmed that different standard proteins were bound to the octadecylated silica monolith and preconcentrated, as is apparent from the change in the colour of the sorbent from white to red for cytochrome C, and brown for hemoglobin and myoglobin. In addition, it was found that the octadecylated silica monolith inside the microchip was very permeable, stable, and no leaking was observed during the experiment.

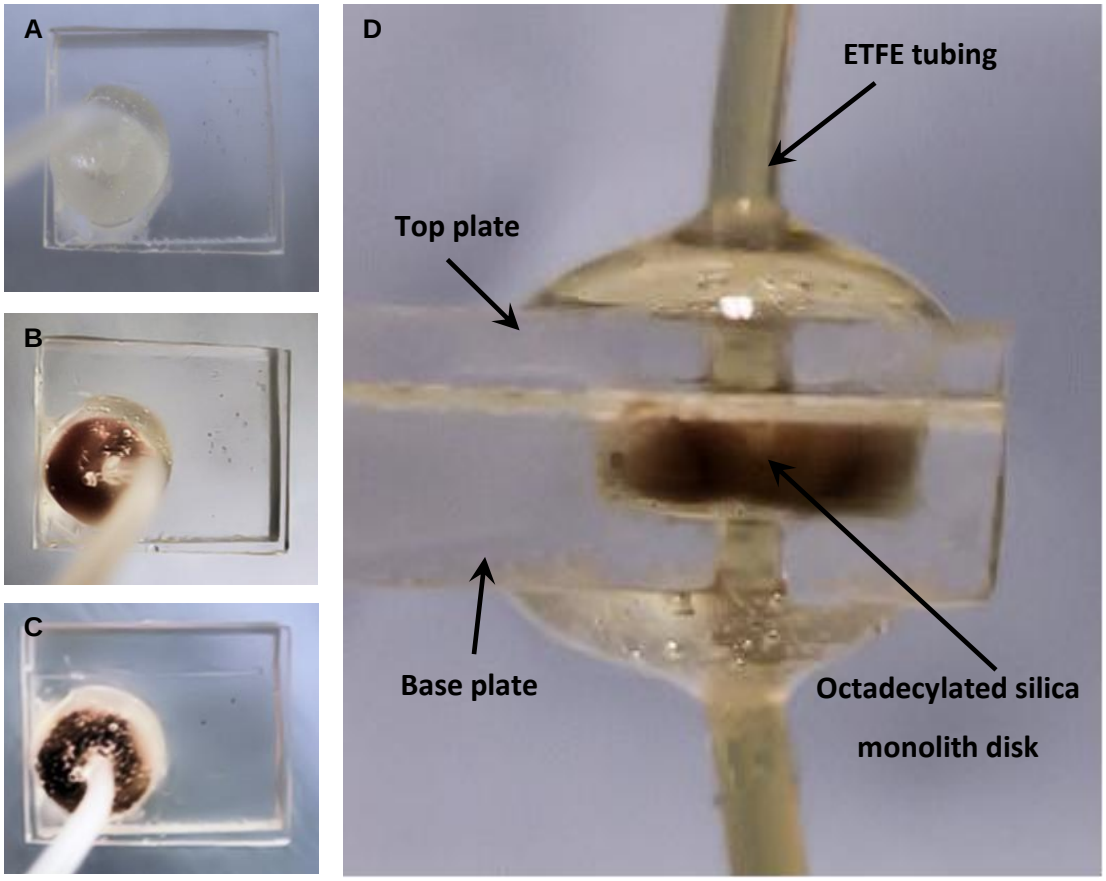

Figure 4.17 The octadecylated silica monolith inside the glass microchip before/during loading protein: (A) before loading protein, (B) during loading cytochrome C, (C) during loading hemoglobin, and (D) cross-section of the glass microchip during loading myoglobin.[121]

The performance of the fabricated octadecylated silica glass microchip in the extraction of protein from the spiked sample was studied using the HPLC-UV detector. The mobile phase was acetonitrile-purified water (50:50) in the presence of 0.1 % (TFA) under isocratic conditions and the flow rate was set at 1 mL min^{-1}; however, it was observed that the peaks were overlapped; therefore, it was decided to decrease the flow rate from 1 to 0.3 mL min^{-1}. Figure 4.18 (A) shows the UV chromatogram of a non-processed protein sample, which shows the peak for cytochrome C (retention time = 5.33 min) was masked by the interfering compounds present in the sample. Figure 4.18 (B) shows the UV chromatogram of the collected solution during washing the fabricated device that shows a peak at 7.03 min, which is related to the detergent (CHAPS), similar to the peak observed in the sample mixture

while the peak of cytochrome C was not observed, which confirmed that washing the octadecylated silica monolith inside the extraction chamber of the glass microchip did not affect the retained protein.

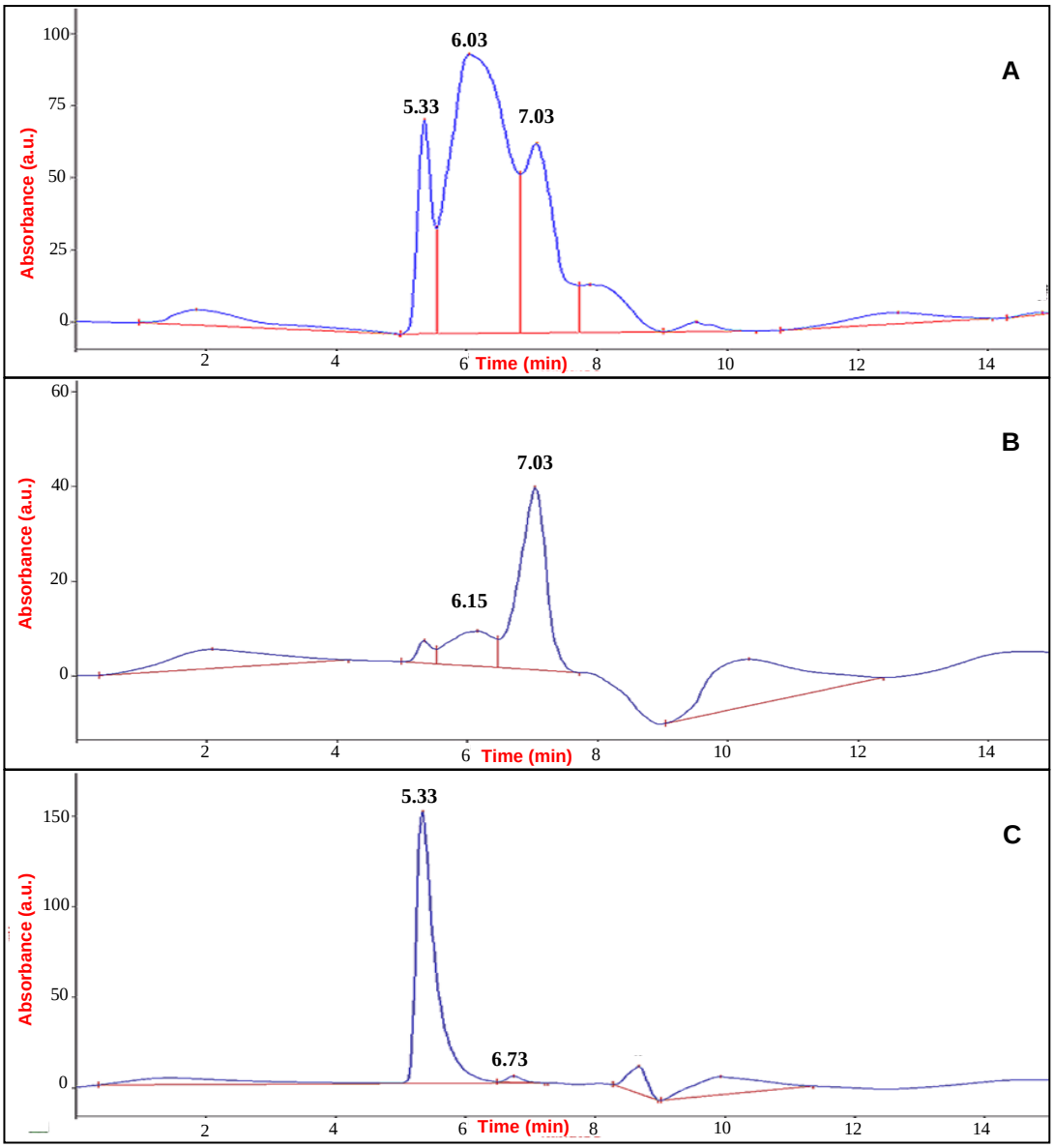

Figure 4.18 The UV chromatogram (A) mixture of 60 µM cytochrome C and 120 µM CHAPS dissolved in a mixture of 1 mL PBS and 4 mL 50 mM tris-HCl buffer solution (pH 7.0) containing 10 mM NaCl and 5 µL TFA, (B) collected solution during washing the fabricated device, and (C) eluent solution. The flow rate was 0.3 mL min^{-1} and the detection wavelength was 210 nm. Between consecutive analyses, a needle for the automated injector was washed with 70 % aqueous methanol.

Figure 4.18 (C) shows the UV chromatogram for the eluent solution. Comparison of the peak area of extracted cytochrome C with the non-processed sample solution shows that the peak area of cytochrome C was increased significantly after preconcentration while the interfering peaks from the interfering compounds present in the sample solution were not observed. In addition, the peak at 6.0 min that was observed in figure 4.18 (A), which could be because cytochrome C interacted with some components in the sample solution, was not observed in the UV chromatogram of the eluent solution, which confirmed that the protein was recovered and no interfering materials were observed. These results indicated that the fabricated device has the ability to clean up the protein and remove impurities and detergent.

The performance of the octadecylated silica monolith inside the glass microchip was also examined with matrix-assisted laser desorption/ionisation time-of-flight mass spectrometry (MALDI-TOF-MS), since it has been used as a fast and efficient technique for analysis of proteins and its sensitivity is better than that of the HPLC-UV detector. Although MALDI-TOF-MS tolerates some degree of contamination and detergents, it is very important to remove detergents, such as CHAPS, before peptide mapping and protein analysis since enzymatic digestion is commonly utilised and this detergent has been found to mask the spectrum of the peptides and add spectral noise. In addition, the presence of CHAPS in the sample solution can affect the co-crystalisation of matrix molecules during the matrix-sample preparation.[290] Therefore, it is important to remove interfering materials before MALDI analysis in order to get a successful spectrum for the target analyte in a complex sample.[291]

After extraction of cytochrome C in the presence of a double concentration of the detergent (CHAPS), the eluent solution was mixed with matrix and studied with the MALDI-TOF-MS instrument. Chait and coworkers [204] mentioned that using 4-hydroxy-α-cyano-cinammic acid (4HCCA) dissolved in a distilled water/2-propanol/formic acid mixture (3:2:1, v/v/v) can enhance the mass resolution of the proteins. Therefore, this method was investigated for preparation of the sample-matrix solution. The MALDI-TOF mass spectrum of cytochrome C in the eluent solution was compared with the MALDI-TOF mass spectrum of non-processed cytochrome C. Figure 4.19 shows the MALDI-TOF mass spectrum of cytochrome C before and after preconcentration using the fabricated octadecylated silica monolith microchip over the

mass range from 4 to 16 kDa. The figure shows the signal intensity of cytochrome C (the peak at m/z 12154) was increased significantly after preconcentration. This result indicated that the fabricated octadecylated silica monolith inside the glass microchip has the ability to preconcentrate cytochrome C. In addition, it can produce a spectrum with a high signal-to-noise ratio.

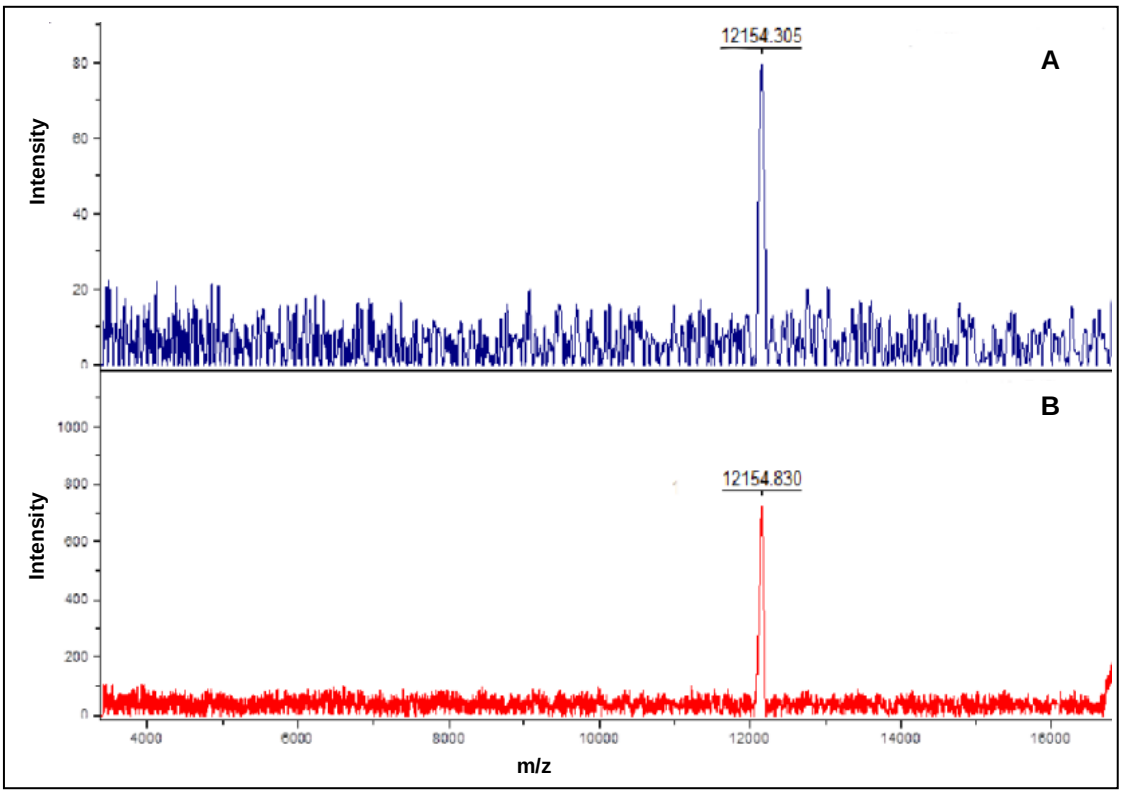

Figure 4.19 Comparison of MALDI-TOF mass spectrum of cytochrome C, with/without purification by fabricated microchip: (A) without and (B) with purification. Matrix solution was 4-hydroxy-α-cyano-cinammic acid (4HCCA) dissolved in a distilled water/2-propanol/formic acid mixture (3:2:1, v/v/v). The mass range was between 4 and 16 kDa.[121]

In the previous MALDI-TOF mass spectra, only one peak that corresponds to cytochrome C was observed. Although the sample solution contained CHAPS and other impurities, these were not observed since the mass range was between 4 and 16 kDa while the molecular weights of CHAPS and salts from PBS were less than 1 kDa. Therefore, the mass range was changed to 1-1000 Da in order to investigate the ability of the fabricated device to preconcentrate protein and remove interfering materials. The MALDI-TOF mass spectra of non-processed sample solution, solution collected

during washing the fabricated microchip, and eluent solution were studied. Figure 4.20 (A) shows the MALDI-TOF mass spectrum of the non-processed sample solution, which contained different peaks related to the interfering materials (CHAPS and salts from PBS) in the sample solution. The peak at m/z 615 is attributed to a CHAPS molecule that could interfere with the digested peptides and affect the MS analysis.[290]

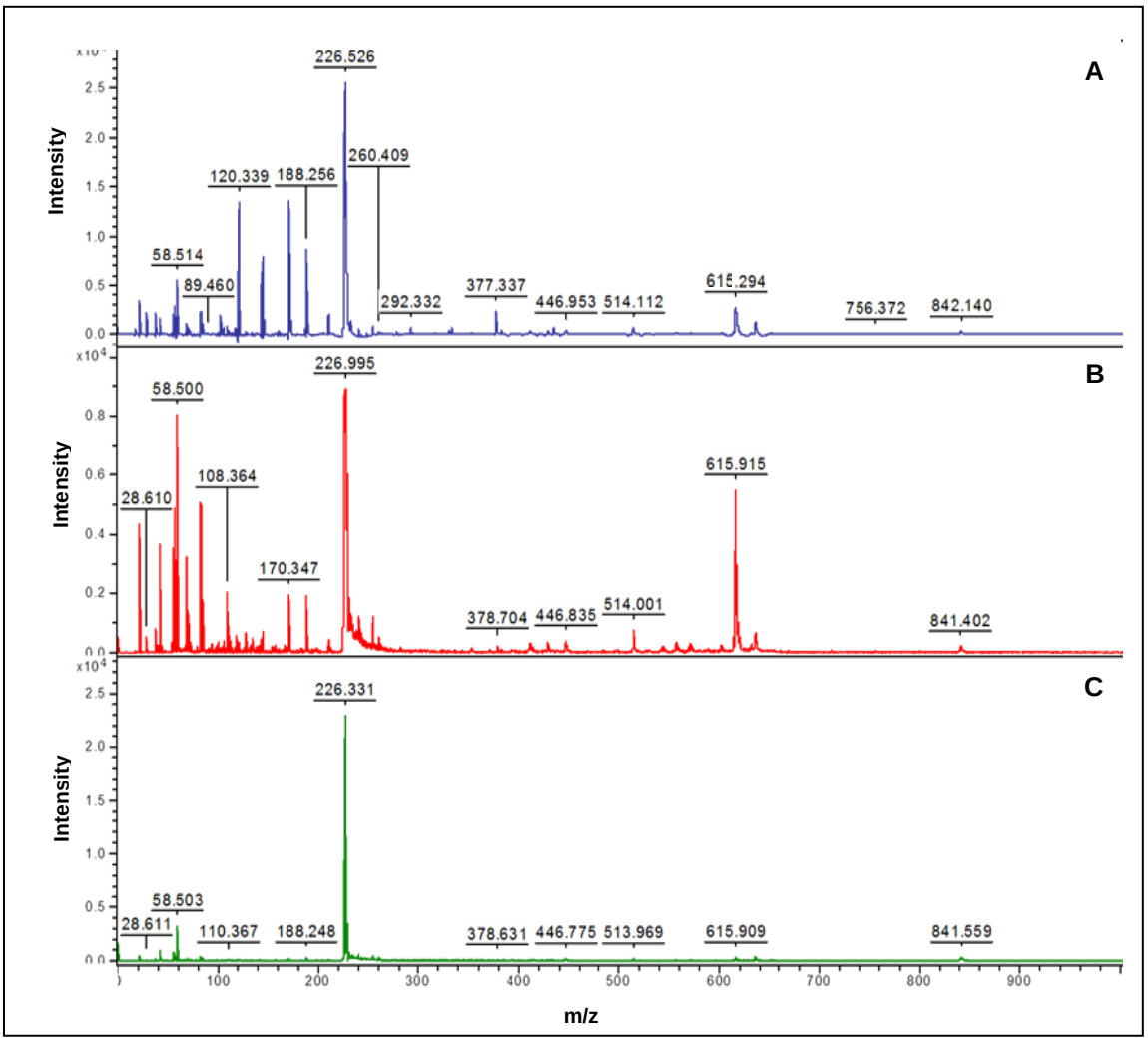

Figure 4.20 MALDI-TOF mass spectra of (A) the non-processed sample solution containing 60 µM cytochrome C and 120 µM CHAPS dissolved in a mixture of 1 mL PBS and 4 mL 50 mM tris-HCl buffer solution (pH 7.0) containing 10 mM NaCl and 5 µLTFA, (B) solution collected during washing the fabricated device, and (C) eluent solution. The MALDI sample preparation was performed as done before in figure 4.19. The mass range was 1-1000 Da.

Figure 4.20 (B) shows the MALDI-TOF mass spectrum of the solution collected during washing the fabricated microchip, showing the signal of CHAPS, the peak at m/z 615, which confirmed that the interfering materials were washed out from the octadecylated silica monolithic disk. Figure 4.20 (C) shows the MALDI-TOF mass spectrum of the eluent solution, which shows that the signal intensities of salts and impurities were decreased and only a strong peak at m/z 226 was observed, which was not known. This result confirms the ability of the octadecylated silica monolith microchip to preconcentrate cytochrome C, although the sample solution containd a high concentration of CHAPS and PBS.

4.2.3 Performance comparison between the C_{18}-bonded silica monolith microchip and a commercial C_{18} cartridge

The performance of the C_{18}-bonded silica monolith inside the glass microchip was compared with a commercial cartridge that was reversed-phase sorbent material (DSC-18), which contained silica particles (50 μm) modified with octadecyl ligands and end capped, which is similar to the fabricated octadecylated silica monolith. The extraction of standard proteins in the presence of a high concentration of CHAPS and PBS was carried out under the same conditions since they are both hydrophobic sorbents. Figure 4.21 shows comparison of the extraction efficiencies of the standard proteins purified with the octadecylated silica monolith microchip and commercial cartridge. Each value represents the mean of three measurements carried out. The figure indicates that a higher extraction efficiency can be achieved using the octadecylsilated silica monolith microchip, ranging from 94.8 to 99.7 %, which is better than the commercial cartridge, where extraction recovery ranging from 48.3 to 91.3 %. The low extraction recovery of the standard proteins using the conventional C_{18}-bonded silica particles could be attributed to the formation of channels in the stationary phase after a few usages resulting in fast movement of the proteins through these channels before they get sufficient equilibration time to interact with the sorbent [286], while there was no deterioration in the performance of the octadecylated silica monolith indicating that the silica monolith has a long lifetime.

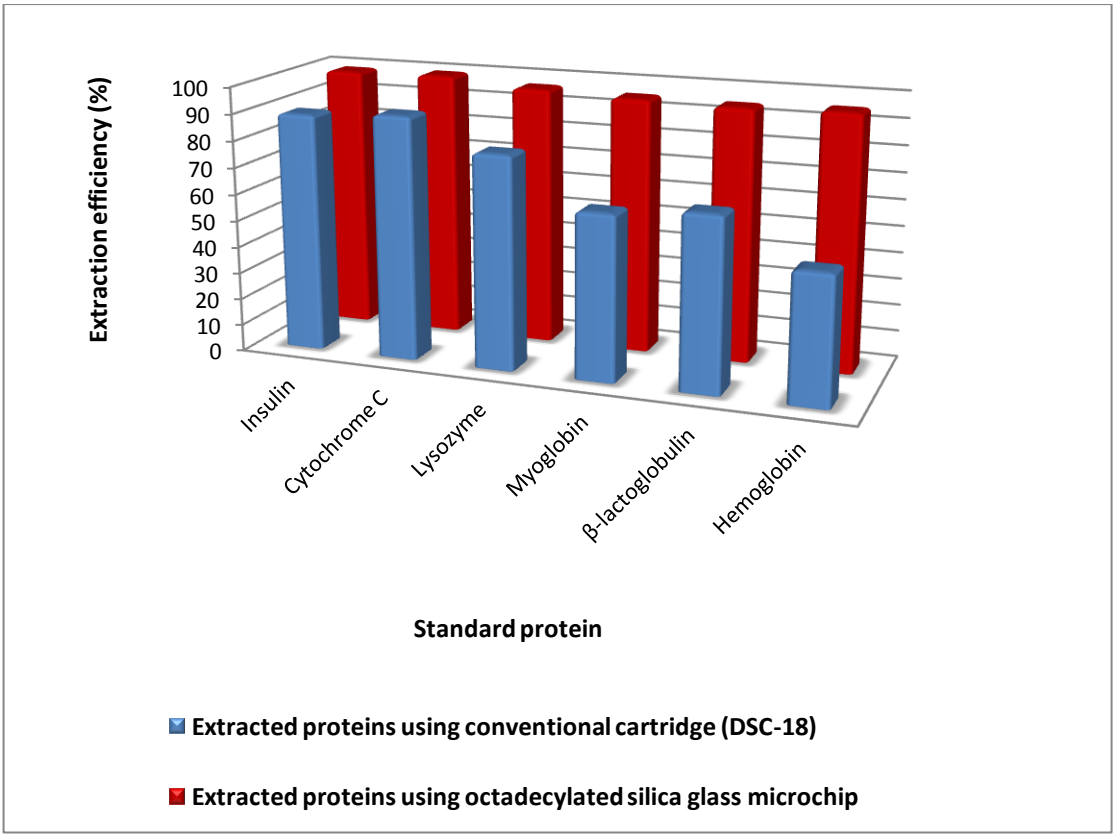

Figure 4.21 Comparison of the extraction efficiencies of the standard proteins (60 µM) purified with conventional DSC-18 cartridge (blue) and fabricated octadecylated silica monolith microchip (red).

It is evident from the results that the fabricated C_{18}-bonded monolithic silica extraction microchip has the ability to preconcentrate different standard proteins and the extraction recovery of the proteins was not decreased if the molecular weight of the standard protein was more than 40 kDa. This result differs from a previous study that reported that the performance of the C_{18}-bonded monolithic silica inside the micropipette tip in extraction of standard proteins was decreased when the molecular weight of protein was more than 40 kDa.[125]

4.2.4 Reproducibility and stability of the fabricated device

One of the most important aspects of using a glass microchip is reusability, since the cost of fabrication is high. The reproducibility of the device was assessed by calculating the relative standard deviation for six standard proteins during extraction.

The intra-batch relative standard deviations for peak area counts were calculated to be between 2.0 - 4.5 % while the inter-batch relative standard deviations ranged from 2.9 to 6.4% (table 4.6).

Precision (RSD %)	**Insulin**	**Cyto C**	**Lysozyme**	**Myoglobin**	**β-lactoglobulin**	**Hemoglobin**
Intra-batch (n=4)	4.1	2.0	3.8	3.7	4.3	4.5
Inter-batch (n=3)	5.8	2.9	4.7	4.2	5.5	6.4

Table 4.6 RSD's of extraction efficiencies showing the intra-chip (run-to-run) and inter-chip (chip-to-chip) reproducibility of the octadecylated silica monolith.

To check the long-term stability of the monolithic silica microchip in the extraction of proteins, the same microchip was used for extraction of proteins several times. It was found that there were no memory effects or deterioration in performance of the fabricated microchip and it was reliably reusable (n > 30 times) with no adverse effect on the extraction efficiency of the standard proteins.

4.2.5 Preconcentration of proteins from real sample

Since the fabricated octadecylated silica monolith microchip shows its ability for preconcentration of standard proteins, it was very important to investigate the performance of the fabricated device to preconcentrate proteins from a real sample. Two real samples were used to check the performance of the fabricated device, namely, skimmed cows milk, and hen egg white. The reasons for choosing these samples were because they are cheap and easy to obtain. In addition, they contain different kinds of proteins that are important and valuable.

4.2.5.1 Skimmed cows' milk

To our knowledge, there has been no published report on the application of a silica-based monolith to extract proteins from a milk sample. Therefore, the performance of the octadecylated silica monolith microchip was examined in the preconcentration of the proteins in liquid skimmed milk containing 0.5 % fat that was used as the real sample. This was performed by diluting 250 μL skimmed milk containing 0.5 % fat with 250 μL tris-HCl buffer solution (50 mM, pH 7.0), containing 10 mM NaCl and then the sample solution was acidified with 0.1 % TFA. The proteins in the liquid milk sample were purified using the octadecylated silica monolith inside the glass microchip and the same optimised extraction conditions used in the preconcentration of the standard proteins were used for the enrichment of milk proteins.

After preconcentration of milk proteins using the fabricated octadecylated silica monolith microchip, they were analysed using MALDI-TOF-MS analysis in the linear positive ion mode, and the matrix solution was prepared as before using 4-hydroxy-α-cyano-cinammic acid (4HCCA) dissolved in a distilled water/2-propanol/formic acid mixture (3:2:1, v/v/v). Figure 4.22 shows the MALDI-TOF mass spectrum of the milk proteins after enrichment using the octadecylated silica monolith microchip in the mass range between 5 and 30 kDa. As can be seen in the figure, the peaks of the whey proteins (α-lactalbumin and β-lactoglobulin) were observed. The strong signal at m/z 14089 corresponds to the singly charged ion of α-lactalbumin [292] with its doubly charged ion (m/z 7101), while the peak at m/z 18265 is attributed to the singly charged ion of β-lactoglobulin with its doubly charged ion (m/z 9101). The peak at m/z 6976 corresponds to a casein proteolytic fragment produced by proteases within the milk sample on β-casein.[179] For casein proteins, two weak signals at m/z 11742 and m/z 23460 correspond to γ_2-casein A_2, which is proteolytic fragments derived from β-casein A_2, and α_{s1}-casein, respectively. Although the signal intensities of the whey proteins were high, the signal intensities of the casein proteins were very weak.

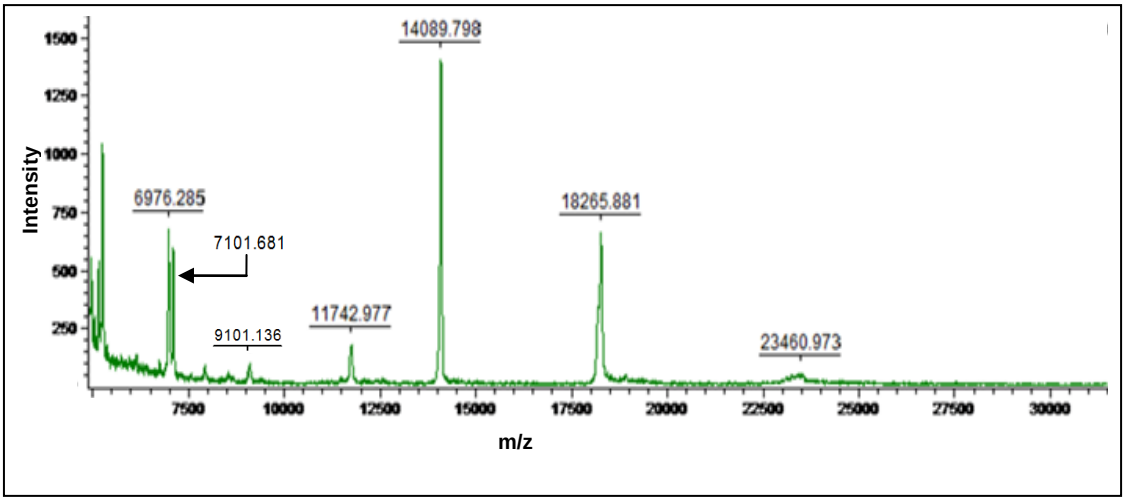

Figure 4.22 MALDI-TOF mass spectrum of the extracted proteins from liquid milk sample using the octadecylated silica monolith microchip. The mass range was 5-30 kDa using linear mode. Matrix solution was 4-hydroxy-α-cyano-cinammic acid (4HCCA) dissolved in a distilled water/2-propanol/formic acid mixture (3:2:1, v/v/v).

It was found that not all casein proteins were observed in the previous MALDI-TOF mass spectrum of the extracted proteins from the liquid milk sample using the octadecylated silica monolith microchip. This could be attributed to factors relating to the MALDI sample preparation since the quality of the MALDI spectrum depends on the sample and matrix preparation; therefore, different matrices and solvents were investigated in order to improve the spectrum of milk proteins particularly for casein proteins. The two-layer sample preparation method was used to prepare the matrix crystal, since this method is shown to be superior to other MALDI sample preparation methods and very effective for analysing complex mixtures. In this work, sinapinic acid (SA) was used as a matrix substance. 0.5 µL of the first layer, which was 6 mg mL^{-1} SA in 60 % MeOH/acetone, was deposited on a MALDI target. The reason for using these solvents is the fast solvent evaporation to form matrix crystals. This was followed by deposition of the second layer, which was 1 µL sample solution and 9 µL saturated matrix solution of SA in 25 % ACN in distilled water containing 0.1 % TFA, on top of the first layer.[205]

The performance of the C_{18}-bonded silica monolith inside the glass microchip to preconcentrate the milk protein was compared with the conventional cartridge (DSC-

18), and the preconcentrated milk proteins were then analysed using MALDI-TOF-MS analysis. All spectra were acquired using identical MS conditions. Figure 4.23 shows the MALDI-TOF mass spectra of proteins in the liquid milk sample for the standard (non-extracted) milk sample, figure 4.23 (A), after enrichment of the milk proteins using the conventional cartridge, figure 4.23 (B), and after enrichment using the fabricated glass microchip containing C_{18}-bonded monolithic silica, figure 4.23 (C). By comparing the MALDI-TOF mass spectra of figure 4.23 (A) and (B), it can be seen that there was a general improvement in the signal intensities of the peaks of milk proteins when using the conventional cartridge. Figure 4.23 (C) displays a further improvement in the mass spectrum of the preconcentrated proteins and displays more peaks corresponding to the milk proteins. The figure has a number of features that need to be emphasised. The two strong signals at m/z 11498 and 11763 correspond to γ_3-casein A_2, and γ_2-casein A_2, respectively. These proteins are proteolytic fragments derived from β-casein A_2. In addition, the peak at m/z 14117 is attributed to α-lactalbumin [292] and the peak at m/z 6999 corresponds to a casein proteolytic fragment produced by proteases within the milk sample on β-casein, as mentioned before.[179] The peak at m/z 8577 can be assigned to ubiquitin, which has been newly identified in milk at very low concentration.[27] A quite broad peak was observed that was related to α_{s1}-, and β-caseins due to the detection of a mixture of those proteins with post-translational modifications. The peak at m/z 23561 is attributed to α_{s1}-casein while the peak at m/z 23934 corresponds to β-casein.[177] In addition to the significantly improved signal intensities of milk proteins, the low-abundance variants of β-lactoglobulin at m/z 18297 (variant A), and m/z 18366 (variant B) were enriched using the fabricated microchip. The peak at m/z 18215 has not been completely assigned; however, the mass difference of 82 Da to the variant A (peak at m/z 18297) might indicate a change in phosphorylation state for this variant. Only three peaks of casein proteins were not observed, which were the peak of κ-casein (m/z 19000), and the peak of γ_1-casein (m/z 21000) while the peak of α_{s2}-casein (m/z 25250) could be overlapped with the peaks of α_{s1}-, and β-caseins.

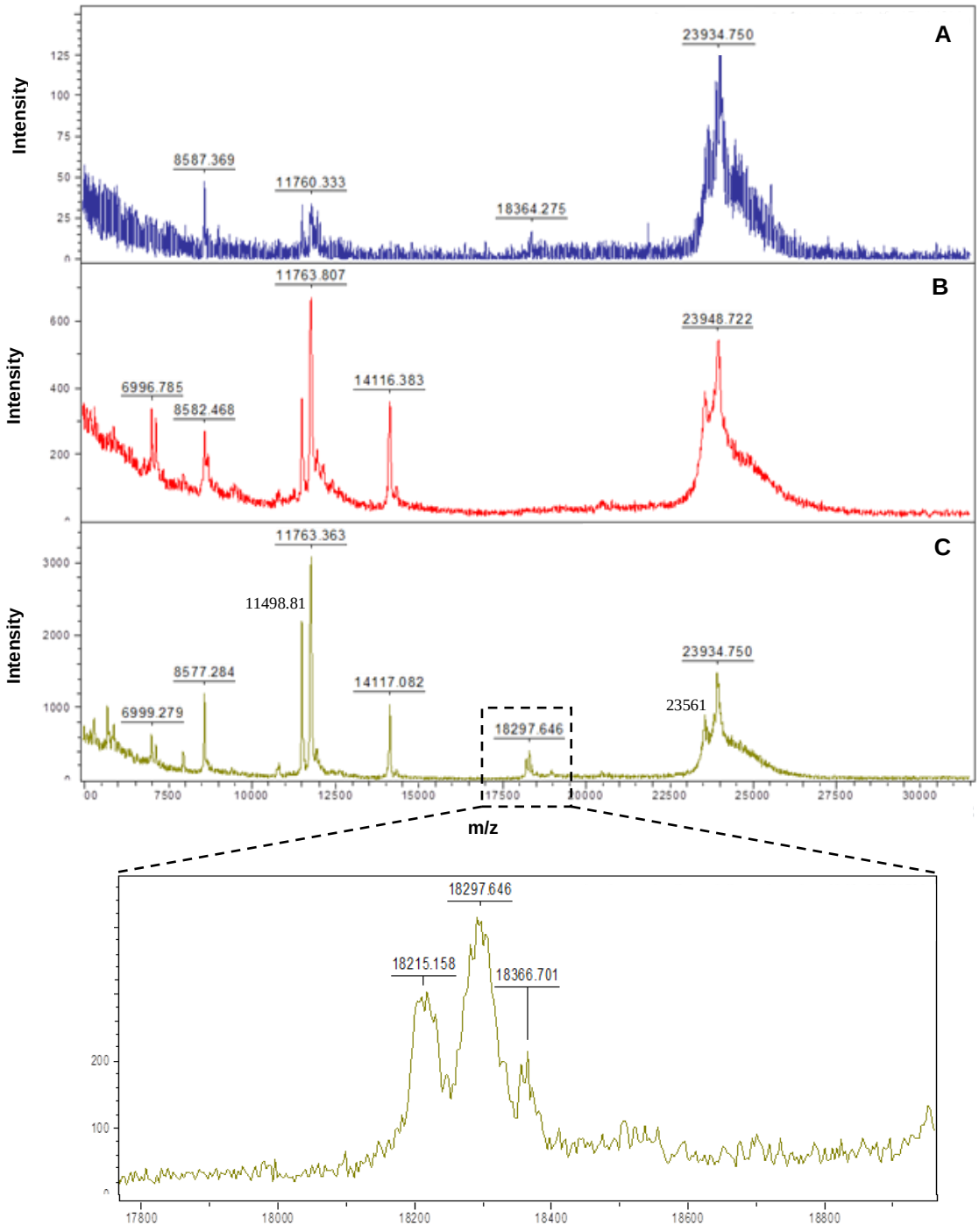

Figure 4.23 Comparison of the MALDI-TOF mass spectra of (A) main milk sample before extraction, (B) after extraction using conventional cartridge, and (C) using octadecylated silica monolith. The matrix crystal was prepared using the two-layer sample preparation method. The first layer was 6 mg mL^{-1} sinapinic acid (SA) in 60 % MeOH/acetone, and the second layer consists of 1 µL sample solution and 9 µL saturated SA in 25 % ACN/0.1 % TFA in water.

These results confirm that the octadecylated silica monolith fabricated inside the glass microchip has the ability to preconcentrate milk proteins that vary in molecular weight, hydrophobicity, and abundance. Moreover, it can produce a clean spectrum free from background interferences, and with a high signal-to-noise ratio. In addition, it was found that the two-layer sample preparation method was effective for analysing milk proteins. The reason for that could be attributed to an increase in the matrix to protein ratio resulting in enhanced isolation between the protein molecules.[205] Therefore, this method of sample preparation was used in all further MS studies.

It was important to calculate the average of the mass to charge ratio of each purified milk protein, since there were slight differences between them. Table 4.7 lists the average mass to charge ratio of the milk proteins that were preconcentrated from the liquid milk sample. From the table, it can be concluded that the relative standard deviation was between 0.01 and 0.46 %.

Milk protein	**The average of the mass to charge ratio (m/z) (n=3)**	**RSD (%)**
Ubiquitin	8577	0.05
γ_3-casein A_2 (proteolytic fragments derived from β-casein A_2)	11496	0.01
γ_2-casein A_2 (proteolytic fragments derived from β-casein A_2)	11757	0.06
α-lactalbumin	14115	0.01
β-lactoglobulin (variant A)	18215	0.46
β-lactoglobulin (variant B)	18321	0.20
α_{s1}-casein	23561	0.03
β-casein	23949	0.09

Table 4.7 The average of the mass to charge ratio of milk proteins identified after preconcentration with the fabricated device, and the repeatability of the molecular mass measured (n=3).

The measured molecular masses of the milk proteins preconcentrated using the octadecylated silica monolith microchip were compared with the reported masses of the milk proteins, as can be seen in table 4.8. The relative percentage error of the molecular masses ranged between 0.03 and 0.90 %. The differences between measured and calculated molecular masses were in agreement with previous studies for milk proteins by MALDI-TOF-MS.[177, 293]

Milk protein	Molecular mass (Da)		Relative percentage error (%)
	Measured	Reported[177, 293]	
Ubiquitin	8577	8500	0.90
γ_3-casein A_2	11496	11500	0.03
γ_2-casein A_2	11757	11800	0.36
α-lactalbumin	14115	14200	0.59
β-lactoglobulin (variant A)	18215	18277	0.33
β-lactoglobulin (variant B)	18321	18360	0.21
α_{s1}-casein	23561	23600	0.16
β-casein	23949	24000	0.21

Table 4.8 Comparison between the measured and reported molecular masses of the milk proteins preconcentrated using the octadecylated silica monolith microchip, and the relative percentage error in the measured molecular masses.

The bar chart 4.24 presents the signal intensities for all the preconcentrated milk proteins, which were significantly increased when using the octadecylated silica monolith compared to the conventional method and unobserved milk proteins enriched using the microchip. This result clearly demonstrates the ability of the fabricated microchip to preconcentrate milk proteins from liquid milk sample.

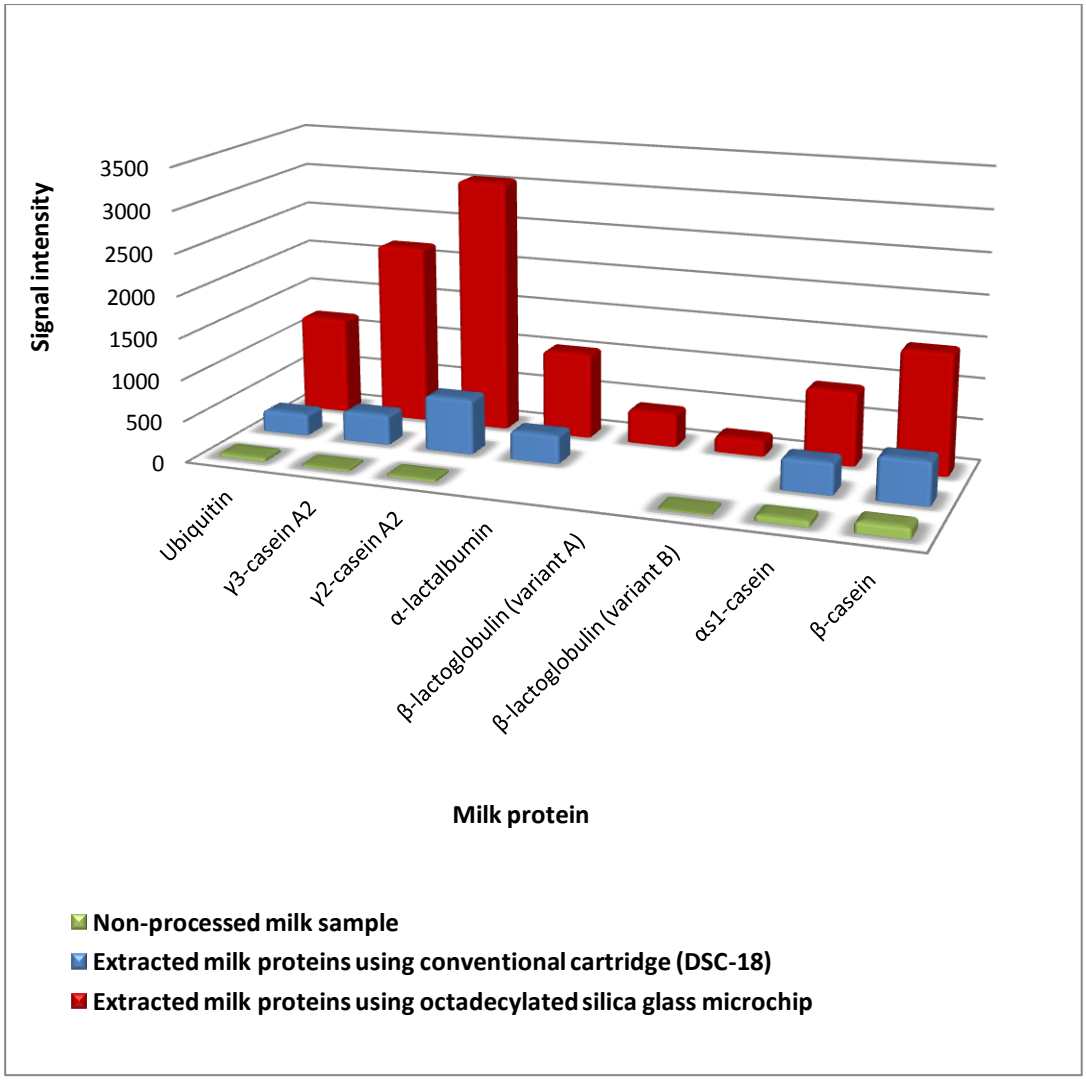

Figure 4.24 The average signal intensities of milk proteins before and after enrichment using the octadecylated silica monolith inside glass microchip and conventional cartridge (DSC-18) for the skimmed milk sample.

4.2.5.2 Hen egg white

In the previous experiment, the milk proteins were preconcentrated from liquid skimmed milk in the mass range 5-30 kDa. It was very important to investigate the performance of the octadecylated silica monolith microchip in preconcentration of a high range of proteins. Therefore, the second real sample investigated was hen egg white.

The sample solution was prepared by separating fresh egg white from egg yolk manually. The egg white sample was diluted more due to the higher viscocity of the

egg white compared with the liquid skimmed milk. This was performed by mixing 150 µL egg white with 350 µL tris-HCl buffer solution (50 mM, pH 7.0), containing 10 mM NaCl and then the sample solution was adjusted with 0.1 % TFA. The proteins in the hen egg white were preconcentrated using the same procedure previously used for the liquid milk sample using the octadecylated silica monolith microchip and the performance of the fabricated device was again compared with the conventional cartridge (DSC-18). The eluent solution was studied using MALDI-TOF-MS and the matrix crystal was prepared using the two-layer sample preparation method as before. Since the proteins in egg white have a very broad molecular mass range, a broad mass range (10-100 kDa) was used. Figure 4.25 shows the MALDI-TOF mass spectra in the mass range between 10 and 100 kDa of the non-processed egg white, figure 4.25 (A), and after preconcentration using the conventional cartridge, figure 4.25 (B), and using the fabricated device, figure 4.25 (C). Generally, there was an improvement in the MALDI-TOF spectrum of the proteins of the egg white after preconcentration using the fabricated device.

As can be seen in figure 4.25 (C), the strong signal at m/z 14236 is attributed to lysozyme while the peak at m/z 44500 corresponds to ovalbumin. The broad peak at m/z 29771 is attributed to ovomucoid. Moreover, two weak peaks were found that belong to ovalbumin Y protein, m/z 53956, and the peak at m/z 18884 is attributed to Hep21 protein, which has been recently identified in hen egg white. In addition, the very weak peak at m/z 22100 corresponds to chondrogenesis-associated lipocalin (CAL γ, prostaglandin H2 D-isomerase), which are transporters for small hydrophobic molecules such as lipids, steroid hormones, and retinoids.[182]

The previous result confirmed the ability of the octadecylated silica monolith to preconcentrate some proteins in hen egg white such as lysozyme, ovomucoid, and ovalbumin. However, it was found that the signal intensities of some proteins, such as Hep21 protein, CAL-γ protein, and ovalbumin Y, were very weak and they were not preconcentrated efficiently. This could be because the egg white sample was very diluted or due to the low abundance of these proteins in the hen egg white. In addition, a known egg white protein, ovotransferrin (molecular weight 77700 Da, *pI* 6.1)[181], was not preconcentrated and detected, although this protein is abundant in hen egg white, accounting for 13 % of the total egg white protein. This could be because the pores of

the octadecylated silica monolith were not of an appropriate size to retain this protein sufficiently. Although this protein was also not preconcentrated with the conventional DSC-18 cartridge.

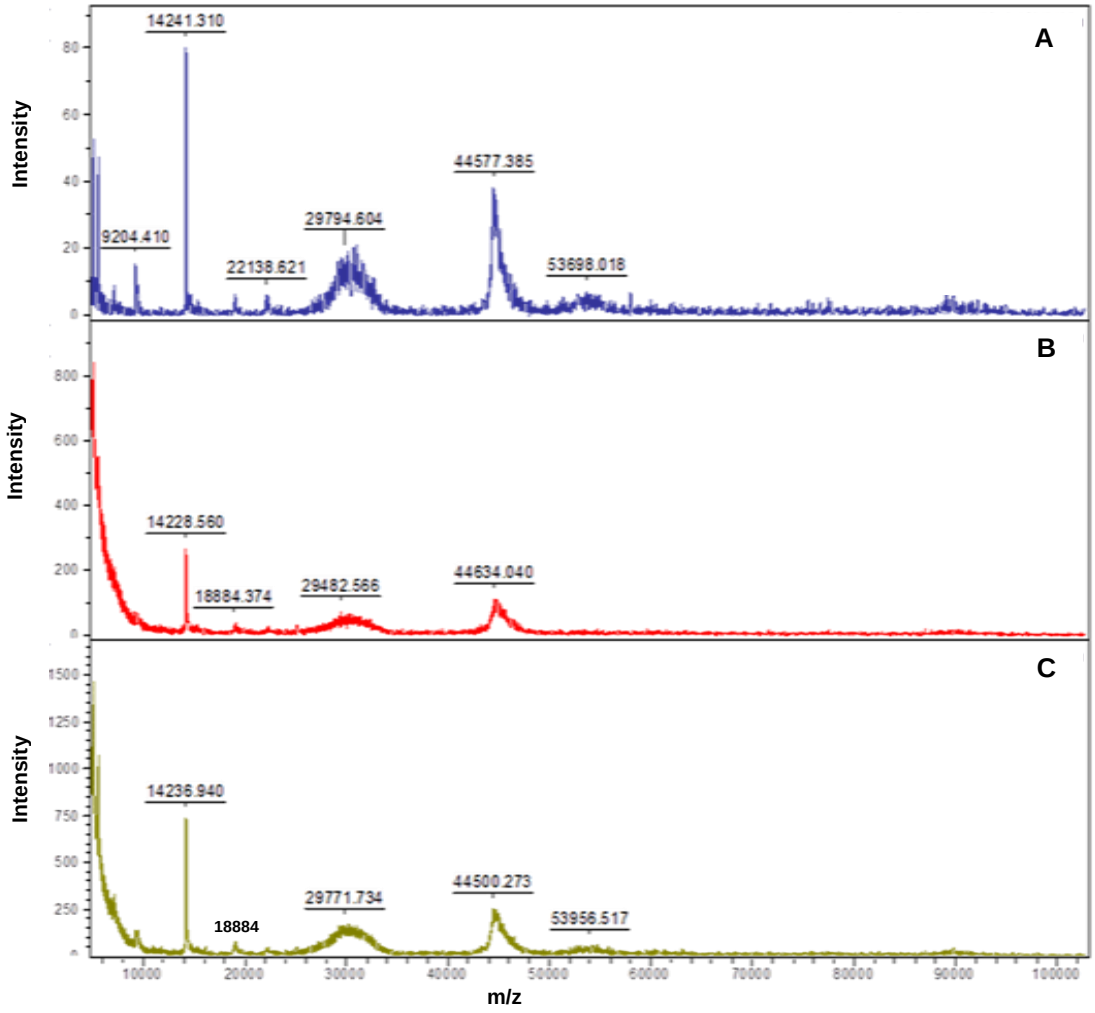

Figure 4.25 Comparison of the MALDI-TOF mass spectra of (A) non-processed egg white sample, 150 µL of the sample solution diluted with 350 µL 50 mM tris-HCl buffer solution (pH 7.0) containing 10 mM NaCl and 0.1%TFA, and after preconcentration of proteins in the egg white (B) using the conventional cartridge (DSC-18) and (C) using octadecylated silica monolith inside the glass microchip. The MALDI sample preparation was performed as done before in figure 4.23. The mass range was 10-100 kDa.

The average of the mass to charge ratio (m/z) for each purified proteins in the hen egg white was calculated, as shown in table 4.9. From the table, it was found that the relative standard deviation in the mass to charge ratio of the preconcentrated hen egg white proteins was in the range 0.05 - 0.59 %.

Egg white protein	**The average of the mass to charge ratio (m/z) (n=3)**	**RSD (%)**
Lysozyme	14235	0.05
Hep21 protein	18927	0.32
CAL-γ protein	22225	0.35
Ovomucoid	29682	0.59
Ovalbumin	44570	0.15
Ovalbumin Y	53827	0.34

Table 4.9 The average of the mass to charge ratio of the egg white proteins identified after preconcentration with the fabricated microchip containing octadecylated silica monolith, and the repeatability of the molecular mass measured (n=3).

The measured molecular masses of the preconcentrated egg white proteins were compared with the reported masses of the egg white proteins, as can be seen in table 4.10. The table shows a somewhat disappointing relative percentage error for the molecular masses, which ranged between 0.11 and 6.00 %. The measured molecular masses of Hep21 protein, ovomucoid, and ovalbumin Y were much higher than those previously reported. The reason for the difference between the measured and previously reported molecular masses was not known; however, due to differences in glycosylation of these proteins.

Egg white protein	Molecular mass (Da)		Relative percentage error (%)
	Measured	Reported[294]	
Lysozyme	14235	14300	0.45
Hep21 protein	18927	18100	4.56
CAL-γ protein	22225	22200	0.11
Ovomucoid	29682	28000	6.00
Ovalbumin	44570	44500	0.15
Ovalbumin Y	53827	53400	0.79

Table 4.10 Comparison between the measured and reported molecular masses of the hen egg white proteins preconcentrated using the octadecylated silica monolith microchip, and the relative percentage error in the measured molecular masses.

The bar chart 4.26 shows the signal intensities of all the preconcentrated hen egg white proteins, which were improved when using the octadecylated silica monolith compared to the conventional cartridge. In all the studies conducted in this research the octadecylated silica monolith has consistently outperformed the conventional DSC-18 SPE cartridge for extraction and preconcentration of proteins. However, the failure of both devices to show the higher molecular weight protein (ovotransferrin) may indicate that more work is still needed on the efficient extraction of very large proteins and this may be a limitation of the current device.

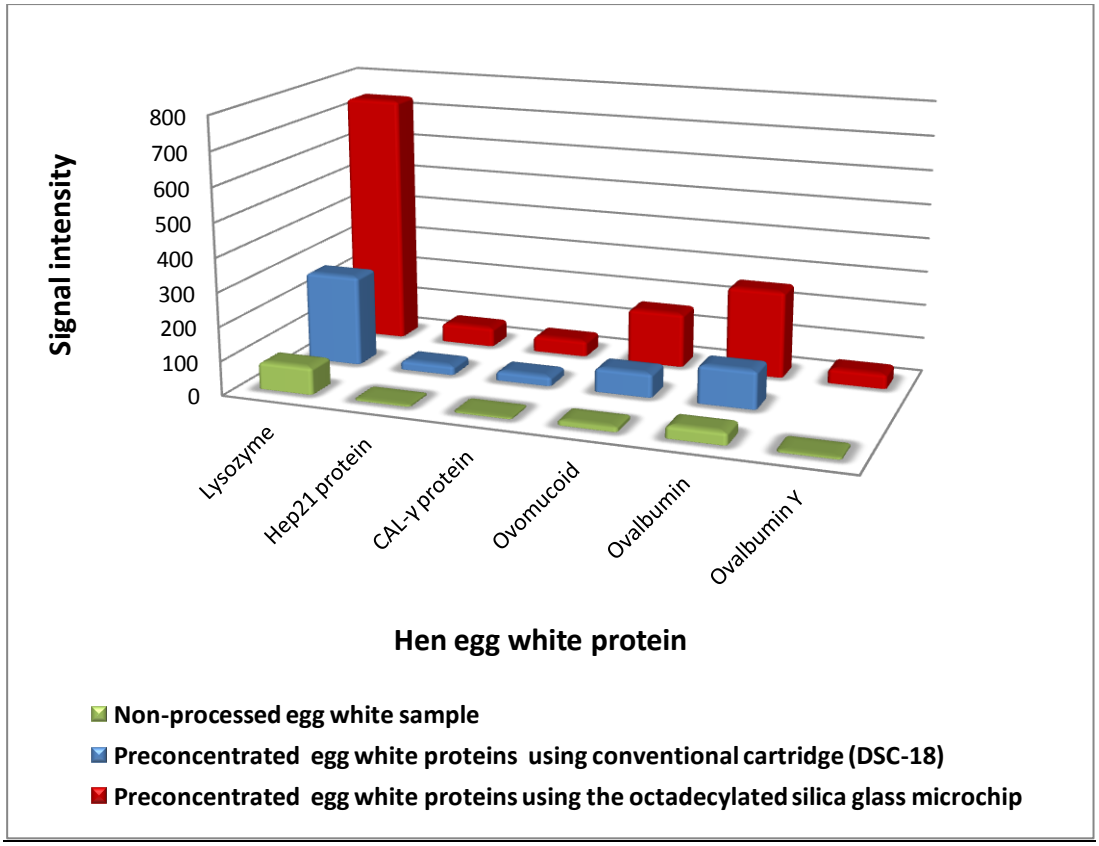

Figure 4.26 The average signal intensities of the proteins in hen egg white sample before, and after enrichment using the fabricated microchip containing octadecylated silica monolith and the conventional cartridge (DSC-18).

4.3 Reduction and alkylation of proteins

Protein identification by mass spectrometry forms the cornerstone of proteomics. Commonly, identification of proteins is based on digestion of proteins into peptides using proteolytic enzymes. Cleavage of the disulphide bonds in proteins before enzymatic digestion and mass spectral analysis is important in order to facilitate the accessibility of the enzyme to cleave the proteins into peptides. As a result, the protein sequence coverage will be increased.[250] The aim of this work was to fabricate a novel microfluidic device containing a monolithic sol-gel bed, which has the ability to reduce the disulphide bonds in a protein in order to make the protein unfold. As a result, the proteins will be accessible to the enzyme to cut at a specific location and produce peptides. The desired fabricated device would be simple, decrease the number

of processing steps, not be time consuming, reduce the risk of loss of the protein sample, compatible with proteins in aqueous solution, and be reproducible.

After fabrication of the glass microchip containing the TCEP-immobilised silica monolith, its performance in the reduction of the disulphide bonds in proteins was evaluated. The main standard protein used to study the performance of the fabricated polymer- and silica-based monoliths in protein extraction was cytochrome C; however, it was not studied here because it does not contain any disulphide bonds.[147] Therefore, the standard proteins used to check the performance of the silica-based monolith coated with TCEP were insulin from bovine pancreas and chicken egg white lysozyme, since these proteins contain a number of disulphide bonds.

4.3.1 Reduction and alkylation of insulin in the two-step procedure

The first protein investigated in order to check the effectiveness of the TCEP-immobilised silica monolith was insulin. It consists of 51 amino acids distributed in two polypeptide chains, α-chain (21 amino acids), and β-chain (30 amino acids). It contains three disulphide bonds; two interchain disulphide bonds between the α- and β-chains and one intrachain linkage in the α-chain.[295, 296]

The sample solution was prepared by dissolving insulin (60 µM) in 50 mM ammonium hydrogen carbonate buffer solution (pH 8.0), then 100 µL of the sample solution was injected inside the microchip using a syringe pump at flow rate 10 µL min^{-1} without causing leaking of the solution from the holes or damage to the monolith inside the glass microchip, which shows the fabricated monolith had high permeability. After sealing the ends of the ETFE tubes with blu-tak, the microchip was incubated at room temperature for 1 hour. During the incubation, the disulphide bonds in the proteins reacted with the reducing reagent (TCEP) that was immobilised on the surface of the silica-based monolith resulting in cleavage of the S-S bond and oxidation of the phosphine. The formation of phosphine oxide prevents reversal of the reaction.[268] Figure 4.27 shows the reaction of the disulphide bonds in a protein with TCEP and forming of two cysteines while TCEP was oxidised.

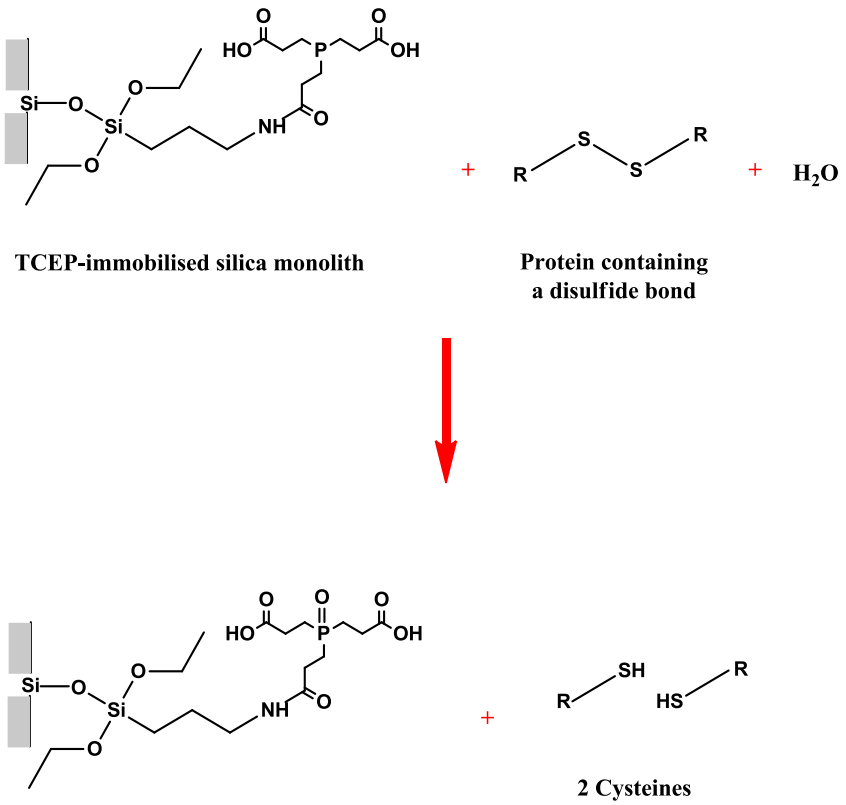

Figure 4.27 Reduction of the disulphide bond in the protein using the reducing reagent (TCEP) that was immobilised on the surface of the silica-based monolith resulting in formation of cysteine residues.

After reduction of the disulphide bonds in the protein, it was important to incorporate an additional processing step, which was alkylation of cysteine residues, since they are highly reactive and could be oxidised with other sulfhydryl groups resulting in reforming of the disulphide bonds prior to proteolytic cleavage.[250] The sulfhydryl-reactive alkylating reagent that was used in this study was iodoacetamide (IAA), since most popular procedures have utilised IAA for the alkylation reaction.[144]

The alkylation of cysteine residues was carried out using 500 µL 15 mM IAA solution that was prepared in 50 mM ammonium hydrogen carbonate buffer solution (pH 8.0). It was injected onto the fabricated microchip at a flow rate of 10 µL min^{-1}. During injection of the alkylating reagent, the microchip was covered with foil, since IAA is sensitive to light. The benefits of using IAA were to elute the reduced protein from the

microchip and to alkylate cysteine residues in order to prevent reformation of the disulphide bond. The solution was collected into an Eppendorf tube that was incubated at room temperature for 1 hour.

During incubation, IAA reacts with cysteine groups resulting in the addition of a carbamidomethyl group to each thiol group, resulting in an increase in mass by 57 Da and blocking the thiol groups preventing the reformation of the disulphide bonds [297], as can be seen in figure 4.28.

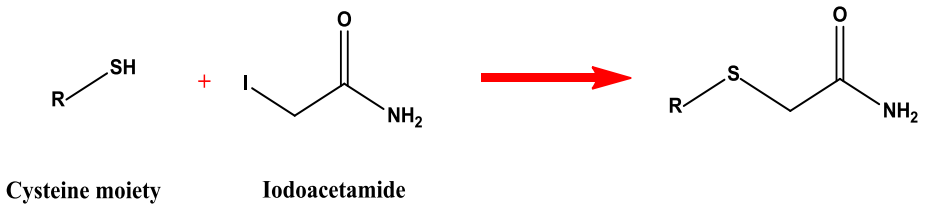

Figure 4.28 The schematic reaction of iodoacetamide (IAA) with the cysteine moiety, leading to a mass shift of 57 Da in order to prevent the reduced cysteine residues from reforming the disulphide bond.

In order to evaluate the performance of the monolithic sol-gel bed within a microchip for reduction of the disulphide bonds in proteins, the mass of insulin was monitored by MALDI-TOF mass spectrometry. Figure 4.29 shows the MALDI-TOF mass spectrum of the reduced and alkylated insulin. The figure shows a strong signal at m/z 5733 corresponding to the singly charged ion of insulin and a very weak signal at m/z 2861 corresponding to the doubly charged ion of insulin. From the spectrum, it was found that insulin was not reduced since insulin was not cleaved into two polypeptide chains, α-chain (2.3 kDa) and β-chain (3.4 kDa). In addition, it was found that the intact insulin was alkylated, since different peaks were observed. The reason for that could be the lack of thiol groups causing alkylation of amines (lysine, N-termini), imidazoles (histidine) and carboxylates (aspartate, glutamate). As a result, multiple alkylation products with different molecular weight and isoelectric point will be formed.[143, 144]

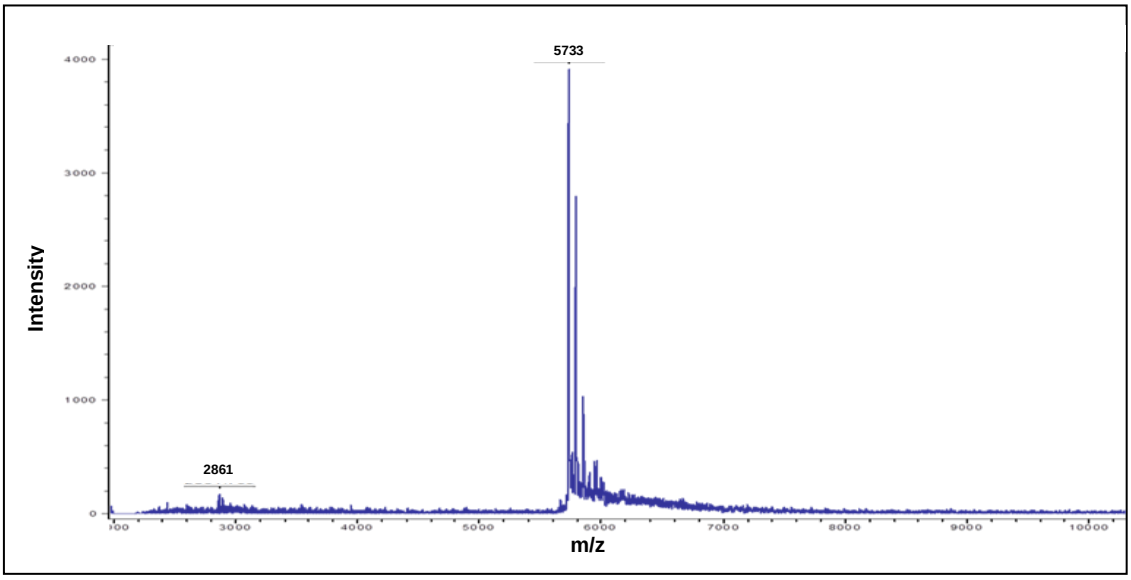

Figure 4.29 The MALDI-TOF mass spectrum of the reduced and alkylated insulin (60 µM) dissolved in 50 mM ammonium hydrogen carbonate buffer solution (pH 8.0). Reduction was performed using TCEP-immobilised silica monolith at room temperature for 1 hour, and alkylation was performed using 500 µL 15 mM IAA solution at room temperature for 1 hour. The MALDI sample preparation was prepared using the two-layer sample preparation.

To solve this problem, it was decided to use a denaturant in order to change the structure of the proteins by destroying hydrogen bonds, hydrophobic interaction, and van der Waals forces. As a result, the ability of the reducing reagent to reduce the disulphide bonds would be increased. Commonly, proteins can be denatured by using a strong acid or base, urea, guanidine-HCl, sodium dodecyl sulphate (SDS), or organic solvents.[298] In this study, urea was used as a denaturant, and denaturation of protein was carried out by mixing 100 µL of the protein sample with 100 µL of 8 M urea solution in an Eppendorf tube that was placed in an oven at 37 °C for 1 hour,[206] followed by reduction and alkylation of insulin, as done before. Figure 4.30 shows a comparison between the MALDI-TOF mass spectrum of the non-reduced insulin and the MALDI-TOF mass spectrum of the reduced insulin using TCEP-immobilised silica monolith. Figure 4.30 (A) shows the singly charged ion of the non-reduced insulin, which is a peak at m/z 5743, and the doubly charged ion, which is a peak at m/z 2866. After reduction of disulphide bonds in insulin, the two linked polypeptide chains linked by disulphide bonds, which are α-chain (2.3 kDa) and β-chain (3.4 kDa),

were cleaved using the fabricated microchip, as can be seen in figure 4.30 (B). The figure shows a complete reduction of insulin, since there was no corresponding peak for the singly and doubly charged ion of insulin. From this experiment, it was found that denaturation of protein using urea before reduction of the disulphide bond was important. In addition, it was concluded that the fabricated microchip has the ability to reduce the disulphide bonds in insulin.

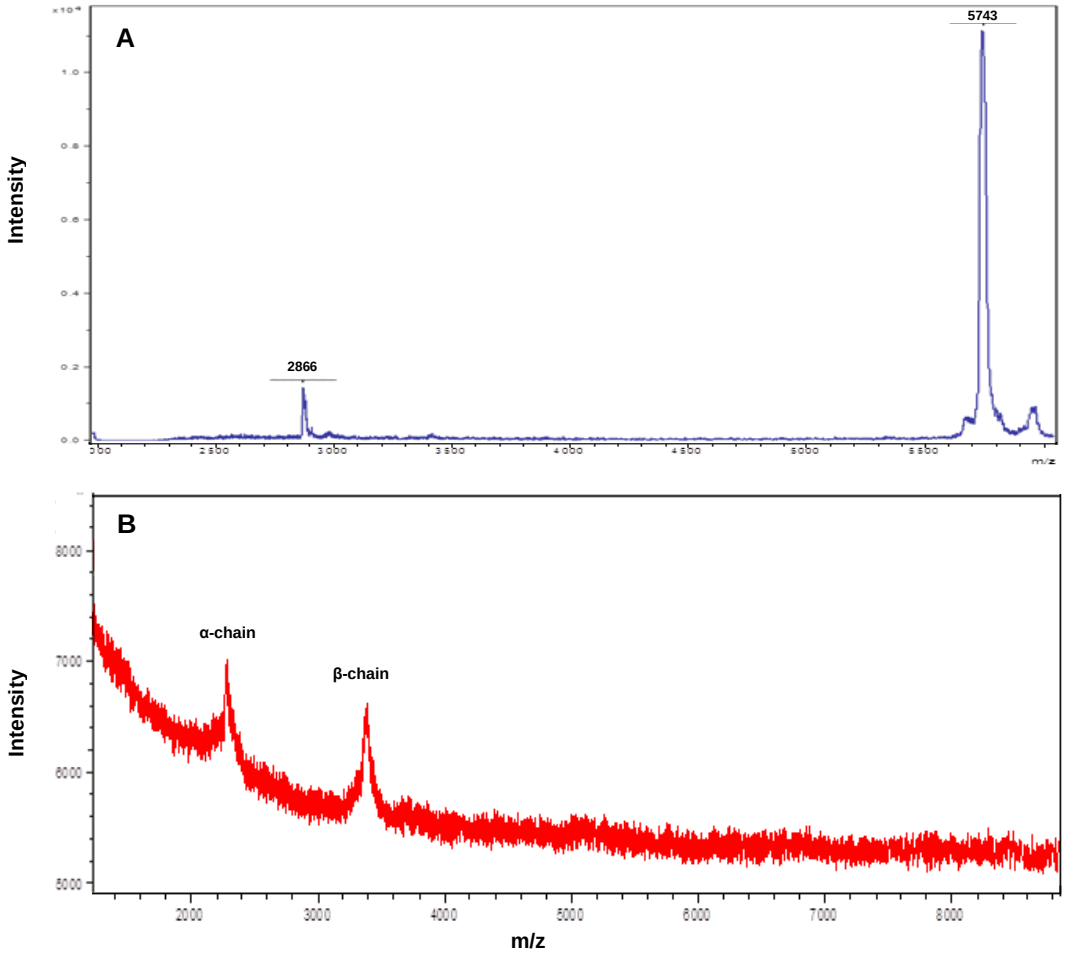

Figure 4.30 MALDI-TOF mass spectrum of the non-reduced insulin (60 µM) dissolved in 50 mM ammonium hydrogen carbonate buffer solution (pH 8.0) (A), and after denaturation of 100 µL insulin using 100 µL 8 M urea solution in an Eppendorf tube that was placed in oven at 37 °C for 1 hour, followed by reduction of the disulphide bonds using the glass microchip containing the TCEP-immobilised silica monolith at room temperature for 1 hour.

After reduction of the disulphide bonds in insulin, the free thiol groups were alkylated using IAA solution in order to prevent reformation of the disulphide bonds. After alkylation reaction, the MALDI-TOF mass spectrum of the alkylated insulin was checked, as can be seen in figure 4.31. Several peaks were observed, which are corresponding to varying degrees of alkylation of α- and β-chains (where υ represents the number of the reacted thiol groups).

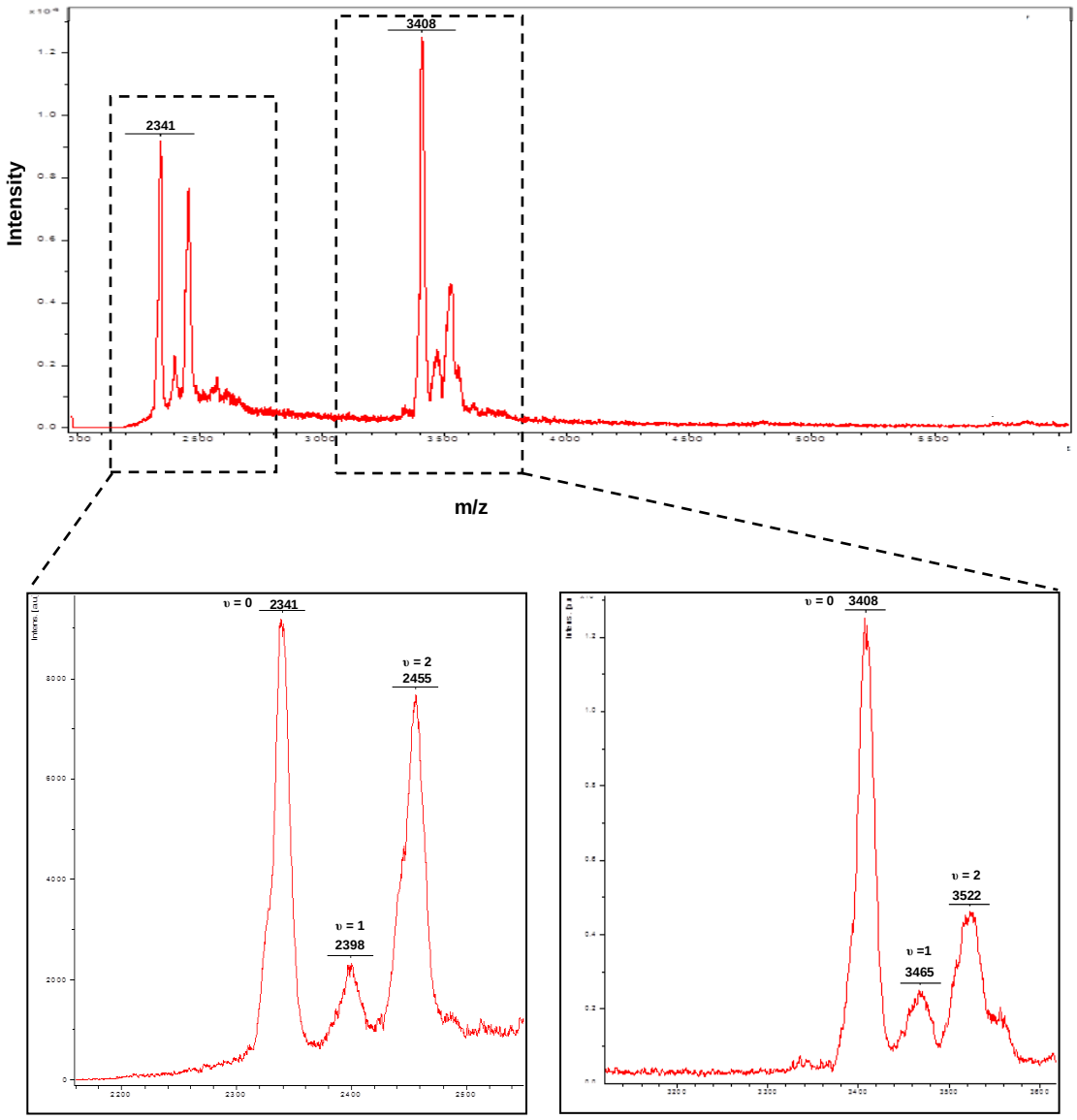

Figure 4.31 MALDI-TOF mass spectrum of the alkylated insulin using 500 µL 15 mM IAA solution that was prepared in 50 mM ammonium hydrogen carbonate buffer solution (pH 8.0) at room temperature for 1 hour.

Many studies have used a high temperature for protein reduction and alkylation in order to accelerate the reaction, thereby increasing the efficiency of reduction and alkylation of proteins and reducing the reaction time. Therefore, the effect of temperature on the reduction and alkylation of insulin was investigated. This was performed by using the same procedure that was used before for reduction and alkylation of insulin except the temperature of reduction and alkylation processes was changed to a high temperature (60 °C) rather than room temperature, and the incubation time was decreased to 30 min. During the reduction reaction, the microchip was kept in a humidified chamber (a petri dish partially filled with deionised water) in the oven in order to decrease evaporation of the solution during incubation.

The progress of the alkylation reaction was monitored by determination of the mass of insulin using MALDI-TOF mass spectrometry. Figure 4.32 shows the MALDI-TOF mass spectrum of the reduced and alkylated insulin using a high temperature (60 °C) for 30 min. By comparing the MALDI-TOF mass spectrum of the reduced and alkylated insulin at room temperature for 1 hour, figure 4.31, with the reduced and alkylated insulin at 60 °C for 30 min, figure 4.32, it can be seen that the number of peaks, which correspond to varying degrees of alkylation of α- and β-chains, were increased when using an elevated temperature (60 °C). This means reduction and alkylation of insulin at 60 °C can drive the reaction to completion in 30 min, which results in decreasing the time of incubation for reduction and alkylation processes.

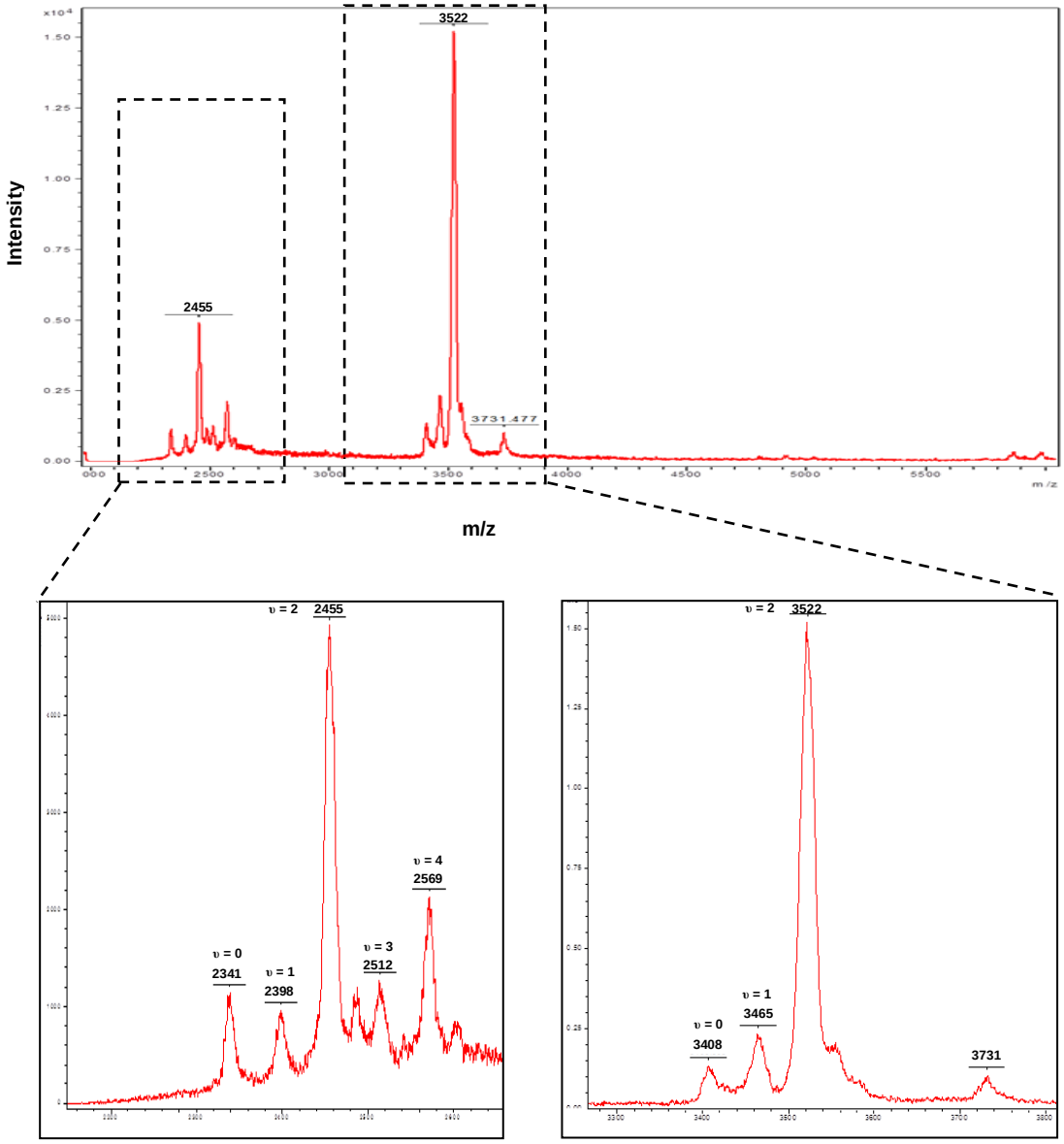

Figure 4.32 MALDI-TOF mass spectrum of the reduced and alkylated insulin at 60 °C for 30 min. For the reduction process, the microchip was kept in a petri dish partially filled with deionised water to decrease evaporation of the solution during incubation.

4.3.2 Reduction and alkylation of insulin in the one-step procedure

In the previous procedure (the two-step procedure), insulin was reduced using a reducing reagent (TCEP) that was immobilised on the surface of a silica-based monolith at room temperature for 1 hour or at elevated temperature (60 °C) for 30 min, followed by alkylation of the reduced cysteine residues using IAA at room

temperature for 1 hour or at elevated temperature (60 °C) for 30 min. Although this procedure was simple and successful in reducing the disulphide bonds in insulin and alkylating the thiol groups, it has some limitations. For example; it is time consuming, it poses the risk of loss of a portion of the protein sample, and it increases the chance of error. Therefore, it was decided to decrease the number of processing steps in order to decrease the time of the reduction and alkylation reactions, and to reduce the risk of loss of the protein sample. Since the main advantages of the reducing reagent (TCEP) are that it is specific to the disulphide bonds in proteins, and it does not need to be removed before adding the alkylation reagents[143], it was possible to perform the reduction and alkylation reactions in a single step. This was performed by injection of a mixture consists of 40 µL denatured insulin and 60 µL IAA solution into the fabricated microchip at a flow rate 10 µL min^{-1}. During injection of the mixture, the microchip was covered with foil, since IAA is unstable and sensitive to light. Both ends of the ETFE tubes were sealed with blu-tak, and then the microchip was placed on a petri dish partially filled with deionised water to minimise evaporation that was placed in the oven at 60 °C for 30 min.

After reduction and alkylation of insulin using the one-step procedure, MALDI-TOF mass spectrometry was used to determine the effectiveness of the procedure. Figure 4.33 shows the MALDI-TOF mass spectrum of insulin after TCEP reduction and alkylation by IAA in a single step at 60 °C for 30 min. From the spectrum, it was found that the signal from intact insulin was not observed, which means the disulphide bonds in insulin were reduced completely. In addition, different peaks were observed, related to varying degrees of alkylation of α- and β-chains. This result confirms the ability of the fabricated device to reduce and alkylate insulin in a single step. Since there are many advantages of the one-step reduction and alkylation using the fabricated device such as decreasing the processing steps, decreasing the time of incubation, and reducing the required sample volume, it was decided to use this procedure for further study.

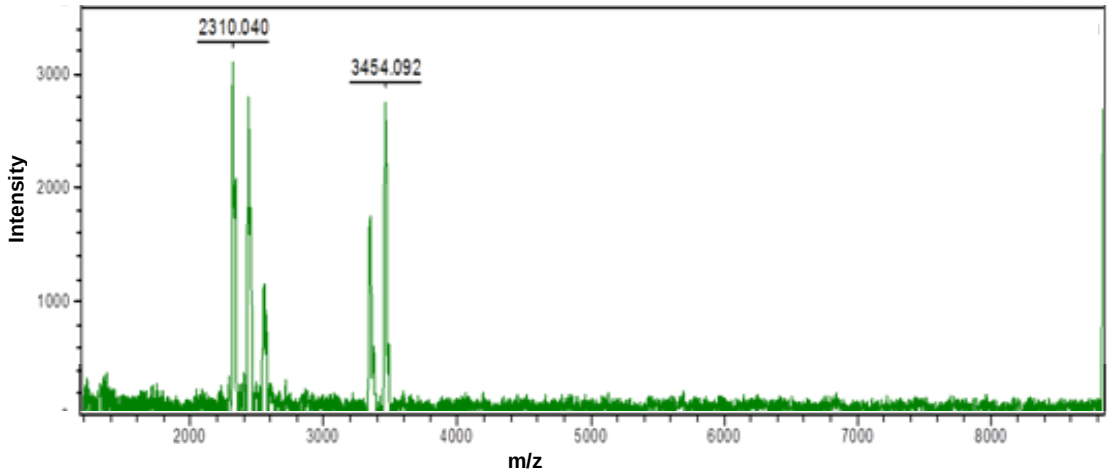

Figure 4.33 MALDI-TOF mass spectrum of the reduced and alkylated insulin using the fabricated device in the one-step procedure. The mixture consists of 40 µL denatured insulin and 60 µL 15 mM IAA solution. During injection of the mixture, the microchip was covered with foil. Both ends of the ETFE tubes were sealed with blu-tak, and the microchip was placed on a petri dish partially filled with deionised water that was placed in the oven at 60 °C for 30 min.

4.3.3 Reduction and alkylation of lysozyme

Another standard protein investigated to check the performance of the fabricated device was chicken egg white lysozyme. It consists of 129 amino acid residues contains four disulphide bonds, and all of them are intra-disulphide bonds.[299] Reduction and alkylation of lysozyme was carried out using the one-step procedure used before for reduction and alkylation of insulin at high temperature (60 °C) for 30 min. The progress of the reduction and alkylation reactions was monitored by determination of the mass of lysozyme by MALDI-TOF mass spectrometry, as can be seen in figure 4.34. Figure 4.34 (A) presents the MALDI-TOF mass spectrum of lysozyme before the reduction and alkylation reactions, which shows a peak at m/z 14296. After reduction and alkylation reactions using the fabricated device at high temperature (60 °C) for 30 min, the peak of the reduced and alkylated lysozyme was at m/z 14581, figure 4.34 (B). By comparing the MALDI-TOF mass spectrum of the non-processed lysozyme with the MALDI-TOF mass spectrum of the reduced and alkylated lysozyme, it was found that there was an increase in the mass of lysozyme

(285 Da) as a result of adding 57 Da to each thiol groups after reduction and alkylation reactions at 60 °C for 30 min, which presents lysozyme alkylation of five cysteines, lysozyme has eight cysteines (four disulphide bridges). This means the alkylation reaction was nearly complete under these conditions. Since not all the reduced cysteine residues were alkylated, it was decided to use the same procedure with an increase in the incubation time to 45 min. Figure 4.34 (C) demonstrates that the molecular mass of lysozyme was further increased and there was an increase in the mass of 513 Da after reduction and alkylation of lysozyme at 60 °C for 45 min, which corresponds to addition of a 57 Da carbamidomethyl group for each of the 8 cysteines in lysozyme, and could be one additional lysine was alkylated with IAA. Completeness of the alkylation reaction is an important procedure to avoid the introduction of variability into protein analysis.[250] Therefore, the alkyation of lysozyme for 45 min was chosen in order to make sure that all thiol residues were completely blocked. Although the peak of the reduced and alkylated lysozyme was wider compared with non-processed lysozyme, which could be because of using a high concentration of urea required, it is likely that the procedure for reduction and alkylation of lysozyme was successful.

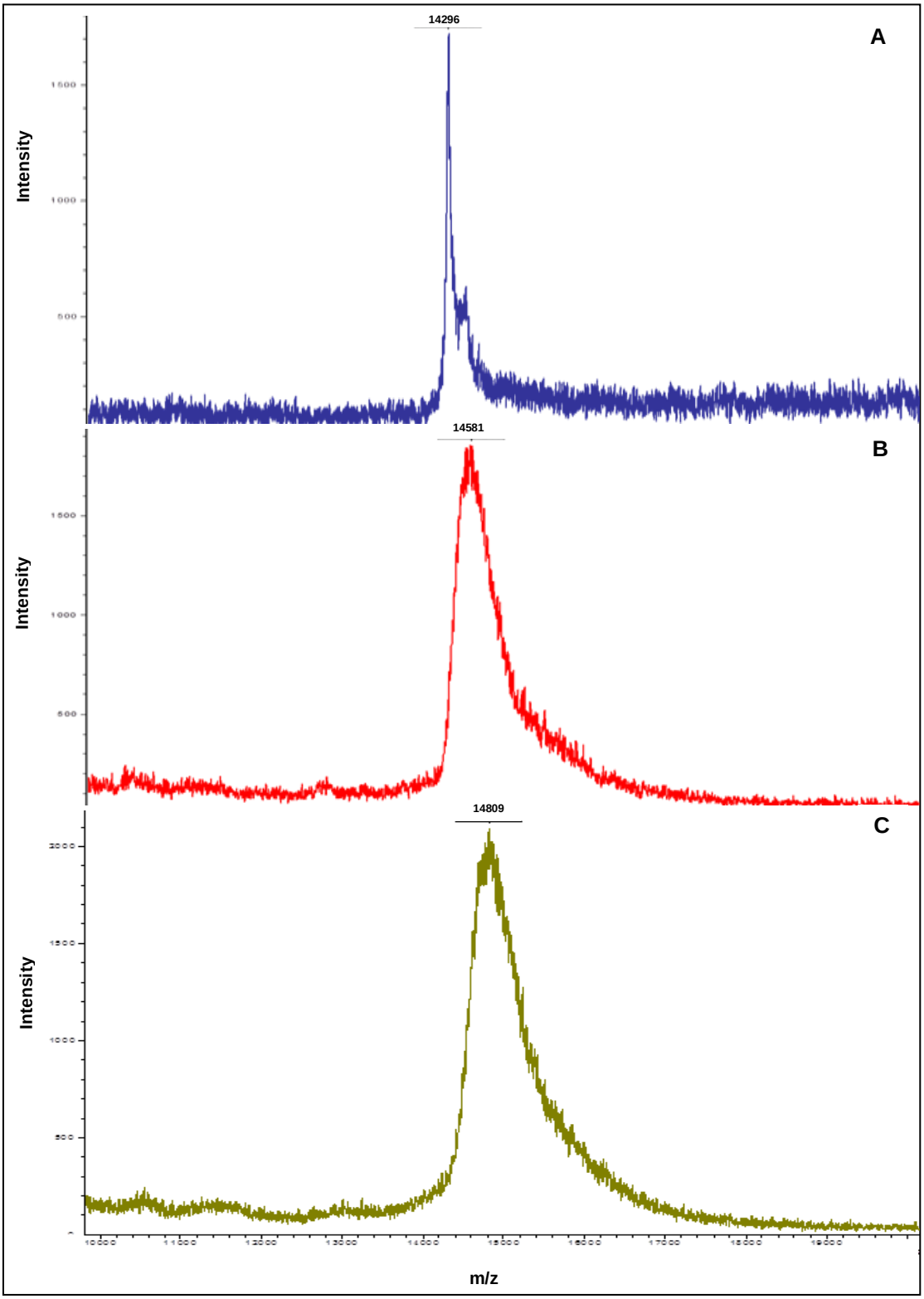

Figure 4.34 MALDI-TOF mass spectrum of the non-processed chicken egg white lysozyme (60 µM) dissolved in 50 mM ammonium hydrogen carbonate buffer solution (pH 8.0) (A), and after reduction and alkylation of denatured lysozyme using the fabricated device in the one-step procedure at 60 °C for 30 min (B) and for 45 min (C).

4.3.4 Reproducibility of the fabricated device

The reproducibility of the fabricated device containing the TCEP-immobilised silica monolith was checked by studying the MALDI-TOF mass spectrum of the reduced and alkylated insulin. It was found that the chip-to-chip (inter-chip) reproducibility of the fabricated device (n=3) was acceptable. Unfortunately, the fabricated device had low run-to-run (intra-chip) reproducibility since the signal from intact insulin was observed while the peaks related to alkylated α-chain and β-chain were not observed, as can be seen in figure 4.35. The reason for this could be that the ability of the immobilised TCEP on the surface of the silica-based monolith to reduce the disulphide bonds was decreased, since the reaction of TCEP with the disulphide bonds involves oxidation of TCEP.

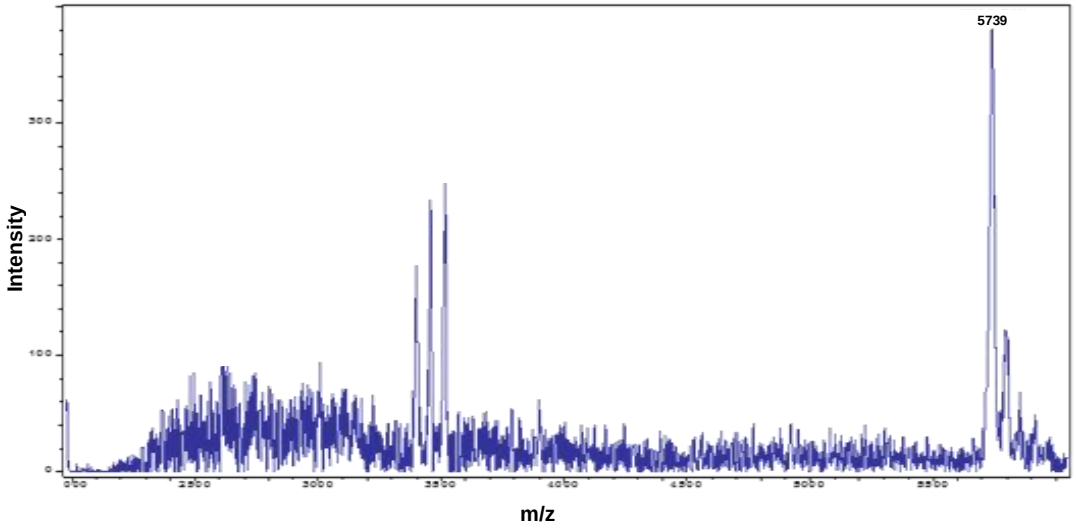

Figure 4.35 MALDI-TOF mass spectrum of the reduced and alkylated insulin using the fabricated device in the one-step procedure after the third use to check the intra-chip reproducibility.

It is possible that the lifetime of the fabricated TCEP-immobilised silica monolith may be extended by rinsing with 50 mM ammonium hydrogen carbonate buffer solution (pH 8.0), or with an organic solvent such as acetonitrile (ACN); however, this problem was not fully resolved. Despite this, the results obtained in this study show the potential utility of the silica sol-gel monolith for reduction of the disulphide bonds in proteins and the overall procedure was simple, easy to use, and resulted in lower protein sample and reagent consumption with decreased sample loss compared with the conventional techniques for protein reduction and alkylation.

5.0 Conclusions and further work

The objective of this PhD project was to fabricate monolithic materials inside a microfluidic device for use in protein sample preparation, with the advantages of decreased sample handling, reduced contamination, and decreased analysis time. This work involved optimisation of the porous properties of the fabricated monolithic materials in order to get the desired properties (large surface area and excellent hydrodynamic properties). The application of the optimised monolithic materials in protein extraction was investigated. Additionally, this project was undertaken to fabricate TCEP-immobilised monolithic silica in a glass microchip and evaluate its performance for protein reduction and alkylation. In this chapter, the major findings and achievements from this work will be summarised, and recommendations for future work on the project will be highlighted.

5.1 Fabrication of the organic monolith and its application for protein extraction

In this study, a butyl methacrylate-*co*-ethylene dimethacrylate (BuMA-*co*-EDMA) monolith was synthesised using UV-initiated polymerisation. Before fabrication of the organic polymer monolith inside the borosilicate tube or the glass microchip, the inner walls were silanised with 3-(trimethoxysilyl) propyl methacrylate (γ-MAPS). The result of this investigation confirms previous findings and contributes additional evidence that the silanisation step after pretreatment is an important procedure to covalently anchor the monolith to the inner walls.[52]

Since the organic monolithic material was prepared by photoinitiated polymerisation reaction, the effect of the energy of the UV light (254 and 365 nm), and the time of exposure to the UV light (8-22 min) on fabrication of the organic polymer monolith were investigated. The results of this investigation showed that the most suitable wavelength for the photoinitiated polymerisation reaction in this study was 365 nm, which supports previous research.[223] In addition, the finding of this study suggests that the optimum time of exposure to the UV light in order to prepare a porous rigid monolith was 20 min. Further work concerning optimisation of the porous properties using different free radical initiators, such as dibenzoyl peroxide (BPO) and lauroyl peroxide (LPO), which have recently been reported for the preparation of methacrylate

monolithic columns providing a compromise between chromatographic performance and analysis time.[300]

Control of the porous properties of the organic polymer monolith was optimised by adjusting the composition of the porogenic solvents. In this study, eight different binary porogenic solvent systems containing 50 % of main solvent (MeOH) and 50 % of co-porogen (EtOH, ACN, chloroform, hexane, tetrahydrofuran, 1-propanol, ethyl acetate, and cyclohexanol) were studied. The characterisation of the bed structures of the fabricated monoliths was carried out by SEM analysis, BET model, and measuring the porosity and permeability of the monoliths. The results of this investigation show that the optimal binary porogenic solvent system to prepare the poly (BuMA-*co*-EDMA) monolith was MeOH/EtOH, which offers high porosity and permeability. In addition, this study found that replacing EtOH with 1-propanol enables the fabrication of the organic polymer monolith with a higher surface area (56.89 m^2 g^{-1}). The present study confirms previous findings and contributes additional evidence that the organic monoliths have low surface area in comparison to the surface area of the silica-based monoliths.[89, 90]

The performance of the optimised monoliths in their ability to extract proteins was investigated. The results showed that the organic polymer monolith prepared using MeOH/EtOH was not suitable for use as a SPE sorbent since the extraction recovery of cytochrome C was very low (17 %), which could be attributed to the lower surface area of this monolith (12.6 m^2 g^{-1}), while the organic monolith prepared using MeOH/1-propanol was able to preconcentrate some standard proteins such as insulin, cytochrome C, myoglobin, and hemoglobin with fairly good extraction recovery (75.3 - 95.7 %). However, the fabricated organic monolith was unable to preconcentrate other investigated standard proteins such as β-lactoglobulin, ovalbumin, and BSA (giving extraction recoveries of less than 26 %).

Further optimisation of the physical properties of the organic polymer monolith using a tertiary porogenic solvent system was also investigated by changing the porogenic solvent system from binary to tertiary, consisting of 50 % MeOH of the total amount of the porogenic solvent and the other 50 % was a combination of different ratios of EtOH and 1-propanol (40:10, 30:20, 25:25, 20:30, and 10:40). This study has found

that by increasing the amount of 1-propanol, the surface area of the monoliths was increased; however, it was found that the main limitation of the five organic polymer-based monoliths prepared using tertiary porogenic solvent system was low surface area (5.06-38.87 m^2 g^{-1}). In addition, investigation of their performance in preconcentration of cytochrome C showed that the extraction recovery of cytochrome C was not high, ranging from 25.3 to 60.7 %.

Since the highest extraction recovery was achieved using MeOH/1-propanol, this was used to fabricate the polymer-based monolith inside a microfluidic device. It was found that fabrication of the organic monolithic materials inside a glass microchip was simple, fast, and the location of the monolith was defined inside the extraction chamber since the reaction is UV-initiated polymerisation. In addition, this study has found that the polymeric-based microchip was able to preconcentrate four standard proteins (insulin, cytochrome C, myoglobin, and hemoglobin) and their extraction recoveries were in range (79.1-98.4 %). However, it was found that the polymer-based monolith lacks the desired permeability and porosity, since it was found that a high flow rate (more than 3.5 µL min^{-1}) during extraction of standard proteins could not be used. The result of this investigation confirms previous findings and contributes additional evidence that the organic monoliths have moderate permeability.[60, 76]

The reproducibility of preparation of butyl methacrylate monoliths was studied by checking the morphology of three different batches of the fabricated monolith and the results of this investigation showed that there was no difference in the morphology of the prepared monoliths. The run-to-run reproducibility of the extraction of the proteins on the same microchip is quite good with RSD values for peak area counts below 6 % (n=4), and the chip-to-chip reproducibility ranged from 4.2 to 7.1 % (n=3). However, the findings of the current study showed that the lifetime of this type of monolithic material was not very long and it should be kept in a solution of distilled water and ACN (50:50) to prevent drying of the organic polymer monolith and minimise cracking.

Future work on the optimisation of fabrication of the polymer-based monolith in order to increase the surface area and the permeability of the monolith by investigating

different parameters needs to be continued. In addition, it would also be interesting to investigate different types of organic monolithic materials such as poly (styrene-*co*-divinylbenzene) monolith since the styrene monomer is also hydrophobic.[52, 301]

5.2 Fabrication of the inorganic monolith and its application for protein extraction

Fabrication of the inorganic silica-based monolith using a sol-gel method was investigated. The present study confirms previous findings and contributes additional evidence that fabrication of the monolithic silica material is associated with shrinkage in the monolithic silica rod associated with the gelation process and that large shrinkage of the monolith occurs during drying of the monolithic silica rod. [233-235]

The internal pore structure of the silica-based monolith was tailored to increase the surface area by converting micropores to mesopores using ammonia or urea solution. This study has found that using ammonia solution can offer mesopores containing materials without changing the colour of the silica-based monolith compared with urea. It is recommended that further research be undertaken in optimisation of the concentration of ammonia solution, the time, or temperature of the thermal decomposition step in order to further increase the total surface area and yield mesopores of narrow pore size distribution.

The effect of the gelation time (1, 2, 3, and 4 days) and the gelation temperature (40 and 50 °C) on the properties of the fabricated silica-based monolith was investigated. This study has shown that increasing the temperature and the time of the gelation process resulted in a slight decrease in the size of macropores, the total surface area, and the porosity of the silica-based monolith. The following conclusion can be drawn from the present study that the optimal gelation condition for fabrication of the silica-based monolith was 40 °C for 1 day.

Surface modification of the silica-based monolith with octadecyl groups has been carried out and was confirmed using SEM analysis, EDX analysis, and the BET model. The finding from this study showed that there was a slight decrease in the surface area, pore volume, average pore diameter, and porosity of the silica-based

monolith after derivatisation of the surface with octadecyl groups due to blocking of the micropores by the bonded phase that attached to the silica surface.

The results of this study indicate that although preparation of the silica-based monolith was a long-term process, which took almost one week and was relatively tedious, it had high porosity, was not affected by organic solvent, and offered high surface area. Furthermore, the silica-based monolith had high permeability, enabling high flow, and lower backpressure; moreover, the results showed that the procedure to fabricate the silica-based monolith was reproducible. A future study investigating ways to speed up fabrication of the silica-based monolith would be very interesting.

The bare silica-based monolith (normal-phase mode) and the octadecylated silica monolith (reversed-phase mode) inside the heat shrinkable tubes were evaluated for their use in performing solid phase extraction for preconcentration of eight standard proteins, which were insulin, cytochrome C, lysozyme, myoglobin, β-lactoglobulin, ovalbumin, hemoglobin, and BSA. The results showed that recovery of the standard proteins was achieved by both sorbents with variable yields; however, the octadecylated silica monolith gave higher extraction recoveries (92.7 to 109.7 %) than the non-modified silica monolith (25.5 to 97.9 %). This is in contrast to previous work, which showed the ability to purify different standard proteins varying in molecular weight more than 40000 Da.[125]

Since a satisfactory extraction recovery of protein was achieved using the octadecylated silica monolith, it was decided to fabricate it inside a glass microchip rather than a shrinkable tube in order to speed up the analysis, and reduce the volume of the analyte and the reagents. In this work, a novel microfluidic device has been successfully developed that contained crack-free monolithic silica modified with octadecyl groups for use in the microchip-based solid phase extraction of proteins. Although the monolithic silica disk was not chemically anchored to the inner walls of the microchip, it was not affected by the thermal bonding step, and the shrinkage of the disk was completely avoided. However, a weakness of this study was that the surface area of the monolith, which could be changed after thermal bonding of the two plates, was not measured since it was difficult to separate the two glass plates. In addition, fabrication of the silica-based monolith inside a glass microchip involves cutting the monolithic silica rod with a scalpel blade and placing the monolithic silica

disk inside the extraction chamber of the base plate of the microchip before bonding the top and the base plates. The variability of the size of the prepared monolith could cause variability of the protein extraction. It is recommended that this variability can be decreased by automation of the preparatory procedure.

The performance of the octadecylated silica microchip was evaluated using the extraction of six standard proteins, namely insulin, cytochrome C, lysozyme, myoglobin, β-lactoglobulin, and hemoglobin in the presence of a high concentration of CHAPS and PBS. The results showed that the octadecylated silica monolith was permeable, has the ability to remove impurities, and achieved a high extraction recovery of the proteins (94.8 - 99.7 %) compared with conventional octadecylated silica particles (48.3 - 91.3 %). This study showed that using the octadecylated silica microchip resulted in a reduction of the volume of sample and reagent needed, and reduction in the time to obtain the result. Good run-to-run reproducibility was achieved with RSD values below 5 % for peak area counts (n=4), and chip-to-chip reproducibility was below 7 % (n=3). Furthermore, the durability of the silica-based monolithic material was evident in that no obvious changes in extraction efficiency for the standard proteins was observed even after more than 30 use. They have high mechanical strength, and relatively high thermal stability, which supports previous studies. [238, 240]

Two real samples have been used to check the performance of the fabricated device, skimmed cows milk, and hen egg white. The results indicate that the octadecylated silica monolith inside the glass microchip has the ability to preconcentrate milk proteins (caseins and whey proteins) from skimmed cows' milk (250 µL sample). This was confirmed by MALDI-TOF-MS spectra, which showed a significant improvement in sensitivity, and produced clean spectra free from background interferences with a high signal-to-noise ratio compared with a conventional cartridge. The three replicate experiments showed that the RSD of the mass to charge ratio of milk proteins ranged from 0.01 to 0.46%. In addition, it was found that there were no significant differences between the observed and reported masses of the milk proteins and the relative percentage error of the molecular masses ranged between 0.03 and 0.90 %.

A satisfactory preconcentration of the proteins in the hen egg white (150 µL sample) such as lysozyme, ovomucoid, and ovalbumin was achieved when using the octadecylated silica monolith compared with the conventional cartridge. However, some proteins such as Hep21 protein, CAL-γ protein, and ovalbumin Y were preconcentrated with low efficiency, which could be attributed to the low abundance of these proteins in the hen egg white or could be because the sample was very diluted. Additionally, a high abundant protein in the hen egg white (ovotransferrin) was not preconcentrated and detected. This could be attributed to the pore size of the octadecylated silica monolith not being sufficient to retain this protein and further work needs to be undertaken to optimise the size of the mesopores. It was found that RSD in the mass spectrum to charge ratio of the preconcentrated hen egg white proteins was in the range 0.05-0.59 %. However, the comparison between the measured and reported molecular masses of the hen egg white proteins showed that the relative percentage error of molecular masses of the preconcentrated hen egg white proteins was high (6.00 %).

Future work might investigate extraction of large proteins such as IgG (MW 150 kDa) [302] after optimisation of the pore size of the octadecylated silica monolith. Moreover, it would also be interesting to investigate more complex samples such as proteins in serum or tissue.

5.3 Fabrication of the TCEP-immobilised silica monolith and its application for protein reduction and alkylation

A novel method to prepare the TCEP-immobilised silica monolith in a glass microchip in order to use it for protein reduction and alkylation has been successfully prepared. This was carried out by derivatisation of the surface of the silica-based monolith with APTES, followed by covalent immobilisation of the reducing reagent on the surface of the treated silica monolith with APTES via amino groups in the presence of coupling reagents (EDC), and coupling enhancer (Sulfo-NHS). The grafted silica-based monolith with APTES and immobilisation of TCEP on the surface of the amino-modified silica monolith were confirmed by using different techniques such as measuring the water contact angle, IR spectroscopy, EDX analysis, and BET

instrument. The results of this investigation showed that the procedure of fabrication of the TCEP-immobilised silica monolith was simple, easy to use, and reproducible.

The performance of the fabricated glass microchip containing the TCEP-immobilised silica monolith to reduce the disulphide bonds in proteins was checked using 60 µM insulin at room temperature for 1 hour, followed by alkylation of the reduced cysteine residues at room temperature for 1 hour. However, it was found that the disulphide bonds in insulin were not reduced. This study has found that denaturation of insulin using 8 M urea solution in an oven at 37 °C for 1 hour increased the ability of the reducing reagent immobilised on the surface of the silica-based monolith to reduce the disulphide bonds, which was confirmed by the MALDI-TOF-MS instrument. Furthermore, this study has focused on the effect of increasing the temperature (60 °C) on the reduction and alkylation of insulin. The results of this investigation showed that increasing the temperature of the reduction and alkylation reactions resulted in decreasing the incubation time to 30 min.

Integration of reduction and alkylation of protein in one single step at 60 °C, followed by studying the reduced and alkylated protein using MALDI-TOF-MS instrument has been investigated. The studies reported here established the ability of the fabricated glass microchip containing the TCEP-immobilised silica monolith to reduce the disulphide bonds and alkylate the reduced cysteine residues of insulin in 30 min, and lysozyme in 45 min. This single step method offered significant advantages in terms of speed, decrease in the number of processing steps, ease of use, reduced risk of contamination, and resulted in lower reagent consumption and sample loss. Therefore, the glass microchip containing the TCEP-immobilised silica monolith can be a powerful tool for reduction and alkylation of proteins. Future work would involve reduction and alkylation of complex proteins such as BSA since it contains 17 disulphide bonds and one free sulfhydryl group.[303]

The limitation of this method was the reduction of disulphide bonds in proteins had to be carried out in the presence of a denaturant (urea), which required sample desalting or other sample processing steps before mass spectrometry. Additionally, it was found that the main drawback of the fabricated microchip was the low run-to-run (intra-chip) reproducibility. Therefore, further work should focus on additional investigations to optimise fabrication of the TCEP-immobilised silica monolith in order to increase the

amount of TCEP on the surface of the silica monolith, and to reactivate the TCEP-immobilised silica monolith after use.

This study has found that the chip-to-chip (inter-chip) reproducibility of the fabricated device was acceptable; therefore, it would be interesting to use an inexpensive disposable plastic microchip rather than the glass microchip for fabrication of a monolithic sol-gel bed within a microchip for protein reduction and alkylation.

Generally, the comparison between the polymer- and silica-based monoliths in the physical properties of the fabricated monolith, and their performance in protein preconcentration indicated that the inorganic silica-based monolith can be a good SPE sorbent for proteomics. It would be interesting to establish a fully integrated device for protein extraction and the existing microchip for proteomics at Hull University (protein digestion with peptide separation) in order to develop a continuous flow proteomics device.

It would be interesting to investigate preconcentration of small peptides, drugs and other small molecules using the fabricated octadecylated silica monolith and use it as separation media for reversed-phase liquid chromatography. In addition, a future study investigating reduction of the disulfide bonds in labile disulfide-containing compounds using TCEP-immobilised silica monolith would be very interesting.

6.0 References

1. P. Righetti and M. Hamdan, *Proteomics Today: Protein Assessment and Biomarkers Using Mass Spectrometry, 2D Electrophoresis, and Microarray Technology*, Wiley, Hoboken, 2005.

2. C. Kerese, *Methods of Protein Analysis*, Ellis Horwood, Michigan, 1984.

3. G. Liumbruno, *Blood Transfusion*, 2008, **6**, 70-85.

4. M. Wilkins, J. Sanchez, A. Gooley, R. Appel, I. Humphery-Smith, D. Hochstrasser and K. Williams, *Biotechnology & Genetic Engineering Reviews*, 1996, **13**, 19-50.

5. P. S. Milksik, *Journal of Separation Science*, 2007, **30**, 1686-1703.

6. M. M. Aebersold, *Nature*, 2003, **422**, 198-207.

7. H. Wang and S. Hanash, *Mass Spectrometry Reviews*, 2005, **24**, 413-426.

8. V. Hlady and J. Buijs, *Current Opinion in Biotechnology*, 1996, **7**, 72-77.

9. R. A. Hartvig, M. van de Weert, J. Østergaard, L. Jorgensen and H. Jensen, *Langmuir*, 2011, **27**, 2634-2643.

10. D. C. Liebler, *Introduction to Proteomics: Tools for The New Biology*, Humana Press, Totowa, 2002.

11. W. Sun, S. Gao, L. Wang, Y. Chen, S. Wu, X. Wang, D. Zheng and Y. Gao, *Molecular & Cellular Proteomics*, 2006, **5**, 769-776.

12. X. Han, A. Aslanian and J. Yates Iii, *Current Opinion in Chemical Biology*, 2008, **12**, 483-490.

13. V. H. Wysocki, K. A. Resing, Q. Zhang and G. Cheng, *Methods*, 2005, **35**, 211-222.

14. C. Wu and M. MacCoss, *Current Opinion in Molecular Therapeutics*, 2002, **4**, 242-250.

15. Y. Shen and R. D. Smith, *Electrophoresis*, 2002, **23**, 3106-3124.

16. F. E. Ahmed, *Journal of Separation Science*, 2009, **32**, 771-798.

17. N. Delaunay, V. Pichon and M. Hennion, *Journal of Chromatography B: Biomedical Sciences and Applications*, 2000, **745**, 15-37.

18. G. Vas and K. Vékey, *Journal of Mass Spectrometry*, 2004, **39**, 233-254.

19. T. Hyötyläinen, *Analytical and Bioanalytical Chemistry*, 2009, **394**, 743-758.

20. K. C. Saunders, A. Ghanem, W. Boon Hon, E. F. Hilder and P. R. Haddad, *Analytica Chimica Acta*, 2009, **652**, 22-31.

21. M. Abdel-Rehim, M. Andersson, E. Portelius, C. Norsten-Höög and L. G. Blomberg, *Journal of Microcolumn Separations*, 2001, **13**, 313-321.

22. L. Nováková and H. Vlčková, *Analytica Chimica Acta*, 2009, **656**, 8-35.

23. J. Jonsson and L. Mathiasson, *Journal of Chromatography A*, 2000, **902**, 205-225.

24. F. L. Moore, *Analytical Chemistry*, 1956, **28**, 997-1001.

25. C. F. Poole, *TrAC-Trends in Analytical Chemistry*, 2003, **22**, 362-373.

26. H. Zhang, J. Huang, H. Wang and Y. Feng, *Analytica Chimica Acta*, 2006, **565**, 129-135.

27. C. Freiburghaus, C. Welinder, U. Tjörnstad, H. Lindmark-Månsson, M. Paulsson and S. Oredsson, *Journal of Dairy Science*, 2010, **93**, 3442-3452.

28. E. M. Thurman and M. S. Mills, *Solid-Phase Extraction: Principles and Practice*, Wiley, New York, 1998.

29. A. Zwir-Ferenc and M. Biziuk, *Polish Journal of Environmental Studies*, 2006, **15**, 677-690.

30. K. Haupt, *Analyst*, 2001, **126**, 747-756.

31. N. Simpson, *Solid-Phase Extraction: Principles, Techniques, and Applications*, Marcel Dekker, New York, 2000.

32. G. Shen and H. K. Lee, *Analytical Chemistry*, 2001, **74**, 648-654.

33. H. Lingeman and S. J. F. Hoekstra-Oussoren, *Journal of Chromatography B: Biomedical Sciences and Applications*, 1997, **689**, 221-237.

34. S. Ulrich, *Journal of Chromatography A*, 2000, **902**, 167-194.

35. M. C. Hennion, *Journal of Chromatography A*, 1999, **856**, 3-54.

36. S. Mysling, G. Palmisano, P. Højrup and M. Thaysen-Andersen, *Analytical Chemistry*, 2010, **82**, 5598-5609.

37. J. X. Shen, C. I. Tama and R. N. Hayes, *Journal of Chromatography B*, 2006, **843**, 275-282.

38. V. Camel, *Spectrochimica Acta Part B: Atomic Spectroscopy*, 2003, **58**, 1177-1233.

39. R. D. Oleschuk, L. L. Shultz-Lockyear, Y. Ning and D. J. Harrison, *Analytical Chemistry*, 1999, **72**, 585-590.

40. H. Sabik, R. Jeannot and B. Rondeau, *Journal of Chromatography A*, 2000, **885**, 217-236.

41. C. F. Poole, A. D. Gunatilleka and R. Sethuraman, *Journal of Chromatography A*, 2000, **885**, 17-39.

42. M. R. Buchmeiser, *Polymer*, 2007, **48**, 2187-2198.

43. A. Akbarzadeh, M. Samiei and S. Davaran, *Nanoscale Research Letters*, 2012, **7**, 1-13.

44. D. Perrett, *Annals of Clinical Biochemistry*, 1999, **36**, 133-150.

45. C. K. Ratnayake, C. S. Oh and M. P. Henry, *Journal of Chromatography A*, 2000, **887**, 277-285.

46. J. Wen, C. Guillo, J. P. Ferrance and J. P. Landers, *Analytical Chemistry*, 2006, **78**, 1673-1681.

47. H. Minakuchi, K. Nakanishi, N. Soga, N. Ishizuka and N. Tanaka, *Journal of Chromatography A*, 1998, **797**, 121-131.

48. J. S. Fritz, P. J. Dumont and L. W. Schmidt, *Journal of Chromatography A*, 1995, **691**, 133-140.

49. T. Nema, E. Chan and P. Ho, *Talanta*, 2010, **82**, 488-494.

50. S. Hjertén, J. Liao and R. Zhang, *Journal of Chromatography A*, 1989, **473**, 273-275.

51. F. Svec and J. Frechet, *Analytical Chemistry*, 1992, **64**, 820-822.

52. H. Zou, X. Huang, M. Ye and Q. Luo, *Journal of Chromatography A*, 2002, **954**, 5-32.

53. S. M. Fields, *Analytical Chemistry*, 1996, **68**, 2709-2712.

54. H. Minakuchi, K. Nakanishi, N. Soga, N. Ishizuka and N. Tanaka, *Analytical Chemistry*, 1996, **68**, 3498-3501.

55. G. Guiochon, *Journal of Chromatography A*, 2007, **1168**, 101-168.

56. Z. Deyl and F. Sevc, *Capillary Electrochromatography*, Elsevier Science, Amsterdam, 2001.

57. K. K. Unger, R. Skudas and M. M. Schulte, *Journal of Chromatography A*, 2008, **1184**, 393-415.

58. H. Oberacher and C. G. Huber, *TrAC-Trends in Analytical Chemistry*, 2002, **21**, 166-174.

59. F. C. Leinweber, D. G. Schmid, D. Lubda, K. Wiesmüller, G. Jung and U. Tallarek, *Rapid Communications in Mass Spectrometry*, 2003, **17**, 1180-1188.

60. F. Svec, *Journal of Separation Science*, 2004, **27**, 747-766.

61. F. Leinweber, D. Lubda, K. Cabrera and U. Tallarek, *Analytical Chemistry*, 2002, **74**, 2470-2477.

62. C. W. Klampfl, *Journal of Chromatography A*, 2004, **1044**, 131-144.

63. F. Svec and A. A. Kurganov, *Journal of Chromatography A*, 2008, **1184**, 281-295.

64. R. D. Arrua, M. C. Strumia and C. I. Igarzabal, *Materials*, 2009, **2**, 2429-2466.

65. I. Nischang, O. Brueggemann and F. Svec, *Analytical and Bioanalytical Chemistry*, 2010, **397**, 953-960.

66. S. Xie, R. Allington, J. Fréchet and F. Svec, *Advances in Biochemical Engineering*, 2002, **76**, 87-125.

67. L. L. Lulia, M. Lazar, Yu. Yang, B. L. Karger, *Electrophoresis*, 2003, **24**, 3655-3662.

68. C. Yu, F. Svec and J. Fréchet, *Electrophoresis*, 2000, **21**, 120-127.

69. C. Viklund, E. Pontén, B. Glad, K. Irgum, P. Hörstedt and F. Svec, *Chemistry of Materials*, 1997, **9**, 463-471.

70. F. Svec, *Journal of Chromatography A*, 2010, **1217**, 902-924.

71. D. Connolly, V. O'Shea, P. Clark, B. O'Connor and B. Paull, *Journal of Separation Science*, 2007, **30**, 3060-3068.

72. M. Merhar, A. Podgornik, M. Barut, M. Žigon and A. Štrancar, *Journal of Separation Science*, 2003, **26**, 322-330.

73. I. Gusev, X. Huang and C. Horváth, *Journal of Chromatography A*, 1999, **855**, 273-290.

74. E. C. Peters, F. Svec and J. Fréchet, *Advanced Materials*, 1999, **11**, 1169-1181.

75. M. Bedair and Z. El Rassi, *Electrophoresis*, 2004, **25**, 4110-4119.

76. Y. Li and M. Lee, *Journal of Separation Science*, 2009, **32**, 3369-3378.

77. F. Svec and J. Frechet, *Chemistry of Materials*, 1995, **7**, 707-715.

78. J. F. Rabek, *Mechanisms of Photophysical Processes and Photochemical Reactions in Polymers: Theory and Applications*, Wiley, Chichester, 1987.

79. C. M. Paleos, *Polymerization in organized media*, Gordon and Breach Science Publishers, Philadelphia, 1992.

80. Z. Liu, Y. Xu, H. Wang, C. Yan and R. Gao, *Analytical Sciences*, 2004, **20**, 673-678.

81. T. Rohr, E. F. Hilder, J. J. Donovan, F. Svec and J. Fréchet, *Macromolecules*, 2003, **36**, 1677-1684.

82. S. Xie, F. Svec and J. Fréchet, *Journal of Polymer Science Part A: Polymer Chemistry*, 1997, **35**, 1013-1021.

83. Á. Sáfrány, B. Beiler, K. László and F. Svec, *Polymer*, 2005, **46**, 2862-2871.

84. J. P. Landers, *Handbook of Capillary and Microchip Electrophoresis and Associated Microtechniques*, Taylor and Francis Group, USA, 2008.

85. F. Svec, T. Tennikova and Z. Deyl, *Monolithic Materials: Preparation, Properties, and Applications*, Elsevier Science, Amsterdam, 2003.

86. V. F. Samanidou, A. S. Ioannou and I. N. Papadoyannis, *Journal of Chromatography B*, 2004, **809**, 175-182.

87. K. Cabrera, G. Wieland, D. Lubda, K. Nakanishi, N. Soga, H. Minakuchi and K. K. Unger, *TrAC-Trends in Analytical Chemistry*, 1998, **17**, 50-53.

88. E. C. Peters, F. Svec and J. Fréchet, *Chemistry of Materials*, 1997, **9**, 1898-1902.

89. S. Xie, F. Svec and J. Fréchet, *Chemistry of Materials*, 1998, **10**, 4072-4078.

90. E. C. Peters, F. Svec, J. Fréchet, C. Viklund and K. Irgum, *Macromolecules*, 1999, **32**, 6377-6379.

91. S. Frantisek, *Journal of Chromatography B*, 2006, **841**, 52-64.

92. J. M. Armenta, B. Gu, P. H. Humble, C. D. Thulin and M. L. Lee, *Journal of Chromatography A*, 2005, **1097**, 171-178.

93. J. M. Armenta, B. Gu, C. D. Thulin and M. L. Lee, *Journal of Chromatography A*, 2007, **1148**, 115-122.

94. C. Schley, R. Swart and C. G. Huber, *Journal of Chromatography A*, 2006, **1136**, 210-220.

95. C. Yu, M. H. Davey, F. Svec and J. Fréchet, *Analytical Chemistry*, 2001, **73**, 5088-5096.

96. O. G. Potter and E. F. Hilder, *Journal of Separation Science*, 2008, **31**, 1881-1906.

97. Y. Hua, A. B. Jemere and D. J. Harrison, *Journal of Chromatography A*, 2011, **1218**, 4039-4044.

98. C. Li and K. H. Lee, *Analytical Biochemistry*, 2004, **333**, 381-388.

99. A. Denizli and E. Pişkin, *Journal of Biochemical and Biophysical Methods*, 2001, **49**, 391-416.

100. A. M. Siouffi, *Journal of Chromatography A*, 2003, **1000**, 801-818.

101. S. H. Lee, T. T. Doan, S. H. Ha, W. Chang and Y. Koo, *Journal of Molecular Catalysis B: Enzymatic*, 2007, **47**, 129-134.

102. M. Kato, K. Sakai-Kato and T. Toyo'oka, *Journal of Separation Science*, 2005, **28**, 1893-1908.

103. N. Ishizuka, H. Kobayashi, H. Minakuchi, K. Nakanishi, K. Hirao, K. Hosoya, T. Ikegami and N. Tanaka, *Journal of Chromatography A*, 2002, **960**, 85-96.

104. A. M. Frolova, M. A. Chukhlieb, A. V. Drobot, A. P. Kryshtal, L. P. Loginova and A. P. Boichenko, *The Open Surface Science Journal* 2009, **1**, 40-45.

105. T. Adam, K. K. Unger, M. M. Dittmann and G. P. Rozing, *Journal of Chromatography A*, 2000, **887**, 327-337.

106. L. Xu, Z. Shi and Y. Feng, *Analytical and Bioanalytical Chemistry*, 2010, **399**, 3345-3357.

107. D. Allen and Z. El Rassi, *Electrophoresis* 2003, **24**, 408-420.

108. T. Keeling-Tucker, M. Rakic, C. Spong and J. D. Brennan, *Chemistry of Materials*, 2000, **12**, 3695-3704.

109. A. Siouffi, *Journal of Chromatography A*, 2003, **1000**, 801-818.

110. L. Rieux, H. Niederländer, E. Verpoorte and R. Bischoff, *Journal of Separation Science*, 2005, **28**, 1628-1641.

111. J. E. Sandoval and J. J. Pesek, *Analytical Chemistry*, 1991, **63**, 2634-2641.

112. J. M. Herrero-Martínez, A. Méndez, E. Bosch and M. Rosés, *Journal of Chromatography A*, 2004, **1060**, 135-145.

113. M. Sanagi, A. Abu Naim, A. Hussain and N. Dzakaria, *Malaysian Journal of Analytical Sciences*, 2001, **7**, 337-343.

114. M. L. Larrivee and C. F. Poole, *Analytical Chemistry*, 1994, **66**, 139-146.

115. A. Gambero, L. T. Kubota, Y. Gushikem, C. Airoldi, J. M. Granjeiro, E. M. Taga and E. F. Alcântara, *Journal of Colloid and Interface Science*, 1997, **185**, 313-316.

116. H. Girault, N. Lion, F. Reymond and J. Rossier, *Current Opinion in Chemical Biology*, 2004, **15**, 31-37.

117. Z. Lin, F. Yang, X. He, X. Zhao and Y. Zhang, *Journal of Chromatography A*, 2009, **1216**, 8612-8622.

118. M. Kelea and G. Guiochon, *Journal of Chromatography A*, 2002, **960**, 19-49.

119. S. L. Cohen and B. T. Chait, *Analytical Chemistry*, 1996, **68**, 31-37.

120. P. K. Jal, S. Patel and B. K. Mishra, *Talanta*, 2004, **62**, 1005-1028.

121. E. Alzahrani and K. Welham, *Analyst*, 2012, **137**, 4751-4759.

122. Q. Luo, Y. Shen, K. K. Hixson, R. Zhao, F. Yang, R. J. Moore, H. M. Mottaz and R. D. Smith, *Analytical Chemistry*, 2005, **77**, 5028-5035.

123. S. Ota, S. Miyazaki, H. Matsuoka, K. Morisato, Y. Shintani and K. Nakanishi, *Journal of Biochemical and Biophysical Methods*, 2007, **70**, 57-62.

124. K. A. Wolfe, M. C. Breadmore, J. P. Ferrance, M. E. Power, J. F. Conroy, P. M. Norris and J. P. Landers, *Electrophoresis*, 2002, **23**, 727-733.

125. S. Miyazaki, K. Morisato, N. Ishizuka, H. Minakuchi, Y. Shintani, M. Furuno and K. Nakanishi, *Journal of Chromatography A*, 2004, **1043**, 19-25.

126. Q. Wu, J. Bienvenue, B. Hassan, Y. Kwok, B. Giordano, P. Norris, J. Landers and J. Ferrance, *Analytical Chemistry*, 2006, **78**, 5704-5710.

127. L. Xu and H. K. Lee, *Journal of Chromatography A*, 2008, **1195**, 78-84.

128. C. S. Sevier and C. A. Kaiser, *Nature Reviews Molecular Cell Biology*, 2002, **3**, 836-847.

129. J. Tetenbaum and L. M. Miller, *Biochemistry*, 2001, **40**, 12215-12219.

130. I. Braakman and D. N. Hebert, *Current Protocols in Protein Science*, John Wiley & Sons, New York, 2001.

131. W. D. Kohn, R. Micanovic, S. L. Myers, A. M. Vick, S. D. Kahl, L. Zhang, B. A. Strifler, S. Li, J. Shang, J. M. Beals, J. P. Mayer and R. D. DiMarchi, *Peptides*, 2007, **28**, 935-948.

132. M. Scigelova, P. Green, A. Giannakopulos, A. Rodger, D. Crout and P. Derrick, *European Journal of Mass Spectrometry***,** 2001, **7**, 29-34.

133. N. J. Hauser and F. Basile, *Journal of Proteome Research*, 2008, **7**, 1012-1026.

134. P. D. Tzanavaras, C. Mitani, A. Anthemidis and D. G. Themelis, *Talanta*, 2012, **96**, 21-25.

135. M. E. Levison, A. S. Josephson and D. M. Kirschenbaum, *Cellular and Molecular Life Sciences*, 1969, **25**, 126-127.

136. J. A. Burns, J. C. Butler, J. Moran and G. M. Whitesides, *The Journal of Organic Chemistry*, 1991, **56**, 2648-2650.

137. E. B. Getz, M. Xiao, T. Chakrabarty, R. Cooke and P. R. Selvin, *Analytical Biochemistry*, 1999, **273**, 73-80.

138. G. E. Begg and D. W. Speicher, *Journal of Biomolecular Techniques*, 1999, **10**, 17-20.

139. S. S. Rhee and D. H. Burke, *Analytical Biochemistry*, 2004, **325**, 137-143.

140. J. C. Han and G. Y. Han, *Analytical Biochemistry*, 1994, **220**, 5-10.

141. S. Wang, K. Liu and Y. Lu, *Biochemical and Biophysical Research Communications*, 2009, **381**, 639-642.

142. W. H. Fischer, D. P. Behan, M. Park, E. Potter, P. J. Lowry and W. Vale, *Journal of Biological Chemistry*, 1994, **269**, 4313-4316.

143. F. Bai, S. Liu and F. A. Witzmann, *Proteomics*, 2005, **5**, 2043-2047.

144. S. Gehanne, D. Cecconi, L. Carboni, P. G. Righetti, E. Domenici and M. Hamdan, *Rapid Communications in Mass Spectrometry*, 2002, **16**, 1692-1698.

145. J. Hale and M. Knierman, *One-Step Reduction and Alkylation of Proteins,* Indiana Proteomics Consortium LLC, USA, 2006.

146. V. N. Luk and A. R. Wheeler, *Analytical Chemistry*, 2009, **81**, 4524-4530.

147. D. Chatterjee, A. J. Ytterberg, S. U. Son, J. A. Loo and R. L. Garrell, *Analytical Chemistry*, 2010, **82**, 2095-2101.

148. R. Tian, X. D. Hoa, J. Lambert, J. P. Pezacki, T. Veres and D. Figeys, *Analytical Chemistry*, 2011, **83**, 4095-4102.

149. E. Maxwell and D. Chen, *Analytica Chimica Acta*, 2008, **627**, 25-33.

150. S. Gygi and R. Aebersold, *Current Opinion in Chemical Biology*, 2000, **4**, 489-494.

151. E. Maxwell and D. Chen, *Analytica Chimica Acta*, 2008, **627**, 25-33.

152. J. Lewis, J. Wei and G. Siuzdak, *Matrix-assisted Laser Desorption/Ionization Mass Spectrometry in Peptide and Protein Analysis in Encyclopedia of Analytical Chemistry*, John Wiley & Sons Ltd., Chichester, 2000.

153. H. D. Kris Gevaert, T. Sklyarova, J. Vandekerckhove and T. Houthaeve, *Electrophoresis*, 1997, **19**, 909-917.

154. O. Vorm, P. Roepstorff and M. Mann, *Analytical Chemistry*, 1994, **66**, 3281-3287.

155. D. Skoog, F. Holler, S. Crouch, *Principles of Instrumental Analysis,* Brooks, Canada, 2007.

156. R. Bayerbach, V. Nguyen, U. Schurr and D. Meier, *Journal of Analytical and Applied Pyrolysis*, 2006, **77**, 95-101.

157. L. Cheng and D. Zhang, *Molecular Genetic Pathology*, Humana Press, Totowa, 2008.

158. R. Zenobi and R. Knochenmuss, *Mass Spectrometry Reviews*, 1998, **17**, 337-366.

159. C. Jurinke, P. Oeth and D. van den Boom, *Molecular Biotechnology*, 2004, **26**, 147-163.

160. S. Higson, *Analytical Chemistry*, Oxford University Press, New York, 2004.

161. P. Kallio and J. Kuncova, *Technology Review*, 2004, **7**, 1-36.

162. Y. Yang, C. Li, K. H. Lee and H. G. Craighead, *Electrophoresis*, 2005, **26**, 3622-3630.

163. N. Lion, T. C. Rohner, L. Dayon, I. L. Arnaud, E. Damoc, N. Youhnovski, Z. Wu, C. Roussel, J. Josserand, H. Jensen, J. S. Rossier, M. Przybylski and H. H. Girault, *Electrophoresis*, 2003, **24**, 3533-3562.

164. T. Rohr, D. F. Ogletree, F. Svec and J. Fréchet, *Advanced Functional Materials*, 2003, **13**, 264-270.

165. C. Zhang, J. Xu, W. Ma and W. Zheng, *Biotechnology Advances*, 2006, **24**, 243-284.

166. S. Ong, S. Zhang, H. Du and Y. Fu, *Frontiers in Bioscience*, 2008, **13**, 2757-2773.

167. D. B. Wolfe, D. Qin and G. M. Whitesides, *Methods in Molecular Biology***,** 2010, **583**, 81-107.

168. G. S. Fiorini and D. T. Chiu, *BioTechniques*, 2005, **38**, 429-446.

169. C. Henry, *Microchip Capillary Electrophoresis, Methods and Protocols*, Humana Press, Totowa, 2006.

170. G. N. Doku, S. J. Haswell, T. McCreedy and G. M. Greenway, *Analyst*, 2001, **126**, 14-20.

171. N. Lion, F. Reymond, H. H. Girault and J. S. Rossier, *Current Opinion in Biotechnology*, 2004, **15**, 31-37.

172. D. Erickson and D. Li, *Analytica Chimica Acta*, 2004, **507**, 11-26.

173. A. G. Crevillén, M. Hervás, M. A. López, M. C. González and A. Escarpa, *Talanta*, 2007, **74**, 342-357.

174. B. Casado, M. Affolter and M. Kussmann, *Journal of Proteomics*, 2009, **73**, 196-208.

175. R. L. Walzem, C. J. Dillard and J. B. German, *Critical Reviews in Food Science and Nutrition*, 2002, **42**, 353-375.

176. M. Galvani, M. Hamdan and P. G. Righetti, *Rapid Communications in Mass Spectrometry*, 2000, **14**, 1889-1897.

177. A. S. Lopes, J. S. Garcia, R. R. Catharino, L. S. Santos, M. N. Eberlin and M. A. Arruda, *Analytica Chimica Acta*, 2007, **590**, 166-172.

178. L. Lin, C. Wang, K. Chen and P. Lin, *Colloids and Surfaces A: Physicochemical and Engineering Aspects*, 2009, **346**, 47-51.

179. M. Galvani, M. Hamdan and P. G. Righetti, *Rapid Communications in Mass Spectrometry*, 2001, **15**, 258-264.

180. X. Tian, J. Gautron, P. Monget and G. Pascal, *Biology of Reproduction*, 2010, **83**, 893-900.

181. A. Cláudia, *Journal of Agricultural Science*, 2006, **63**, 291-298.

182. C. Guérin-Dubiard, M. Pasco, D. Mollé, C. Désert, T. Croguennec and F. Nau, *Journal of Agricultural and Food Chemistry*, 2006, **54**, 3901-3910.

183. Y. Mine and F. Shahidi, *Nutraceutical Proteins and Peptides in Health and Disease*, Taylor and Francis, London, 2006.

184. E. Li-Chan and S. Nakai, *Critical Reviews in Poultry Biology*, 1989, **2**, 21-59.

185. D. Vadehra and K. Nath, *Critical Reviews in Food Technology*, 1973, **4**, 193-308.

186. J. Bienvenue, J. Ferrance, B. Giordano, B. Hassan, Y. Kwok, J. Landers, P. Norris and Q. Wu, *Analytical Chemistry*, 2006, **78**, 5704-5710.

187. F. Svec, T. Tennikova and Z. Deyl, *Monolithic Materials: Preparation, Properties and Applications*, Elsevier Science, Amsterdam, 2003.

188. N. Ishizuka, H. Minakuchi, K. Nakanishi, N. Soga, H. Nagayama, K. Hosoya and N. Tanaka, *Analytical Chemistry*, 2000, **72**, 1275-1280.

189. R. Wu, L. Hu, F. Wang, M. Ye and H. Zou, *Journal of Chromatography A*, 2008, **1184**, 369-392.

190. A. S. Maria Chong and X. S. Zhao, *Applied Surface Science*, 2004, **237**, 398-404.

191. D. S. Peterson, T. Rohr, F. Svec and J. Fréchet, *Analytical Chemistry*, 2003, **75**, 5328-5335.

192. D. J. Vanhoutte, S. Eeltink, W. T. Kok and P. J. Schoenmakers, *Analytica Chimica Acta*, 2011, **701**, 92-97.

193. C. Yu, M. Xu, F. Svec and J. Fréchet, *Journal of Polymer Science Part A: Polymer Chemistry*, 2002, **40**, 755-769.

194. T. McCreedy, *TrAC-Trends in Analytical Chemistry*, 2000, **19**, 396-401.

195. J. Babin, J. Iapichella, B. Lefèvre, C. Biolley, J. P. Bellat, F. Fajula and A. Galarneau, *New Journal of Chemistry*, 2007, **31**, 1907-1917.

196. C. Xie, M. Ye, X. Jiang, W. Jin and H. Zou, *Molecular and Cellular Proteomics*, 2006, **5**, 454-461.

197. M. Etienne and A. Walcarius, *Talanta*, 2003, **59**, 1173-1188.

198. N. O. Dhoot, C. A. Tobias, I. Fischer and M. A. Wheatley, *Journal of Biomedical Materials Research Part A*, 2004, **71A**, 191-200.

199. P. Fletcher, S. Haswell, P. He, S. Kelly and A. Mansfield, *Journal of **Porous** Materials*, 2010, **18**, 501-508.

200. K. Chuda, J. Jasik, J. Carlier, P. Tabourier, C. Druon and X. Coqueret, *Radiation Physics and Chemistry*, 2006, **75**, 26-33.

201. C. P. Jaroniec, R. K. Gilpin and M. Jaroniec, *Journal of Chromatography A*, 1998, **797**, 103-110.

202. M. Furuno, N. Ishizuka, H. Minakuchi, S. Miyazaki, K. Morisato, K. Nakanishi and Y. Shintani, *Journal of Chromatography A*, 2004, **1043**, 19-25.

203. E. Alzahrani and K. Welham, *Analyst*, 2011, **136**, 4321-4327.

204. S. Cohen and B. Chait, *Analytical chemistry*, 1996, **68**, 31-37.

205. Y. Dai, R. M. Whittal and L. Li, *Analytical Chemistry*, 1999, **71**, 1087-1091.

206. Promega,http://www.promega.com/resources/protocols/technical-manuals/0/immobilized-trypsin-protocol/, accessed March 2012.

207. J. Lichtenberg, N. F. de Rooij and E. Verpoorte, *Talanta*, 2002, **56**, 233-266.

208. N. Ahn and A. Wang, *Current Opinion in Chemical Biology***,** 2008, **12**, 1-3.

209. M. M. Zheng, G. D. Ruan and Y. Q. Feng, *Journal of Chromatography A*, 2009, **1216**, 7739-7746.

210. D. Allen and Z. El Rassi, *Analyst*, 2003, **128**, 1249-1256.

211. D. Lubda, K. Cabrera, K. Nakanishi and W. Lindner, *Analytical and Bioanalytical Chemistry*, 2003, **377**, 892-901.

212. G. T. Gibson, S. M. Mugo and R. D. Oleschuk, *Polymer*, 2008, **49**, 3084-3090.

213. D. R. Baker, *Capillary Electrophoresis*, John Wiley and Sons, New York, 1995.

214. D. J. Throckmorton, T. J. Shepodd and A. K. Singh, *Analytical Chemistry*, 2002, **74**, 784-789.

215. Z. E. Mohammed Bedair, *Electrophoresis*, 2004, **25**, 4110-4119.

216. F. Lin and W. Chen, *Analytical Chemistry*, 2001, **73**, 3875-3883.

217. D. Bandilla and C. D. Skinner, *Journal of Chromatography A*, 2003, **1004**, 167-179.

218. K. Nakanishi, H. Shikata, N. Ishizuka, N. Koheiya and N. Soga, *Journal of High Resolution Chromatography*, 2000, **23**, 106-110.

219. C. Barner-Kowollik, T. P. Davis and M. H. Stenzel, *Polymer*, 2004, **45**, 7791-7805.

220. Z. J. Norman W. Smith, *Journal of Chromatography A*, 2008, **1184**, 416-440.

221. M. Wu, R. Wu, Z. Zhang and H. Zou, *Electrophoresis*, 2011, **32**, 105-115.

222. J. Urban, P. Jandera and P. Schoenmakers, *Journal of Chromatography A*, 2007, **1150**, 279-289.

223. V. Augustin, T. Stachowiak, F. Svec and J. Fréchet, *Electrophoresis*, 2008, **29**, 3875-3886.

224. G. Ma, F. Gong, G. Hu, D. Hao, R. Liu and R. Wang, *China Particuology*, 2005, **3**, 296-303.

225. V. F. Samanidou, A. S. Ioannou and I. N. Papadoyannis, *Journal of Chromatography B*, 2004, **809**, 175-182.

226. Z. Altun, *New Techniques for Sample Preparation in Analytical Chemistry: Microextraction in Packed Syringe and Methacrylate Based Monolithic Pipette Tip*, Karlstad University, Sweden, 2008.

227. B. Beiler and Á. Sáfrány, *Radiation Physics and Chemistry*, 2007, **76**, 1351-1354.

228. E. Byström, C. Viklund and K. Irgum, *Journal of Separation Science*, 2010, **33**, 191-199.

229. E. C. Peters, M. Petro, F. Svec and J. Fréchet, *Analytical Chemistry*, 1998, **70**, 2288-2295.

230. I. Nischang, F. Svec and J. Fréchet, *Analytical Chemistry*, 2009, **81**, 7390-7396.

231. D. Lubda, W. Lindner, M. Quaglia, C. Hohenesche and K. Unger, *Journal of Chromatography A*, 2005, **1083**, 14-22.

232. K. Nakanishi, *Journal of Porous Materials*, 1997, **4**, 67-112

233. H. Yang, Q. Shi, B. Tian, S. Xie, F. Zhang, Yan, B. Tu and D. Zhao, *Chemistry of Materials*, 2003, **15**, 536-541.

234. N. Huesing, C. Raab, V. Torma, A. Roig and H. Peterlik, *Chemistry of Materials*, 2003, **15**, 2690-2692.

235. N. A. Melosh, P. Davidson and B. F. Chmelka, *Journal of the American Chemical Society*, 2000, **122**, 823-829.

236. N. Tanaka, H. Kobayashi, N. Ishizuka, H. Minakuchi, K. Nakanishi, K. Hosoya and T. Ikegami, *Journal of Chromatography A*, 2002, **965**, 35-49.

237. N. Ishizuka, H. Minakuchi, K. Nakanishi, N. Soga and N. Tanaka, *Journal of Chromatography A*, 1998, **797**, 133-137.

238. D. Allen and Z. El Rassi, *Electrophoresis*, 2003, **24**, 408-420.

239. Q. Qu , Q. Gu , L. Shi , Z. Gu and X. Hu, *Analytical Methods*, 2012, **4**, 3200-3205.

240. R. Takahashi, S. Sato, T. Sodesawa, T. Goto, K. Matsutani and N. Mikami, *Materials Research Bulletin*, 2005, **40**, 1148-1156.

241. R. Roux, G. Puy, C. Demesmay and J. Rocca, *Journal of Separation Science*, 2007, **30**, 3035-3042.

242. H. Minakuchi, K. Nakanishi, N. Soga, N. Ishizuka and N. Tanaka, *Journal of Chromatography A*, 1997, **762**, 135-146.

243. P. Fletcher, S. Haswell, P. He, S. Kelly and A. Mansfield, *Journal of Porous Materials*, 2011, **18**, 501-508.

244. G. L. Drisko, X. Wang and R. A. Caruso, *Langmuir*, 2011, **27**, 2124-2127.

245. X. Zhao, G. Lu and X. Hu, *Chemical Modification and Characterisation of MCM-41 and Adsorption Study*, presented in 2nd Pacific Basin Conference on Adsorption Science and Technology, 2000, 386-390.

246. P. He, S. Haswell, P. Fletcher, S. Kelly and A. Mansfield, *Beilstein Journal of Organic Chemistry*, 2011, **7**, 1150-1157.

247. J. Le Bideau, M. Y. Miah, A. Vioux, F. Fajula and A. Galarneau, *Journal of Materials Chemistry*, 2010, **20**, 964-971.

248. M. H. Sorouraddin, M. Amjadi and M. Safi-Shalamzari, *Analytica Chimica Acta*, 2007, **589**, 84-88.

249. D. Lubda and W. Lindner, *Journal of Chromatography A*, 2004, **1036**, 135-143.

250. J. E. Hale, J. P. Butler, V. Gelfanova, J. You and M. D. Knierman, *Analytical Biochemistry*, 2004, **333**, 174-181.

251. N. Jiang, X. Chang, H. Zheng, Q. He and Z. Hu, *Analytica Chimica Acta*, 2006, **577**, 225-231.

252. D. Brandhuber, H. Peterlik and N. Husing, *Journal of Materials Chemistry*, 2005, **15**, 35-36.

253. G. Arslan, M. Ozmen, B. Gunduz, X. Zhang and M. Ersoz, *Turkish Journal of Chemistry*, 2006, **30**, 203-210.

254. M. Zhu, M. Z. Lerum and W. Chen, *Langmuir*, 2011, **28**, 416-423.

255. Y. Zhu, C. Gao, X. Liu and J. Shen, *Biomacromolecules*, 2002, **3**, 1312-1319.

256. M. Lin, C. Chu, L. Tsai, H. Lin, C. Wu, Y. Wu, D. Shieh, Y. Su and C. Chen, *Nano Letters*, 2007, **7**, 3656-3661.

257. C. M. Crudden, M. Sateesh and R. Lewis, *Journal of the American Chemical Society*, 2005, **127**, 10045-10050.

258. F. Darain, P. Yager, K. L. Gan and S. C. Tjin, *Biosensors and Bioelectronics*, 2009, **24**, 1744-1750.

259. J. Shim, H. Na, Y. Lee, H. Huh and Y. Nho, *Journal of Membrane Science*, 2001, **190**, 215-226.

260. L. Jang and H. Liu, *Biomedical Microdevices*, 2009, **11**, 331-338.

261. R. F. Lenza and W. L. Vasconcelos, *Materials Research*, 2001, **4**, 189-194.

262. K. M. de Lathouder, D. T. van Benthem, S. A. Wallin, C. Mateo, R. F. Lafuente, J. M. Guisan, F. Kapteijn and J. A. Moulijn, *Journal of Molecular Catalysis B: Enzymatic*, 2008, **50**, 20-27.

263. X. Wang, K. Lin, J. Chan and S. Cheng, *The Journal of Physical Chemistry B*, 2005, **109**, 1763-1769.

264. Y. Chen, Q. Chen, L. Song, H. Li and F. Hou, *Microporous and Mesoporous Materials*, 2009, **122**, 7-12.

265. M. Yamaura, R. L. Camilo, L. C. Sampaio, M. A. Macêdo, M. Nakamura and H. E. Toma, *Journal of Magnetism and Magnetic Materials*, 2004, **279**, 210-217.

266. L. D. White and C. P. Tripp, *Journal of Colloid and Interface Science*, 2000, **232**, 400-407.

267. S. Han and Y. Kim, *Tetrahedron*, 2004, **60**, 2447-2467.

268. G. Hermanson, *Bioconjugate Techniques*, Academic Press, London, 2008.

269. F. Albericio, *Current Opinion in Chemical Biology*, 2004, **8**, 211-221.

270. S. Ravindran, S. Chaudhary, B. Colburn, M. Ozkan and C. Ozkan, *Nano Letters*, 2003, **3**, 447-453.

271. G. K. Toworfe, R. J. Composto, I. M. Shapiro and P. Ducheyne, *Biomaterials*, 2006, **27**, 631-642.

272. H. Yang, F. Li, C. Shan, D. Han, Q. Zhang, L. Niu and A. Ivaska, *Journal of Materials Chemistry*, 2009, **19**, 4632-4638.

273. G. T. Lu and Y. Huang, *Journal of Materials Science*, 2002, **37**, 2305-2309.

274. P. K. Sahoo, S. S. Kamal, M. Premkumar, T. Kumar, B. Sreedhar, A. K. Singh, S. K. Srivastava and K. Sekhar, *International Journal of Refractory Metals and Hard Materials*, 2009, **27**, 784-791.

275. Infrared Spectroscopy, http://www.chemistry.ccsu.edu/glagovich/teaching/316/ir/table.html, accessed June 2012.

276. L. Xu, X. Dong and Y. Sun, *Electrophoresis*, 2009, **30**, 689-695.

277. B. Hames, *Gel Electrophoresis of Proteins: A Practical Approach (Practical Approach Series)*, Oxford University Press, New York, 1998.

278. D. Marshak, J. Kadonaga, R. Burgess, M. Knuth, W. Brennan and M. Lin, *Strategies for Protein Purification and Characterization: A Laboratory Course Manual*, Cold Spring Harbor Laboratory Press, Woodbury, 1995.

279. H. Liang, M. K. Scott, D. J. Murry and K. M. Sowinski, *Journal of Chromatography B: Biomedical Sciences and Applications*, 2001, **754**, 141-151.

280. V. Pattabhi and N. Gautham, *Biophysics*, Springer, New Delhi, 2002.

281. J. Dong, J. Ou, X. Dong, R. Wu, M. Ye and H. Zou, *Journal of Separation Science*, 2007, **30**, 2986-2992.

282. Y. Ueki, T. Umemura, J. Li, T. Odake and K. Tsunoda, *Analytical Chemistry*, 2004, **76**, 7007-7012.

283. Y. Xu, W. Zhang, P. Zeng and Q. Cao, *Sensors*, 2009, **9**, 3437-3446.

284. I. Liska, *Journal of Chromatography A*, 1993, **655**, 163-176.

285. C. Xie, J. Hu, H. Xiao, X. Su, J. Dong, R. Tian, Z. He and H. Zou, *Electrophoresis*, 2005, **26**, 790-797.

286. T. Nema, E. Chan and P. Ho, *Talanta*, 2010, **82**, 488-494.

287. L. Snyder, J. Kirkland and J. Dolan, *Introduction to Modern Liquid Chromatography*, John Wiley and Sons, Hoboken, 2009.

288. M. le Maire, P. Champeil and J. V. Møller, *Biochimica et Biophysica Acta - Biomembranes*, 2000, **1508**, 86-111.

289. J. L. Norris, N. A. Porter and R. M. Caprioli, *Analytical Chemistry*, 2003, **75**, 6642-6647.

290. N. Zhang and L. Li, *Rapid Communications in Mass Spectrometry*, 2004, **18**, 889-896.

291. K. Shrivas and H. Wu, *Analyst*, 2012, **137**, 890-895.

292. R. Cozzolino, S. Passalacqua, S. Salemi, P. Malvagna, E. Spina and D. Garozzo, *Journal of Mass Spectrometry*, 2001, **36**, 1031-1037.

293. R. Siciliano, B. Rega, A. Amoresano and P. Pucci, *Analytical Chemistry*, 1999, **72**, 408-415.

294. A. Alleoni, *Scientia Agricola*, 2006, **63**, 291-298.

295. W. R. Gray, *Protein Science*, 1993, **2**, 1732-1748.

296. G. I. Bell, W. F. Swain, R. Pictet, B. Cordell, H. M. Goodman and W. J. Rutter, *Nature*, 1979, **282**, 525-527.

297. A. L. McClerren, L. E. Cooper, C. Quan, P. M. Thomas, N. L. Kelleher and W. A. van der Donk, *Proceedings of the National Academy of Sciences*, 2006, **103**, 17243-17248.

298. J. Ma, J. Liu, L. Sun, L. Gao, Z. Liang, L. Zhang and Y. Zhang, *Analytical Chemistry*, 2009, **81**, 6534-6540.

299. R. Yazdanparast, P. C. Andrews, D. L. Smith and J. E. Dixon, *Journal of Biological Chemistry*, 1987, **262**, 2507-2513.

300. V. Zafón, M. Cambra, E. Alfonso and J. Martínez, *Journal of Chromatography A*, 2010, **1217**, 3231-3237.

301. C. W. Huck and G. K. Bonn, *Journal of Chromatography A*, 2000, **885**, 51-72.

302. S. Mirzadeh, M. W. Brechbiel, R. W. Atcher and O. A. Gansow, *Bioconjugate Chemistry*, 1990, **1**, 59-65.

303. N. Kolodny and F. A. Robey, *Analytical Biochemistry*, 1990, **187**, 136-140.

7.0 Publications and presentations

7.1 Journal articles

E. Alzahrani and K. Welham, "Fabrication of an octadecylated silica monolith inside a glass microchip for protein enrichment", *Analyst*, 2012, 137 (20), 4751- 4759. Doi**:** 10.1039/C2AN16018H.

E. Alzahrani and K. Welham, "Design and evaluation of synthetic silica-based monolithic materials in shrinkable tube for efficient protein extraction", *Analyst*, 2011, 136 (20), 4321-4327. Doi: 10.1039/C1AN15447H.

7.2 Oral presentations

E. Alzahrani and K. Welham, "Characterisation of silica-based monoliths with bimodal pore size distribution", *International Conference on Materials Science and its Applications*, Taif University, Kingdom of Saudi Arabia (2012).

E. Alzahrani and K. Welham, "Preparation of monolithic materials and their applications in proteomic analysis", *2nd International Conference on Analytical Proteomics*, Ourense, Spain (2011).

E. Alzahrani and K. Welham, "Design and evaluation of synthetic silica-based monolithic materials for efficient protein extraction", *Analytical Research Forum 2011*, University of Manchester, Manchester, UK (2011).

E. Alzahrani and K. Welham, "Development of a microfluidic device for efficient protein extraction", *5th Saudi International Conference*, University of Warwick, Coventry, UK (2011).

Oral presentation prize awarded.

E. Alzahrani and K. Welham, "Development of a microfluidic device for protein separation", *4th Saudi International Conference*, University of Manchester, Manchester, UK (2010).

7.3 Poster presentations

E. Alzahrani and K. Welham, "Application of synthetic silica-based monolithic materials in reduction of the disulfide bonds in proteins", *6th Saudi International Conference*, Brunel University, Uxbridge, UK (2012).

E. Alzahrani and K. Welham, "Development of a microfluidic device for efficient protein extraction", *2nd International Symposium on Hyphenated Techniques for Sample Preparation*, Bruges, Belgium (2012).

E. Alzahrani and K. Welham, "Fabrication of the monolithic materials and their applications in proteomics analysis", *Emerging Analytical Professionals Conference*, Manchester, UK (2012).

E. Alzahrani and K. Welham, "Development of a microfluidic device for efficient protein extraction", *Lab-on-a-Chip European Congress*, Heriot-Watt University, Edinburgh, UK (2012).

E. Alzahrani and K. Welham, "Design and evaluation of synthetic silica-based monolithic materials in shrinkable tube for efficient protein extraction", *5th Saudi International Conference*, University of Warwick, Coventry, UK (2011).

Poster presentation prize awarded.

E. Alzahrani and K. Welham, "Protein separation by organic monolithic capillary electrochromatography", *Analytical Research Forum 2010*, University of Loughborough, Loughborough, UK (2010).